

**A STUDY OF TRANSMISSION, REFLECTION AND STABILITY  
OF LOW-CRESTED RUBBLE MOUND BREAKWATERS  
UNDER WAVE ACTION**

by

I Gusti Bagus Sila Dharma

Submitted  
in partial fulfillment of the requirements  
for the degree of

DOCTOR OF PHILOSOPHY

Major Subject: Civil Engineering

at

DALHOUSIE UNIVERSITY

Halifax, Nova Scotia

November, 2001

© Copyright by I Gusti Bagus Sila Dharma, 2001



National Library  
of Canada

Acquisitions and  
Bibliographic Services

395 Wellington Street  
Ottawa ON K1A 0N4  
Canada

Bibliothèque nationale  
du Canada

Acquisitions et  
services bibliographiques

395, rue Wellington  
Ottawa ON K1A 0N4  
Canada

*Your file Votre référence*

*Our file Notre référence*

The author has granted a non-exclusive licence allowing the National Library of Canada to reproduce, loan, distribute or sell copies of this thesis in microform, paper or electronic formats.

The author retains ownership of the copyright in this thesis. Neither the thesis nor substantial extracts from it may be printed or otherwise reproduced without the author's permission.

L'auteur a accordé une licence non exclusive permettant à la Bibliothèque nationale du Canada de reproduire, prêter, distribuer ou vendre des copies de cette thèse sous la forme de microfiche/film, de reproduction sur papier ou sur format électronique.

L'auteur conserve la propriété du droit d'auteur qui protège cette thèse. Ni la thèse ni des extraits substantiels de celle-ci ne doivent être imprimés ou autrement reproduits sans son autorisation.

0-612-77599-2

Canada

**Dalhousie University**  
**Faculty of Engineering**

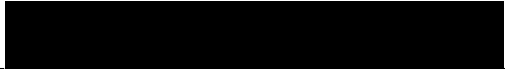
The undersigned hereby certify that they have examined, and recommend to the Faculty of Graduate Studies for acceptance, the thesis entitled "**A Study of Transmission, Reflection and Stability of Low-Crested Rubble Mound Breakwaters under Wave Action**" by I Gusti Bagus Sila Dharma in partial fulfillment of the requirements for the degree of Doctor of Philosophy.

Dated: Feb. 4, 2002

Supervisor:


  
\_\_\_\_\_  
Dr. Mysore Satish

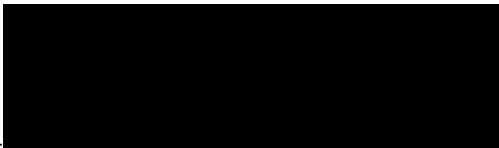
External Examiner:

  
\_\_\_\_\_  
Dr. René Kahawita, École Polytechnique  
de Montréal

Examiners:

  
\_\_\_\_\_  
Dr. Rafiqul Islam

  
\_\_\_\_\_  
Dr. Matiur Rahman

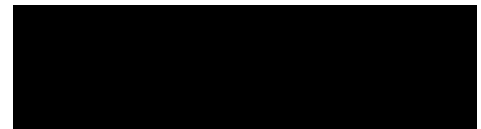
  
\_\_\_\_\_  
Dr. Kevin Hall, Queen's University

**Dalhousie University**  
**Faculty of Engineering**

Date: JAN, 2002

AUTHOR : I Gusti Bagus Sila Dharma  
TITLE : A Study of Transmission, Reflection and Stability of Low-  
crested Rubble Mound Breakwaters Under Wave Action  
MAJOR SUBJECT : Civil Engineering  
DEGREE : Doctor of Philosophy  
CONVOCATION : May, 2002

Permission is herewith granted to Dalhousie University to circulate and to have copied for non-commercial purposes, at its discretion, the above thesis upon the request of individuals or institutions.



Signature of Author

The author reserves other publication rights, and neither the thesis nor extensive extracts from it may be printed or otherwise reproduced without the author's written permission.

The author attests that permission has been obtained for the use of any copyrighted material appearing in this thesis (other than brief excerpts requiring only proper acknowledgement in scholarly writing), and that all such use is clearly acknowledged.



# TABLE OF CONTENTS

LIST OF TABLES .....	ix
LIST OF FIGURES .....	x
LIST OF SYMBOLS .....	xv
ACKNOWLEDGEMENTS .....	xviii
ABSTRACT.....	xix
<b>I INTRODUCTION .....</b>	<b>1</b>
1.1 COASTAL EROSION AND PROTECTION .....	1
1.2 LOW CRESTED BREAKWATER AS COASTAL DEFENCE.....	2
1.3 THE DESIGN OF LOW CRESTED BREAKWATERS .....	4
1.4 OBJECTIVES OF PRESENT INVESTIGATION.....	5
1.5 THESIS OUTLINE.....	6
<b>II REVIEW OF RELATED LITERATURE .....</b>	<b>8</b>
2.1 INTRODUCTION .....	8
2.2 CLASSIFICATION OF LOW CRESTED STRUCTURES.....	11
2.3 STABILITY OF RUBBLE MOUND STRUCUTRES .....	13
2.3.1 Design Formula.....	14
2.3.2 Parameters Affecting Stability.....	22
a. Effect of Wave Period.....	22
b. Effect of Wave Groups .....	23
c. Effect of Wave Duration.....	24
d. Effect of Irregular Waves.....	26
e. Effect of Water Depth.....	27
f. Effect of Permeability .....	29
g. Effect of Structure Slope.....	29
2.4 DAMAGE CRITERIA.....	30
2.5 WAVE TRANSMISSION AND REFLECTION .....	33
2.5.1 Predictive Equations for Wave Transmission.....	34
2.5.2 Predictive Equations for Wave Reflection.....	36
2.6 WAVE ENERGY DISSIPATION.....	37
2.7 CONCLUDING REMARKS.....	38

<b>III</b>	<b>THEORETICAL BACKGROUND .....</b>	<b>40</b>
3.1	INTRODUCTION .....	40
3.2	WAVE CHARACTERISTICS .....	40
3.2.1	Wave Height Distribution .....	41
3.2.2	Wave Energy Spectrum .....	42
3.2.3	Parameters Derived from the Wave Spectrum.....	46
3.2.4	Wave Groups .....	48
3.2.5	Wave Height and Wave Period.....	50
3.3	WAVE-STRUCTURE INTERACTION .....	51
3.3.1	Wave Reflection.....	52
3.3.2	Wave Runup/rundown .....	54
3.3.3	Wave Transmission.....	56
3.3.4	Wave Energy Dissipation .....	56
3.4	STRUCTURAL STABILITY .....	61
3.4.1	Initiation of Damage .....	61
3.4.2	Forces on Armour Unit .....	63
3.5	MODELING OF WAVE-STRUCTURE INTERACTION.....	66
3.6	DIMENSIONAL ANALYSIS .....	68
3.6.1	Governing Variables of Wave Transmission.....	69
3.6.2	Governing Variables for Stability.....	70
3.7	DEVELOPMENT OF RESEARCH PLAN.....	73
<b>IV</b>	<b>EXPERIMENTAL SET UP, INSTRUMENTATION AND DATA COLLECTION .....</b>	<b>75</b>
4.1	EXPERIMENTAL SETUP.....	75
4.1.1	Wave Flume .....	75
4.1.2	Test Structures .....	77
a.	Cross-sectional Geometry.....	77
b.	Breakwater Material .....	77
c.	Model Construction .....	80
d.	Test Conditions .....	80
4.1.3	Data Acquisition .....	82
4.1.4	Wave Measurement .....	82
4.1.5	Measurement of Damage .....	84
4.2	DATA COLLECTION .....	85
4.3	TEST CONDITION AND PROCEDURE .....	88
4.3.1	Calibration .....	88
a.	Wave Machine .....	88
b.	Wave Probes and Profiler .....	88
4.3.2	Wave Signals Generation.....	89
4.3.3	Wave Conditions.....	93

4.3.4	Wave Calibration .....	95
4.3.5	Stability Tests .....	96
<b>V</b>	<b>DATA ANALYSIS AND RESULTS.....</b>	<b>100</b>
5.1	INTRODUCTION .....	100
5.2	DATA ANALYSIS.....	100
5.2.1	Time Domain Analysis: Zero-crossing Method .....	101
5.2.2	Frequency Domain Analysis: Spectral Method .....	101
5.2.3	Reflection Analysis.....	102
5.3	VISUAL OBSERVATIONS .....	104
5.4	RESULTS .....	105
5.4.1	Wave Calibration .....	105
5.4.2	Transmission Tests .....	106
	a. Time Series Transformations.....	107
	b. Spectral Transformations.....	108
	c. Wave Transmission.....	111
	d. Wave Reflection.....	114
5.4.3	Stability Tests .....	117
5.5	WAVE TRANSMISSION, REFLECTION AND STABILITY .....	123
5.5.1	Wave Transmission.....	123
	a. Effect of Relative Crest Height.....	123
	b. Effect of Wave Steepness .....	126
	c. Effect of Crest Width.....	128
	d. Effect of Gradation (armour size).....	129
	e. Effect of the Breakwater Slope.....	130
	f. Effect of Core Permeability .....	131
	g. Effect of Surface Friction and Internal Flow .....	132
	h. Comparison with Existing Design Equations .....	134
5.5.2	Wave Reflection.....	137
	a. Effect of Surf Similarity Parameter .....	137
	b. Effect of Crest Width.....	138
	c. Effect of Armour Size.....	140
	d. Effect of Water Depth.....	140
	e. Effect of Core Permeability .....	141
	f. Comparison with Existing Design Equations .....	141
5.5.3	Stability of the Breakwater .....	143
	a. Initiation of Damage .....	143
	b. Effect of Wave Height .....	145
	c. Effect of Wave Period.....	146
	d. Effect of Water Depth.....	147
	e. Effect of Structure Slope .....	149
	f. Effect of Wave Duration.....	149

g.	Effect of Grouped Waves.....	150
h.	Effect of Core Permeability .....	151
i.	Comparison with Existing Design Equations .....	153
5.6	SUMMARY .....	156
<b>VI DEVELOPMENT OF PREDICTIVE MODELS.....</b>		<b>159</b>
6.1	INTRODUCTION .....	159
6.2	DEVELOPMENT OF THE WAVE TRANSMISSION MODEL .....	160
6.2.1	General Consideration .....	160
6.2.2	Development of the Model .....	161
6.2.3	Evaluation of Predictive Equation .....	164
6.3	DEVELOPMENT OF WAVE REFLECTION MODEL .....	167
6.3.1	Development of the Model .....	169
6.3.2	Evaluation of Predictive Equation .....	171
6.4	VALIDITY OF THE MODELS .....	173
6.5	CALIBRATION OF THE MODEL .....	174
6.5.1	Brief Description of Seabrook's 3-D Testing .....	175
6.5.2	Comparison of the Recent Model and the 3-D Results .....	177
6.6	DEVELOPMENT OF THE 3-D MODEL FOR $K_t$ .....	180
6.6.1	Effect of Wave Direction .....	182
6.6.2	Effect of Angle of Location from the Breakwater .....	183
6.6.3	Effect of Relative Radial Distance .....	185
6.6.4	Statistical Development .....	185
6.7	LIMITATION OF THE PROPOSED EQUATIONS.....	189
<b>VII SOURCES OF ERROR .....</b>		<b>191</b>
7.1	POSSIBLE ERRORS.....	191
7.2	INSTRUMENTAL ERROR .....	191
7.3	HUMAN ERROR .....	192
7.4	MATERIAL VARIABILITY .....	192
7.5	REPEATABILITY .....	193
<b>VIII CONCLUSIONS AND RECOMMENDATIONS .....</b>		<b>194</b>
8.1	CONCLUSIONS.....	194
8.2	RECOMMENDATION FOR FUTURE WORKS .....	196
<b>REFERENCES.....</b>		<b>198</b>
<b>APPENDICES .....</b>		<b>209</b>
APPENDIX A	Wave Characteristics based on Linear Theory .....	209

APPENDIX B	Wave Generation Routines .....	210
APPENDIX C	Wave Analysis Routines .....	214
APPENDIX D	Profile Analysis Routines .....	221
APPENDIX E	Wave Generation Characteristics.....	223
APPENDIX F	Boundary Conditions for Transmission and Stability Tests .....	252
APPENDIX G	Photographs .....	270

# LIST OF TABLES

Table 2.1.	A summary of the previous investigations .....	39
Table 3.1.	Runup coefficients proposed by van der Meer and Stam (1992) ....	56
Table 4.1.	Characteristics of armour and core model. ....	80
Table 4.2.	Structural configurations of wave transformation tests. ....	81
Table 4.3.	Wave test conditions of armour gradation 1. ....	93
Table 4.4.	Wave test conditions of armour gradation 2 and 3. ....	94
Table 4.5.	Waves target of wave calibration.....	96
Table 4.6.	Stability test characteristics. ....	97
Table 4.7.	Wave climate generated for this study.....	99
Table 5.1.	Wave height relationship for different damage levels (CERC, 1984). ....	153
Table 6.1.	The valid range of variables for transmission and reflection equations. ....	174
Table 6.2.	A Summary of data sets used in the calibration.....	177

# LIST OF FIGURES

Figure 2.1.	Example of reef-type breakwater (from van der Meer and Daemen, 1994).....	11
Figure 2.2.	Example of low-crested breakwater (from van der Meer and Daemen, 1994).....	11
Figure 2.3.	Example of submerged breakwater (from van der Meer and Daemen, 1994).....	12
Figure 2.4.	Permeability factor P of various types of structures (van der Meer, 1988).....	19
Figure 2.5.	Effect of the wave period in term of surf similarity parameter $\xi$ (from Losada and Giménez-Curto, 1979).....	24
Figure 2.6.	Effect of wave duration on stability (from van der Meer, 1988). ....	26
Figure 2.7.	Stability of each section of breakwater for Iribaren Damage (from Vidal et al. 1993). ....	29
Figure 3.1.	A schematic frequency spectrum. ....	43
Figure 3.2.	Comparison of Pierson-Moskowitz and JONSWAP spectra.....	46
Figure 3.3.	Reflection coefficient as function of surf similarity parameter $\xi$ (from Battjes, 1974). ....	54
Figure 3.4.	Sketch of different breaker types (from Wiegel, 1964). ....	62
Figure 3.5.	Definition sketch of forces acting on armour units.....	64
Figure 4.1.	Wave flume and model setup.....	76
Figure 4.2.	Cross-section of permeable breakwater model at water depth above the crest. ....	77
Figure 4.3.	Cross-section of impermeable breakwater model at water depth above the crest. ....	78
Figure 4.4.	Gradation curve of core material. ....	78
Figure 4.5.	Gradation curves of armour stones. ....	79
Figure 4.6.	Wave probe instrumentation. ....	83
Figure 4.7.	Mechanical profiler.....	86
Figure 4.8.	Irregular wave generation. ....	91
Figure 4.9.	Grouped wave generation. ....	92
Figure 5.1.	Example of surface elevation time series recorded at probe 5. ....	102
Figure 5.2.	The first 50 seconds of wave record for Figure 5.1. ....	102
Figure 5.3.	Example of wave spectrum of the wave record by VSD for $f_p = 0.5$ Hz.....	103
Figure 5.4.	Reflection characteristics of the beach slope without breakwater (1 <sup>st</sup> array).....	106
Figure 5.5.	Reflection characteristics of the energy absorber at rear end of flume without breakwater (2 <sup>nd</sup> array).....	106
Figure 5.6.	Typical wave time series record for $H_{mo} \sim 10$ cm, $T_p \sim 2.0$ s, water depth $h = 0.43$ m. ....	107

Figure 5.7.	Wave spectral transformations in various wave periods and water depths. ....	108
Figure 5.8.	Comparison of peakedness factor, $Q_p$ , between the transmitted and incident wave spectra (test $T_6$ ). ....	111
Figure 5.9.	Influence of relative crest height on transmission (variable wave heights, $B = 0.30\text{m}$ and $T_p \sim 2\text{s}$ ). ....	112
Figure 5.10.	Influence of relative crest height on transmission (variable wave periods, $B = 0.30\text{m}$ and $H_{mo} \sim 7.5\text{cm}$ ). ....	112
Figure 5.11.	Influence of crest width on transmission (variable wave height, $h_c/h = -0.3$ , $T_p \sim 2\text{s}$ ). ....	112
Figure 5.12.	Influence of crest width on transmission (variable wave periods, $h_c/h = -0.3$ , $H_{mo} \sim 7.5\text{cm}$ ). ....	112
Figure 5.13.	Influence of armour diameter on transmission (variable wave heights, $h_c/h = -0.3$ , $T_p \sim 2\text{s}$ ). ....	113
Figure 5.14.	Influence of armour diameter on transmission (variable wave periods, $h_c/h = -0.3$ , $H_{mo} \sim 7.5\text{cm}$ ). ....	113
Figure 5.15.	Influence of slope structure on transmission (variable wave heights, $h_c/h = -0.3$ , $T_p \sim 2\text{s}$ ). ....	114
Figure 5.16.	Influence of slope structure on transmission (variable wave periods, $h_c/h = -0.3$ , $H_{mo} \sim 7.5\text{cm}$ ). ....	114
Figure 5.17.	Influence of permeability on transmission (variable wave heights, $h_c/h = -0.3$ , $T_p \sim 2\text{s}$ ). ....	114
Figure 5.18.	Influence of permeability on transmission (variable wave periods, $h_c/h = -0.3$ , $H_{mo} \sim 7.5\text{cm}$ ). ....	114
Figure 5.19.	Influence of relative crest height on Reflection (variable wave heights, $B = 0.30\text{m}$ , $T_p \sim 2\text{s}$ ). ....	116
Figure 5.20.	Influence of relative crest height on reflection (variable wave periods, $B = 0.30\text{m}$ , $H_{mo} \sim 7.5\text{cm}$ ). ....	116
Figure 5.21.	Influence of crest width on reflection (variable wave heights, $h_c/h = -0.3$ , $T_p \sim 2\text{s}$ ). ....	116
Figure 5.22.	Influence of crest width on reflection (variable wave periods, $h_c/h = -0.3$ , $H_{mo} \sim 7.5\text{cm}$ ). ....	116
Figure 5.23.	Influence of armour size on reflection (variable wave heights, $h_c/h = -0.3$ , $T_p \sim 2\text{s}$ ). ....	116
Figure 5.24.	Influence of armour size on reflection (variable wave periods, $h_c/h = -0.3$ , $H_{mo} \sim 7.5\text{cm}$ ). ....	116
Figure 5.25.	Influence of slope structure on reflection (variable wave heights, $h_c/h = -0.3$ , $T_p \sim 2\text{s}$ ). ....	117
Figure 5.26.	Influence of slope structure on reflection (variable wave periods, $h_c/h = -0.3$ , $H_{mo} \sim 7.5\text{cm}$ ). ....	117
Figure 5.27.	Influence of permeability on reflection (variable wave heights, $h_c/h = -0.3$ , $T_p \sim 2\text{s}$ ). ....	117
Figure 5.28.	Influence of permeability on reflection (variable wave periods, $h_c/h = -0.3$ , $H_{mo} \sim 7.5\text{cm}$ ). ....	117



Figure 5.29.	Influence of wave height on stability of breakwater (tests SH4, SH5, SH6, SH7, water depth $h = 0.23$ m).....	118
Figure 5.30.	Influence of wave period on stability of breakwater (tests ST5, ST6, ST7, water depth $h = 0.23$ m).....	118
Figure 5.31.	Influence of water depth on stability of breakwater (tests SD1, SD3, and SD4). ....	119
Figure 5.32.	Influence of grouped waves on stability of breakwater (tests SG4 and SG41). ....	120
Figure 5.33.	Influence of wave number (duration) on stability of breakwater (tests SN1, SN2 and SN3).....	120
Figure 5.34.	Influence of wave climate on stability of breakwater (tests SC1, SC2, SC3, SC4, and SC5).....	121
Figure 5.35.	Influence of slope structure on stability of breakwater (test SD1, slope 1:2). ....	122
Figure 5.36.	Influence of slope structure on stability of breakwater (test SS1, slope 1:1). ....	122
Figure 5.37.	Influence of core permeability on stability of breakwater (tests SH7 and SP2).....	123
Figure 5.38.	Wave transmission as a function of relative crest height $h_c/H_i$ (Test T1). ....	124
Figure 5.39.	Wave transmission coefficients as a function of relative crest height, $h_c/H_i$ (all of the test data). ....	125
Figure 5.40.	Wave transmission coefficients as a function of relative crest height $h_c/D_{50}$ for T1 test series.....	126
Figure 5.41.	Effect of wave steepness related to $h_c/H_i$ on transmission (test series T1).....	127
Figure 5.42.	Effect of wave steepness related to $h_c/D_{50}$ on transmission (test series T1).....	127
Figure 5.43.	Effect of relative wave height on transmission (test series T1).....	128
Figure 5.44.	Effect of dimensionless crest width $B/H_i$ on transmission (tests series T1-T6).....	129
Figure 5.45.	Effect of dimensionless armour size on transmission (tests series T12, W22 and W32). ....	130
Figure 5.46.	Effect of breakwater slope on wave transmission of breakwater (tests series T1, T12 and T14). ....	131
Figure 5.47.	Effect of core permeability on transmission (tests series T1 and IM1). ....	132
Figure 5.48.	Effect of surface friction on transmission (tests series T1-T6).....	133
Figure 5.49.	Effect of the internal flows on transmission (tests series T1-T6).....	134
Figure 5.50.	Comparison of Ahrens' Equation and present test data.....	135
Figure 5.51.	Comparison of van der Meer's values and present test data for various crest width. ....	136

Figure 5.52.	Comparison of Seabrook's Equation and present test data for submerged conditions. ....	137
Figure 5.53.	Effect of surf similarity on reflection for different water depths (test T1). ....	138
Figure 5.54.	Effect of crest width on reflection (tests series T1, T2, T3 and T4). ....	139
Figure 5.55.	Effect of submergence on $K_r$ - $\xi$ relationship. ....	139
Figure 5.56.	Effect of armour size on reflection (tests series T12, W22 and W32). ....	140
Figure 5.57.	Effect of core permeability on reflection (tests series T1 and IM1 at $h = 0.43\text{m}$ ). ....	141
Figure 5.58.	Comparison of Allsop's (1990) and Seelig & Ahrens' (1981) Eq. with the test data. ....	142
Figure 5.59.	Photograph of the initiation of damage ( $S_A = 1$ ). ....	144
Figure 5.60.	Damage curve (tests SH4, SH5, SH6, SH7, $T_p \sim 1.5\text{s}$ and $h = 0.23\text{m}$ ). ....	145
Figure 5.61.	Effect of wave period on stability of breakwater at $h=0.23\text{m}$ (Test series ST). ....	146
Figure 5.62.	Effect of water depth at initiation of damage ( $S_A = 0-1$ ). ....	148
Figure 5.63.	Effect of water depth on stability for $T_p=1.5$ sec. and $\cot \alpha = 2.0$ . ....	148
Figure 5.64.	Effect of slope on stability for $T_p \sim 2.0$ sec. and $H_i \sim 0.15\text{m}$ . ....	149
Figure 5.65.	Effect of number of waves ( $N$ ) on stability. ....	151
Figure 5.66.	Effect of wave grouping on stability (tests series SG). ....	152
Figure 5.67.	Effect of core permeability on stability for $T_p \sim 1.5\text{s}$ at various water depth. ....	152
Figure 5.68.	Comparison of the test data and Hudson's Equation for $K_D = 4$ (non-breaking). ....	155
Figure 5.69.	Comparison of the test data and van der Meer's Equation on initiation of damage ( $S_A = 0-1$ ) at $h = 0.23\text{m}$ . ....	155
Figure 5.70.	Comparison of the test data and van der Meer's Equation on intermediate of damage ( $S_A = 5-8$ ) at $h = 0.23\text{m}$ . ....	156
Figure 6.1.	Estimated $K_t$ compared to $K_t$ based on impermeable data by applying $D_{50}/D_{50c} = 1.5$ . ....	164
Figure 6.2.	Estimated $K_t$ compared to experiment data for both permeable and impermeable conditions. ....	165
Figure 6.3.	Normal probability of $K_t$ residuals. ....	166
Figure 6.4.	Sensitivity of $K_t$ to variation of +95% confidence interval in regression coefficients. ....	167
Figure 6.5.	Estimated $K_r$ compared to experiment data. ....	172
Figure 6.6.	Normal probability of $K_r$ residuals. ....	172
Figure 6.7.	Sensitivity of $K_r$ to variation of +95% confidence interval in regression coefficients. ....	173

Figure 6.8.	3-D Testing set up at waves direction of 90°. (from Seabrook, 1997) .....	176
Figure 6.9.	3-D Testing set up at waves direction of 60°. (from Seabrook, 1997) .....	176
Figure 6.10.	Comparison between 2-D equation and 3-D test results for probe 2 at $\varphi_0 = 90^\circ$ . .....	178
Figure 6.11.	Comparison between 2-D equation and 3-D test results for probe 4 at $\varphi_0 = 60^\circ$ .....	178
Figure 6.12.	Comparison between diffracted energies calculated using $K_d$ and measured data.....	179
Figure 6.13.	Wave diffraction behind a breakwater for oblique incidence of waves.....	182
Figure 6.14.	Effect of incident wave direction (probes 2 and 4 at the same location and distance to the breakwater).....	183
Figure 6.15.	Effect of angle from the breakwater to the point of interest at normally incident waves (probes 2 and 4 at the same distance to the breakwater). .....	184
Figure 6.16.	Effect of angle from the breakwater to the point of interest at normally incident waves (probes 1 and 2 at the center line of the breakwater). .....	184
Figure 6.17.	Effect of relative radial distance from the tip of breakwater to the point of interest at normally incident waves. ....	185
Figure 6.18.	Estimated and measured $K_t$ of 3-D equation. ....	187
Figure 6.19.	Normal probability of $K_t$ residuals for 3-D equation.....	188
Figure 6.20.	Sensitivity of $K_t$ to variation of +95% confidence interval in regression coefficients. ....	188
Figure 6.21.	Comparison between 3-D equation and 2-D data for submerged conditions.....	189

# LIST OF SYMBOLS

The following symbols are used throughout this thesis to denote the quantity or property given in the table below.

Symbol	Brief Definition	Dimensions
$A_t$	= area of the breakwater cross section;	$L^2$
$A_e$	= eroded area of breakwater cross-section;	$L^2$
$B$	= crest width of breakwater;	$L$
$C$	= velocity of propagation;	$LT^{-1}$
$C_g$	= velocity of wave group propagation	$LT^{-1}$
$D_{50}$	= nominal diameter of armour units $(M_{50}/\rho_a)^{1/3}$	$L$
$E_r$	= the reflected wave energy per unit width;	$MLT^{-2}$
$E_i$	= the incident wave energy per unit width;	$MLT^{-2}$
$E_d$	= the dissipated wave energy per unit width;	$MLT^{-2}$
$e$	= porosity;	-
$f$	= wave frequency;	$T^{-1}$
$f_p$	= peak wave spectral frequency;	$T^{-1}$
$GF$	= wave groupiness factor;	-
$g$	= gravitational acceleration;	$LT^{-2}$
$H$	= wave height;	$L$
$H_b$	= breaking wave height;	$L$
$H_o$	= deep water wave height;	$L$
$H_D$	= wave height at initiation of damage;	$L$
$H_s$	= significant wave height, $H_{1/3}$ or $H_{mo}$ ;	$L$
$H_i$	= incident wave height, $H_{1/3}$ or $H_{mo}$ ;	$L$
$H_t$	= transmitted wave height;	$L$
$H_{1/3}$	= average wave height of one-third the highest waves;	$L$
$H_{mo}$	= significant wave height derived from spectrum = $4\sqrt{m_o}$ ;	$L$
$h$	= water depth at the breakwater;	$L$
$h_s$	= height of the breakwater from the bottom;	$L$
$h_c$	= freeboard or depth of submergence ( $h_s-h$ );	$L$
$h_b$	= water depth at breaking point;	$L$
$K_D$	= coefficient of damage;	-
$K_d$	= diffraction coefficient;	-
$K_t$	= wave transmission coefficient = $H_t/H_i$ ;	-
$K_r$	= wave reflection coefficient;	-

k	= wave number = $2\pi/L$ ;	$L^{-1}$
L	= wave length = $gT^2/2\pi$ ;	L
$L_o$	= deepwater wave length;	L
$L_p$	= local depth wave length;	L
$M_{50}$	= average mass of stones;	M
m	= beach slope;	-
$m_o$	= area under wave spectra;	$L^2$
$m_1$	= 1 <sup>st</sup> moment, spectral density function;	$L^2T^{-1}$
$m_2$	= 2 <sup>nd</sup> moment, spectral density function;	$L^2T^{-2}$
N	= number of waves;	-
$N_s$	= stability number = $H_s/\Delta D_{50}$ ;	-
n	= energy flux parameter = $C_g/C$ ;	-
	= index referring to moment of the spectrum;	-
P	= permeability coefficient;	-
$Q_p$	= spectral peakedness factor;	-
$Re$	= Reynold's number = $\sqrt{gH_s} D_{50}/\nu$ ;	-
$R_u$	= height of the wave runup;	L
r	= radial position;	L
S	= damage parameter;	-
$S_A$	= damage parameter based on eroded area;	-
$S_N$	= damage parameter based on number of stones displaced;	-
$S(f)$	= spectral density function;	$L^2T$
$s_{op}$	= wave steepness obtained from deep water wave length;	-
$s_p$	= wave steepness obtained from local wave length= $H_i/L_p$ ;	-
T	= wave period;	T
$T_p$	= peak period of spectrum = $1/f_p$ ;	T
$T_m$	= average wave spectra period;	T
t	= time;	T
U	= wind speed;	$LT^{-1}$
u	= water particle velocity;	$LT^{-1}$
$\alpha$	= angle between horizontal and slope of breakwater;	-
$\alpha_p$	= Philips constant = 0.0081;	-
$\Delta$	= relative mass density = $(\rho_a - \rho_w)/\rho_w$ ;	-
$\varepsilon$	= spectral width factor;	-
$\phi$	= frictional angle of the unit;	-
$\gamma$	= peak enhancement factor;	-
$\gamma_b$	= breaker index;	-
$\eta$	= water level fluctuation;	L
$\phi_o$	= wave direction;	-
$\phi$	= angle between incident wave and breakwater to the point of interest;	-

$\mu$	= dynamic viscosity of the water;	$ML^{-1}T^{-1}$
$\nu$	= spectral bandwidth parameter;	-
$\rho_a$	= mass density of armour;	$ML^{-3}$
$\rho_w$	= mass density of water;	$ML^{-3}$
$\sigma$	= standard deviation of water surface position; = surface tension of the water;	- $MT^{-2}$
$\nu$	= kinematic viscosity of the water = $\mu/\rho_w$ ;	$L^2T^{-1}$
$\xi$	= surf similarity parameter computed using deep water wave length = $\tan \alpha / \sqrt{H_i/L_o}$ ;	-
$\xi_b$	= surf similarity at the breaking point = $\tan \alpha / \sqrt{H_b/L_o}$ ;	-
$\xi_o$	= surf similarity in deep water = $\tan \alpha / \sqrt{H_o/L_o}$ ;	-
$\xi_p$	= surf similarity parameter computed using local water wave length = $\tan \alpha / \sqrt{H_i/L_p}$ ;	-

# ACKNOWLEDGEMENTS

The author would like to express his gratitude to Dr. M.G. Satish, his supervisor at Dalhousie University. Sincere thanks to him for his continuous support and encouragement provided when the author faced difficult situations throughout the course of this study. He also gave freely and amply of his time, many times interrupting his own important work, to render valuable assistance to me.

This thesis is result of research that has been carried out at the Queen's University Coastal Engineering Research Laboratory (QUCERL) under supervision of Dr. Kevin Hall to whom the author is deeply grateful. The author wishes to thank to him for his both financial and professional support provided throughout this study. His time, suggestions and efforts are greatly appreciated.

The author also wishes to thanks to the staff of the Civil Engineering Department and the Coastal Laboratory of Queen's University who assisted him in this research. In particular special thanks to Stuart Seabrook to allow me to use his data for this study, and for his valuable discussions and technical assistance while conducting this study at the Coastal Lab. The financial support from Indonesian Government through the EEDP is highly appreciated. The author should also thanks Dalhousie Graduate Studies for awarding a Graduate Scholarship.

The author also indebted to many of fellow students and friends, especially at GIS lab for their kindness and friendships.

Finally, the author wishes to thanks his wife, his children and his family in Bali, Indonesia for their encouragement and support to achieve and succeed.

# ABSTRACT

Two-dimensional physical models of low crested breakwaters were tested at the Queen's University Coastal Engineering Research Laboratory (QUCERL) to establish the effects of water depth, crest width, structure slope, stone size, core permeability and incident wave characteristics on the wave transmission and reflection processes. Effects of structure slope, core permeability, water depth and incident wave characteristics, (including wave groups) on the processes leading to damage were also studied. The breakwater models consisted of a core and two armour layers attacked by irregular waves.

Results of the experiments show the strong influence of water depth, crest width and wave period on wave transmission process. In the wave reflection process, results show the strong influence of water depth and wave period. The stability of low crested breakwaters was observed to be strongly influenced by the water depth and wave period.

Comparisons of the test results with the existing design equations do not seem to predict the wave transmission and reflection accurately for the range of the test data, especially for wide crest structures. Results of the irregular wave conditions required to initiate damage are compared to the design equations of Hudson and of van der Meer. The results and analysis presented herein support and are consistent with the design equation proposed by van der Meer. The equation takes into account the effects of wave height, wave period, structure slope, permeability and wave duration.

Alternative empirical models for the transmission and reflection coefficients were developed on the basis of dimensional analysis considerations and graphical inspection of the 2-D test results. The alternative models were evaluated on the basis of statistical measures and practical design considerations. The proposed relationships are useful in predicting wave transmission and reflection over a wide range of wave heights and covers variety of wave conditions and structural geometry. The models were verified with 3-D test results, showing that the proposed models predict the 3-D test data relatively well.

Given the complex nature of the processes at low crested breakwaters that cannot be clearly described using 2-D test data, a model has also been developed which describes the wave transmission characteristics based on a series of 3-D model tests. The 3-D model predicts relatively well  $K_t$  for both 2-D and 3-D test data.



# Chapter I

## INTRODUCTION

### 1.1 COASTAL EROSION AND PROTECTION

The unabated increase in exploration of natural resources from the ocean and the utilization of the coastline for harbours, waterways, industrial complexes as well as tourism in recent years, require a better understanding of the processes that govern coastline behavior. Improperly designed coastal developments have often caused severe problems to the environment, such as erosion and pollution, with irreparable damage. Recent issues, such as global warming have increased the pressure on the coastal environment even further. The rise of sea level due to global warming has an inevitable impact on the erosion and flooding of precious low lands. The most common coastal problem is shore or coastal erosion. Coastal erosion may be defined as the inward change of the coastline, which is mainly due to wave action. Erosion is known as abrasion if the change is taking place in the steep coast in which the changes are caused due to wave action as well as the rock weathering or sliding. All of these consequences, natural or man-made, impose on engineers and scientists a fair amount of responsibility to face challenges of the problem and evolve methods to mitigate the adverse impacts.

Often, in tropical coastal areas coral reefs function as wave absorbers and reduce the wave energy that reaches the beach. In some beaches, the habitat of coral reefs is often destroyed by human activity and the reefs no longer protect the beach. Hence, artificial reefs like breakwaters may be provided to protect the beach from wave actions. This structure with a wide crest can be built parallel to the shoreline

and the crest is set up below or a little above the water level. The primary function of this structure is to protect the coastal area from wave action by reducing the incoming waves or by acting as a barrier to sea waves. This structure is usually desirable in situations where only partial attenuation of the incoming waves will suffice. When a conventional breakwater gets damaged, it may have its crest at or below the water level, and yet function to attenuate the waves in the protected area of the coastal zone.

## **1.2 LOW CRESTED BREAKWATER AS COASTAL DEFENCE**

The Coastal Engineering Research Center (1984) divided shore protection systems into three classes:

- Structures to prevent waves from reaching erodible material (seawalls, bulkheads, revetments, and offshore breakwaters).
- Structures to retard the long shore transport (groins).
- An artificial supply of beach sand to make up for a deficiency in sand supply through natural process (beach nourishment).

The first two classes are related to structural shore protection while the last is related to non-structural protection. Seawalls are vertical structures to protect that behind them from both the waves and waters of the sea. Therefore these structures may be located right along the coastline or set back beyond the active beach. Bulkheads are vertical structures that are constructed primarily to prevent sliding or retention of the land or to protect uplands areas from damage due to wave action. Revetments are shoreline structures that are built parallel to the shoreline to protect shoreline feature against erosion by dissipating wave energy as the wave is directed up the slope. Breakwaters are structures to prevent the shoreline from damage due to wave action by breaking or dissipating incoming waves before they reach it. These structures are usually constructed parallel to the shoreline. Groins are structures that are usually built perpendicular to the shoreline to interrupt sand moving along the shoreline.

Low crested structures as a type of offshore breakwater can be classified into three categories: dynamically stable reef breakwater, statically stable low-crested breakwater and statically stable submerged breakwater (van der Meer, 1991). The use of low crested breakwaters (including submerged breakwaters) has become very attractive in beach restoration projects (Pina et al. 1990). A submerged breakwater is a low crested breakwater structure in which the initial crest level is placed below still water level (SWL). Submerged breakwaters can be relatively ineffective during the high tides. For the greatest effectiveness at all times, submerged breakwater should be used only in locations having a small tidal range. The main purpose of the low crested breakwater is to reduce the wave energy reaching the beach as a result of breaking, dissipation, friction, and reflection.

The construction cost for rubble-mound breakwaters is usually of the order of millions of dollars for shore protection projects (Smith, 1986a, 1986b). Repairing costs of a failed structure may approach the original construction cost due to expensive mobilization. Another cost, which is to be accounted for during maintenance, is due to inconvenience of operation of the breakwaters. To minimize all of these costs due to breakwater failure, the structure should be designed to allow for minimum damage.

The primary advantage of a low-height breakwater is its economics, since the cost of rubble mound breakwater will increase rapidly with the height of the crest. Low crest breakwaters allow wave overtopping and transmission. Several projects have been designed with low crests and large number of research projects on the functional performance of low crested breakwaters has been carried out. Walker et al. (1975) reported on the performance of low crested breakwater structures developed for a wave defense system of a harbour and for beach protection. They discussed many factors that affect the stability of overtopped rubble mound breakwaters. Bremner et al. (1980) reported the surprisingly good performance of the damaged Rosslyn breakwater during Cyclone David in 1976 in Australia. Previously, the Rosslyn breakwater was a non-overtopped breakwater and was reduced to a

submerged breakwater after the cyclone. Abdul Khader and Rai (1980) performed a series of experiments to investigate the effectiveness of submerged breakwaters in the dissipation of wave energy. Wave transmission was found very much dependent on their relative height. Dick and Brebner (1969) and Dattatri et al., (1978) observed the transformation of regular waves at submerged breakwaters. Van der Meer (1991) studied the stability and transmission at low crested structures and developed a set of design equations

Usually construction of a shore protection system has a constraint that the benefits realized by a proposed plan must exceed all the lifecycle costs (Smith, 1986a). The project with the maximum net benefit cost ratio is selected for the project design. Low crested reef type breakwaters reduce construction costs since less material is required. Low crested reef type breakwaters use a homogeneous stone size instead of traditional multi layer construction, thereby require less accuracy in stone placement during construction and as a result will have reduced construction costs.

### **1.3 THE DESIGN OF LOW CRESTED BREAKWATERS**

In the past, certain structures have been over designed, whereas some others have suffered damages that needed considerable repairs. The experience gained on these has proved to be very useful in evolving guidelines for breakwaters. General guidelines for designing low-crested breakwaters can be obtained from the CERC (1984). Design formulae of low crested breakwaters are also discussed by van der Meer (1987, 1988). A general view on designing a breakwater may be had from several past investigations. Some of the important observations are:

- Design water level, i.e. the level that is to be selected for the design of a breakwater not only depends on the characteristics of the water level frequency diagram, but also on the value of the property that is to be protected. The higher

the value of the area to be protected, higher is the design water level chosen as the basis for the breakwater design.

- The design wave is dependent upon the design water level that has been chosen. The height of the waterline and the wave height/period are the two essential conditions for a breakwater design. Usually it is difficult to find the wave data for a study area. In this case, computations have to be made based on wind and tide data. For design purposes, wave analysis can be limited to determining a certain maximum design wave height and wave period.
- As far as armour stability is concerned, several researchers including Hudson (1959) and Bruun (1985) concluded that wave attack is usually the heaviest on that part of the slope, which lies in the vicinity of half the wave height below the average water level. It is difficult to determine what type of armour will be required on various parts of the breakwater slope. The relation between the characteristic of the waves and type of construction is also difficult to determine. The removal of one unit armour by wave action may lead to others being at risk.

#### **1.4 OBJECTIVES OF THE PRESENT INVESTIGATION**

Design of rubble mound structures is usually done using semi empirical formulae developed from a limited range of variables involved. In many cases, the limitation of variables has led to either an unsafe or a conservative design of the structures. In order to achieve more rational results, the design formulae should involve as wide a range of variables as possible. It will help to advance the understanding of the principles of design and evolve cost effective breakwaters. Hence, this study was conducted to investigate the performance and effectiveness of the shore protection systems, particularly those of low crested breakwaters for a wide range of variables. These systems can have application in low-lying coastal areas subject to large storm surges. A two dimensional physical hydraulic modeling was

conducted to investigate the performance of these systems, including stability of the breakwater subject to irregular waves. The hydraulic characteristics of the structure to absorb wave energy were investigated in order to provide additional information on the wave transmission and reflection phenomenon. Wave induced damage of rock armour was investigated in wide range of parameters to advance the understanding of the performance of existing designs in breakwater stability.

To summarize, the objectives of the present study may be stated as follows

- Study wave-structure interaction in the process of wave transmission, reflection, dissipation and other processes related to the wave-structure interaction.
- Study the influences of wave characteristics and cross-sectional geometry of the breakwater on stability.
- Analyze the wave transmission and reflection data for low crested breakwaters, including the present observations, and bring out clearly the role of different dimensionless parameters.
- Review previous design equations relating to low crested breakwaters and suggest alternative relationships using the present data.

## **1.5 THESIS OUTLINE**

In the previous section, the general importance of low crested breakwaters and objective of this research is highlighted. The literature review on wave transmission and stability of low crested breakwaters, presented in Chapter 2, shows that a significant amount of research has already been conducted using both a mathematical and experimental approach.

Chapter 3 provides a brief discussion on the theory relating to wave transformation at a structure, wave characteristics based on linear wave theory, and dimensional analysis of factors influencing wave transmission, reflection and stability of structure. The development of a research plan is also presented within this chapter.

A description of the experimental testing is given in Chapter 4. The experimental facility, setup, and procedures undertaken for this study are described. Two-dimensional testing was employed to study the process of wave transmission, reflection and stability of the rubble mound breakwater. Parameters affecting wave transmission and stability such as wave height, wave period, wave duration, water depth, crest width of structure, face slope, armour gradation, and permeability were varied. Results of this study are reported in Chapter 5, including the observations recorded, assessment of the test results and an assessment of the particular factors that influence the transmission, reflection and stability of the structure.

In Chapter 6, a development of the models to predict wave transmission and reflection using statistical analysis is described following the relationship between parameters described in Chapter 5, together with some discussion on possible limitations of the models. A discussion of the wave transmission process in the 3-D environment is also presented followed by a development of the model. The possible error that may occur in obtaining the data is presented in Chapter 7.

Finally, conclusions based on this study are presented in Chapter 8. A recommendation for future work is also made.

## Chapter 2

# REVIEW OF RELATED LITERATURE

### 2.1 INTRODUCTION

Shore protection using physical construction can be attained by several methods, i.e.: absorbing the wave's energy, changing of long-shore transport, strengthening the beach, and beach nourishment. Pilarzcyk and Zeidler (1996) described various shore protection measures such as shore structures (groins, jetties), shore-parallel structures (offshore breakwaters, sea walls, revetment), headland structures, and beach nourishment. Tschirky et al. (1998) explained a method in shore protection measures using bioengineering approach. CERC (1984) divides the shore protection measures into two classes: structures to prevent erodible material being removed by the wave action (seawalls, revetments) and a supply of beach sand to fill in the eroded beach. Groins and jetties are used to prevent the beach from erosion by long-shore current.

In recent years, a number of low crested breakwaters including submerged breakwaters as shore protection systems have been built. The primary function of this structure is to protect a beach from wave attack by reducing the incoming wave energy or acting as a barrier to sea waves. This structure is usually built in situations where only partial attenuation of the incoming waves is allowed. A number of papers have noted that low crested rubble mound breakwaters are more likely to be economical over traditional mound breakwaters (Abul-Azm 1993, Losada et al. 1992, Ahrens 1984, 1989 and Abdul Khader and Rai 1980). Walker et al. (1975) stated that the primary advantage of low crest breakwaters is economics. Abdul Khader and Rai (1980) noted that submerged breakwaters are less costly to construct and maintain



than conventional breakwaters. Ahrens (1984) described reef type breakwater as possibly the optimum structure for many situations. He also noted that a low crested breakwater with infrequent overtopping is considerably less expensive per unit length than traditional breakwaters since the cost of a rubble mound increases rapidly with the height of the crest. Abul-Azm (1993) has indicated that submerged breakwaters may be a logical selection when the water depth increases and breakwater extends to the full water depth. Losada et al. (1992) has stated that submerged mound breakwaters have been used for shoreline protection because of their low cost and aesthetics.

Numerous studies on low crested breakwaters (including submerged breakwaters or obstacles) to evaluate the stability and wave transformation at the structure have been performed. Early studies were focused on the observation of general transformations of regular waves at submerged breakwaters (Dick and Brebner 1969, and Dattatri et al. 1978). Petti and Ruol (1991 and 1992), Liberatore and Petti (1992), Driscoll et al. (1992) have also investigated submerged structures using irregular waves. Concerning hydraulics stability, Hudson (1959), Losada and Giménez-Curto (1979), Hedar (1986) and van der Meer (1987, 1988) provided simple approaches for breakwater design applications. However, these equations are based on tests involving a limited range of variables. Beji and Battjes (1993) investigated the propagation of irregular waves over a submerged obstacle. The tests found that high frequency energy was generated when waves propagate over a submerged bar. Losada and Giménez-Curto (1981), Ahrens and Titus (1985) described the runup and rundown phenomena on different smooth and rough slopes due to regular and irregular waves. Their results show that runup on smooth slopes is mostly influenced by the surf similarity parameter,  $\xi$ , while on a rough permeable slope runup is influenced by friction and permeability of the armour layer. Bruun and Johannesson (1976) and Bruun (1985) described the importance of the wave group while causing damage to breakwater exposed to waves, while the design formula of van der Meer (1987, 1988) did not incorporate wave grouping. Johnson et al. (1978) found that

wave group could cause greater damage to the rubble mound structures than an individual wave. Their analysis is based on the Smoothed Instantaneous Wave Energy History (SIWEH) techniques, described by Funke and Mansard (1980). Medina et al. (1990) noted that wave groups could contribute up to 50% of the variability in damage to an armour layer of a structure. They proposed the concept of an envelope exceedance coefficient to explain the degree of wave grouping, which controls the stability. According to them, wave groups are more appropriately described by the parameter involving the envelope exceedance coefficient.

The stability of rubble mound structures has been treated experimentally by various researchers, resulting in many design formulae. One well-known design formula for conventional breakwaters was derived by Hudson (1959). Low crested rubble mound structures were studied by van der Meer and Pilarczyk (1990), specifically to observe the stability of front slope and crest. Vidal et al. (1992) tested low crested breakwaters and developed damage criteria for the front side, crest and backside of the structure.

The previous studies that are relevant to the present experiments are reviewed in the following section and are organized in the following topic wise.

## **2.2 CLASSIFICATION OF LOW CRESTED STRUCTURES**

Little literature is available on the subject of classification of low crested structures. The criteria for distinction of low crested breakwaters are the distance from still water level to the breakwater crest and the structure type of material used for construction of the structural section of breakwater (Pilarczyk and Zeidler, 1996). Van der Meer and Pilarczyk (1990) and van der Meer and Daemen (1994), divided low crested structures into three categories such as dynamically stable reef breakwater, statically stable low crested breakwaters, and statically stable submerged breakwaters. A reef breakwater is a low crested homogeneous pile of stones without



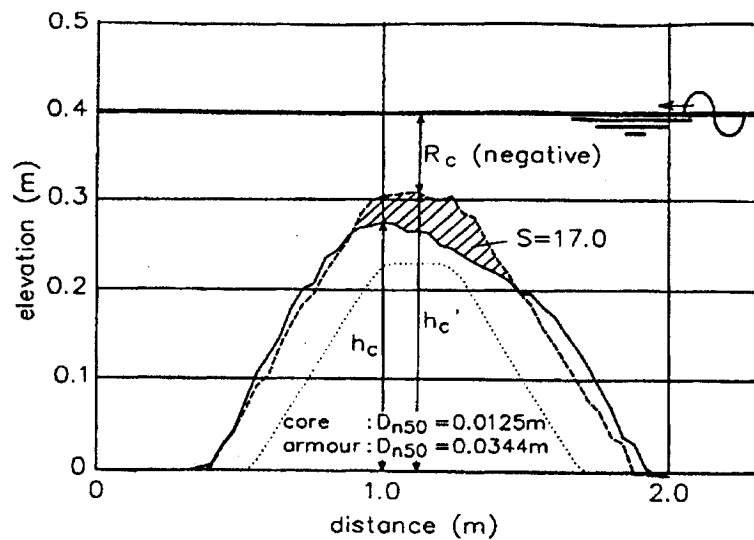


**Figure 2.3.** Example of submerged breakwater (from van der Meer and Daemen, 1994).

Ahrens (1989) described the performance of reef type breakwaters, referred to as low crested rubble mound breakwaters without traditional multi layer cross section. This type of breakwater is of homogeneous stones with similar weight and usually used in the armor and first under layer of conventional breakwater. It was found that reef breakwaters are stable because of their high porosity and as they dissipate wave energy effectively.

### 2.3 STABILITY OF RUBBLE MOUND STRUCTURES

The performance of a breakwater under action of wave is usually linked with the stability. The existing design methods for rubble mound breakwaters use semi empirical and empirical equations based on laboratory data. The most important quantity to be determined in the design is weight of the armour units to be provided in the breakwater armour layers.

Damage of mound breakwaters usually gets initiated as a process by which failure of one armour unit occurs. Bruun and Kjelstrup (1983) classified different kinds of stability associated with mound breakwaters as follows.

1. The overall stability of the mound. The primary concern is for sliding of the armor layer; mass departures of blocks of armor layer; toe failures; and mass breakdowns by heavy rundown waves.
2. The unit stability, is the stability of the individual units of the mound. Any unit must not leave or move considerably relative to other units.
3. The structural stability of a group of individual members of the mound. This stability is concerned with the ability of a collection of units as a structural element to stay in place.

Various authors have listed different governing variables that influence the rubble mound breakwater stability. Commonly, variables affecting rubble mound breakwater stability are divided into two groups: variables related to environmental conditions, and variables related to the physical characteristics of the breakwater.

The environmental variables are:

- wave height ( $H_s$ ),
- wave period ( $T_p$ ),
- duration of wave activity, represented by the number of waves ( $N$ ),
- wave direction ( $\phi_0$ ),
- wave group, represented by groupiness factor ( $GF$ ),
- water density ( $\rho_w$ ),
- dynamic viscosity of the water ( $\mu$ ) and,
- surface tension of the water ( $\sigma$ ).

The physical variables of the breakwater related to characteristics of material and the geometry of the structure are:

- nominal diameter of armour stones ( $D_{50}$ ),
- uniformity of armour stones and filter ( $D_{85}/D_{15}$ ),

- density of armour stones and filter ( $\rho_a$ ),
- shape of the armour stones and roughness,
- thickness of the armour and filter layer ( $t_a$ ),
- permeability of the core (P),
- slope of the structure ( $\cot \alpha$ ),
- the width of the crest (B) and,
- the height of the structure ( $h_s$ ).

Another factor is the method of construction. Construction methods have a significant effect on the stability of breakwaters. Lording and Scott (1971) and Brown (1978) noted that by placing of the rock with its long axis perpendicular to the slope, insuring careful interlocking and friction between units, the stability of units could be increased.

### 2.3.1 Design Formula

Recently several formulae have been developed for predicting the stability of the armour layer. All formulae are based on experimental study and most of the formulae consider the wave height, mass or water density, slope angle, and diameter of armour units as main parameters. Hudson (1959) has developed an empirical formula for design of rubble mound breakwaters based on the data of mostly small-scale model tests. His formula for determining the weight of an armour unit as a function of wave height, specific weight of the water and the units, breakwater slope  $\alpha$  and  $K_D$  a coefficient that reflects the shape of armour unit, is as follows.

$$M_{50} = \frac{\rho_a H^3}{K_D (S_r - 1)^3 \cot \alpha} \quad [2.1]$$

where  $M_{50}$  is mass of armour,  $S_r$  is specific gravity of armour stone and  $\rho_a$  is density of armour stone. Equation [2.1] can be re-arranged in terms of  $H_s/\Delta D_{50}$  (van der

Meer, 1988), or the stability number,  $N_s$  (Ahrens 1987, 1989) to get the following form.

$$\frac{H_s}{\Delta D_{50}} = (K_D \cot \alpha)^{1/3} = N_s \quad [2.2]$$

where  $H_s$  is significant wave height,  $\Delta = \left( \frac{\rho_a - \rho_w}{\rho_w} \right) = (S_r - 1)$  is the relative mass density of the armour material,  $D_{50}$  is the nominal diameter of armour stone related to the mass by  $M_{50} = \rho_a (D_{50})^3$ ,  $\rho_w$  is the density of water,  $\cot \alpha$  is slope structure,  $K_D$  is stability coefficient depending on the type and shape of armour units, the thickness of armour layer, the method of placement, slope angle, wave characteristics (breaking or non breaking), porosity of the core, and damage level. The values of  $K_D$  were derived from model tests using regular waves with permeable cross sections subject to non-overtopping. The  $K_D$  values for breaking and non-breaking waves for quarry stones were 2.0 and 4.0 respectively as suggested by CERC (1984), while CERC (1977) recommends the  $K_D$  values for breaking and non-breaking waves as 3.5 and 4.0 respectively. The values of coefficient  $K_D$  are reported in more detail in CERC (1984), but the exact choice of this coefficient may not be easy.

Equation [2.1] is used to determine the weight of the armour unit required if uniform size (range of  $0.25 M_{50}$  to  $1.25 M_{50}$ ) is used and is applicable for structure with slopes ranging from 1 on 1.5 to 1 on 5 and for non-overtopped breakwaters or overtopped breakwaters with crest height greater than a wave height above water level. It is well known because of its simplicity, though there are a number of shortcomings. This equation was developed on the basis of tests with regular waves and does not include the influence of wave period and wave duration. The method of placement of armour stones in the model structure has a strong influence on the stability of breakwaters. However, no specific techniques are available to determine the exact method of placement of armour stones.

Losada and Giménez-Curto (1979) proposed a design formula to predict minimum stability for values of surf similarity parameter  $\xi$  in the range of collapsing breakers. Their formula was developed on the basis of regular waves that include the influence of wave period and slope structure through the surf similarity parameter. The formula can be written as

$$\frac{H}{\Delta D_{50}} = [A(\xi - \xi_0) \exp\{B(\xi - \xi_0)\}]^{-1/3} \quad [2.3]$$

and the surf similarity parameter defined as

$$\xi = \frac{\tan \alpha}{\sqrt{H/L_0}} = \frac{\tan \alpha}{\sqrt{2\pi H/gT^2}} \quad [2.4]$$

where  $L_0 = gT^2/2\pi$  represents the deep-water wave length, A and B are constants that depend on the slope of structure and armour type. From Eq. [2.3] the minimum value of  $\xi$  which will result in positive values of H is  $\xi_0$ . From the experimental results it was found that  $\xi_0 = 2.65 \tan \alpha$ .

CERC (1984) recommends Hudson's formula as a design equation. Since Hudson's equation was originally developed for regular waves, CERC (1977) recommends that  $H_{1/10}$  be used in that formula in place of regular wave H where  $H_{1/10}$  is defined as the average wave height of the highest 10% waves. CERC (1984) too recommends the use of  $H_{1/10}$  instead of  $H_{1/3}$  where  $H_{1/3}$  is defined as average wave height of one-third the highest waves. Feuillet and Sabaton (1980) also found  $H_{1/10}$  more suitable than  $H_{1/3}$  in Hudson's formula.

Hedar (1986) presented design formulae on the basis of regular wave attack. He has developed two different equations for pervious and impervious under-layer. The influence of the wave climate, the difference between the angle of repose and the slope angle, the material and fluid density, and the permeability of the under-layer



was examined. It shows that permeability of the under-layer has a significant influence on the weight of armour units to resist damage. Also it was reported that for steeper slopes of breakwaters, downrush flow is critical for causing damage while uprush flow is critical on milder slopes. Hedar's formulae can be written in terms of a nominal diameter for stone that leads to stability as,

- a. Uprush condition  
for permeable under layer

$$D_{50} = \left(\frac{\pi}{6}\right)^{1/3} \left[ \frac{0.33(h_b + 0.7H_b)(\tan \phi + 2)}{\Delta(3.6 - e^{-4\tan\beta})\cos \alpha(\tan \phi + \tan \alpha)} \right] \quad [2.5]$$

for impermeable under layer

$$D_{50} = \left(\frac{\pi}{6}\right)^{1/3} \left[ \frac{0.41(h_b + 0.7H_b)(\tan \phi + 2)}{\Delta(3.3 - e^{-4\tan\beta})\cos \alpha(\tan \phi + \tan \alpha)} \right] \quad [2.6]$$

in which  $\beta = \alpha + (\phi - 48^\circ)$

- b. Downrush condition  
for permeable under layer

$$D_{50} = \left(\frac{\pi}{6}\right)^{1/3} \left[ \frac{(h_b + 0.7H_b)(\tan \phi + 2)}{\Delta(13.7 + e^{4\tan\beta})\cos \alpha(\tan \phi - \tan \alpha)} \right] \quad [2.7]$$

for impermeable under layer

$$D_{50} = \left(\frac{\pi}{6}\right)^{1/3} \left[ \frac{1.6(h_b + 0.7H_b)(\tan \phi + 2)}{\Delta(16.5 + e^{4\tan\beta})\cos \alpha(\tan \phi - \tan \alpha)} \right] \quad [2.8]$$

in which  $\beta = \alpha - (\phi - 48^\circ)$

where  $H_b$  is wave breaker height,  $h_b$  is breaker depth,  $\alpha$  is angle between slope and horizontal,  $\phi$  is angle of repose,  $\beta$  is an angle depending on degree of interlocking.

Van der Meer (1987, 1988) presented design equations for the stability of rubble mound breakwater and revetment under wave attack based on an extensive model tests. Two sets of design formulae were developed, one for plunging and the other for surging waves. These formulae are:

$$\frac{H_s}{\Delta D_{50}} = 6.2 \xi_m^{-0.5} P^{0.18} \left( \frac{S}{\sqrt{N}} \right)^{0.2} \quad \text{for plunging waves} \quad [2.9]$$

$$\frac{H_s}{\Delta D_{50}} = P^{-0.13} \left( \frac{S}{\sqrt{N}} \right)^{0.2} \sqrt{\cot \alpha} \xi_m^P \quad \text{for surging waves} \quad [2.10]$$

where  $P$  is notional permeability factor,  $\xi_m$  is a surf similarity parameter obtained using an average wave period ( $T_m$ ),  $N$  is a number of zero crossing waves,  $S$  is a damage level that is defined as  $A_e/D_{50}^2$  where  $A_e$  is eroded area of the structure cross section, and  $\cot \alpha$  is slope of structure. It was mentioned that  $S \sim 2$  may be considered as the initiation of damage,  $S = 5$  means moderate damage and  $S = 8 - 12$  was associated with severe damage, depending on the slope structure. According to Meer, surf similarity parameter for irregular waves is defined in term of the significant wave height ( $H_s$ ) and the average wave period  $T_m$ , and can be written as

$$\xi_m = \frac{\tan \alpha}{\sqrt{\frac{2\pi H_s}{g T_m^2}}} \quad [2.11]$$

The permeability factor,  $P$ , affects structure stability as it includes the relative size of filter layer and core. The value of  $P$  can vary from  $P = 0.1$  to  $P = 0.6$ . The lower value of  $P$  is a structure with armour layer thickness of two diameter and an impermeable core. Between cover layer and core is a thin filter layer with a thickness of 0.5 armour diameter. The upper values of  $P$  represent a homogeneous structure without filter and core. Figure 2.4 shows the values of  $P$  as shown in van der Meer (1887, 1988). The notional permeability above were used by van der Meer to get the best fit on his statistical models and has no physical basis. This condition will limit the use of the permeability factor.

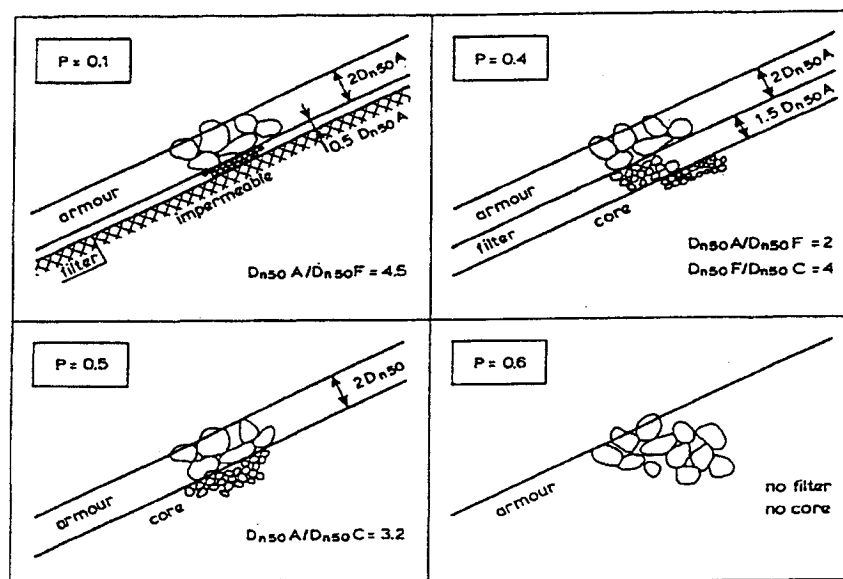


**Figure 2.4.** Permeability factor,  $P$ , of various types of structures (from van der Meer, 1988).

For transition between plunging and surging waves, which results in a minimum stability, the surf similarity parameter can be calculated as

$$\xi_m = \left(6.2P^{0.31} \sqrt{\tan \alpha}\right)^{1/(P+0.5)} \quad [2.12]$$

According to Meer,  $\xi_m$  lies between 2.4 – 4.0 for rubble mound breakwaters. Bruun (1990) noted those wave parameters  $H_s$  and  $T_m$  give a limited description of the wave condition contained in random sea-state. In the reply to the discussion of Bruun, van der Meer stated that irregular wave maybe parameterized by  $H_s$  and  $T_p$ .

The stability of reef breakwater, referred to as a low crested rubble mound breakwater without a multi layer cross section was conducted by Ahrens (1987, 1989) using physical model tests subjected to irregular waves. The stability was measured in terms of reduction in crest height due to wave attack. A number of dimensionless parameters were defined to describe the behavior of the structure. Relative crest height reduction factor,  $h'_s/h_s$ , is the main parameter to determine the deformation of the structure where  $h'_s$  is the crest height after completion of the test, and  $h_s$  is the initial crest height. The values of this ratio are 1.0 for no deformation and 0.0 for a structure not present anymore (completely destroyed). Ahrens described the reduced crest height as

$$h'_s = \sqrt{\frac{A_t}{\exp(aN_s^*)}} \quad [2.13]$$

where  $A_t$  is area of structure cross section,  $N_s^*$  is the spectral (modified) stability number and 'a' is a coefficient. The spectral stability number,  $N_s^*$ , is given by

$$N_s^* = \frac{H_s^{2/3} L_p^{1/3}}{\Delta D_{50}} \quad [2.14]$$

where  $L_p$  is the wave length based on the Linear Waves Theory in term of wave energy density spectrum ( $T_p$ ) and water depth at toe of the structure ( $h$ ). The equation for coefficient 'a' Eq. [2.13] is given by Ahrens (1989) as

$$a = 0.046 \left( \frac{h_s - h'_s}{h} \right) + 0.2083 \left( \frac{h'_s}{h} \right)^{1.5} - 0.144 \left( \frac{h'_s}{h} \right)^2 + \frac{0.4317}{\sqrt{B_n}} \quad [2.15]$$

where

$$B_n = A_t / D_{50}^2 = \text{bulk number} \quad [2.16]$$

The spectral stability number,  $N_s^*$ , is similar to the stability number described by Hudson (1959). The only difference is that wave period is introduced through the variable  $L_p$ . The model was reported to predict accurately the response of rubble mound over a wide range of wave conditions and structural heights.

Van der Meer and Daemen (1994) presented a summary of the important results from the earlier work of van der Meer and Pilarczyk (1990). Their report included data from others such as Ahrens (1987, 1989), van der Meer (1988) and Seelig (1980). The result of the analysis for reef type breakwaters show that the breakwater response slope  $C'$  and  $C$  had to be included in stability analysis, where  $C'$  refers to initially built slope and  $C$  refers to after test slope. The breakwater response slope are defined by

$$C = \frac{A_t}{h_s^2} \quad \text{and} \quad C' = \frac{A_t}{h_s'^2} \quad [2.17]$$

The change in crest height due to wave action (i.e. the crest height reduction) of the breakwater can be described by

$$h_c = \sqrt{\frac{A_t}{\exp(aN_s^*)}} \quad [2.18]$$

where the coefficient 'a' is given as

$$a = -0.028 + 0.045C + 0.034 \left( \frac{h_s}{h} \right) - 6.10^{-9} B_n^2 \quad [2.19]$$

For a statically stable low crested breakwater where overtopping takes place, either Hudson's formula or van der Meer formula (1987, 1988) applicable for non-overtopping breakwaters could be used by applying a reduction factor to the required rock armour diameter. The reduction factor for  $D_{50}$  is given by

$$\text{Reduction factor} = \frac{1}{1.25 - 4.8R_p^*} \quad [2.20]$$

where  $R_p^* = \frac{R_c}{H_s} \sqrt{\frac{s_{op}}{2\pi}}$ ,  $R_c$  is crest height above SWL,  $s_{op}$  is wave steepness =  $(2\pi H_{mo}) / (gT_p^2)$ , and  $R_p^*$  is a dimensionless crest height. The stability of submerged breakwater only associated with the relative crest height,  $h_s/h$ , the damage level,  $S$ , and the spectral stability number,  $N_s^*$ . Thus, design formula of submerged breakwater as suggested by van der Meer and Daemen is as follows.

$$\frac{h_s}{h} = (2.1 + 0.1S) \exp(-0.14N_s^*) \quad [2.21]$$

### 2.3.2 Parameters Affecting Stability

It is expected that a number of parameters like wave period, wave grouping duration of the wave, wave irregularity, water depth, permeability of the rubble mound and the angle of slope of the front face of the mound will affect the stability of the breakwater. A brief description on the role of each parameter is given below.

#### a. Effect of Wave Period

Analysis for breakwater stability did indicate that stability is a function of wave period (Bruun and Gunbak 1976, Losada and Giménez-Curto 1979 and van der Meer 1987, 1988). Cartens et al. (1966) found that long period swells were more damaging than shorter period storm waves. Ahrens (1975) investigated the combined effect of structure slope and wave steepness. He concluded that stability was dependent on

breaker type and the minimum stability occurs for collapsing breakers. He explained that during the uprush, the collapsing breaker have a significant impact directed parallel to the slope which dislodges stones. The downrush is in turn strong enough to loosen the stones. During the downrush period the drag velocity is maximum and together with breaking of waves result in significant uplift force on the armour layer. This situation gives the minimum stability to the armour layer (Bruun and Johannesson, 1976). The breaking type wave is identified by a suitable value of the surf similarity parameter,  $\xi$ .

As described previously, the Hudson's equation (1959) does not include wave period, while other studies do include (e.g. Losada-Gimenez-Curto 1979, Allsop 1983, Ahrens 1987, 1989 and van der Meer 1987, 1988). Their results show that longer wave periods will give lower stability. The contrary, results of a laboratory investigation by Camfield (1996) to determine the response of quarry stone armour units show that shorter wave periods cause more damage than longer wave periods. Similar results by Mansard et al. (1996) also show that minimum stability occurred for shorter wave periods. Losada and Giménez-Curto (1979) introduced a parameter  $Q = (H/\Delta D_{50})^{-3}$  and plotted it against surf similarity parameter,  $\xi$ , as shown on Figure 2.5. Parameter Q in a way shows the relative importance of shear stress acting on the unit compared to the submerged weight of the unit. A high value of Q indicates potential instability of the unit. The minimum stability was found for  $\xi$  lying in the range of 2 to 4.

#### **b. Effect of Wave Groups**

Some researchers pointed out the importance of wave grouping on the stability of rubble mound breakwaters. Burcharth (1979) based on the model tests, described the effect of wave group on stability of onshore structures. He pointed out that shorter waves were more damaging than longer waves, while Johnson et al. (1978) found that wave grouping with longer waves were more damaging than shorter waves. On the other hand, van der Meer (1987, 1988) did not notice significant

correlation between wave grouping and the breakwater stability. Therefore, the wave groupiness factor was not taken into account in his stability formula for rubble mound breakwater design. Medina et al. (1994) emphasized that wave grouping should be considered in engineering design, and their recommendation is similar with that of Bruun and Kjelstrup (1983) who suggested the wave groupiness be considered when testing rubble mound breakwaters for their stability.

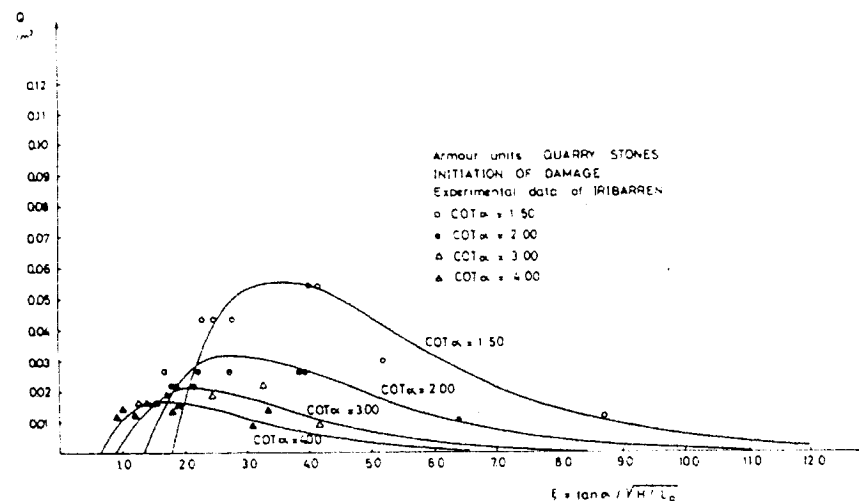


**Figure 2.5.** Effect of the wave period in term of surf similarity parameter  $\xi$  (from Losada and Giménez-Curto, 1979).

### c. Effect of Wave Duration

The damage to a rubble mound structure is progressive; therefore, damage to the structure depends not only on the intensity but also on the duration of wave action. Once the units lose their interlocking, the initial damage occurs. The damage usually increases gradually with time. After a number of stones get displaced rapidly, the damage tends to decrease and the structure settles in and then gradually reaches equilibrium. Font (1968) stated that the duration of the waves is not important for the initial movement of the stones, but is important for advancing damage. Rogan (1968)



investigated the influence of duration of wave attack on a breakwater using regular and irregular waves to generate the destructive conditions on the breakwater cover layers. The destruction of the breakwater was formulated in terms of a risk criterion as follows.

$$\frac{t}{T} = -a \ln\left(\frac{H^2}{\nu T}\right) + b \quad [2.22]$$

where  $t$  is storm duration,  $T$  is wave period,  $H$  is wave height,  $\nu$  is kinematics viscosity, and  $a$ ,  $b$  are constants. The equation permits to determine the time  $t$  needed for the destruction of the cover layer by knowing other variables. The expression shows that the storm duration to cause total damage increases with decreasing the wave height. This expression should be applied for wave heights larger than the “no damage” wave height. Equation [2.22] can be applied to irregular waves as well by selecting  $H_s$  as the design wave height.

Ergin and Pora (1971) conducted experimental tests to study the effect of irregular waves on rubble mound breakwaters. The results show a linear increase in the damage with time, while CERC (1984) described that armour damage is independent of the storm duration. However, it is obvious that damage of the armour should increase if the wave duration increases. Design formula of van der Meer (1987, 1988) accounts for the wave duration influence on the damage inflicted to breakwaters by including the number of waves in it. This relation can be described by a square root function when number of waves  $N$  is between 1000 and 7000 waves. Meer decided using  $N$  equal to 5000 as a bench-mark to ascertain damage that would occur after 3000 waves. The relation can be written as

$$\frac{S}{S(5000)} = \frac{\sqrt{N}}{\sqrt{5000}} = 0.0141\sqrt{N} \quad [2.23]$$

Figure 2.6 is taken from van der Meer (1988) showing the parameter  $S/S(5000)$  as function the number of waves.

The relationship between damaging stability number  $S$  and number of waves  $N$  has also been reported by many authors (Medina and McDougal 1990, Teisson 1990, Smith et al. 1992, and Sakakiyama and Kajima 1996). Almost all researchers agree that wave duration is an important factor influencing the damage level, but the number of waves required to reach equilibrium profile is not yet clearly established. The number of waves,  $N$ , varies between 1000-7000.

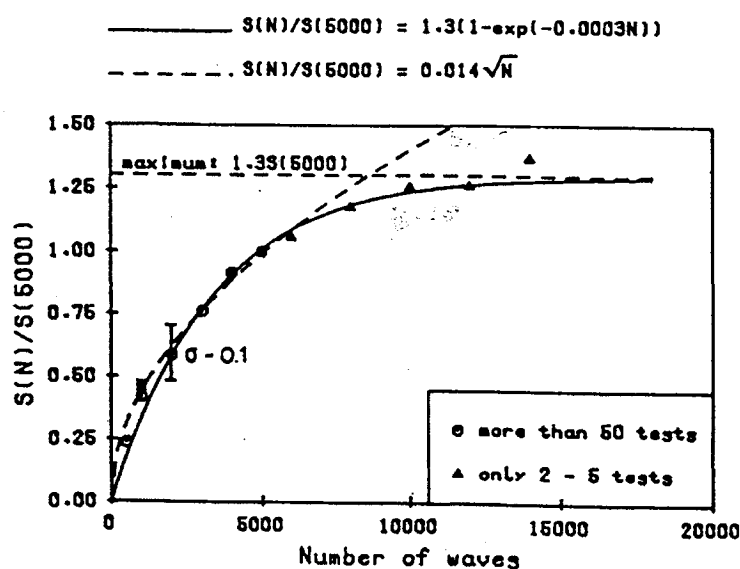


Figure 2.6. Effect of wave duration on stability (from van der Meer, 1988).

#### d. Effect of Irregular Waves

Existing design methods for rubble mound breakwaters use height of regular waves as the equivalent significant wave height to determine action of irregular waves on a rubble mound (e.g. Hudson 1959, Losada and Giménez-Curto 1979, Hedar, 1986). Researchers have questioned this assumption because the effect of isolated large waves on structural stability is not clear. A regular wave represents a different physical phenomenon than an irregular wave, and there is no relationship

between  $H$ , which represents a regular wave, and the irregular wave represented by  $H_s$  or the spectrum wave height,  $H_{mo}$ . Ergin and Pora (1971) studied the influence of irregular wave action on rubble mound breakwaters. The tests were carried out in the 2-D wave flume with a breakwater slope of 1:2 and non-overtopped conditions for all waves. Using the effective energy concept, they concluded that in place of regular wave height  $H$  and period  $T$ , wave height  $H_{1/3}$  and period  $T_m$  could be used in the design to account for an irregular wave climate. The effective energy is the summation of the individual wave energies for waves bigger than the no-damage wave height. Based on the assumption that damage on a rubble mound breakwater is caused by wave trains is proportional to the effective energy of the wave, Ergin and Pora observed that

- Irregular waves result in higher damage than caused by regular waves, and have higher effective energy for waves which are smaller than approximately 1.25 times the design wave.
- Both regular and irregular waves cause the same damage at approximately 1.25 times the design wave.
- For waves greater than 1.25 times the design wave, irregular waves have less effective energy, resulting in less damage than caused by regular waves.

A similar result in the effect of regular and irregular wave action on the stability of breakwaters was also found by Jensen et al. (1996). It was found that irregular waves more damaging than regular waves. The correspondence between the damage level for regular and irregular waves exists when normal  $H_{1/3}$  of irregular waves is considered equivalent to  $H_{1/20}$ , i.e. the effective  $H_{1/3}$  is brought down.

#### e. **Effect of Water Depth**

Walker et al. (1975) conducted two-dimensional hydraulic model study to determine the stability of back-slope of breakwater sections subject to overtopping waves. It was found that the back-slope of low crested breakwaters is more susceptible to damage than the seaward slope, as Raichlen (1972) and Magoon et al.

(1974) also have reported. Walker et al. used monochromatic waves for both breaking and non-breaking waves. The stability was composed based on displacement of 5 percent of the armor stones as an index. The result of the tests showed that two section were severely damaged for  $h_c/H = 0.57$  with  $M_b/M_f = 0.79$ , and  $h_c/H = 1.7$  with  $M_b/M_f = 0.5$ , where  $h_c/H$  is the crest height relative to wave height and  $M_b/M_f$  is back slope armour mass relative to the seaward slope armour mass. It was also found that back slope damage occurs due to internal pressures within the body of the section, impact of overtopping jet, scour of the toe by wave overtopping, and entrapment of pressure due to permeability of the crest.

Vidal et al. (1992) performed 3-D tests to analyze the stability of submerged and low crested rubble mound breakwaters. The breakwater cross section was composed of a permeable core having armoring with two layers of stones. The crest width of the structure was equivalent to  $6D_{50}$  and the slope of the structure was 1:1.5. Two different peak periods,  $T_p$ , of 1.4 and 1.8s were used and one-hour time series were synthesized using the random phase spectra method. Various zero moment wave heights were generated having values of 5 to 19cm. Four areas of breakwater sections, the front slope, the crest, the back slope and the total slope (including front slope, crest and back slope) were evaluated for their stability. They expressed the stability in terms of conventional stability number,  $N_s$ , and the normalized free board,  $F_d$ , where

$$F_d = h_c/D_{50} ; \text{ and } h_c = h_s - h \quad [2.24]$$

They found that the stability of low crested rubble mound breakwater, specifically stability of back slope, was very dependent on the freeboard. For a given water depth, incident wave characteristics, and duration of wave the damage level is a function of the stability number,  $N_s$ , and normalized free board,  $F_d$ . A design curve of the breakwater stability for each section is shown in Figure 2.7.

#### f. Effect of Permeability

The permeability of a rubble mound breakwater has a significant effect on the stability of armour layer. Permeability determines the intensity of the flow through the interstices, as well as the elevation of the water surface within the breakwater core. Impermeable breakwaters are less stable than permeable breakwaters.

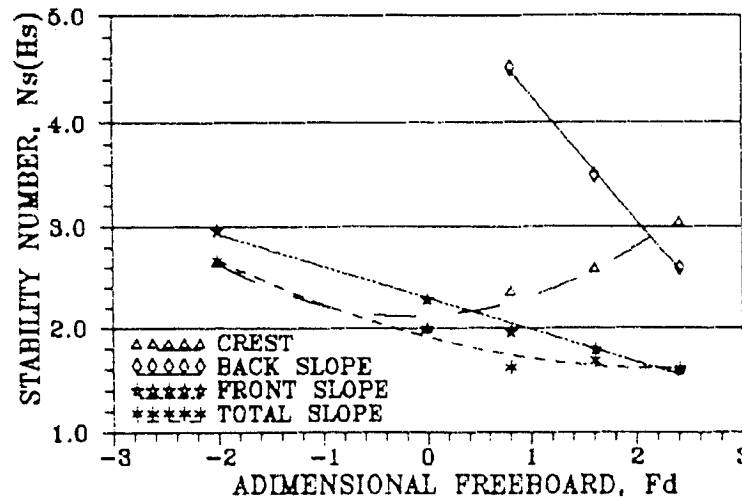


**Figure 2.7.** Stability of each section of breakwater for Irribaren Damage (from Vidal et al., 1993).

Sigurdsson (1962) conducted tests with regular waves to measure the force acting on spheres which formed the armour layer of different core materials. Two different core permeabilities were used, one impervious and another pervious. He found that the normal forces were almost the same in magnitude for both impervious and pervious cores, while Hedar (1986) and van Gent (1996) found that a permeable structure has higher stability than the impermeable structure.

#### g. Effect of Structure Slope

Hudson (1959) and van der Meer (1987, 1988) suggested design formulae taking into account the effect of structure slope. The slope of rubble mound breakwater influences the type of breaking of the wave and the necessary weight of

the stone to impart stability. Steep slopes will reduce stability compared to milder slopes. It was also reported in the work of van der Meer (1988, 1995) that in case of steeper slopes the threshold of stability decreases. It means a lower wave height causes instability for steeper slopes.

## 2.4 DAMAGE CRITERIA

In the analysis of the stability of a breakwater it is important to evolve a proper definition of damage. In the classical definition, damage has been defined as the percentage of armor units displaced from their initial place with respect to the total number of armour units used in the construction of the main layer. The term 'displacement' describes the act of the unit moving a distance greater than the overall length of the unit. This definition would be significant if the dimensions of the armour layer are standardized in the relation to the size of armour unit. Hudson (1959) defined the stability based on a 'no-damage' criteria as one in which a permissible damage by way of displacement of 1% of the armour cover layer subject to wave of certain height and 0.5 hour of duration is allowed. Other definition from van der Kreeke (1969) considers damage as the percentage of the displaced armor units with respect to the number of units contained in a strip around the still water level. This definition has no clue regarding the total damage caused to the breakwater. CERC (1984) accepts damage as a percentage of stones removed from the active zone, i.e.

$$\% \text{ Damage} = \frac{\text{number of stone displaced}}{\text{number of stone within active zone}} \times 100 \% \quad [2.25]$$

where the active zone is defined as area of breakwater from the middle of the crest down to one no-damage wave height below the still water level. The no-damage wave

height,  $H_D$ , is determined from the model armour unit using Hudson's (1959) formula in the following form.

$$H_D = \left( M_{50} \frac{K_D}{\rho_a} \cot \alpha \right)^{1/3} (S_r - 1) \quad [2.26]$$

Using this relationship, it can be seen that for waves smaller than  $H_D$ , the number of armour units actually exposed to wave action is less than the number in the active zone, as the active zone is having a constant area. Hence, actual percent damage will appear to be much smaller than permissible limit of 1% since the damage is actually concentrated in a relatively small range around the still water level. For waves larger than  $H_D$ , the percent damage will be high because the active zone is smaller than the actual area influenced by wave action.

The above damage criteria were proposed based on a number of armour units displacement. Other techniques to quantify damage level are based on the area of erosion (e.g. Ahrens, 1984, van der Meer and Pilarczyk, 1984, van der Meer, 1987 and 1988) and by visual assessment (Vidal et al., 1991). Ahrens (1984) divided types of breakwater damage into two categories in order to quantify the stability of reef breakwaters. First is volumetric damage. This type of damage is defined as the number of stones moved from their original place to another place. The second category is the reduction of the crest height of structure under wave attack. He introduced two dimensionless variables to define the two aspects of stability. These two variables are the relative crest height,  $h'_s/h$ , and the dimensionless damage,  $D'$ . The dimensionless damage,  $D'$ , is defined as

$$D' = \frac{A_e}{(W_{50}/W_a)^{2/3}} \quad [2.27]$$

where  $A_e$  is area of erosion,  $W_a$  is weight of armour. Note that  $D'$  is a measure of the number of stones remove from the damage area.

Van der Meer and Pilarczyk (1984) applied a dimensionless damage parameter in their rubble mound breakwater tests in order to describe the stability of the structure in the following form.

$$S = \frac{A_e}{(D_{50})^2} \quad [2.28]$$

where  $A_e$  the area of erosion. A physical interpretation of this equation is that  $S$  indicates the number of squares of stones with the average diameter,  $D_{50}$ , that fit into the eroded area. Using this measure,  $S \leq 2$  was considered as 'no-damage'. The no-damage criterion as proposed by Hudson (1959) is taken in the range of  $S$  between 1 and 3.

In visual assessment, Vidal et al. (1991) proposed four different degree of armour damage. These are initiation of damage (ID), Irribaren's damage (IR), start of destruction (SD) and destruction (D). Initiation of damage is defined as the condition when a certain number of armor units are moved from their original position to another place with distance equal to or larger than nominal diameter. Irribaren's damage is defined as the condition when the extent of the failure of the outer armor layer is large enough for waves to attack the lower layer that will be cause units to displace. Start of destruction is defined as the condition when a small number of units of the second layer are displaced. Finally, destruction defined as the condition when the filter layer is removed by wave attack. It was found that for initiation of damage and Irribaren's damage, some 3-D test sections started to fail earlier than 2-D sections. For the smaller wave heights, 2-D test section reaches the destruction level of damage earlier than 3-D test sections.



## 2.5 WAVE TRANSMISSION AND REFLECTION

The design of low crested coastal structures requires that the expected amount of wave transmission and reflection be determined with confidence. Wave runup and overtopping of the structures will cause wave transmission. There is a decrease in the transmitted energy because of reflection and dissipation of some of the transmitted wave energy. The wave transmission coefficient,  $K_t$ , is defined as

$$K_t = \sqrt{\frac{E_t}{E_i}} \quad \text{or} \quad K_t = \frac{H_t}{H_i} \quad [2.29]$$

where  $H_t$  is the zero-moment transmitted wave height, and  $H_i$  is the zero moment incident wave height. Another important parameter, the reflection coefficient is defined as (Goda and Suzuki, 1976)

$$K_r = \sqrt{\frac{E_r}{E_i}} \quad [2.30]$$

where  $E_r$  is the reflected wave energy and  $E_i$  is the incident wave energy of the spectrum.

The behaviour of many types of breakwaters in transmission and reflection was examined by many researchers in different ways; bring many results and expressions (e.g. Dick and Brebner 1968, Ahren and Mc Cartney 1975, Dattatri et al. 1978, Bade and Kaldenhoff 1980, Abdul Khader and Rai 1980, Seelig 1980, Alssop 1983, van der Meer 1991 and van der Meer and Daemen 1994). Most of the results suggested that water depth and structure geometry are the most significant parameters affecting wave transmission. Wave characteristics (wave height and period) and structure permeability was also found to affect wave transmission. In wave reflection, results show that water depth and wave characteristics are the significant parameters.

Slope of structure and diameter of armour units also found to be affecting wave reflection.

### 2.5.1 Predictive Equations for Wave Transmission

Seelig (1980) performed a comprehensive test for wave transmission on rubble mound breakwaters. He proposed the following equation to estimate the wave transmission coefficient.

$$K_t = \sqrt{(K_t)_o^2 + (K_t)_p^2} \quad [2.31]$$

where  $K_t$  is the total value of the coefficient,  $(K_t)_o$  is transmission coefficient due to overtopping and  $(K_t)_p$  is transmission coefficient due to penetration through the breakwater body. The wave transmission over the crest due to overtopping is given as

$$(K_t)_o = c \left( 1 - \frac{h_c}{R_u} \right) \quad \text{for } 0 \leq (K_t)_o \leq 1 \quad [2.32]$$

where

$R_u$  is run-up height,

$$c = 0.51 - \frac{0.11B}{(h_s)}$$

Seelig also proposed a formula to predict the runup height as

$$\frac{R_u}{H} = \frac{0.692\xi}{1 + 0.504\xi} \quad \text{where } \xi = \tan \alpha / \sqrt{H/L_o} \quad [2.33]$$

Van der Meer (1991) and van der Meer and Daemen (1994) presented a linear relationship between wave transmission coefficient,  $K_t$ , and the relative crest height,  $h_c/D_{50}$ . The relationship is as follows.

$$K_t = a \frac{h_c}{D_{50}} + b \quad [2.34]$$

with

$$a = 0.031 H_i / D_{50} - 0.24 \quad [2.35]$$

Equation [2.34] can be applied for conventional and reef type breakwaters. Further, The coefficient b for conventional breakwaters is given by

$$b = -5.42s_{op} + 0.0323 \frac{H_i}{D_{50}} - 0.0017 \left( \frac{B}{D_{50}} \right)^{1.84} + 0.51 \quad [2.36]$$

whereas, for reef type breakwaters, coefficient b is defined by

$$b = -2.6s_{op} - 0.05 \frac{H_i}{D_{50}} + 0.85 \quad [2.37]$$

The above formula is reported to be valid for

$$1 < \frac{H_i}{D_{50}} < 6 \quad \text{and} \quad 0.01 < s_{op} < 0.05$$

Seabrook and Hall (1998) and Hall and Seabrook (1998) found that van der Meer's relationship does not remain within acceptable physical limits of  $K_t$ . A wide range of crest widths cannot be accounted for by this relationship. They introduced an improved design equation defining the transmission process for submerged breakwaters. This equation represents the effect of wave breaking, wave overtopping, frictional losses and internal flow losses and is as follows.

$$K_t = 1 - \left\{ e^{-0.65 \left( \frac{-h_c}{H_i} \right) - 1.09 \left( \frac{H_i}{B} \right)} + 0.047 \left( \frac{-Bh_c}{L_p D_{50}} \right) - 0.067 \left( \frac{-H_i h_c}{B D_{50}} \right) \right\} \quad [2.38]$$

where  $H_i$  is the incident  $H_{mo}$  value and  $L_p$  is the wave length at the local depth. Limits for application of the equation are

$$0 \leq \frac{-Bh_c}{L_p D_{50}} \leq 7.08 \quad \text{and} \quad 0 \leq \frac{-H_i h_c}{B D_{50}} \leq 2.14.$$

### 2.5.2 Predictive Equations for Wave Reflection

Seelig (1983) presented a method for predicting wave reflection coefficients on a variety of typical coastal structures. The wave reflection coefficient is given in terms of  $\xi$  as

$$K_r = \frac{a_1 \xi^2}{\xi^2 + b_1} \quad [2.39]$$

where  $a_1$  is equal 0.6 and  $b_1$  is equal 6.6. Equation [2.39] indicates that factors affecting wave reflection include wave period, wave height and slope of structure implicitly as represented by  $\xi$ . Seelig also pointed out that wave reflection from porous structures is a function of the water depth in front of the toe ( $h$ ), beach slope, the characteristic diameter of armour units ( $D_{50}$ ) and number of armour layer. A similar equation by Allsop (1990) representing wave reflection shows good agreement with Equation [2.39] for two armour layers wherein the values of  $a_1$  is 0.64 and  $b_1$  is 8.85.

Davidson et al. (1996a), based on the full-scale data of rock island breakwaters, derived an equation to parameterize wave reflection in term of a dimensionless reflection number  $R$  and expressed it as

$$K_r = \frac{0.635\sqrt{R}}{41.2 + \sqrt{R}} \quad \text{or} \quad K_r = 0.151R^{0.11} \quad [2.40]$$

and

$$R = \frac{L_o^2 h \tan \alpha}{H_i D_{50}^2} = \xi \left( \frac{L_o^{1.5} h}{D_{50} H_i^{0.5}} \right) \quad [2.41]$$

The dimensionless reflection number  $R$  gives weight ages to the wave height and wave length. Its also includes other important physical parameters such as water depth and armour diameter. The equation was reported to predict well wave reflections for the full-scale case, while poor predictions resulted for laboratory conditions. The discrepancies may be due to the limited parameter-space of the data used.

## 2.6 WAVE ENERGY DISSIPATION

Energy dissipation on a rubble mound breakwater is a complex phenomenon on wave-structure interaction. Theoretical analysis of this problem generally involves a number of simplifying assumptions; such as the cross section of the breakwater is rectangular rather than trapezoidal (Madsen and White, 1976a). Prediction of wave transmission through the body and reflection from porous rubble mound breakwaters was developed by Madsen and White (1976b). They found that the most important parameter affecting energy dissipation is the friction factor. To support their theoretical analysis, a simple experimental investigation was also conducted.

Muttray et al. (1992) tested the wave energy dissipation in rubble mound structures. Various layers of an accropode armoured the breakwater that was attacked by regular and irregular waves. The dissipated energy was found to decrease when the

wave period started increasing. Single armour layer dissipated less wave energy than double armour layers. As expected, it was also found that the wave energy dissipation is stronger in the outer layer than in the filter layer.

## 2.7 CONCLUDING REMARKS

Wave-structure interaction and stability of coastal structures have been studied mostly in physical modeling involving large number of governing variables. In structural stability, wave height, period, water depth, structure geometry and material properties are the important parameters. Initially regular waves were applied. With ability to generate irregular waves in the model facilities, most investigations are then concerned under this type. However, many design formulae are still based on regular waves (e.g. Hudson 1959, Losada and Giménez-Curto 1979 and Hedar 1986). Most of the design formulae presented here are based on tests involving a limited range of variables and of an empirical nature. Hence, should be used cautiously within their range of validity. For example, Hudson's (1959) formula was derived based on tests under regular waves and non-overtopped conditions. The choice of the coefficient  $K_D$  of his formula may be difficult. Van der Meer (1988) introduced permeability factor  $P$  on his stability formulae. This permeability coefficient has no physical meaning, but was introduced to ensure that permeability is taken into account. The use of this coefficient for different condition may give different results.

With respect to wave-structure interaction (i.e. wave transmission and reflection), past research efforts have adequately addressed this issue. Since of the complex nature of most wave transmission and reflection processes, techniques for the prediction of these processes rely heavily on empirical studies that are conducted in the laboratory or the field. Techniques for predicting wave transmission and reflection usually in the form of a transmission and reflection coefficient  $K_t$  and  $K_r$ , respectively. Many empirical or semi-empirical formulae have been developed from a

limited range of variables involved and have led to either an unsafe or conservative design of the structures. It is, however, important to note that the empirical expressions are to day as popular as ever, mainly due to their simplicity and their ability to provide reasonably accurate estimates. At the same time, these expressions also should be used cautiously and within their domain of applicability. A summary of the principal findings of the previous investigations is given in Table 2.1.

**Table 2.1.** A summary of the previous investigations

Reference	Structure Types	Slope ( $\cot \alpha$ )	Wave types	Testing Types
Ahrens (1980)	Revetment	1.5 – 2.5	Irregular	2-D
Ahrens and Seelig (1980)	Revetment	2.0	Irregular	2-D
Dattatri et al. (1978)	Submerged breakwaters	Vertical-trapezoidal	Regular	2-D
Hudson (1959)	Breakwaters	1.25 – 5.0	Regular	2-D
Seabrook (1997)	Submerged breakwaters	1.5 – 5.0	Regular, Irregular	2-D and 3-D
Seelig (1980)	Breakwaters	1.5 – 2.6	Regular, Irregular	2-D
Seelig and Ahrens (1981)	Revetment	2.5, 15.0	Regular, Irregular	2-D
Vidal et al. (1992)	Breakwaters	-	Irregular	3-D
Van der Meer (1991)	Low-crested breakwaters	-	Irregular	2-D

There thus is still a need for an investigation that attempts to adequately observe and predict the performance characteristics of breakwaters. A physical model provides a relatively easy way of modeling the structures and its loads for a large number of variables involved in the processes, using a small-scale model. It was decided, therefore, to conduct physical tests over a wider range of input variables for the present study.

## Chapter 3

# THEORETICAL BACKGROUND

### 3.1 INTRODUCTION

The main objective of this thesis is to study wave transmission, reflection and stability of shore protection systems in coastal areas subject to storm surge. Since physical modeling will be adopted as the method of analysis of this subject, a brief review of the hydraulics of modeling will be presented. As the relationships between test variables will be described in dimensionless forms, it is important to review the theory of dimensional analysis. The external stability of a breakwater deals primarily with the stability of the armour layer. The stability of the units of armour is dependent upon both the characteristics of the breakwater and the load acting on it. The load acting on a breakwater is primarily caused by waves. Hence, a brief description of the wave forces acting on a breakwater and the wave characteristics for a simple sinusoidal oscillatory wave will be presented.

The following sections deal first with the description of the wave characteristics of irregular type. Following this, wave-structure interactions and structural stability of breakwater is discussed. Wave-structure interaction modeling and dimensional analysis are described in Sections 3.5 and 3.6, respectively.

### 3.2 WAVE CHARACTERISTICS

Usually, irregular waves should be considered for design formulae related to breakwaters since they reflect a better representation of the naturally occurring



random sea state. The wave height parameter for irregular waves is characterized by the significant wave height,  $H_s$  (van der Meer, 1987, 1988) where  $H_s$  is the average height of the highest 33% of waves in a given record. CERC (1984) recommends using the average height of the highest 10% of waves ( $H_{1/10}$ ) or  $H_{1/20}$  instead of significant wave height for non-breaking conditions, while Vidal et al. (1995) recommends using  $H_{1/30}$ .

This section describes briefly the wave characteristics such as wave energy spectrum, wave height and wave period, which are usually used in the design calculations of coastal structures. Common expressions for waves based on linear wave theory are presented in Appendix A.

### 3.2.1 Wave Height Distribution

The primary forces on structures are due to the action of waves and the most common waves are generated by winds. Wave characteristics are usually random. To describe the wave characteristics such as the wave height, the wave period, celerity, etc., statistical methods can be used. As described previously, several wave height parameters can be used to characterize the wave sea state such as  $H_{1/3}$  or significant wave height  $H_s$ , and the maximum wave height,  $H_{max}$ .

Commonly the Rayleigh distribution is used to determine the probability of distribution of wave heights. This theoretical distribution function is based on the assumption of random phase and a narrow spectrum (Dean and Dalrymple, 1984). The probability distribution function of heights exceeding a given wave height can be written as

$$P(H) = \exp\left[-2\left(\frac{H}{H_s}\right)^2\right] \quad [3.1]$$

If a record contains  $N$  waves and  $n$  ( $\leq N$ ) waves exceed a given wave height  $H$ , the probability of exceedance is  $n/N$  so that

$$H_s = \frac{H}{\left[ \frac{1}{2} \ln \frac{N}{n} \right]^{1/2}} \quad [3.2]$$

For  $n = 1$ , the probable of maximum wave height in a record of  $N$  waves becomes

$$H_{\max} = H_s \left[ \frac{\ln(N)}{2} \right]^{1/2} \quad [3.3]$$

The following approximations can be made based on the Rayleigh distribution, according to Muir-Wood (1981).

$$H_s \approx 1.60\bar{H};$$

$$H_s \approx 1.41H_{\text{rms}};$$

$$H_{1/10} \approx 1.28H_s;$$

$$H_{1/100} \approx 1.68H_s;$$

$$H_{\max} \approx 1.80H_s.$$

where  $H_{\text{rms}}$  is the root mean square of the wave height,  $\bar{H}$  is the average wave height and fractions 1/10, 1/100 define the highest 10% and 1% of waves.

### 3.2.2 Wave Energy Spectrum

The wave energy spectrum is used to express the linear statistical properties of a wind generated wave surface. Several types of spectrum are available for the design of offshore structures. There are various theoretical frequency spectra describing ocean waves. The Pierson-Moskowitz (PM) and the JONSWAP spectrum, two of the commonly used spectra are presented below.

The wave energy spectrum is usually plotted as energy density  $S(f)$  versus the wave frequency  $f$ . The energy density of a wave is given by  $\rho g H^2 / 8$ . Figure 3.1 shows a schematic frequency spectrum. It can be seen that the shape of a wave

spectrum has a tail reach and an upper limit; however the exact shape of the spectrum will depend on many factors such as the wind speed and position of the observation station within the fetch (Sorensen, 1993). Fetch is the unhindered distance the wind blows over the water to generate waves.

- a. The Pierson-Moskowitz spectrum (1964): This is one of the most popular distributions and is given as:

$$S(f) = \frac{\alpha_p g^2}{(2\pi)^4 f^5} \exp\left(\frac{B_1}{f^4}\right) \quad [3.4]$$

where

$S(f)$  = spectral density,

$f$  = frequency,

$\alpha_p$  = Phillips' constant = 0.0081

$B_1$  =  $-0.74[g/(2\pi U)]^4$ ,  $U$  being wind speed,

$g$  = gravitational acceleration

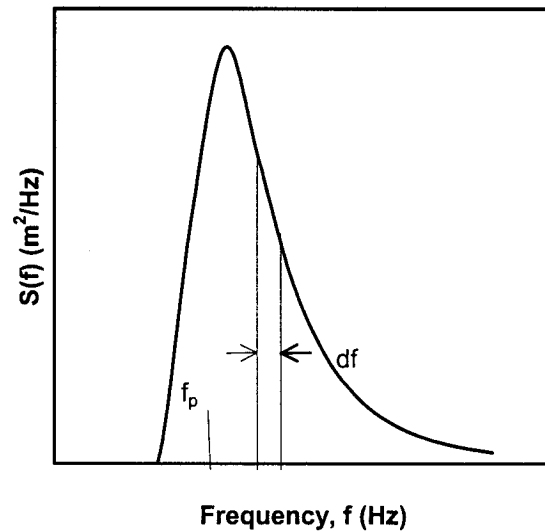


**Figure 3.1.** A schematic frequency spectrum.

From the above equation it can be seen that Pierson-Moskowitz (PM) spectrum is dependent only on the wind speed  $U$ . This spectrum is applicable to fully developed conditions, where the water depth, wind duration and fetch are unlimited. Ochi (1982) stated that for fully developed seas, there would be a distinct dependence of the significant height and peak period on the wind speed  $U$ . The relationships are given below.

$$H_{mo} = \frac{0.21U^2}{g} \quad [3.5]$$

$$f_p = \frac{0.87g}{2\pi U}, \text{ } f_p \text{ is the peak frequency} \quad [3.6]$$

Combining Equations [3.4] and [3.6] by eliminating  $U$ , the Pierson-Moskowitz spectrum can be rewritten as follows as a frequency dependent quantity.

$$S(f) = \frac{\alpha g^2}{(2\pi)^4 f^5} \exp\left[-\frac{5}{4}\left(\frac{f_p}{f}\right)^4\right] \quad [3.7]$$

b. The JONSWAP spectrum (Hasselmann et al., 1973)

The JONSWAP spectrum is derived from the JOint North Sea WAVE Project by Hasselmann et al. (1973) to account for the effect of fetch restrictions and provide a much more peaked spectrum. The spectrum is described by

$$S(f) = \frac{\alpha_p g^2}{(2\pi)^4 f^5} \exp\left[-\frac{5}{4}\left(\frac{f}{f_p}\right)^{-4}\right] \gamma^{\exp\left[\frac{(f-f_p)^2}{2\sigma^2 f_p^2}\right]} \quad [3.8]$$

$$\sigma = \begin{cases} 0.07 & \text{for } f < f_p \\ 0.09 & \text{for } f \geq f_p \end{cases} \quad [3.9]$$

$$\alpha_p = 0.076 \left( \frac{gF}{U^2} \right)^{-0.22} \quad [3.10]$$

$$f_p = \frac{3.5g}{U} \left( \frac{gF}{U^2} \right)^{-0.33} \quad [3.11]$$

where  $S(f)$  is the spectral density,  $\alpha_p$  is the Philips constant,  $g$  is the acceleration of gravity,  $\gamma$  is the ratio of the maximum spectral energy or the spectral peak shape factor to the maximum of the corresponding Pierson-Moskowitz spectrum (1964) with the same value of  $\alpha_p$  and  $f_p$ ,  $f_p$  is the peak frequency and  $F$  is the fetch length. The value of  $\gamma$  (commonly named JONSWAP spectrum parameter) specifies the width of the frequency spectrum and ranges from about 1.6 to 6 with a recommended value of 3.3. Small values of the spectrum give broad peaks and large values of the spectrum give narrow peaks. The Philips' (1958) constant number and peak frequency vary considerably with the fetch and wind speed. These indicate that the growth of wave energy,  $S(f)$ , is proportional to  $\alpha_p$  and peak frequency, which in turn depends on the wave length corresponding to the spectral peak. For  $\gamma$  equal 1 and  $\alpha_p=0.0081$ , the JONSWAP spectrum reduces to the Pierson-Moskowitz spectrum. Figure 3.2 shows the superimposed JONSWAP and Pierson-Moskowitz spectra by letting  $f=f_p$  in the JONSWAP spectrum. It shows the significance of  $\gamma$ , the ratio of the magnitude of the JONSWAP spectral peak to the Pierson-Moskowitz spectral peak.

For wave synthesis, the spectrum is usually specified by  $\gamma$ ,  $f_p$  and significant wave height,  $H_s$ . The choice of  $\gamma$  in ascertaining the shape of the wave energy spectrum is important for a number of engineering applications. A low peak of the input wave spectrum may result in an underestimation of the forces on a structure corresponding to the peak frequency (Rye, 1977).

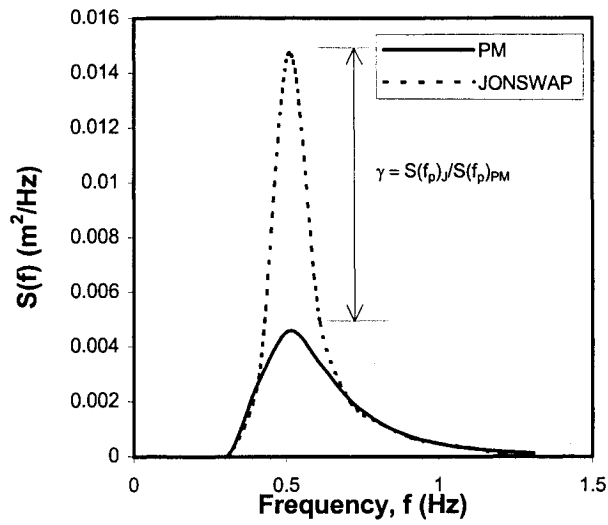


**Figure 3.2.** Comparison of Pierson-Moskowitz and JONSWAP spectra.

### 3.2.3 Parameters Derived from the Wave Spectrum

The moments of a wave spectrum are important in characterizing the spectrum. The moments of the wave spectrum are defined as

$$m_n = \int_0^{\infty} S(f) f^n df \quad n = 0, 1, 2, \dots \quad [3.12]$$

The zero moment ( $n = 0$ ) is therefore the area under the spectral curve  $S(f)$ , which is equal to total energy of the spectrum and is defined as

$$m_0 = \int_0^{\infty} S(f) df = \sigma^2 \quad [3.13]$$

where  $\sigma$  is standard deviation of water surface position.

The spectral shape parameters  $\varepsilon$ ,  $\nu$  and  $Q_p$  are often used in order to describe the shape or narrowness of spectrum. Parameter  $\varepsilon$  is the spectral bandwidth or broadness factor and is defined as

$$\varepsilon^2 = 1 - \frac{m_2^2}{m_0 m_4} \quad [3.14]$$

where  $m_0$ ,  $m_2$  and  $m_4$  are the zero, second and fourth moments of the wave spectrum. This parameter was introduced by Cartwright and Longuet Higgins (1956) in order to describe the width of a spectrum. The value of  $\varepsilon = 0$  represents a narrow frequency spectrum while  $\varepsilon \sim 1$  represents a wide band spectrum.

Subsequently, Longuet-Higgins (1975) introduced the parameter spectral width  $\nu$  to describe the narrowness of a spectrum. This parameter is defined as

$$\nu^2 = \frac{m_2 m_0}{m_1^2} - 1 \quad [3.15]$$

where  $m_0$ ,  $m_1$  and  $m_2$  are the zero, first and second moments of the wave spectrum, ranging from 0 to 1.

A spectral peakedness parameter,  $Q_p$ , was introduced by Goda (1974) to describe the peakedness of a wave spectrum. This parameter is defined by

$$Q_p = \frac{2}{m_0^2} \int_0^{\infty} f[S(f)]^2 df \quad [3.16]$$

which depends only on the first moment of the density spectrum. Generally a small  $\varepsilon$  implies a large  $Q_p$ , and a large  $\varepsilon$  implies a small  $Q_p$ . The value of  $Q_p$  varies from 1 to 2 for wind waves and greater than 2 for swells.

### 3.2.4 Wave Groups

Although the waves may look very random, inspection of wave records and observation of ocean waves show that large waves occur in groups rather than individually. The concept of wave group formation helps to describe the variation of wave energy in a wave train of irregular waves. A wave group can be defined as a superimposition of two or more waves exceeding some specified height such as  $H_s$  but having almost the same period. The superimposed waves are commonly known as a wave run and the number of waves in it is the run length. The number of waves between the first wave run and the one following it is the total run of waves. The wave group consists of a series of individual waves that increase in size and then decrease. When two wave trains have the same height with slightly different frequencies and wave number, their propagation in the same direction results in a new profile. This profile propagates with a velocity called the group velocity,  $C_g = \Delta\sigma/\Delta k$  (Rahman, 1995), where  $\sigma$  is wave angular frequency, and  $k$  being the wave number ( $= 2\pi/L$ ). In the limit as  $\Delta k \rightarrow 0$ ,  $C_g = d\sigma/dk$ . Using the dispersion relationship,  $\sigma^2 = gk \tanh kh$ , the group velocity can be expressed as  $C_g = nC$ , where

$$n = \frac{1}{2} \left( 1 + \frac{2kh}{\sinh 2kh} \right); \quad [3.17]$$

In deep water, the value of  $n$  is equal to  $1/2$ , while in shallow water,  $n$  is equal to 1. Therefore in deep water, a group of waves will propagate at half the velocity of the individual waves, and in shallow water the group of waves and the individual wave profiles travel at the same velocity.

Funke and Mansard (1980) defined the groupiness in terms of the Smoothed Instantaneous Wave Energy History (SIWEH),  $E(t)$ , as follows

$$E(t) = \frac{1}{T_p} \int_{-\infty}^{\infty} \eta^2(t + \tau) Q(\tau) d\tau \quad [3.18]$$



where:

$$\begin{aligned} \tau &= \text{time lag.} \\ \eta &= \text{water level variation.} \\ Q(\tau) &= \text{Bartlett window.} \\ Q(\tau) &= 1 - |\tau|/T_p \quad \text{for } -T_p \leq \tau \leq T_p \end{aligned}$$

From the SIWEH, the groupiness factor (GF) is defined as

$$GF = \frac{\sqrt{\frac{1}{T_R} \int_0^{T_R} (E(t) - s^2)^2 dt}}{s^2} \quad [3.19]$$

where

$$s^2 = \frac{1}{T_R} \int_0^{T_R} E(t) dt \quad [3.20]$$

$T_R$  is the record length and  $s$  is the square root of the smoothed instantaneous wave energy history  $E(t)$ . The groupiness factor is the standard deviation of the SIWEH about its mean and is normalized with respect to this mean. The groupiness factor concept is a preferred method of describing grouped waves because this approach allows researchers to synthesize time series with different degrees of grouping, while maintaining the frequency domain characteristics of the variance spectral density distribution. At present there is no technique, which utilizes run length statistics in a simulation. For review of wave grouping parameters and analysis that is commonly used, one can refer to Medina and Hudspeth (1990).

The stability of armour units on a rubble mound breakwater has been shown to be influenced by the characteristics of wave groupiness (Medina et al. 1990). The characteristics of wave grouping that influence the damage of rubble mound breakwaters are the mean wave run length and the groupiness factor, GF, as defined by Funke and Mansard (1980). Medina et al. (1990, 1994) proposed that the envelope

exceedance coefficient ( $\alpha_m$ ) and groupiness factor (GF) are parameters that can be used to describe wave group characteristics affecting the stability of the armour layer.

### 3.2.5 Wave Height and Wave Period

Because of the randomness of waves in nature and the complex transformations that occur through refraction, shoaling and diffraction, it is difficult to choose wave conditions appropriate for the design of rubble mound structures. A wave condition characterization that has been applied extensively is the significant wave height,  $H_s$ , and the peak wave period,  $T_p$ . The term significant wave height is usually denoted as  $H_{1/3}$  or  $H_{mo}$ , depending on the origin. The significant wave height  $H_{1/3}$  is typically estimated from wave records using zero-crossing analysis or by hindcasting based on meteorological conditions and defined as the average height of the highest one-third of the individual waves. However, the significant wave height  $H_{mo}$  is related to the total energy density as given by the zero moment of the wave spectrum. To distinguish between significant wave heights estimated from time domain analysis and from frequency analysis, the term characteristic wave height,  $H_{ch}$ , is used as defined by

$$H_{ch} = H_{mo} = 4\sqrt{m_0} = 4\sigma \quad [3.21]$$

Quite often  $H_{mo}$  and  $H_{1/3}$  are used interchangeably, although they may differ slightly. Thompson and Vincent (1985) found that in deep water  $H_{1/3}$  and  $H_{mo}$  are about equal, however, as the wave propagates into shallow water and wave steepness increases,  $H_{1/3}$  become larger than  $H_{mo}$  due to shoaling. The following equation may be used to equate  $H_{1/3}$  from energy-based wave parameters (Hughes and Borgman, 1987):

$$\frac{H_{1/3}}{H_{mo}} = \exp \left[ C_0 \left( \frac{h}{gT_p^2} \right)^{-C_1} \right] \quad [3.22]$$

where

- $C_0, C_1$  = regression coefficients given as 0.00089 and 0.834, respectively,
- $h$  = local water depth (i.e. toe of structure),
- $g$  = gravity acceleration,
- $T_p$  = peak period of energy density of the wave spectrum.

The wave height in a random sea state can be described by the Rayleigh probability distribution as described in section 3.2.1. Theoretically, the highest waves will generate the highest wave forces on the structure that might cause instability of the armour units. Since many structures are situated in shallow water, the highest waves can break in front of the structure thereby reduce the wave forces on it.

The peak period,  $T_p$ , is usually used to represent the wave period in the spectrum and can be obtained by differentiating the wave spectrum equation and equating it with zero i.e.

$$\frac{d}{df}[S(f)] = 0 \quad [3.23]$$

This period corresponds to the frequency associated with the maximum energy density in the wave spectrum.

### 3.3 WAVE-STRUCTURE INTERACTION

In nature, as a wave propagates towards the coastline, change will occur when they interact with various coastal structures or beaches. The transformations that usually occur during wave-structure interaction, especially offshore breakwaters, are wave refraction and diffraction, wave reflection and runup as well as wave overtopping and transmission past structures. In general, the interaction of wave-structure during wave propagation can be explained by the following mechanisms.

When the waves reach the front face of the structure, a part of the wave energy will be reflected by the front slope of the structure, while the rest will cause waves to break and transmit energy. On reaching the specific breaking depth, they will break, runup, and overtop the structure if the runup is sufficiently high. The wave overtopping and reaching the leeside of the breakwater regenerates waves that have different wave periods than the incident waves. For permeable structures, the wave energy may also propagate through the structure and interact with the waves regenerated by wave overtopping.

Following the above discussion, the wave transformation elements that are most pronounced at structures can be listed as wave reflection, wave energy dissipation, generation of wave harmonics, wave runup/rundown and wave overtopping. These components are intimately related to transmission of energy across coastal structures. Wave transmission occurs in conjunction with runup and overtopping while energy dissipation occurs through wave breaking, turbulence, generation of eddies and friction on the surface of the structure. The amount of wave reflection, wave dissipation, and wave transmission depends on wave characteristics such as wave period, wave height, and water depth; type of structures such as permeable or impermeable, smooth or rough slope; and structural geometry such as slope of structures, elevation and width of crest. This section describes in general the various wave transformations at structures.

### **3.3.1 Wave Reflection**

Wave reflection is a process of transferring energy from one direction of movement to another direction when the incident wave is intercepted by a structure. A part or all of the incident wave energy gets reflected by the structure and moves out into the sea. The reflected wave energy has been found to be strongly dependent on the depth of submergence in case of submerged breakwaters (Ahrens 1987, van der Meer 1991). It has been observed that the slope of the structure has no significant influence on wave reflection (Datattri et al., 1978).

As described in the previous chapter, the reflection coefficient is defined as (Goda and Suzuki, 1976)

$$K_r = \sqrt{\frac{E_r}{E_i}} \quad [3.24]$$

where  $E_r$  is the reflected wave energy and  $E_i$  is the incident wave energy of the spectrum. This coefficient can vary from 1 for total reflection to zero for no reflection. The reflection coefficient can also be determined from the envelope of wave records using the relationship

$$K_r = \frac{H_{\max} - H_{\min}}{H_{\max} + H_{\min}} \quad [3.25]$$

where  $H_{\max}$  and  $H_{\min}$  are the maximum and minimum wave height of the wave envelope.

Battjes (1974) presented an equation for smooth slopes using observations of Hunt (1959) and rewrote it in the form

$$K_r = 0.1\xi^2 \quad [3.26]$$

This equation is plotted in Figure 3.3, which is reproduced from Battjes (1974). From this figure it can be seen that full reflection occurs for a value of  $\xi$  equal or greater than 3.2. It may be noted that  $\xi$  is based on the incident wave characteristics. Seelig (1983) proposed a similar equation to predict wave reflection in relation to surf similarity parameter from deepwater conditions.

$$K_r = \frac{a\xi^2}{b + \xi^2} \quad [3.27]$$

with:  $a = 1.0$  and  $b = 5.5$  for smooth slopes,  
 $a = 0.6$  and  $b = 6.6$  for rough permeable slopes.

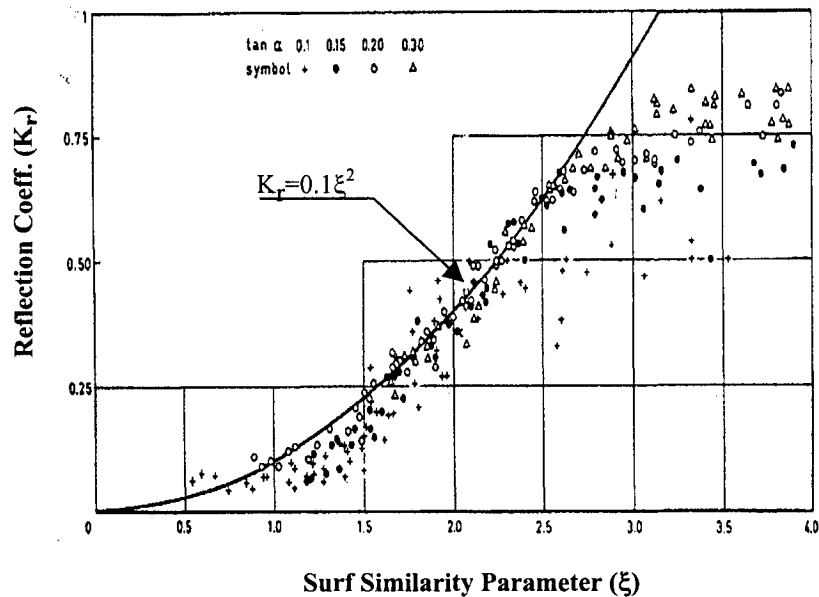


**Figure 3.3.** Reflection coefficient as function of surf similarity parameter,  $\xi$ . (from Battjes, 1974).

### 3.3.2 Wave Runup/rundown

Wave runup is an important parameter that affects the overtopping of coastal structures. The runup,  $R_u$ , of a wave on a slope is defined as the maximum vertical rise of the water above the still water level. The runup phenomenon on a slope is complex since it is affected by the occurrence of preceding and following waves. In general, wave runup also depends on the characteristics of the coastal structures such as the slope, roughness and porosity. Of course, the wave characteristics such as the wave height, wave period, wave duration and the shape of spectrum play a significant role on the wave runup.

Most techniques presently available to predict the runup of irregular waves are empirical or semi-empirical. However, numerical models have also been developed

by Wuryanto and Kobayashi (1993) for one-dimensional flow and by van der Meer et al. (1992) for the two-dimensional case. All computational methods require parameters that have to be defined precisely, thereby reducing their application domain in practice.

Prediction of runup on permeable and impermeable structures has been made by van der Meer and Stam (1992). The formula was derived based on physical scale-models and presented as a function of the surf similarity parameter,  $\xi_m$ . For impermeable structures, runup is defined as

$$\frac{R_{ux}}{H_s} = a\xi_m \quad \text{for } \xi_m < 1.5 \quad [3.28]$$

$$\frac{R_{ux}}{H_s} = b\xi_m^c \quad \text{for } \xi_m > 1.5 \quad [3.29]$$

and for permeable structures, runup is defined as

$$\frac{R_{ux}}{H_s} = d \quad [3.30]$$

in which  $R_{ux}$  refers to the runup level exceeded by  $x\%$  of the runup heights,  $H_s$  is the significant wave height at the toe of the structures,  $\xi_m$  is the surf similarity based on the mean wave period,  $T_m$ , and  $a$ ,  $b$ ,  $c$ ,  $d$  are empirical coefficients obtained from the laboratory data through the least square analysis as given in Table 3.1.

Runup has an important role for non-submerged breakwaters, and in particular it can affect the energy transmission process for low-crested structures due to overtopping. However, the runup has not been explicitly studied in the present investigation and its role is implicitly included in the analysis of transmission coefficient  $K_t$ .

**Table 3.1.** Runup coefficients proposed by van der Meer and Stam (1992).

Runup levels (%)	a	b	c	d
0.13	1.12	1.43	0.55	2.58
1	1.01	1.24	0.48	2.15
2	0.96	1.17	0.46	1.97
5	0.86	1.05	0.44	1.68
10	0.77	0.94	0.42	1.45
Significant	0.72	0.88	0.41	1.35
Mean	0.47	0.60	0.34	0.82

### 3.3.3 Wave Transmission

Wave transmission at rubble mound breakwaters may be caused by wave overtopping and runup at the structure. This phenomenon is affected by many factors such as crest width, water depth, slope angle, porosity and nominal diameter of rubble mound. Wave overtopping and runup result in wave transmission by the regeneration of waves on the leeside of the structure. If the structure is sufficiently permeable, the transmission also occurs by penetration of wave energy through the structure. The transmitted wave is likely to be more complex than the incident wave since a part of the wave may break on the structure and generate waves with different periods than that of the incident wave, while another part of the wave passes over the structure.

Since the wave transmission process is complex, the prediction of wave transmission is usually based on empirical studies. The level of wave transmission is generally represented by a transmission coefficient,  $K_t$ , and defined in terms of the incident wave height,  $H_i$ , and transmitted wave height,  $H_t$ , as,

$$K_t = \frac{H_t}{H_i} \quad [3.31]$$

### 3.3.4 Wave Energy Dissipation

Wave energy dissipation at coastal structures occurs primarily through wave breaking and friction on the surface of the structure. Wave breaking can occur both



for waves approaching shallow water boundaries such as the coastlines as well as structures located in deeper water. For permeable structures, energy dissipation also occurs within the permeable zones of the structure.

Wave breaking usually accounts for the major portion of dissipated energy. It also results in a heavy loading on a coastal structure, which can damage the structure. When the horizontal orbital velocity of particle  $u$  at the free surface exceeds the velocity of propagation  $C$  of the wave itself, wave breaking occurs. As the steepness increases, it results in particle velocities at the wave crest which are greater than the wave velocity. Consequently, instability of the profile develops.

In deep water, the maximum height of a wave that can occur is limited by the maximum wave steepness,  $H/L$ . Michell (1893) based on theoretical considerations found that this limit of the wave steepness may be represented as follows.

$$\left( \frac{H_o}{L_o} \right)_{\max} = 0.142 \approx 1/7 \quad [3.32]$$

where  $H_o$  and  $L_o$  are the wave height and wave length in deep water, respectively.

When the wave propagates into the surf zone, the wave celerity slows down, and the wavelength shortens. Therefore the wave steepness increases and eventually the wave breaks. In the shoaling zone the limiting steepness is a function of both the relative  $h/L$  and the slope of the beach or structure, measured perpendicular to the direction of wave advance. The breaking criterion in the surf zone is limited by the water depth and is often written as follows.

$$H_b = \gamma_b h_b \quad [3.33]$$

where  $H_b$  and  $h_b$  are wave height and water depth at breaking point respectively, and  $\gamma_b$  is a breaker index. Expression such as Equation [3.33] only allows the calculation of one of the two variables,  $H_b$  or  $h_b$ , once the other variable is known. The procedure

to compute the breaking wave height consists of calculating the local wave height corresponding to depth  $h$ , by means of some propagation model, and then compare it with the estimated breaking wave height,  $H_b$ . As long as  $H < H_b$ ,  $H$  is assumed as the correct wave height and the calculations are repeated for other  $h$  values, until the condition  $H = H_b$  is satisfied.

Miche (1944) from theoretical considerations, proposed another well-known criterion relating the breaking wave height to the wave length and depth

$$H_b = 0.142 \tanh\left(\frac{2\pi h_b}{L_b}\right) \quad [3.34]$$

where  $L_b$  is the wave length at the breaking point. In shallow water (i.e., when  $kh \rightarrow 0$ ), Miche's equation becomes

$$\frac{H_b}{h_b} = 0.89 \quad [3.35]$$

while Munk (1949) derived the breaker index for solitary wave as

$$\frac{H_b}{h_b} = 0.78 \quad [3.36]$$

It is easy to see that the above equations relate  $H_b$  only with the water depth. However, many laboratory tests and field observations indicate that the breaker index  $\gamma_b$  is not a constant. Other parameters like beach slope should be taken into account to determine the height of breaking waves within the surf zone (e.g. Horikawa and Kuo 1966, Goda 1970, Battjes and Stive 1984).

Goda (1970) proposed the following breaking criterion:

$$H_b = A_G L_o \left[ 1 - \exp\left\{-1.5 \frac{\pi h_b}{L_o} (1 + 15m^{4/3})\right\} \right] \quad [3.37]$$

where  $L_o$  is deep-water wave length and  $A_G$  is a constant ranging between 0.12 and 0.18.

Weggel (1972) re-evaluated some of the breaker data from many other researchers' work and proposed the following equation for  $\gamma_b$  to be used in Equation [3.33].

$$\gamma_b = \left[ \frac{1.56}{(1.0 + e^{-19.5m})} - 43.8(1.0 - e^{-19m}) \right] \frac{H_b}{gT^2} \quad [3.38]$$

where  $m$  = beach slope.

Later, Battjes and Stive (1984) proposed the following formula for breaker index,  $\gamma_b$ .

$$\gamma_b = a + b \tanh(33m) \quad [3.39]$$

with  $a = 0.5$  and  $b = 0.4$  and  $m$  is the beach slope.

All of the above equations were obtained using tests conducted with regular waves-waves that have the same height and period as in small amplitude wave theory. The results pertaining to irregular waves will be discussed in the following section. Khampuis (1991) proposed two criteria for breaking waves as follows.

$$H_b = 0.095e^{4m}L_{bp} \tanh\left(\frac{2\pi h_b}{L_{bp}}\right) \quad [3.40]$$

and

$$H_b = h_b [0.56 \exp(3.5m)] \quad [3.41]$$

where  $m$  is a beach slope and  $L_{bp}$  is the breaking wave length based on  $h_b$  and  $T_p$ . Equations [3.40] and [3.41] describe wave breaking when the limiting wave steepness is exceeded (wave steepness criterion) and when the water limits the wave height (depth limited criterion), respectively.

Breaking waves can be classified into three types, namely, surging breakers, plunging breakers and spilling breakers depending on wave steepness and beach slope. Galvin (1968) and Sleath (1984) gave a definition of surging breakers as the one where the wave only surges up and down the slope with relatively small air entrainment. Surging breakers occur for low  $H/L$  on steeper beach slopes. Spilling breakers are specified when the crest of the wave spills down the front face of a wave. Plunging breakers are identified when the wave steepens, followed by the overturning of a jet that plunges forward into the trough water ahead and encloses an air pocket. Plunging breakers usually occur for steep waves on mild slopes. Galvin also introduced an additional type of breaking called a collapsing breaker, corresponding to a surging breaker whose front face becomes steep and eventually collapses. These occur with the steepest waves on the steepest beaches. Galvin proposed criteria in terms of the surf similarity parameter,  $\xi_o$ , to classify the breaker types in deep water. These are,

$\xi_o > 3.3$	surging breaker occur,
$0.5 < \xi_o < 3.3$	plunging breaker occur,
$\xi_o < 0.5$	spilling breaker occur.

where:

$$\xi_o = \frac{\tan \alpha}{\sqrt{H_o/L_o}} .$$

A combination of the beach slope and the wave steepness, usually called the surf similarity parameter at the breaking point,  $\xi_b = m/(H_b / L_o)^{1/2}$ , where  $H_b$  is

breaking wave height, was suggested by Battjes (1974) for use to classify types of breakers. Based on Battjes description, the following criteria to describe the breaker type were obtained.

Surging or collapsing occurs if	$\xi_b > 2.0$
Plunging occurs if	$0.4 < \xi_b < 2.0$
Spilling occurs if	$\xi_b < 0.4$

Figure 3.4 shows the sketches of these different breaker types. Battjes also found that Galvin's classification of the breakers type could serve equally well with  $\xi_b$ .

### 3.4 STRUCTURAL STABILITY

#### 3.4.1 Initiation of Damage

The initiation of damage to a rubble mound structure for a given wave height occurs when the resultant of the driving forces exceed the resisting force, so that armour units with poor interlocking will get removed from the initial place. The resisting forces of units depend upon the gravity force that gets on the individual units and frictional forces activated by neighbouring units. The degree of damage depends on the steepness of incoming wave besides other parameters. After the waves break and the wave runup reach its maximum level, the wave downrush results in a secondary drag, inertia and lift force. Differences in the permeability of the armour layer, core and filter layers results in uplift pressures against the armour layer. In this case wave uprush is usually greater than the wave downrush. Thus, Bruun (1985) concluded that the ability of armour units to resist the forces caused by waves is determined by some parameters such as the weight of the armour unit, water depth, free board of structure, crest width and structure slope.

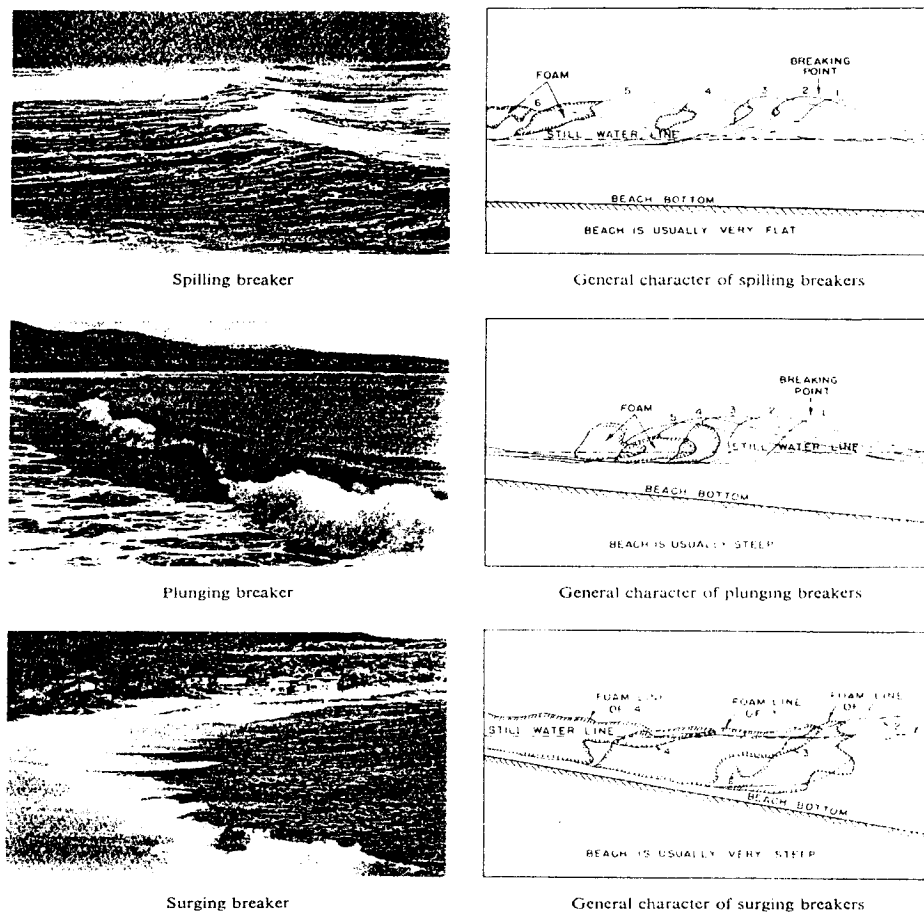


Figure 3.4. Sketch of different breaker types (from Wiegel, 1964).

Modes of failure of the units of armour of breakwaters is often referred to as rolling, sliding or lifting and is caused by a combination of the buoyancy, inertia and drag forces. In addition, the hydrostatic pressure from within the core enhances the mechanisms of failure. The rolling motion take place when the overturning moment acting on the armour unit overcomes the restoring moment. The sliding movement occurs when the sliding forces exceed the tangential resisting forces that depends upon the buoyant forces, gravitational forces and friction between armour units. This movement is usually due to decrease in the friction forces between the armour and sub layer by upliftment of the armour. The lifting movement occurs due to a complex

combination of forces resulting from uprush or downrush of water and the resulting hydrostatic pressures. These pressures are highly variable depending on the permeability of the armour layer and core.

### 3.4.2 Forces on Armour Unit

The wave force acting on an armour unit moving with the wave of velocity  $u$  may be described by the following formulae.

$$\text{Drag force } F_D = \frac{1}{2} \rho_w C_D C_1 D_{50}^2 u^2 \quad [3.42]$$

$$\text{Lift force } F_L = \frac{1}{2} \rho_w C_L C_1 D_{50}^2 u^2 \quad [3.43]$$

$$\text{Inertia force } F_I = \rho_w C_M C_2 D_{50}^3 \frac{du}{dt} \quad [3.44]$$

where  $\rho_w$  is water density,  $C_D$ ,  $C_L$ ,  $C_M$  are the coefficient of drag, lift and inertia respectively,  $D_{50}$  is diameter of armour units,  $C_1$ ,  $C_2$  are area and volume coefficients of armour unit.

The drag and inertia forces act upslope or downslope in the direction of the velocity, whereas, the lift force acts normal to the slope. The submerged weight of the unit and frictional forces act as the restoring forces against the hydrodynamic forces. The submerged weight acts vertically downward and can be written as

$$\text{Submerged weight } W_s = g C_3 D_{50}^3 (\rho_a - \rho_w) \quad [3.45]$$

Figure 3.5 shows a definition sketch of the forces acting on an armour layer. The slope angle is given by  $\alpha$  and the natural angle of repose by  $\phi$ .

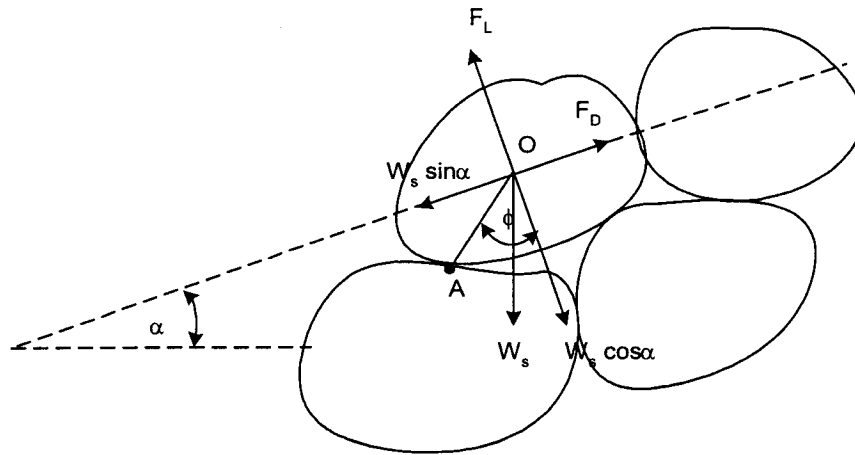


**Figure 3.5.** Definition sketch of forces acting on armour units.

Stability condition against lifting can be expressed as

$$F_L \leq W_s \cos \alpha \quad [3.46]$$

in which the friction between armour units is neglected. The incipient instability occurs when the moments taken at the point of support, A, sum to zero. The hydrodynamic force is assumed to act at the stone's center of gravity, O, and A is assumed such that an increase in the slope angle,  $\alpha$ , to the natural angle of repose,  $\phi$ , places point O directly above point A. Assuming the distance between A and O is half of diameter, this condition can be described as

$$\frac{D_{50}}{2} [F_L \sin \phi - F_D \cos \phi - W_s \sin(\phi - \alpha)] = 0 \quad [3.47]$$

Substituting  $\sin(\phi - \alpha) = \sin \phi \cos \alpha - \sin \alpha \cos \phi$  and dividing through by  $(D_{50}/2) \cos \phi$ , this becomes



$$[F_L \tan \phi - F_D - W_s(\tan \phi \cos \alpha - \sin \alpha)] = 0 \quad [3.48]$$

Substituting Equations [3.42], [3.43] and [3.45] into Equation [3.48], this becomes with Equation [3.49].

$$\frac{1}{2} \rho_w C_L C_1 D_{50}^2 u^2 \tan \phi - \frac{1}{2} \rho_w C_D C_1 D_{50}^2 u^2 - g C_3 D_{50}^3 (\rho_a - \rho_w) (\tan \phi \cos \alpha - \sin \alpha) = 0 \quad \dots[3.49]$$

The water particle velocity,  $u$ , in shallow water is related to the wave height,  $H$ , and can be expressed as

$$u \approx \sqrt{gH} \quad [3.50]$$

Equation [3.49] becomes:

$$\frac{1}{2} \rho_w C_L C_1 D_{50}^2 gH \tan \phi - \frac{1}{2} \rho_w C_D C_1 D_{50}^2 gH - g C_3 D_{50}^3 (\rho_a - \rho_w) (\tan \phi \cos \alpha - \sin \alpha) = 0 \quad \dots\dots[3.51]$$

Hudson (1959) assumed for rubble structures  $\tan \phi=1$ , which reduces Equation [3.51] becomes:

$$\frac{1}{2} \rho_w C_L C_1 D_{50}^2 gH - \frac{1}{2} \rho_w C_D C_1 D_{50}^2 gH - g C_3 D_{50}^3 (\rho_a - \rho_w) (\cos \alpha - \sin \alpha) = 0 \quad [3.52]$$

Equation [3.52] can be simplified to:

$$\frac{1}{2} C_L C_1 gH - \frac{1}{2} C_D C_1 gH - g C_3 D_{50} \Delta (\cos \alpha - \sin \alpha) = 0 \quad [3.53]$$

with

$$\Delta = \frac{\rho_a - \rho_w}{\rho_w} \quad [3.54]$$

Hudson combined all coefficients to one coefficient,  $K_D$ , and replaced the term  $(\cos\alpha - \sin\alpha)$  by  $(\cot\alpha)^{1/3}$ . Hence, Equation [3.53] can be simplified to:

$$\frac{H}{\Delta D_{50}} = (K_D \cot \alpha)^{1/3} \quad [3.55]$$

Equation [3.55] is similar to the well-known Hudson formula as discussed in Chapter 2, in which

$$D_{50} = (M_{50}/\rho_a)^{1/3} \quad [3.56]$$

The term  $H/\Delta D_{50}$  determines the stability of a unit under wave attack.

### 3.5 MODELING OF WAVE-STRUCTURE INTERACTION

Two general approaches can be used in order to solve a physical problem. These approaches are mathematical and physical modeling. A mathematical model expresses the physics of a problem based on theoretical reasoning, and is usually presented in the form of a set of equations. This model can be solved either analytically or numerically. In contrast, a physical model has advantages when the analysis of the physics of a problem is complicated or is uncertain and cannot be solved analytically. Often, physical model results can be used to validate numerical simulation results to find accurate solutions. An empirical relationship can be formulated from model tests that may be useful as an input for the analytical

prediction equation. On the other hand, one has to be cautious since scale effects will result if the model properties are not scaled properly. Use of large scale models will minimize scale effects, but will increase the cost of investigation. However, it is possible to conduct tests on small-scale ratio models by paying careful attention to the Reynolds Number criterion. Hence, a small-scale model was constructed with several breakwater configurations and experiments were carried out by maintaining sufficiently large Reynold number ( $\geq 1.7 \times 10^4$ ) in all of the tests.

In physical modeling, it is important that the model must possess dynamic as well as physical similarity. The principle of dynamical similarity requires that all corresponding forces acting on the prototype and model should be in the same ratio. To underscore this point Bruun (1985) stated that a hydraulic model study should not be run without proper scaling all the factors concerned because the model is supposed to imitate nature.

Three basic forces have to be considered in physical modeling of breakwaters: gravity, viscosity and surface tension. If the gravity forces are dominant everywhere and other forces can be ignored, the scaling of the model can be based on the Froude criterion of similarity. The Froude Number represents the ratio of inertial forces to gravitational forces. The Reynolds Number represents the ratio of inertial forces to viscous forces and the Weber Number represents the ratio of inertial forces to surface tension forces. These parameters can be written as

$$\text{Froude Number } (F_r) = \frac{u^2}{gD_{50}} \quad [3.57]$$

$$\text{Reynolds Number } (R_e) = \frac{\rho_w u D_{50}}{\mu} \quad [3.58]$$

$$\text{Weber Number } (W_e) = \frac{u^2}{\sqrt{\sigma/\rho_w D_{50}}} \quad [3.59]$$

where  $u$  is the water velocity,  $\mu$  is the dynamic viscosity of water at  $15^\circ\text{C}$ ,  $g$  is gravitation acceleration,  $D_{50}$  is diameter of the armour unit,  $\rho_w$  is the water density and  $\sigma$  is the effect of surface tension.

In wave-structure interaction, the wave forces acting on the hydraulic structure are dominated by gravity (hydrostatic and weight of the unit) and surface tension (impact of breaking). Therefore the model should be based on a Froude criterion. In modeling the internal flow or transmission of fluid through a structure, it is necessary to reproduce the frictional effects within the internal flow. However, for the external flow the scale effects of friction are relatively small compared to the gravitational forces, provided the Reynolds Number of flow in the model exceeds a value of  $3.0 \times 10^4$  (Dai and Kamel 1969 and Jensen and Klinting 1983), while van der Meer (1988) stated that the lowest Reynolds Number to avoid scale effects could be set in the range of  $1.0 \times 10^4$  to  $4.0 \times 10^4$ . In the present tests the lowest Reynolds Number for the experiments undertaken works out to be  $1.7 \times 10^4$ , hence the wave acting on the structure are not affected by scale effects. The effect of surface tension  $\sigma$  can usually be neglected when the typical wave length generated in the model is greater than 2 cm (Dalrymple, 1985). The wave lengths considered in this study were in the range of 1.40m to 1.60m, therefore the effect of surface tension is assumed to be insignificant.

### 3.6 DIMENSIONAL ANALYSIS

Dimensionless group of numbers are widely used in different branches of science, including hydraulic engineering, because of large number of advantages they offer. The main advantage comes from the requirement that all mathematical equations that describe certain physical phenomena must be dimensionally homogeneous. It means that the equation must be true, regardless of the system of units being used. Another benefit, which is very important to many experimental

investigations, is that lesser number of plots is required to convey the interrelationship among different variables of a physical phenomenon. Multiple functional relationships can also be deduced from a single dimensionless correlation.

Wave-structure interaction is a complex phenomenon, which cannot be described precisely using a theoretical approach. In order to describe the response of a structure subject to irregular waves, a model study seems to be the only viable solution. The model should no doubt be similar to the prototype in such cases. Using dimensional analysis, the laws of similitude for the model and prototype can be derived.

Based on literature review, a list of governing variables can be derived to qualitatively describe the influences of these variables on wave transformation and stability of breakwater. Since it is hardly feasible to investigate all variables, the previous work of other researchers will be selected.

### 3.6.1 Governing Variables of Wave Transmission

In the wave transmission processes, the transmitted wave height  $H_t$  can be denoted as

$$H_t = f(H_i, T_p, \rho_w, g, \mu, D_{50}, e, \alpha, h_c, h_s, h, B) \quad [3.60]$$

where  $H_i$  is wave incident,  $T_p$  is peak period of wave,  $\rho_w$  is water density,  $g$  is gravitational acceleration,  $\mu$  is viscosity of water,  $D_{50}$  is nominal diameter of armour stones,  $e$  is porosity,  $\alpha$  is an angle between horizontal bottom and structure,  $h_c$  depth of submergence or freeboard,  $h_s$  is structure height,  $h$  is water depth and  $B$  is crest width. Wave transmission is usually described by a coefficient  $K_t$ , where  $K_t$  is defined as the ratio of transmitted wave height,  $H_t$ , to the incident wave height,  $H_i$ .

Hence, choosing three dimensionally independent variables  $H_i$ ,  $\rho_w$  and  $g$  as repeaters, the functional relationship for  $K_t$  takes the following form:

$$K_t = \frac{H_t}{H_i} = f\left(\frac{B}{H_i}, \frac{h_c}{H_i}, \frac{h_s}{H_i}, \frac{h}{H_i}, \frac{D_{50}}{H_i}, \rho_w H_i \frac{\sqrt{gH_i}}{\mu}, e, \alpha, P\right) \quad [3.61]$$

The dimensionless viscosity term in Equation [3.61] is a form of Reynolds number. For test conditions considered here, Reynolds numbers were found to be in the turbulent flow range where the viscous forces become independent of Reynolds number. By multiplying or dividing each other various dimensionless terms can be combined from the above list to form relevant dimensionless parameters, which can either help to explain the phenomenon or help to conduct limited tests more systematically.

### 3.6.2 Governing Variables for Stability

As described in the previous chapter, the stability of rubble mound breakwaters depends on environmental conditions and the physical characteristics of the breakwaters. For convenience, the following list summarizes the relevant parameters under different categories.

- a. Wave Characteristics
  - wave height ( $H_s$ ),
  - wave period ( $T_p$ ),
  - groupiness of waves (GF) and spectral shape,
  - number of waves (N),
  - angle of wave attack ( $\phi_o$ ),
- b. Fluid Characteristics
  - mass density of water ( $\rho_w$ ),
  - dynamic viscosity of water ( $\mu$ ),
  - surface tension of water ( $\sigma$ ),
- c. Material Characteristics
  - nominal diameter of the armour stone ( $D_{50}$ ),

- uniformity of the stone ( $D_{85}/D_{15}$ ),
  - mass density of the stone ( $\rho_a$ ),
  - shape of the armour stones and roughness,
- d. Geometry of the structure
- thickness of the armour and filter layer ( $t_a$ ),
  - permeability of the core ( $P$ ),
  - slope of the structure ( $\cot \alpha$ ),
  - width of the crest ( $B$ ),
  - height of the structure ( $h_s$ ),
- e. Other Characteristics
- water depth ( $h$ ),
  - gravitational acceleration ( $g$ ),
  - construction method.

Summarizing, the structural variables are function of:

$$S = f (H_s, T_p, GF, N, \varphi_o, \rho_w, \rho_a, \mu, \sigma, D_{50}, D_{85}/D_{15}, t_a, P, \cot \alpha, B, h_s, h, g \text{ and construction method}) \dots\dots[3.62]$$

The angle of wave attack was not covered in this test; therefore the influence of this variable is not included as a governing variable. The most severe condition for stability of a breakwater is often the result of perpendicular attack of wave. The viscous effects are not important as long as the Reynolds number exceeds a few thousand, therefore variable  $\mu$  will not be taken into account. The surface tension effect can also be neglected since the wave length adopted for this test was greater than 2.5 cm. The thickness of the armour stone and height of the structure were kept constant, therefore these variables too will not be included in the formulation. The construction method is also assumed to be standardized as a consequence it will not have significant effect on the stability of the breakwater. The width of the crest  $B$  and

the uniformity of material,  $D_{85}/D_{15}$ , were also kept constant and will not be taken into account. Considering the above, Equation [3.62] can be rewritten as

$$S = f(H_s, T_p, GF, N, \rho_w, \rho_a, D_{50}, P, \cot \alpha, h_s, h, g) \quad [3.63]$$

As described previously, stability of breakwater is usually represented by the damage level, the amount of displacement of armour units in the structure's lifetime and under design conditions. Damage level can be measured by counting the number of displaced armour units or by comparing the initial profile with the profile after the event and is expressed as (van der Meer, 1988),

$$S = \frac{A_e}{D_{50}^2} \quad [3.64]$$

The wave period is often expressed as a wavelength and related to the wave height, resulting in the wave steepness. The wavelength, related to deep water, can be defined as

$$L_o = \frac{gT_p^2}{2\pi} \quad [3.65]$$

and the wave steepness can be defined as

$$s_{op} = \frac{2\pi H_s}{gT_p^2} = \frac{H_s}{L_o} \quad [3.66]$$

The wave steepness can also be related to the slope angle of the structure, and expressed as the surf similarity parameter in term of



$$\xi = \frac{\tan \alpha}{\sqrt{H_s/L_o}} \quad [3.67]$$

Summarizing, the wave height  $H_s$ , can be described by the dimensionless variable  $H_s/\Delta D_{50}$ , and the wave period can be described by the dimensionless variables  $s_{op}$  and  $\xi$ . The group of dimensionless variables for stability of breakwater becomes;

$$S = f(H_s/\Delta D_{50}, s_{op}, \xi, GF, N, P, \cot \alpha, h/H_s) \quad [3.68]$$

The above dimensionless variables represent the wave height parameter,  $H_s/\Delta D_{50}$ , the wave period parameters,  $s_{op}$  and  $\xi$ , the groupiness of waves, GF, number of waves, N, permeability, P, slope of structure,  $\cot \alpha$ , and the crest height as function of wave height. The variables  $\rho_w$ ,  $\rho_a$ , and  $g$  were used to defined the dimensionless parameters  $H_s/\Delta D_{50}$ ,  $s_{op}$  and  $\xi$ .

### 3.7 DEVELOPMENT OF RESEARCH PLAN

Based on the discussion presented in the previous chapters, it appears that wave height and wave period are the two most important parameters, which should be considered in undertaking breakwater research, such as wave transformation and structure stability. In the research plan described in the subsequent chapter, test on physical models were conducted. A wide-range of wave heights was generated as an irregular type. Both grouped and non-grouped waves were generated to attack the breakwaters in order to assess the effect of wave group on stability. Four different wave periods were generated for the wave transformation and stability tests and various water depths were created to observe the effect of water depth. Three water depths to lie below the crest of the breakwater; three water depths above the crest and

one at the crest level were used in the transmission tests. To observe the breakwater stability, tests were conducted at three different water depths, water depth below the crest, above the crest and at the crest level.

Effect of geometry of structure on wave attenuation, such as effect of crest width and slope were observed for six different crest widths and three different slopes of the structure. Only one crest width and two slope angles were used as regards observations on the stability is concerned. Effect of permeability of the core also was also studied by placing a plywood board vertically within the core. Since the board reflects the waves almost totally, it was assumed that the core of the breakwater is impermeable. Three different sizes of stone armour layers were introduced to assess the effect of gradation on transmission and reflection.

## Chapter 4

# EXPERIMENTAL SET UP, INSTRUMENTATION AND DATA COLLECTION

Experiments were carried out using the facilities of the Queen's University Coastal Engineering Research Laboratory (QUCERL) at Kingston. This experimental study provided an opportunity to investigate the mechanism of wave transmission, reflection and stability of low crested breakwaters, including submerged rubble mound breakwaters, under a wide range of design conditions. The parameters that are likely to affect wave transmission, reflection and stability were varied over as wide a range as feasible in the setup. The parameters are wave height, wave period, wave duration, wave grouping, core permeability, armour stone size, the crest width of the structure, and slope of the structure. Analysis of the data acquired and results from these tests are presented in Chapter 5.

### **4.1 EXPERIMENTAL SETUP**

#### **4.1.1 Wave Flume**

The flume was 47m long, 1.0m wide and 1.2m deep and was equipped with a flapper type wave paddle. The wave paddle generated both regular and irregular waves. Energy dissipating materials were placed at the ends of the wave flume on a beach with 1:10 slope to dampen wave energy reflection. A horizontal platform with a 1:10 front slope was constructed from thick plywood in the test section to support the model breakwater and allow the waves generated in the deeper section of the flume to pass by. Details of the wave flume are shown in Figure 4.1.

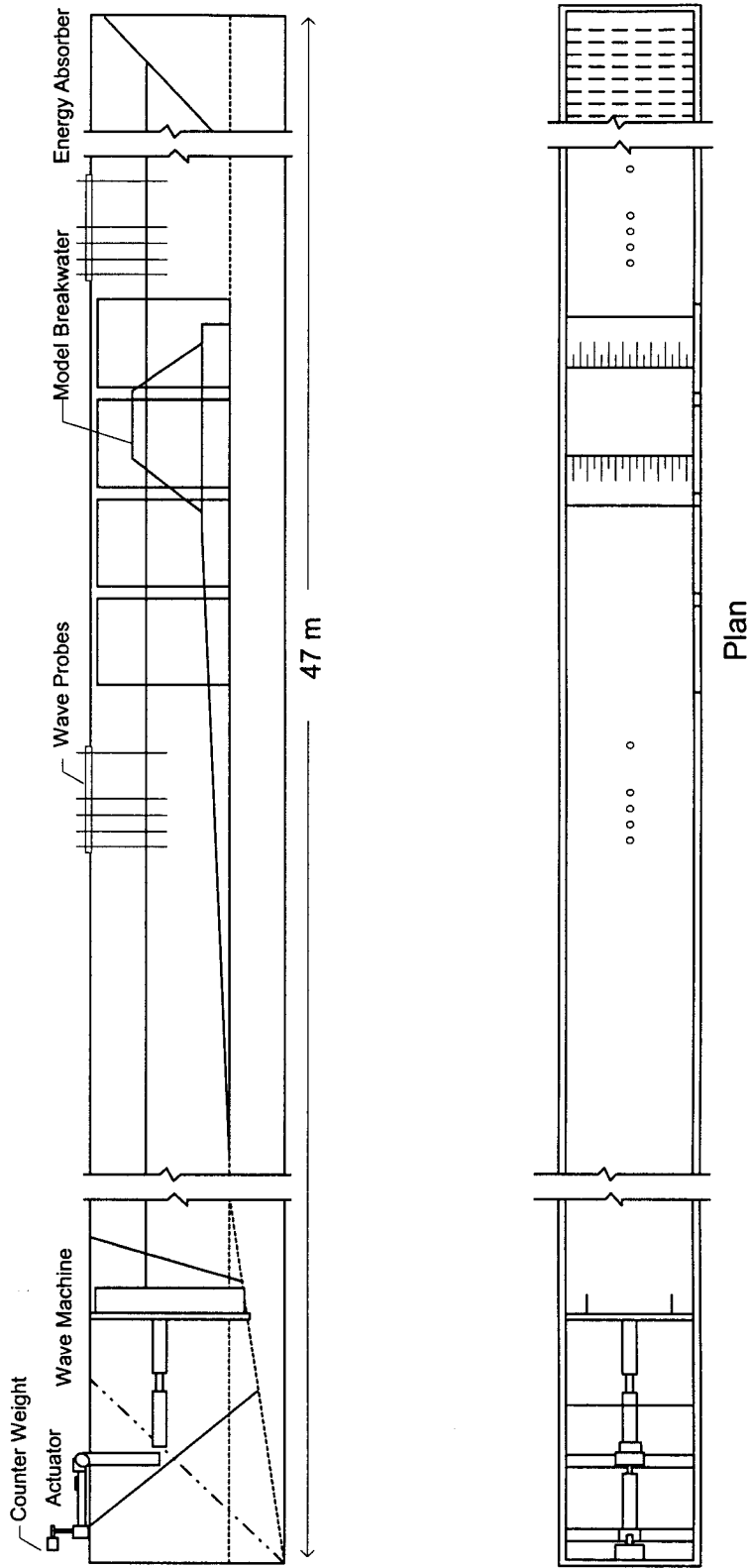
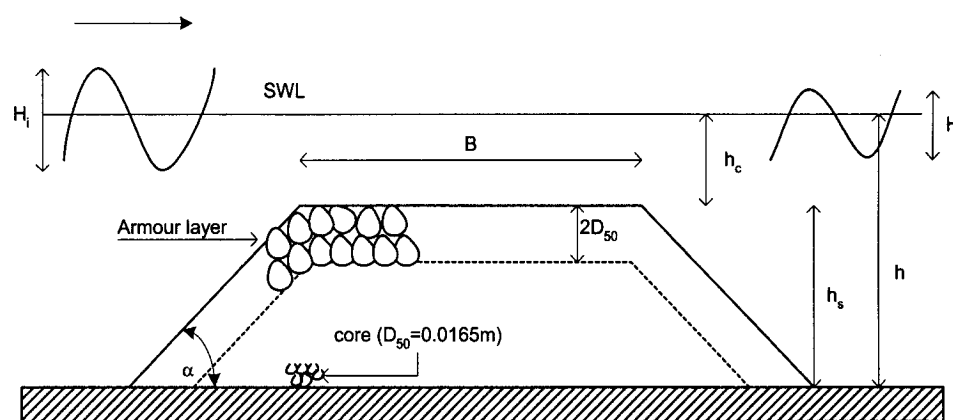


Figure 4.1. Wave flume and model setup (not to scale).

## 4.1.2 Test Structures

### a. Cross-sectional Geometry

The breakwater models were constructed on a horizontal platform preceded by a 1:10 beach slope. A wide range of breakwater cross sections were evaluated during the tests. The geometry of breakwaters was modeled using various crest widths of 0.30m, 0.60m, 0.90m, 1.20m, 1.50m and 2.00m and front slopes (cot  $\alpha$ ) of 1, 2 and 4, combined in different ways. The slopes were chosen to represent steep, mild and very mild sloping structures. The breakwaters were built using both a permeable and an impermeable core and armoured with two identical layers of rocks. For simulating an impermeable core, a plywood board was placed within the core. A typical cross-section of the permeable and impermeable breakwater models is shown in Figure 4.2 and 4.3, respectively.



**Figure 4.2.** Cross-section of permeable breakwater model at water depth above the crest (not to scale).

### b. Breakwater material

For transmission tests, the breakwaters were built with a core comprised of crushed stones that had nominal diameter,  $D_{50}$ , equal to 0.0165 m. This value was obtained by sieving a sample of about 25 kg of core material. The gradation of core

material was characterized by a  $D_{85}/D_{15}$  of 1.25. Figure 4.4 illustrates the grading curve of core material. The core material was kept constant for all tests conducted. The two layers of armor stones protecting the core had an average mass,  $M_{50}$ , of 107g, 249g, and 406g, respectively. These sizes of armour stones were chosen to observe the effect of varying armour stone size in the wave transmission process.

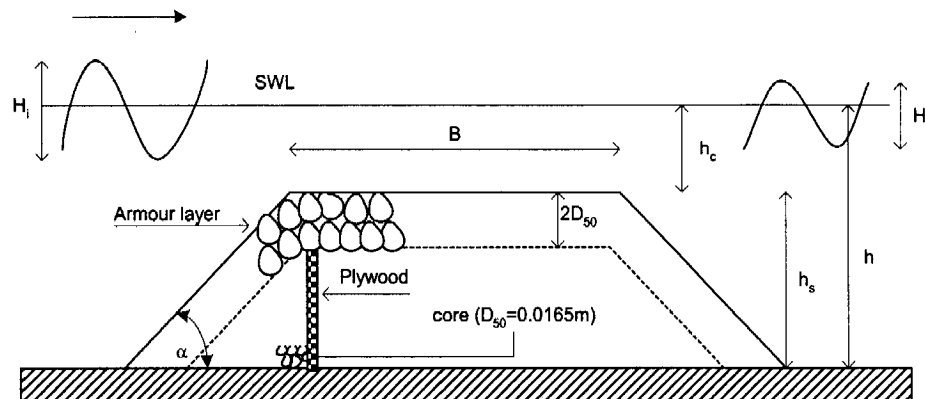


**Figure 4.3.** Cross-section of impermeable breakwater model at water depth above the crest (not to scale).

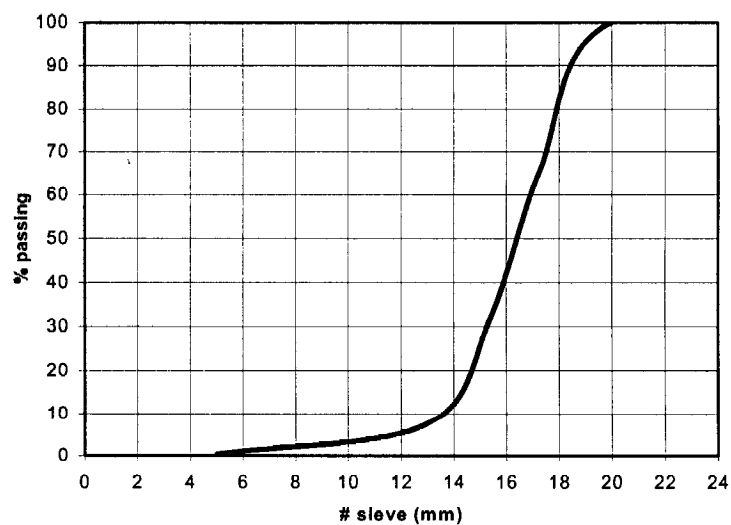


**Figure 4.4.** Gradation curve of core material.

For stability tests, an assessment of weight of the armour stone size was made based on the Van der Meer's (1991) method as discussed in Chapter 2. By assuming relative crest height,  $h_s/h$ , equal to 1 and allowing the damage level,  $S$ , to be equal to 8, the spectral stability number,  $N_s^*$ , works out to be 8. Using the definition  $N_s^* = \frac{H_s S_{op}^{-1/3}}{\Delta D_{50}}$  and the estimated  $H_s = 20\text{cm}$  (the highest wave that can be generated for these tests), the nominal diameter of the armour stone,  $D_{50}$ , is equal to 0.033m and the nominal mass,  $M_{50}$ , is equal to 95g ( $\rho_a = 2630 \text{ kg/m}^3$ ). Hence, armour stones were obtained from a representative sample of crushed stones by individual weighing and had  $D_{50} = 0.034\text{m}$ . Only stones that had similar shapes were accepted. Some main characteristics of the armour stones and core material are provided in Table 4.1. Figure 4.5 shows the gradation curves of three different armour stones expressed as a function of mass.

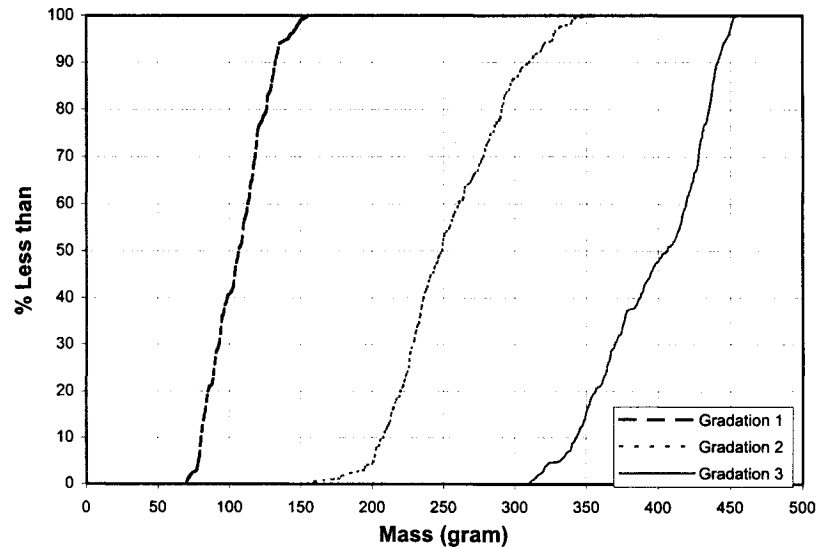


**Figure 4.5.** Gradation curves of armour stones.

**Table 4.1.** Characteristics of armour and core model.

<b>Parameter</b>	<b>Armour</b>			<b>Core</b>
D <sub>15</sub> (cm)	3.1	4.3	5.1	1.44
D <sub>85</sub> (cm)	3.7	4.8	5.5	1.80
D <sub>50</sub> (cm)	3.4	4.6	5.4	1.65
D <sub>85</sub> /D <sub>15</sub>	1.2	1.1	1.1	1.25
M <sub>50</sub> (g)	107	249	406	-
M <sub>85</sub> /M <sub>15</sub>	1.57	1.39	1.25	-
M <sub>max</sub> (g)	155	360	457	-
M <sub>min</sub> (g)	70	159	310	-
$\rho_a$ (kg/m <sup>3</sup> )	2630	2630	2630	2630

### c. Model Construction

Before building the model in the flume, the cross section of the breakwater was drawn on the sidewalls and the model was built following the outline perpendicular to the flume. Core material was first dumped and leveled by hand without pressing too hard in order to prevent the permeability from being affected. The armour stones were individually placed by hand such that a fitted surface was obtained. In the stability tests, a colour coding, i.e. painting of the armour units with different colours for each section, was employed in order to determine armour stone displacement. The same technique was used throughout the tests to place the stones in the model in order to obtain consistency in the experiments. The configurations of the model offered an opportunity to determine the effects of core permeability, stones size, crest width, and slope on the stability and on wave transformations when attacked by irregular waves.

### d. Test Conditions

Both permeable and impermeable cores were tested at water levels corresponding to the relative crest height,  $h_c/h$ , of -0.3, -0.2, -0.1, 0.0, +0.1, +0.2, and +0.3, where  $h_c$  is vertical distance between crest and water level ( $h_s-h$ ). The negative sign represents submerged breakwaters, while the positive values represent



breakwaters whose crest protrudes above the still water level. The models were placed with their longitudinal axis parallel to the wave board. All tests were conducted with a constant crest height of 0.30m, measured from the bottom of the horizontal platform. The transformation tests were divided into twelve series of tests. Various combinations of water depth, wave characteristics, stone sizes and breakwater geometry were investigated for each test series. A summary of important characteristics of the transformation test configurations is provided in Table 4.2.

**Table 4.2.** Structural configurations of wave transformation tests.

Test Series	Slope ( $\cot\alpha$ )	Crest Width (m)	$M_{50}$ armour (g)	Core	Relative water depth ( $h_c/h$ )
T1	1	0.30	107	Permeable	-0.3; -0.2; -0.1; 0.0; 0.1; 0.2; 0.3
IM1	1	0.30	107	Impermeable	-0.3; -0.2; -0.1; 0.0; 0.1; 0.2; 0.3
T2	1	0.60	107	Permeable	-0.3; -0.2; -0.1; 0.0; 0.1; 0.2; 0.3
T3	1	0.90	107	Permeable	-0.3; -0.2; -0.1; 0.0; 0.1; 0.2; 0.3
T4	1	1.20	107	Permeable	-0.3; -0.2; -0.1; 0.0; 0.1; 0.2; 0.3
T5	1	1.50	107	Permeable	-0.3; -0.2; -0.1; 0.0
T6	1	2.00	107	Permeable	-0.3; -0.2; -0.1; 0.0
T12	2	0.30	107	Permeable	-0.3; -0.2; -0.1; 0.0; 0.1; 0.2; 0.3
IM2	2	0.30	107	Impermeable	-0.3; -0.2; -0.1; 0.0; 0.1; 0.2; 0.3
T14	4	0.30	107	Permeable	-0.3; -0.2; -0.1; 0.0; 0.1; 0.2; 0.3
W22	2	0.30	250	Permeable	-0.3; -0.2; -0.1; 0.0; 0.1; 0.2; 0.3
W32	2	0.30	400	Permeable	-0.3; -0.2; -0.1; 0.0; 0.1; 0.2; 0.3

### 4.1.3 Data Acquisition

The response of the following instruments was sampled during the experiments.

- Wave probes
- The displacement and rotation of the electro-mechanical profiler (for stability tests).

A sampling rate of 20 Hz was employed for the wave probe transducers and it was controlled using the GEDAP (Generalized Experiment Data control and Analysis Package) data acquisition and experiment control program. This software package was developed by the National Research Council of Canada (NRC). GEDAP data acquisition files (DAC) were generated and stored on a personal computer running on Windows NT operating system. Profiler data acquisition was controlled and collected using LABTECH Notebook software package. A sampling rate of 10 Hz was used for the profiler.

### 4.1.4 Waves Measurement

To measure the water surface fluctuations with time, the wave flume was equipped with 10 wave probes. These probes are capacitance type water level gauges. The wave probes consist of a hollow tube, insulated probe wire, and a transducer box. Figure 4.6 shows a schematic of a wave probe. The capacitance of the probe is proportional to the current that it carries and is converted into a voltage signal by an amplifier. The voltage time series was acquired using a special Real Time Control (RTC) package available with the GEDAP software package. The voltage time series is converted into a water surface elevation by applying conversion factors and is stored in a calibration file. This data file is then analyzed using programs available in the GEDAP package to obtain the desired wave characteristics. Before each test, these probes were calibrated to avoid errors in collecting data. The probes were calibrated at three different water levels to provide a conversion from voltage to water surface elevation. A maximum error of the linearity under 1% was accepted as

a good calibration. The linearity of the probes was found to be better than 0.8% and the resolution of the probes better than 1 mm of water.

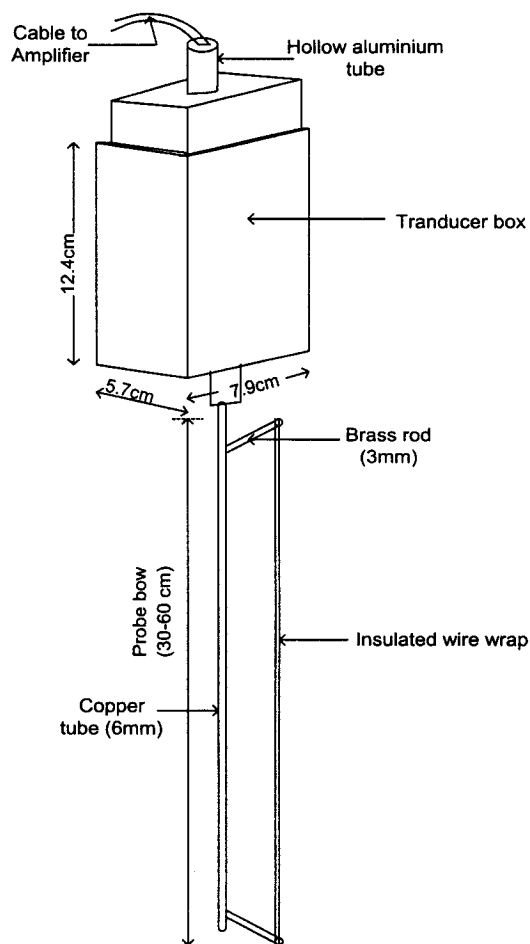


**Figure 4.6.** Wave probe instrumentation.

The ten wave probes were grouped into two five-probe arrays. The first array with large bows (60 cm) was setup in front of the breakwater and the second array with smaller bows (30 cm) was located behind the test breakwater. The probes were setup so as to permit measurement of transformations in the waves passing the

breakwater. Use of a five-probe array allows for the direct calculation of incident and reflected wave characteristics (Funke and Mansard, 1980). The stream wise distances between the first probe (probe nearest to the wave paddle) and each one of the other probes in the array were 0.18m, 0.40m, 0.66m and 1.25m, respectively.

The measurement of wave heights was made each time different wave signals were used to operate the paddle for run. Visual observation on wave breaking over the breakwater, wave setup, movement of stones and wave transformations were made during the test. Sampling of the incident and reflected waves was generally started at 100 wave cycles for each test in order to allow for wave stabilization. Before each wave signal was generated, the water surface was allowed to be calm to prevent residual agitation.

#### **4.1.5 Measurement of Damage**

Common measures for rubble mound damage are visual assessment and profiling. Visual assessment includes counting the number of armour units displaced and profiling includes measurement of the eroded profile.

Count of the number of stones dislodged, photographs and profiles of the breakwater were all used to record damage caused to the breakwater for evaluating its stability. In the counting method, the displacement of armour stones from the initial place during the test gets counted only once. Further displacement of the same units of the armour was not considered as unit removal. The removal of up to one per cent of the total number of armour units in each section of the armour layer was considered as having suffered no-damage. The cross section of the breakwater model was divided into three parts; the front slope (FS), crest (C), and back slope (BS).

Profiling of the armour layer was performed by electro-mechanical equipment developed at QUCERL. This profiler rig consists of a long beam, a carriage with pivoting arm, a profiler box, pulley and crank. As a main support, a 510 cm long and 7.5x7.5 cm hollow aluminum beam is used. This beam is equipped with two pulleys, one small and one large, setup at each end of the beam. A carriage

carries the profiler rod and the profiler box assembly between the pulleys. The pivoting arm is equipped with a 2 cm diameter rubber wheel to move over the armour surface. Details of the profiler equipment are shown in Figure 4.7.

Two rotary potentiometers were used to measure the horizontal displacement and angle respectively. When the carriage gets displaced and the arm rotates, it turns the potentiometers and hence causes a change in the resistances of the potentiometers. The change will alter the applied voltage of the potentiometers, which will be conveyed as a voltage signal through a channel amplifier to the A/D converter. When the voltages are converted, they give the distance and the vertical coordinate of the point on which the free end of the rod is resting. Three separate cross-sectional profiles, 15 cm apart, were taken before each test and after a specified duration of wave action to find out the change, if any, of the armor layer.

Sampling of the potentiometers was completed at a rate of 10 Hz for durations of 60 seconds each. Six hundred data points were collected for each profile. The profiler was dragged slowly in order to gather as many points as possible on the profile.

## **4.2 DATA COLLECTION**

Analog signals from wave probe transducers were converted to digital form and stored in computer data files using the GEDAP software package. This software has been designed to provide some features such as: a standard data file format, an extensive set of data analysis programs and an interactive graphics capability. The basic analysis consists of a spectral and zero crossing analysis.

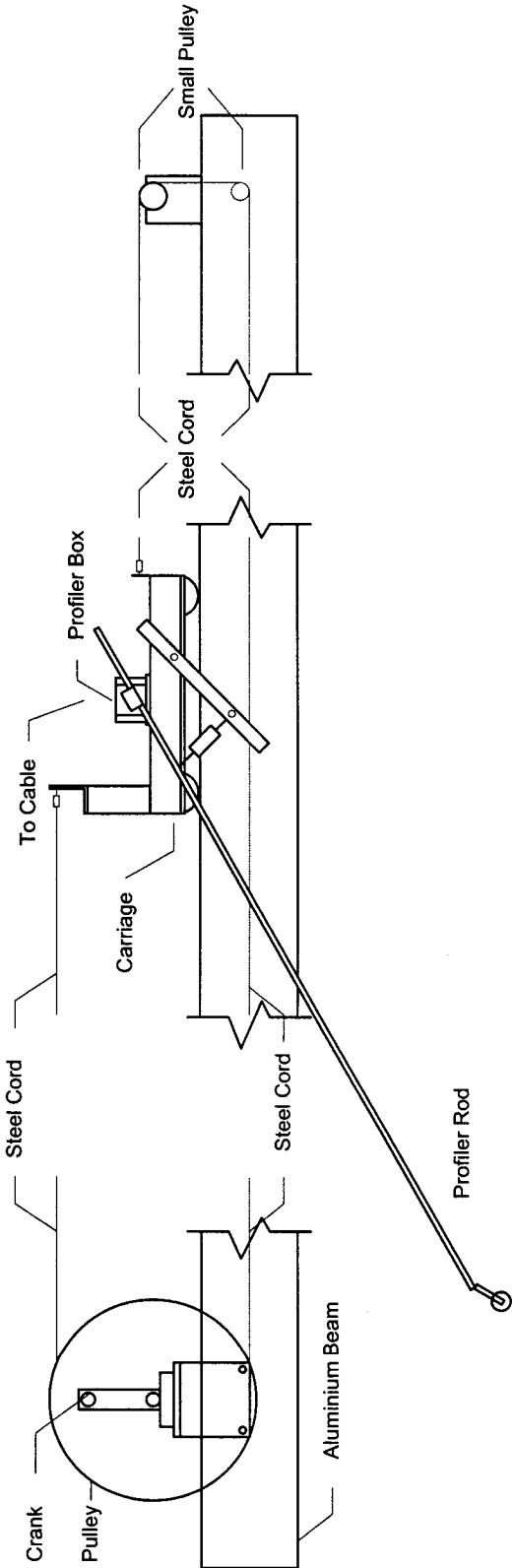


Figure 4.7. Mechanical profiler (not to scale).

Each of the two probe arrays recorded the incident and reflected wave trains respectively. Two types of analysis were performed to determine individual wave heights and periods i.e. spectral analysis and the zero crossing method. Spectral analysis was performed on the time history of the water level data using a Fast Fourier Transform. The reflected and incident wave from the two probe arrays were analyzed using a least square approach. Mansard and Funke (1980) give details of the reflection analysis used in this study.

For stability tests, only one probe array was used for data acquisition and it was setup in front of the breakwater structures. Profile data were collected using Labtech Notebook. Sampling output from profiler device consisted of two data files called R(t) and Theta(t), where R is the horizontal distance of the carriage along the beam of the profiling rod, and Theta is the angle between the profiling beam and the rod. Once the data acquisition was complete, all of the profile data were converted using a calibration factor to create a file of breakwater surface coordinates at constant increments. The calibration factor for the profiler was determined from the profiler calibration, discussed later. Once the data conversion gets complete, the profile data files get converted to a GEDAP format by running the program IMPORT that is available on the GEDAP software package. Profile analysis was then performed by running program MERGE\_BW to determine the X and Z coordinates that are calculated from the data files R(t) and Theta(t). The relationship between R, Theta, X, and Z as an output file were:

$$X = R - \text{rod length} \times \cos(\text{theta}) \quad [4.1]$$

$$Z = \text{elevation of beam} - \text{rod length} \times \sin(\text{theta}) \quad [4.2]$$

The program reads important information such as an input data including the length of the profiling rod, the depth offset, etc. The depth offset is determined by measuring the normal distance from the end of the profiling rod to the center of the carriage.

### **4.3 TEST CONDITION AND PROCEDURE**

This section describes the test conditions and procedures applied for this study. The calibration procedure for the equipment used for the experiment is discussed first. In the following, generation of wave signals and wave calibration are presented.

#### **4.3.1 Calibration**

##### **a. Wave Machine**

The wave machine was calibrated using a static calibration process in GEDAP program. To obtain a static calibration drive signal, the program RWREP2 was run. The standard static calibration control signal that was produced by RWREP2 was sent to the wave machine controller, drives the wave machine to full forward and reverse stroke of the wave paddle. The displacement of the wave paddle was then measured for both forward and backward stroke positions. Depth of water was also measured at the paddle, as was the gap between the bottom of the paddle and the floor. These measurements were used in obtaining the wave machine calibration file.

The GEDAP program WMCAL was run to generate a wave machine calibration file named WMCAL.001 that contains the static calibration data such as type of wave machine, articulation mode, wave machine elevation, polarity and displacement of wave board. Waves generation was performed by running the program RWREP2 in conjunction with the wave machine calibration file WMCAL.001.

##### **b. Wave Probes and Profiler**

The wave probes and profiler were calibrated before collecting data. Calibration of the wave probes was done by running the NDAC Data Acquisition and Control Package. This package in conjunction with the GEDAP software, provides real-time data acquisition and control functions using National Instruments analog I/O card.



The wave probes were calibrated at three different positions along the span to provide a conversion from voltage to water surface elevation. The sampling rate was set at 20 Hz. and the sampling time was 30 seconds. The voltage value recorded from each probe was then plotted with respect to still water level. The maximum error in the linearity of less than 1% is accepted as a good calibration. Calibration was carried out daily and also when the probes were moved from their original place. In cases where the water level changed from the initial level, the wave probe calibration was re-zeroed. The linearity of the probes during the test was found to be better than 1% and the resolution of the probes was better than 1mm. The calibration parameters were found to be influenced by water temperature.

Calibration of the profiler was undertaken twice, once for angle calibration and the other time for displacement since the profiler recorded both vertical and horizontal position of the profile. Calibration of the profiler was completed using Labtech Notebook developed by Laboratory Technologies Corp, running on an IBM PC compatible. Two data blocks were used in this setup. One block was used for the horizontal voltages and the other was used for the angle voltages. While calibrating the angle, the pivoting arm was held at three different angles. The voltage value recorded for each angle was then plotted against the angle. Horizontal calibration was conducted at four different positions with distances of 0.50 m for each position. Each value of the horizontal calibration was plotted against the distance. Both calibration factors for angle and displacement were used in the profiling analysis. Similar to the wave probe calibration accuracies, a maximum error of less than 1% was accepted as a good calibration.

#### **4.3.2 Wave Signal Generation**

Waves were synthesized using the GEDAP Real Time Data Acquisition and Control package (Miles, 1989). First, the desired target wave spectrum was defined using a theoretical parametric spectral model by running the program PARSPEC. The target wave spectrum was synthesized using the JONSWAP spectra having value of

Philips Alpha,  $\alpha_p = 0.0081$ , a peak enhancement factor,  $\gamma = 3.3$  and a variable zero moment wave height  $H_{mo}$ . Other input parameters included significant wave height, water depth for power calculation and peak period. The output of this program was a file containing expected variance spectral density of the expected wave.

The wave trains for the transformation tests were synthesized by running the program RWSYN. The input of this program was the output file produced by PARSPEC. The output file of program RSWYN was a file containing a water surface elevation time series (wave train). This output file was used as input for the RWREP2 program, which generates a voltage signal for various combinations of wave height and wave period required. The voltage signal file produced by program RWREP2 was then used to drive the wave machine. The program RWREP2 also obtained all of the required data concerning the particular wave machine by running the program WMCAL. The wave amplification factor then was changed to obtain the desired wave height in cases where the measured waves were not matching with the expected wave heights. The wave amplification factor is input in the RWREP2 program and has default value of one. The output file containing the wave signals consists of several specific wave height and period combinations. Diagram of the irregular wave generation can be seen on Figure 4.8.

In the stability tests, target waves were synthesized containing grouped waves and non-grouped waves. The program SYSI from the GEDAP package was run to generate a target SIWEH using the temporary theoretical SIWEH spectral density proposed by Funke and Mansard (1980) used by the program SYW. The input data for the program SYSI includes the peak frequency of the SIWEH spectral density, repetition period of the SIWEH, groupiness factor and mean value of the SIWEH. The output file obtained from SYSI contains the SIWEH spectral density.

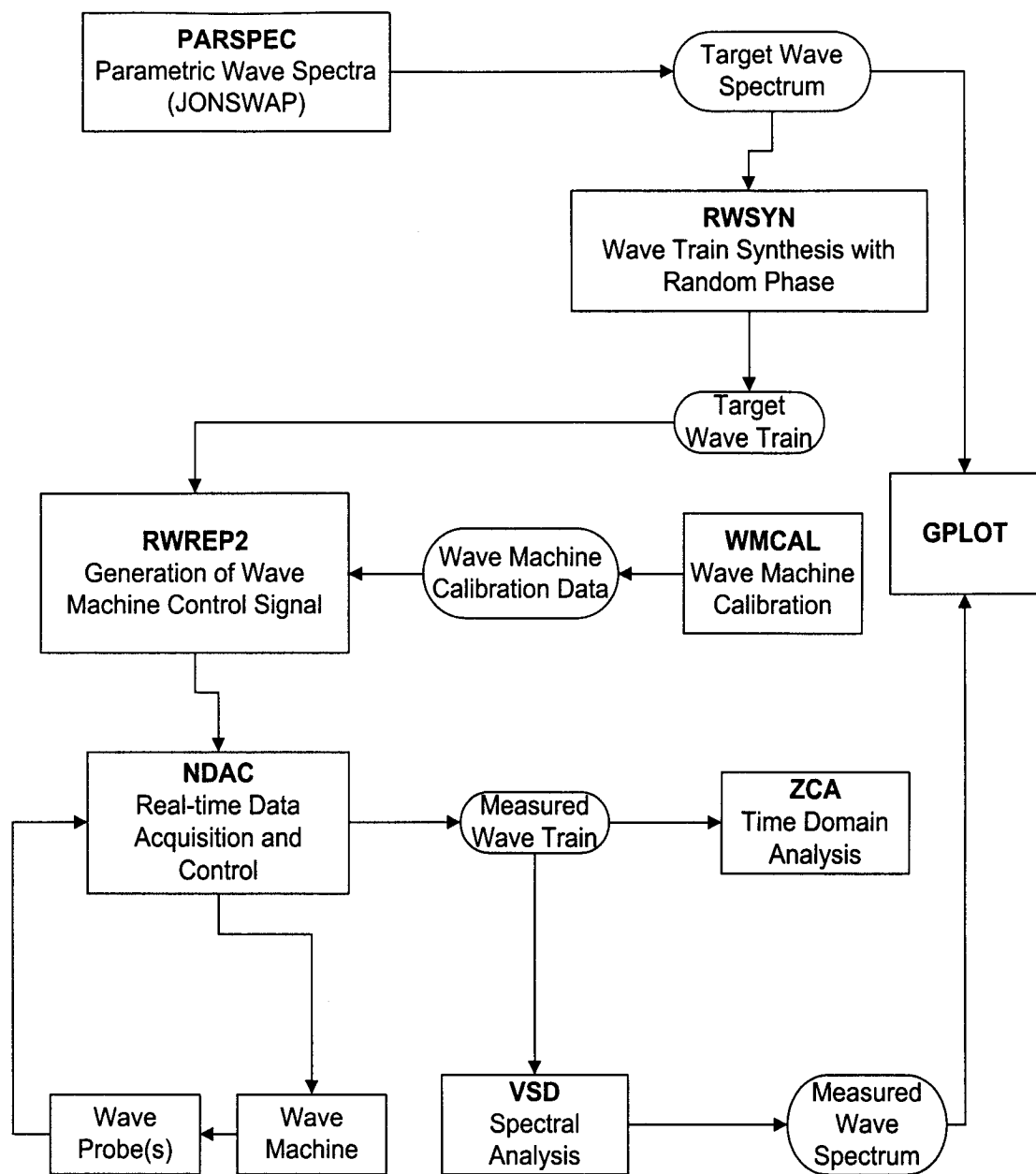


**Figure 4.8.** Irregular wave generation.

The grouped waves were synthesized by running program SYW. This program needs two input files, SIWEH spectral density from SYSI and variance spectral density from PARSPEC. The output file of the program SYW contain the synthesized grouped wave train, used by the program RWREP2 to generate the wave machine control signal (see Figure 4.9).

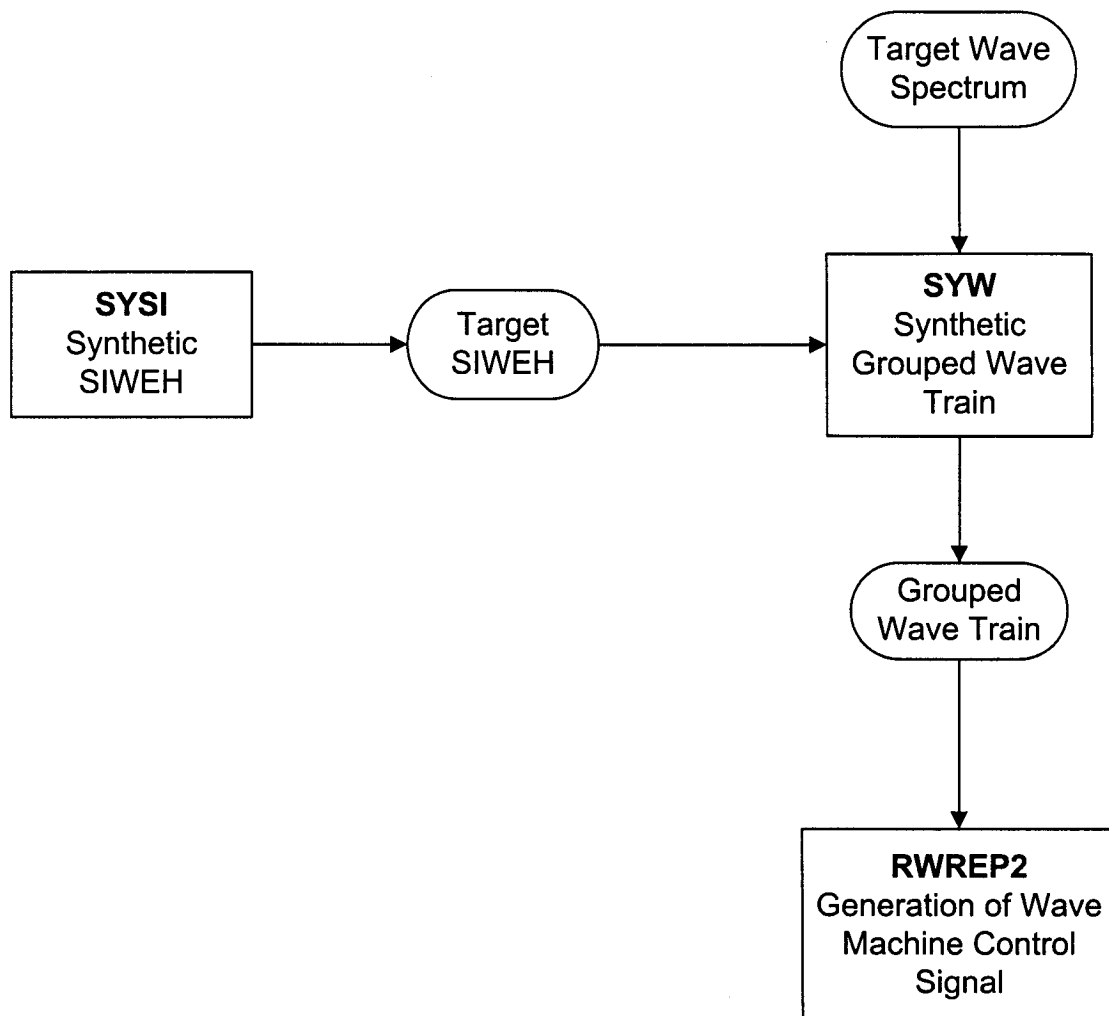


**Figure 4.9.** Grouped wave generation.

### 4.3.3 Wave Conditions

All tests were carried out using irregular waves. For the transmission tests, waves were generated from the lowest target wave height of 5cm up to 20cm with increments of 2.5cm, and for periods ranging from 1 to 2.5 seconds. In cases where the breakwater model was built with the smallest weight of stone (107g), the range of target waves generated in the flume was varied from 5cm to 15cm for submerged conditions and from 5cm to 7.5cm for non-submerged conditions. This was done to prevent the armour layers from being damaged during the transmission tests. Following the earlier tests, using the smallest stone weight, it was observed that the armour stones were not stable with the larger waves. Considerable damage was done to the crest and front slope of the breakwater. A summary of the spectral characteristics of the incident wave target spectra for the different stone gradations used in the transmission tests are provided in Tables 4.3 and 4.4.

Generally, the duration of wave action for transmission test was 200 waves for all wave periods and water depths. The duration of the waves for the stability tests was 3000 waves to allow the breakwater to reach an equilibrium profile i.e. until no new units get displaced by the waves.

**Table 4.3.** Wave test conditions of armour gradation 1.

Relative water depth ( $h_c/h$ )	Wave period ( $T_p$ ) (sec.)	Wave height ( $H_{m0}$ ) (cm)
-0.3	1.0	5, 7.5, 10, 12.5, 15
	1.5	5, 7.5, 10, 12.5, 15
	2.0	5, 7.5, 10, 12.5
	2.5	5, 7.5, 10, 12.5
-0.2	1.0	5, 7.5, 10, 12.5
	1.5	5, 7.5, 10, 12.5
	2.0	5, 7.5, 10,
	2.5	5, 7.5, 10,
-0.1	1.0	5, 7.5, 10
	1.5	5, 7.5, 10
	2.0	5, 7.5, 10
	2.5	5, 7.5, 10

**Table 4.3.** Wave test conditions of armour gradation 1 (Cont'd).

Relative water depth ( $h_c/h$ )	Wave period ( $T_p$ ) (sec.)	Wave height ( $H_{m0}$ ) (cm)
0.0	1.0	5, 7.5, 10
	1.5	5, 7.5, 10
	2.0	5, 7.5, 10
	2.5	5, 7.5, 10
0.1	1.0	5, 6.5, 7.5
	1.5	5, 6.5, 7.5
	2.0	5, 6.5, 7.5
	2.5	5, 6.5, 7.5
0.2	1.0	5, 6.5, 7.5
	1.5	5, 6.5, 7.5
	2.0	5, 6.5, 7.5
	2.5	5, 6.5, 7.5
0.3	1.0	5, 6.5, 7.5
	1.5	5, 6.5, 7.5
	2.0	5, 6.5, 7.5
	2.5	5, 6.5, 7.5

Note: negative  $h_c/h$  ratios indicate submerged conditions.

**Table 4.4.** Wave test conditions of armour gradation 2 and 3.

Relative water depth ( $h_c/h$ )	Wave period ( $T_p$ ) (Sec.)	Wave height ( $H_{m0}$ ) (cm)
-0.3	1.0	5, 7.5, 10, 12.5, 15, 20
	1.5	5, 7.5, 10, 12.5, 15, 20
	2.0	5, 7.5, 10, 12.5, 17.5
	2.5	5, 7.5, 10, 12.5, 17.5
-0.2	1.0	5, 7.5, 10, 12.5, 17.5
	1.5	5, 7.5, 10, 12.5, 17.5
	2.0	5, 7.5, 10, 15
	2.5	5, 7.5, 10, 15
-0.1	1.0	5, 7.5, 10, 12.5, 17.5
	1.5	5, 7.5, 10, 12.5, 17.5
	2.0	5, 7.5, 10, 15
	2.5	5, 7.5, 10, 15
0.0	1.0	5, 7.5, 10, 12.5, 17.5
	1.5	5, 7.5, 10, 12.5, 17.5
	2.0	5, 7.5, 10, 15
	2.5	5, 7.5, 10, 15

**Table 4.4.** Wave test conditions of armour gradation 2 and 3  
(Cont'd)

Relative water depth ( $h_c/h$ )	Wave period ( $T_p$ ) (sec.)	Wave height ( $H_{mo}$ ) (cm)
0.1	1.0	5, 7.5, 12.5
	1.5	5, 7.5, 12.5
	2.0	5, 7.5, 12.5
	2.5	5, 7.5, 12.5
0.2	1.0	5, 7.5, 12.5
	1.5	5, 7.5, 12.5
	2.0	5, 7.5, 12.5
	2.5	5, 7.5, 12.5
0.3	1.0	5, 7.5, 12.5
	1.5	5, 7.5, 12.5
	2.0	5, 7.5, 12.5
	2.5	5, 7.5, 12.5

Note: negative  $h_c/h$  ratios indicate submerged conditions.

#### 4.3.4 Wave Calibration

Initial testing was performed in the wave flume without a breakwater in place to determine the performance of the flume and the characteristics of waves that were generated in the flume. Testing covered all of wave conditions shown in Table 4.5. Waves were generated from lowest wave target of 5cm up to 20cm with increment of 2.5cm for all cases. Four water depths of 0.73m, 0.80m, 0.88m and 0.93m were maintained in the beginning of the flume for this test. The water depths above the horizontal test platform were therefore 0.23m, 0.30m, 0.38m and 0.43m, respectively. Probe arrays 1 and 2 were located at a distance of 12m and 28.3m, respectively from the rear of the flume (wave absorber location) in order to obtain wave characteristics at the test site and in the deep water.

**Table 4.5.** Waves target of wave calibration.

<b>Water depth (m)</b>	<b>Wave period (<math>T_p</math>) (sec.)</b>	<b>Wave height (<math>H_{mo}</math>) (cm)</b>
0.43	1.0	5, 7.5, 10, 12.5, 15, 20
	1.5	5, 7.5, 10, 12.5, 15, 20
	2.0	5, 7.5, 10, 12.5, 17.5
	2.5	5, 7.5, 10, 12.5, 17.5
0.38	1.0	5, 7.5, 10, 12.5, 15, 17.5
	1.5	5, 7.5, 10, 12.5, 15, 17.5
	2.0	5, 7.5, 10, 12.5, 15
	2.5	5, 7.5, 10, 12.5, 15
0.30	1.0	5, 7.5, 10, 12.5, 17.5
	1.5	5, 7.5, 10, 12.5, 17.5
	2.0	5, 7.5, 10, 15
	2.5	5, 7.5, 10, 15
0.23	1.0	5, 7.5, 10, 12.5, 15
	1.5	5, 7.5, 10, 12.5, 15
	2.0	5, 7.5, 10, 12.5, 15
	2.5	5, 7.5, 10, 12.5, 15

It was observed that the generated wave spectra and wave characteristics varied to some degree from the target values. This variation could be due to the dynamics of the wave generator and the physical limitations of the wave flume. In an effort to achieve the target spectrum and target waves, each wave signal was modified by applying an amplification factor.

#### 4.3.5 Stability Tests

Tests were performed for stability of all structural configurations provided in Table 4.6 below. Each wave was allowed to attack the breakwater until an equilibrium profile was attained after which the breakwater was rebuilt prior to the attack by the next higher wave. The general procedure followed for the stability test sequence was as follows:

- Construct the breakwater model in the wave flume.
- Calibrate the wave gauges.



- Calibrate the electro mechanical profiler.
- Survey the breakwater to document its initial condition by profiling and photographs.
- Start the wave generator and run waves.
- Sample wave data from wave probes.
- Visual observations of wave-breakwater interaction.
- Stop the wave generator.
- Survey the breakwater to document its final condition by counting, profiling and photography.

Tests were not commenced until the water level surface in the flume was completely calm in order to avoid wave agitation.

In order to simulate the growth and decay of waves similar to the ones expected in the prototype-sea state, the wave consisted of combination of several wave heights and wave periods starting with smaller waves of 7.5cm increasing with increment of 2.5cm up to 15cm, then decreasing to 7.5cm shown in Table 4.7. This wave climate was used to study the stability of the breakwaters.

**Table 4.6.** Stability test characteristics.

Slope	: 1:2 (excepting in Test SS1 and SS2)
Crest width	: 0.30 m
$M_{50}$	: 107 g
$D_{50c}$	: 0.0165m
Crest height	: 0.30 m

Test #	Relative water depth ( $h_c/h$ )	Wave height (cm)	Wave period (sec.)	Wave duration (minutes)
ST1	-0.2	12.5	1	50
ST2	-0.2	12.5	1.5	75
ST3	-0.2	12.5	2.0	100
ST4	-0.2	12.5	2.5	125
ST5	0.3	12.5	1.0	50
ST6	0.3	12.5	1.5	75

Table 4.6. Stability test characteristics (Cont'd).

Test #	Relative water depth ( $h_c/h$ )	Wave height (cm)	Wave period (sec.)	Wave duration (minutes)
ST7	0.3	12.5	2	100
SH1	-0.2	10.0	1.5	75
SH2	-0.2	15.0	1.5	75
SH3	-0.2	17.5	1.5	75
SH4	0.3	7.5	1.5	75
SH5	0.3	10.0	1.5	75
SH6	0.3	12.5	1.5	75
SH7	0.3	15	1.5	75
SD1	-0.2	15	2	100
SD3	0.0	15	2	100
SD4	0.3	15	2	100
SG1*	0.3	7.5	1.5	75
SG2*	0.3	10	1.5	75
SG3*	0.3	12.5	1.5	75
SG4*	0.3	15	1.5	75
SG11**	0.3	7.5	1.5	75
SG21**	0.3	10	1.5	75
SG31**	0.3	12.5	1.5	75
SG41**	0.3	15	1.5	75
SC1	0.3	7.5	1	50
SC2	0.3	10	1.5	75
SC3	0.3	12.5	2	100
SC4	0.3	10	1.5	75
SC5	0.3	7.5	1	50
SS1***	-0.2	15	2	100
SS2***	0.3	15	2	100
SN1	0.3	12.5	1.5	3 x 75
SP1****	-0.2	15	1.5	75
SP2****	0.3	15	1.5	75

Note:

- \* : GF ~ 0.5
- \*\* : GF ~ 1.0
- \*\*\* : slope 1:1
- \*\*\*\* : Impermeable core

### Purpose of each test

- ST1 - ST7 : to assess the effect of wave periods ranging from 1s to 2.5s in submerged and crest above water level.
- SH1 - SH7 : to assess the effect of wave heights
- SD1 - SD4 : to assess the effect of water depths
- SG1 - SG4 and SG11-SG41: to assess the effect of wave groupiness
- SC1 - SC5 : to assess the effect of wave climate (see Table 4.7)
- SS1- SS2 : to asses the effect of structure slope
- SN1- SN3 : to assess the effect of number of waves
- SP1- SP2 : to assess the effect of core permeability

**Table 4.7.** Wave climate generated for this study.

Wave height (cm)	Wave period (s)	Duration (min)
7.5	1	50
10	1.5	75
12.5	2	100
15	2.5	125
12.5	2	100
10	1.5	75
7.5	1	50

## Chapter 5

# DATA ANALYSIS AND RESULTS

### 5.1 INTRODUCTION

This chapter deals with data analysis and the results of this study. Two-dimensional testing was undertaken to investigate the effect of various variables on the wave transmission and reflection processes and the stability of wide crown breakwaters. A total of twelve series of transmission and reflection tests were conducted where for each series of test, water depth and wave condition were varied. For the stability tests, a total of thirty-six tests were carried out, in which the following parameters were varied:

- water depth,  $h$ ,
- wave height,  $H_i$ ,
- wave period,  $T_p$ ,
- number of waves attacking the structure/wave duration,  $N$ ,
- wave groupiness, represented by  $GF$ ,
- core permeability and,
- slope of the structure,  $\cot\alpha$ .

### 5.2 DATA ANALYSIS

As described in Chapter 4, data from all the waves generated in the flume were collected and analyzed using the GEDAP software package. The analysis

consisted of time domain using zero-crossing method, frequency domain using spectral method and reflection analysis. Zero-crossing and spectral methods were performed for records of each probe of the two probe arrays, while reflection analysis was performed for each array of the two probe arrays. The Zero-crossing method is a statistical approach, whereas, spectral method is based on wave energy considerations.

### **5.2.1 Time Domain Analysis: Zero-crossing Method**

The Zero-crossing Analysis (ZCA) performs a time domain zero crossing on a time series signal. Both zero up-crossing and zero down-crossing were performed. The important output parameters derived from the ZCA are significant wave height ( $H_s$ ), maximum wave height ( $H_{max}$ ), peak period ( $T_p$ ), average period ( $T_m$ ), etc. Analysis of the test data was performed using the option setting as provided by the GEDAP software. The outputs of the test data from these experiments were collected in a separate file for the purpose of this thesis. An example of wave time series is shown in Figure 5.1. Figure 5.2 shows in detail the first 50 seconds of wave record. The Zero Crossing Analysis is usually used for the wave records with a narrow frequency band.

### **5.2.2 Frequency Domain Analysis: Spectral Method**

The Variance Spectral Density (VSD) program contained in the GEDAP software package is a program for analysis based on wave frequencies. This program solves for parameters such as zero moment wave height ( $H_{m0}$ ), frequency of spectral peak ( $f_p$ ), peak period ( $T_p$ ) corresponding to  $f_p$ , etc., using Fourier transforms analysis. The water level fluctuation as shown in Figure 5.1 for example, is transformed into wave variance spectral density function, known as wave spectrum. The smoothing bandwidth values used in the spectral analysis were the default values computed by the spectral analysis program. The upper and lower cut-off frequencies used in this analysis were selected as 0 and Nyquist frequency respectively. Nyquist frequency is

the highest frequency that can be defined from a time series. Typical example of a wave spectrum as a result of the VSD program is shown in Figure 5.3.

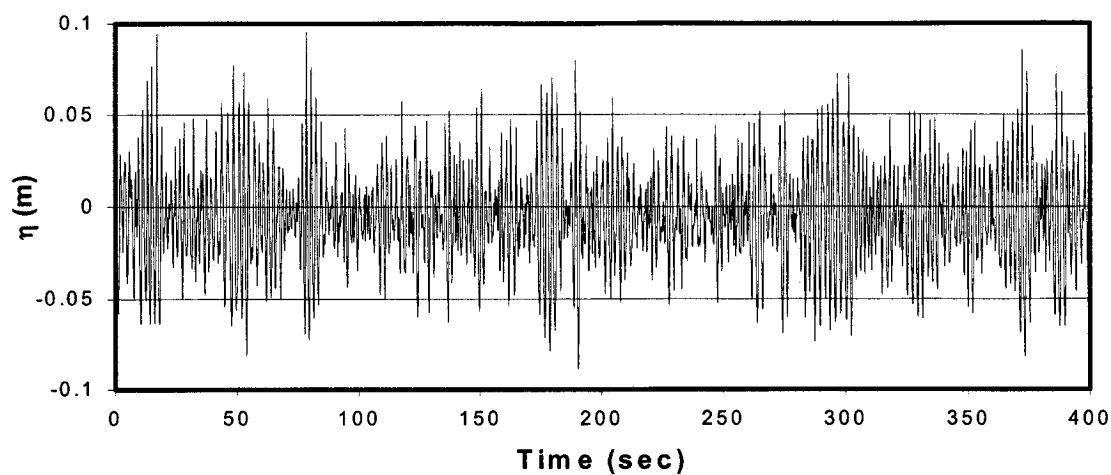


**Figure 5.1.** Example of surface elevation time series recorded at probe 5.

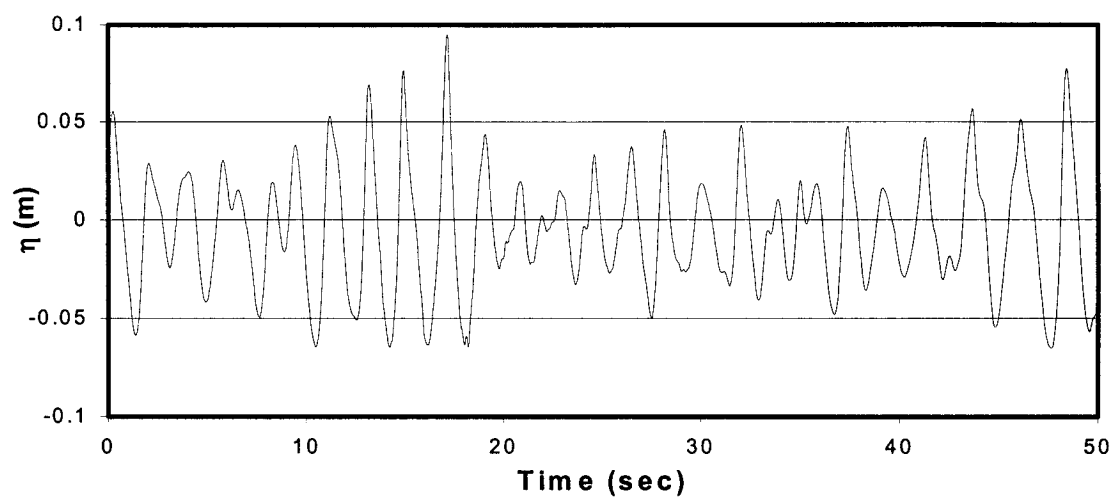


**Figure 5.2.** The first 50 seconds of wave record for Figure 5.1.

### 5.2.3 Reflection Analysis

Reflection analysis of the wave data was performed using REFLA program as provided in the GEDAP software. This program separates the incident and the

reflected spectra from measured data. The analysis is based on the Least Square method as described by Mansard and Funke (1980) using data from the three wave probes. This method was initially proposed by Goda and Suzuki (1976) using two-wave probes set up on the axis of the flume and improved by Mansard and Funke for an array of three probes. The least square method is used to minimize the noise signal for all three probe as described by Mansard and Funke (1980). Laboratory tests by Mansard and Funke show good agreement between incident wave spectra calculated by the least squares method and the spectra measured without a reflective structure.

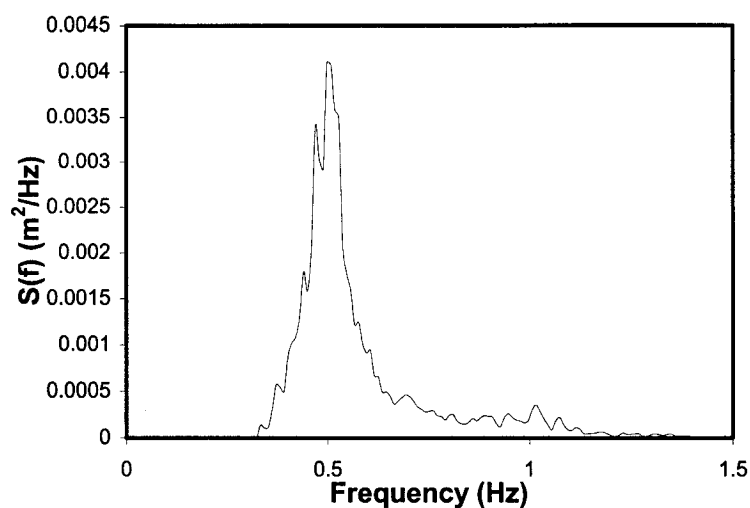


**Figure 5.3.** Example of wave spectrum of the wave record by VSD for  $f_p = 0.5$  Hz.

Since the REFLA program needs the cross-spectral density data between probe 1 and 2 and probe 1 and 3 as an input file, the cross spectral analysis was first performed for the three probes using the GEDAP routine XSPEC program. The standard probe spacing is provided in program PRBSP for selecting automatically the three of five possible probe spacing before running of program XSPEC. The REFLA program provides an option to enter the parameters that are needed in the analysis, if program PRBSP is not used. The GEDAP output file of the REFLA program provides the incident spectrum, reflected spectrum error threshold values and parameters such as wave height of the incident spectrum (HCHR), peak frequency ( $f_p$ ) and peak period

( $T_p$ ) of the incident spectrum. The reflection coefficient is also provided in this program or can be computed from the wave height of the reflected and incident spectrum.

### 5.3 VISUAL OBSERVATIONS

Observations were made during the wave calibrations, at a section where no breakwater was placed in the flume. It was done to determine the characteristics of the wave flume and to observe the characteristics of wave propagation in the flume. It was observed that during the higher wave series, some waves were breaking on the beach slope and the horizontal platform.

In the transmission tests, in which the breakwater was in place, wave breaking was observed on the front slope and crest of the breakwater for submerged conditions, mainly on the front of the breakwater when the water level was below the crest. For certain heights of waves attacking the narrow crest breakwater, wave breaking occurred behind it. A water level setup behind the breakwater was also observed for the case of the longer wave periods resulting in return flow velocities. Generation of higher frequency of waves on the crest and behind the structure was visually evident. For smaller waves, having the water level below the crest, it was observed that wave runup never reached the crest. For the bigger waves, most of the waves broke on the crest, and for some, overtopped and broke behind the structure.

In the stability tests, it was observed during the tests that the uprush and downrush of the waves causes displacement of the armour units. The impact of the wave action on an armour unit was not playing an important role on the unit displacement. In many cases, the uprush tends to loosen or rock a unit in the armour layer while the downrush carries it away if the unit was loosened sufficiently.

When the water level was above the crest, the wave form changes, and for a given wave height and wave period, several armour stones were lifting and rocking



because of the return flow from the previous waves. For a still water level at the crest, waves broke on the crest and on the front slope.

As the water level further decreases (the crest elevation protrudes more above the water level), the wave runup exceeds the elevation of the permeable core for the lower waves, and the elevation of the crest for the higher waves. This condition results in flow through the structure and causes lifting on the units over the crest and the slope.

## **5.4 RESULTS**

### **5.4.1 Wave Calibration**

Analyzed data from the two wave probe arrays using GEDAP software provides the incident and reflected wave characteristics of each array. Reflection characteristics recorded by the two probe arrays are shown in Figures 5.4 and 5.5. The 1<sup>st</sup> probe array computed the reflection coefficients of the entire test apparatus. The reflection coefficients generally ranged from 2.4% to 13.02% with the average of 5.9%. The reflected waves that were measured at the 1<sup>st</sup> wave probe were as a result of interaction of waves and the beach slope platform. However, at the 2<sup>nd</sup> wave probe array, the reflection coefficients were higher than those found at the 1<sup>st</sup> probe array. The coefficient  $K_r$ , ranged from 4.8% to 37.5% and has an average value of 14.8%. It increases as the water depth decreases. The incident waves in this region are the transmitted waves from the 1<sup>st</sup> wave probe array located (seaward) and are generally smaller than incident waves measured at the 1<sup>st</sup> wave probe because of breaking, dissipation and reflection from the beach slope. Yet, the reflection from the end wall is higher due to the inability of the wave absorber to dissipate the incident wave energy, especially for longer wave periods.

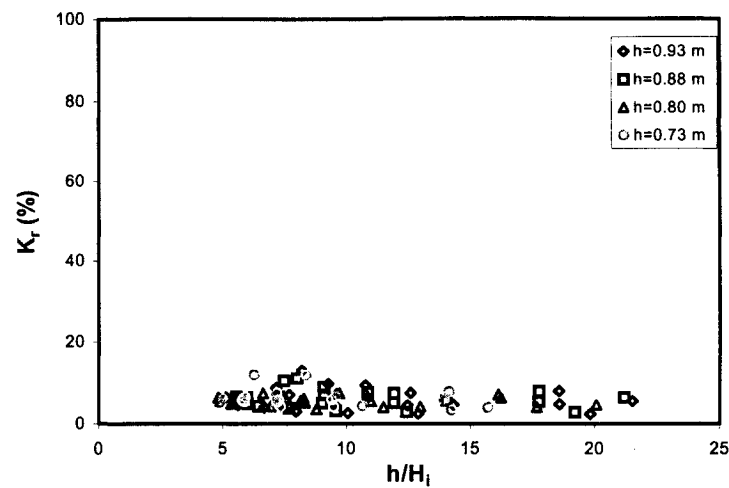


**Figure 5.4.** Reflection characteristics of the beach slope without breakwater (1<sup>st</sup> array).

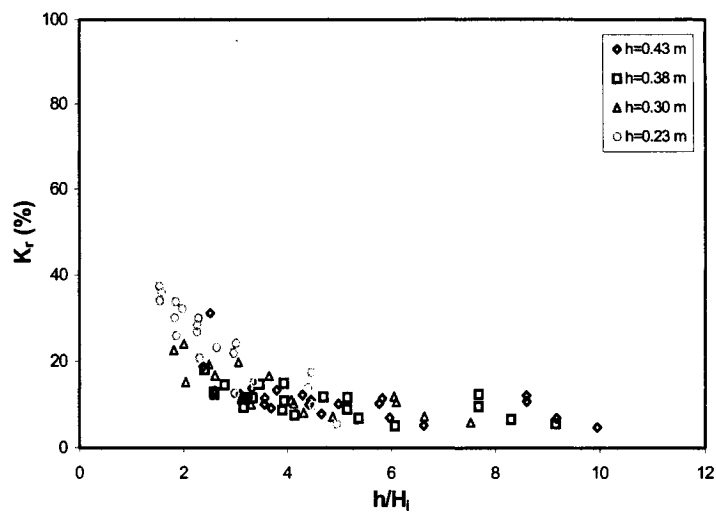


**Figure 5.5.** Reflection characteristics of the energy absorber at rear end of flume without breakwater (2<sup>nd</sup> array).

#### 5.4.2 Transmission Tests

The smaller armour stone ( $D_{50} = 0.034\text{m}$ ) was not stable when larger waves and longer wave periods were generated especially for waves higher than 15cm and wave periods of 2.5s. Several stones were displaced from their initial place.

Considerable damage occurred on the crest and front slope for both submerged and non-submerged conditions. Since these tests were to address the wave transmission processes, attention was paid to preserve the stability of the structure. To prevent the breakwater from damage, incipient damage conditions were used as the limiting factor for the range of tests conducted. Details of the wave test conditions are given in Table 4.3 - 4.4.

**a. Time Series Transformations**

From the zero crossing analysis, it can be seen that the transmitted wave heights are lower than the incident wave heights, but have higher wave frequencies (Figure 5.6). Higher frequency of waves on the crest and behind of the breakwater mostly occurred when the water level was in the vicinity of the crest. For certain incident wave heights, wave setup occurred behind the breakwater due to mass transfer across the crest, which is produced by the breaking wave resulting in return flows to the breakwater. Wave breaking mostly occurs on the front slope and crest for wider crest structures. For narrow crest structures, wave breaking usually occurred behind the structure. Petti and Ruol (1990, 1992) and Liberatore and Petti (1992) found that water setup behind a breakwater results in lower frequency of wave energy in front of the breakwater.

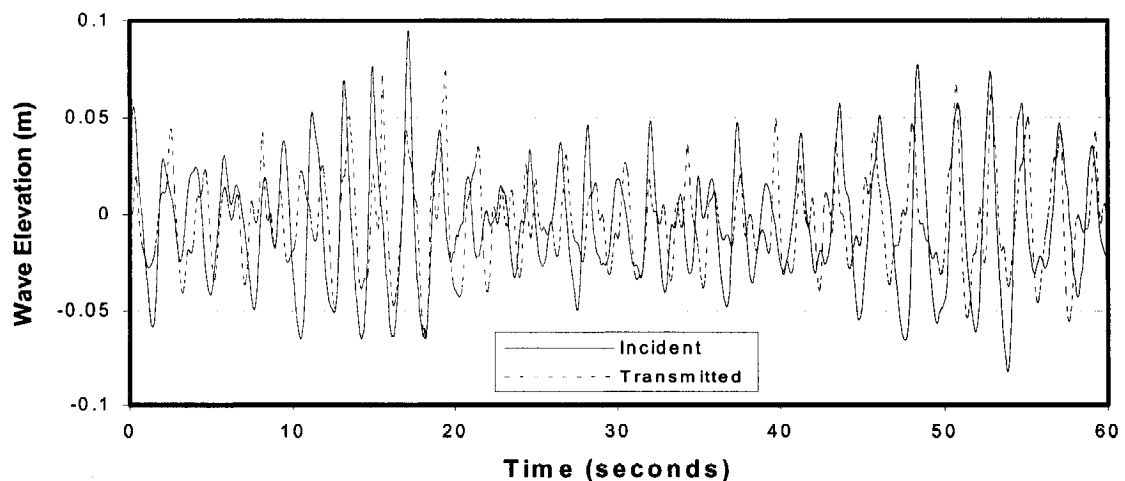
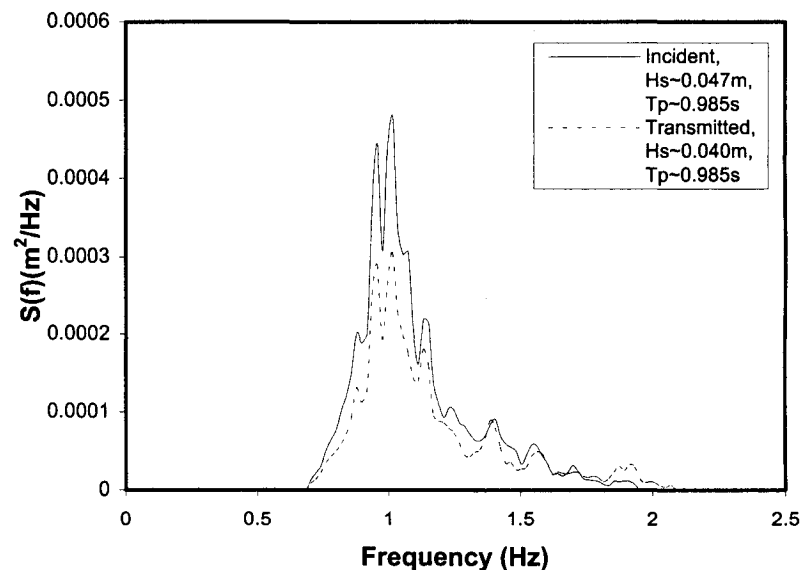


**Figure 5.6.** Typical surface elevation time series record for  $H_{mo} \sim 0.10\text{m}$ ,  $T_p \sim 2.0\text{s}$ , water depth  $h = 0.43\text{m}$ .

### b. Spectral Transformations

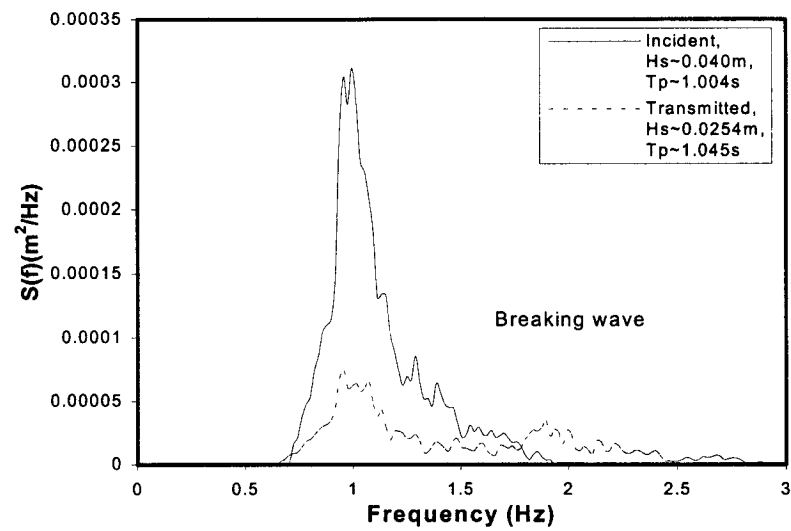
Transfer of energy occurs with the wave transmission process. For the present layout of the breakwater, transmitted waves have higher frequency than incident waves. The generation of higher frequency is associated with breaking condition as shown in Figures 5.7b and 5.7d. It is also shown from these figures that wave breaking reduce the wave energy near the peak frequency. Inspection of Figures 5.7c and 5.7d shows that the frequency of the transmitted wave increases lot more for breaking wave condition when the time period of the incident wave is large. This could be due to the non-linear wave transformation and harmonic generation behind the structure.

Wave breaking is associated with the relative crest height,  $h_c/H_i$ . At breaking condition, it is evident that wave energy decrease considerably that could be observed from the series of Figure 5.7. It can be concluded that relative crest height is an important parameter in spectral transformation, therefore will influence the wave transmission process.

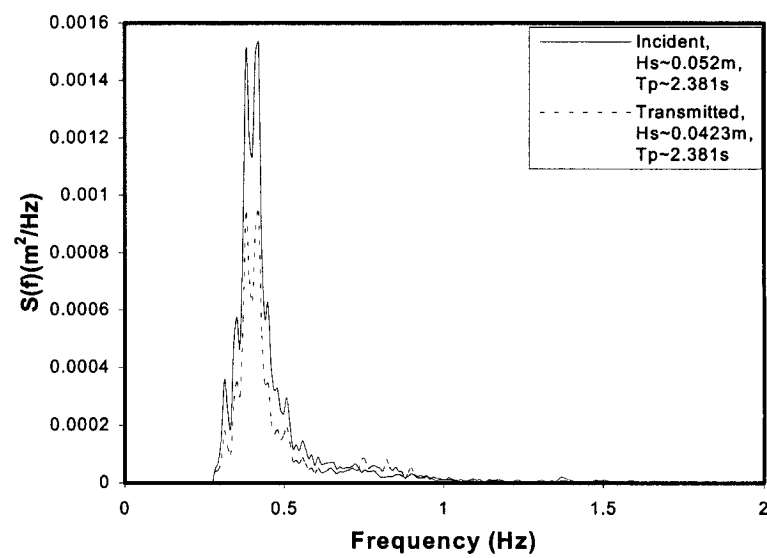


(a)  $B = 0.30m$ ,  $H_{mo} \sim 0.05m$ ,  $T_p \sim 1.0s$ ,  $h_c/h = -0.3$

**Figure 5.7.** Wave spectral transformations in various wave periods and water depths.

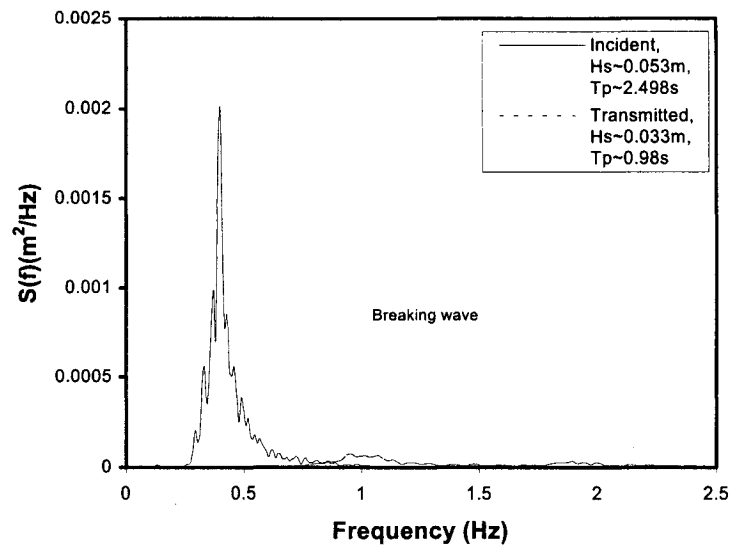


(b)  $B = 0.30\text{m}$ ,  $H_{mo} \sim 0.05\text{m}$ ,  $T_p \sim 1.0\text{s}$ ,  $h_c/h = -0.1$



(c)  $B = 0.30\text{m}$ ,  $H_{mo} \sim 0.05\text{m}$ ,  $T_p \sim 2.5\text{s}$ ,  $h_c/h = -0.3$

**Figure 5.7.** Wave spectral transformations in various wave periods and water depths (Cont'd).



(d)  $B=0.30\text{m}$ ,  $H_{mo}\sim 0.05\text{m}$ ,  $T_p\sim 2.5\text{s}$ ,  $h_c/h=-0.1$

**Figure 5.7.** Wave spectral transformations in various wave periods and water depths (Cont'd).

During wave transmission over the breakwater, some shift occurs in the distribution of wave energy. The spectral shapes of transmitted wave conditions show significant variation from the incident spectral shapes. A parameter usually used to describe the shape of the spectrum is spectral peakedness factor,  $Q_p$ , as described in Chapter 3. Inspection of the  $Q_p$  in Figure 5.8 shows that transmitted waves have lower  $Q_p$  than incident waves indicates that the transmitted waves have wider spectrum than the incident waves, as noted by Beji and Battjes (1993). It is also evident that small change in the relative crest height of breakwater influences  $Q_p$  significantly.

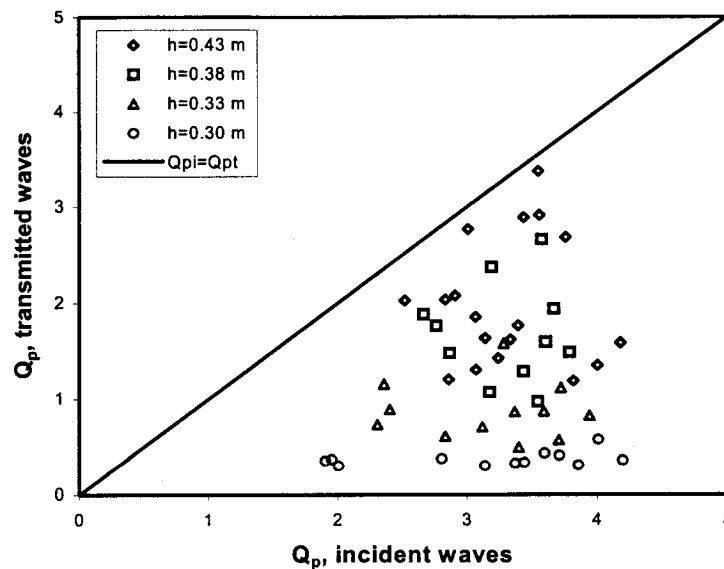


**Figure 5.8.** Comparison of peakedness factor,  $Q_p$ , between the transmitted and incident wave spectra (test series  $T_6$ ).

### c. Wave Transmission

Wave transmission at low crested breakwaters is usually caused by wave overtopping and penetration through the porous structure which effects dissipation of energy. This phenomenon is influenced by many factors such as crest width, water depth, slope angle, permeability and wave characteristics such as wave period and wave height. For 2-D tests, the zero moment wave height,  $H_{m0}$ , is usually used to parameterize the wave height.  $H_{m0}$  is based on the total energy of spectrum measured for the incident waves.

Selected plots of the transmission coefficient as a function of wave height, wave period, water depth, crest width, slope structure, permeability and armour diameter are presented to evaluate the influence of each parameter are shown in Figures 5.9 through 5.18. Figures 5.9 and 5.10 show the influence of water depth, represented by relative crest height,  $h_c/h$ , on  $K_t$  as variable wave heights and wave periods, respectively. The plots show the strong influence of water depth, with higher water depths giving rise to higher  $K_t$  values. Figures 5.11 and 5.12 show the influence

of crest width  $B$  on  $K_t$ . As may be expected, the test results indicate an increase in transmission as the crest width is decreased. In the case of wider crests, the wave breaks somewhere along the crest, resulting in lower transmission.

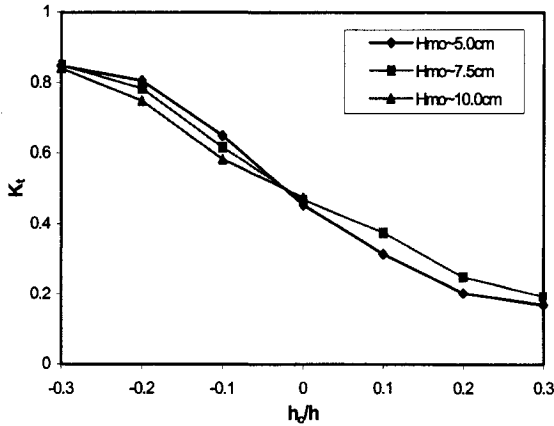


**Figure 5.9.** Influence of relative crest height on transmission (variable wave heights,  $B=0.30\text{m}$  and  $T_p \sim 2\text{s}$ ).

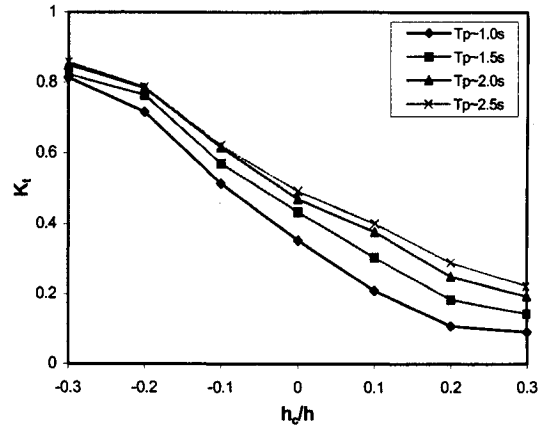


**Figure 5.10.** Influence of relative crest height on transmission (variable wave periods,  $B=0.30\text{m}$  and  $H_{mo} \sim 7.5\text{cm}$ ).

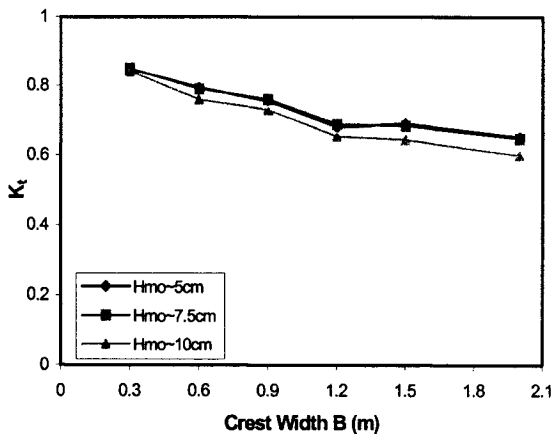


**Figure 5.11.** Influence of crest width on transmission (variable wave height,  $h_c/h=0.3$ ,  $T_p \sim 2\text{s}$ ).

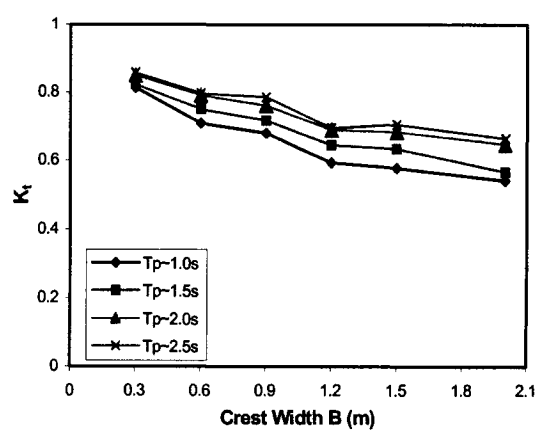


**Figure 5.12.** Influence of crest width on transmission (variable wave periods,  $h_c/h=0.3$ ,  $H_{mo} \sim 7.5\text{cm}$ ).



The influence of armour size is shown in Figures 5.13 and 5.14. For the limited tests carried out, the plots indicate a slight increase in transmission as the armour size is increased. Figures 5.15 and 5.16 indicate the effect of slope on  $K_t$ . For the range of tests conducted, flatter slopes initially result in a slight reduction of  $K_t$  and further reduction in the slope does not result in any appreciable change in the value of  $K_t$ . Only two tests were conducted related to the effect of permeability on  $K_t$ . Based on these two tests, permeable core related to an impermeable core indicates a slight increase on  $K_t$ , as shown in Figures 5.17 and 5.18. Overall, the inspection of the plots shows the strong influence of water depth and wave period in most cases. Longer wave periods have higher wave transmission than shorter wave periods. Wave height also slightly influences the wave transmission. Slope of structure and core permeability has less impact on the wave transmission for the range of variable tested. The crest width appears as one of the important parameters in this process.

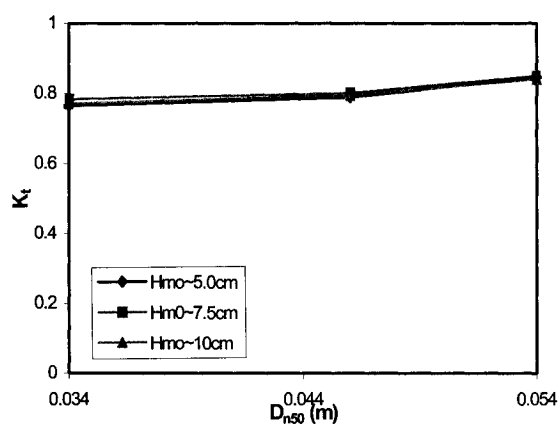


**Figure 5.13.** Influence of armour diameter on transmission (variable wave heights,  $h_c/h = -0.3$ ,  $T_p \sim 2$ s).

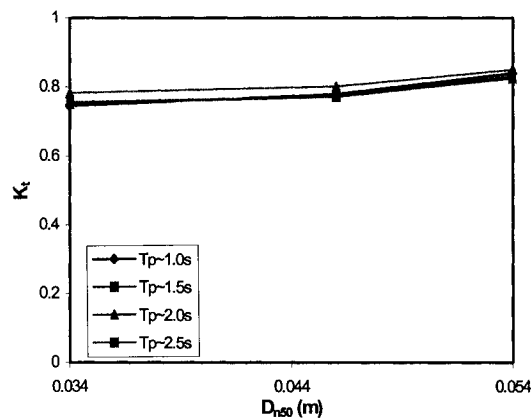


**Figure 5.14.** Influence of armour diameter on transmission (variable wave periods,  $h_c/h = -0.3$ ,  $H_{m0} \sim 7.5$ cm).

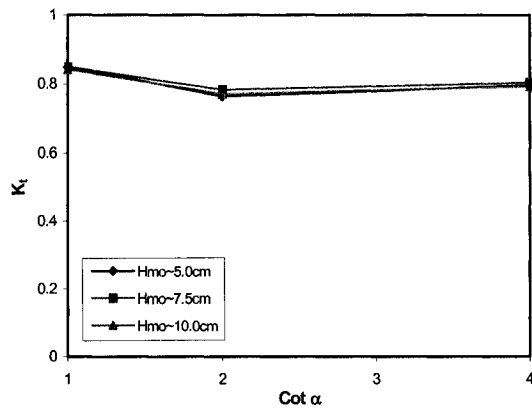


**Figure 5.15.** Influence of slope structure on transmission (variable wave heights,  $h_c/h = -0.3$ ,  $T_p \sim 2\text{s}$ ).

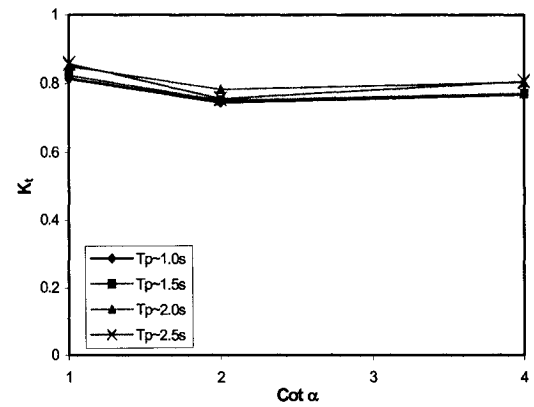


**Figure 5.16.** Influence of slope structure on transmission (variable wave periods,  $h_c/h = -0.3$ ,  $H_{mo} \sim 7.5\text{cm}$ ).

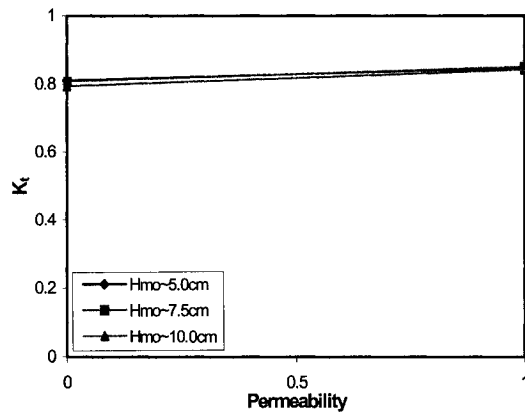


**Figure 5.17.** Influence of permeability on transmission (variable wave heights,  $h_c/h = -0.3$ ,  $T_p \sim 2\text{s}$ ).

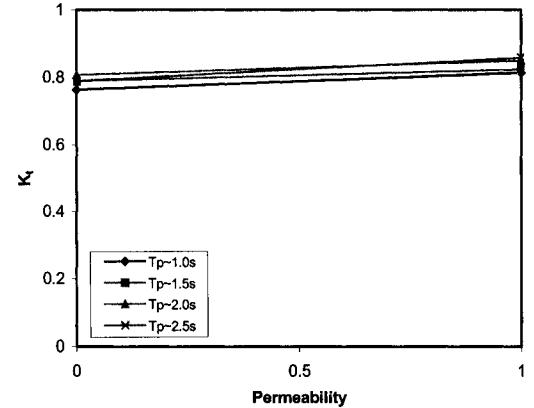


**Figure 5.18.** Influence of permeability on transmission (variable wave periods,  $h_c/h = -0.3$ ,  $H_{mo} \sim 7.5\text{cm}$ ).

#### d. Wave Reflection

Wave reflection is a process of propagation of energy from one direction to another direction when a wave encounters a coastal structure or beach. A part or whole of the wave energy of incident wave is reflected by the structure and moved away from the structure. In the present study, the incident and reflected waves move

in opposite directions. In some cases, the reflected waves and incident waves get superimposed on each other which leads to increase in the magnitude of water particle velocities and the water level in front of the structure.

Selected plots of the reflection coefficient as a function of wave height, wave period, water depth, crest width, slope structure, permeability and armour diameter are presented to evaluate the influence of each parameter, as shown in Figures 5.19 through 5.28. Figures 5.19 and 5.20 give indication of the influence of water depth, represented by  $h_c/h$ , for wave reflection. Lower water depths give higher reflection than higher water depths. This is because for lower water depths, only a small amount of wave energy is transmitted, while the rest is sustained by the breakwater, thus increasing the reflection. Figures 5.21 and 5.22 show the influence of crest width in reflection. The plots indicate a slight decrease in reflection as the crest width is increased. For wider crests, the wave breaks along the crest, resulting in lower reflection. Trends between  $K_r$  and armour size are observed using Figures 5.23 and 5.24. For the limited range of armour size tested, the plots suggest that armour size has no significant influence on reflection could be observed. Tests with three different slopes of the breakwater, as shown in Figures 5.25 and 5.26, indicate that with steeper slopes result in higher  $K_r$  values. The reduction of the reflection for milder slopes may be attributed partially to the combination of friction along the slope and breaking processes. Figures 5.27 and 5.28 show the influence of core permeability on reflection. Based on these two tests, permeable core indicates a slight decrease in  $K_r$  relative to an impermeable core.

Overall, the plots generally show the strong influence of water depth and wave period in most cases. Waves with longer periods have lower wave reflection coefficients,  $K_r$ , than waves with shorter periods. Wave height also slightly influences reflection for the range of variable tested. Slope of the structure and core permeability indicated little contribution to the wave reflection process. The width of the crest also does not appear to be an important parameter in this process for the cases tested.

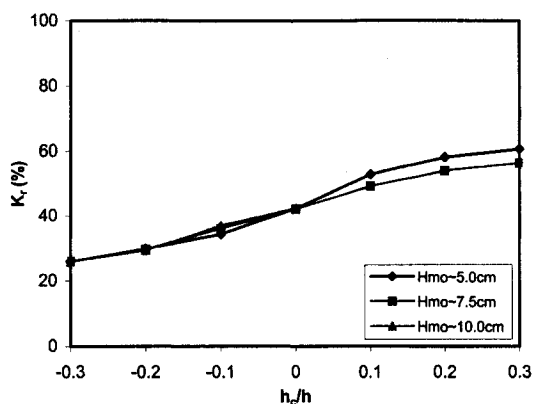


**Figure 5.19.** Influence of relative crest height on Reflection (variable wave heights,  $B=0.30$ m,  $T_p \sim 2$ s).

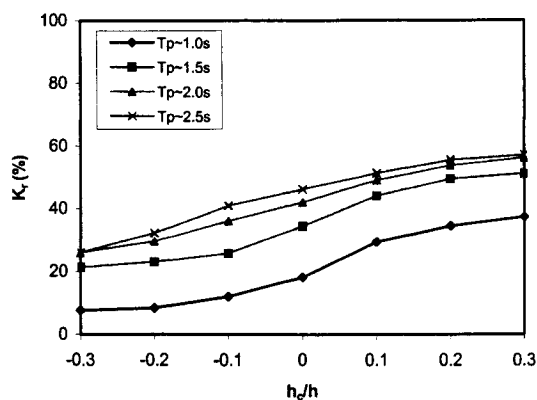


**Figure 5.20.** Influence of relative crest height on reflection (variable wave periods,  $B=0.30$ m,  $H_{m0} \sim 7.5$ cm).

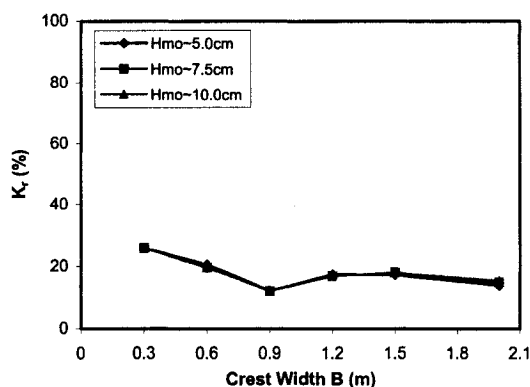


**Figure 5.21.** Influence of crest width on reflection (variable wave heights,  $h_c/h = -0.3$ ,  $T_p \sim 2$ s).

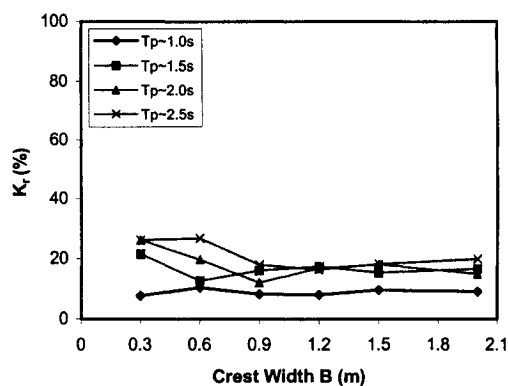


**Figure 5.22.** Influence of crest width on reflection (variable wave periods,  $h_c/h = -0.3$ ,  $H_{m0} \sim 7.5$ cm).

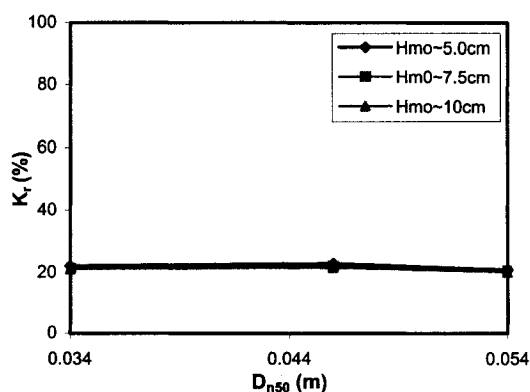


**Figure 5.23.** Influence of armour size on reflection (variable wave heights,  $h_c/h = -0.3$ ,  $T_p \sim 2$ s).

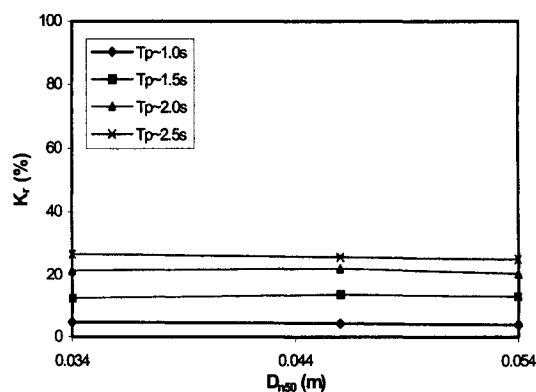


**Figure 5.24.** Influence of armour size on reflection (variable wave periods,  $h_c/h = -0.3$ ,  $H_{m0} \sim 7.5$ cm).

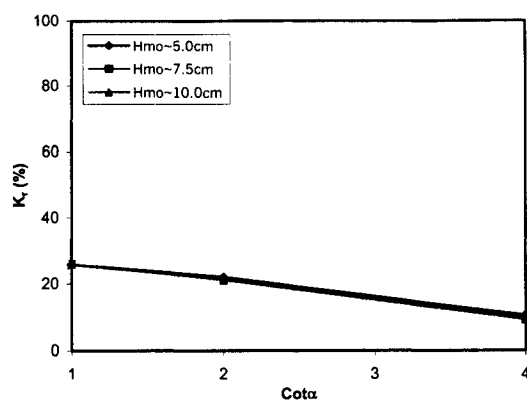


**Figure 5.25.** Influence of slope structure on reflection (variable wave heights,  $h_c/h=0.3$ ,  $T_p \sim 2\text{s}$ ).

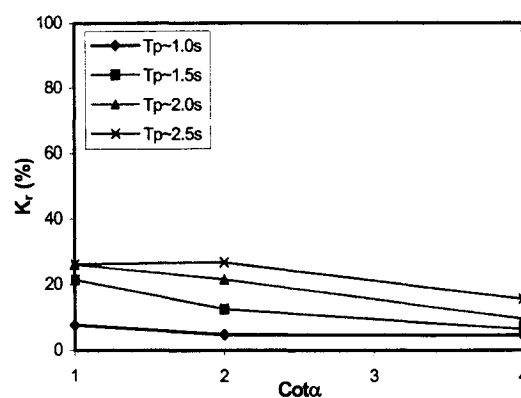


**Figure 5.26.** Influence of slope structure on reflection (variable wave periods,  $h_c/h=0.3$ ,  $H_{mo} \sim 7.5\text{cm}$ ).

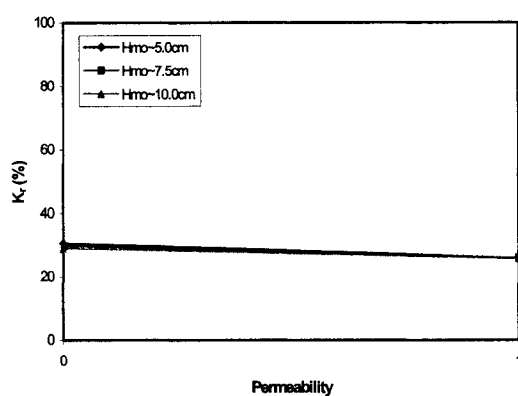


**Figure 5.27.** Influence of permeability on reflection (variable wave heights,  $h_c/h=0.3$ ,  $T_p \sim 2\text{s}$ ).

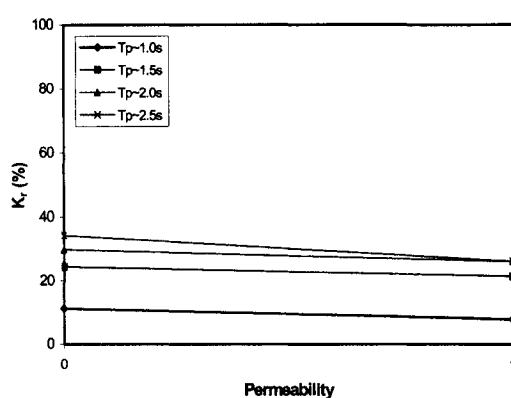


**Figure 5.28.** Influence of permeability on reflection (variable wave periods,  $h_c/h=0.3$ ,  $H_{mo} \sim 7.5\text{cm}$ ).

### 5.4.3 Stability Tests

Initial and final profiles of the structure were plotted after a certain number of waves (3000 waves) attacked the breakwater. It helped to evaluate whether the test variables had any influence on the breakwater stability or not. Only one parameter was varied while preparing each plot in order to observe the influence of that particular parameter. Selected plots of the profiles as a function of wave height, wave period, wave duration, grouped waves, water depth, slope of the structure, and permeability are presented to depict the influence of each parameter. Figure 5.29

shows that erosion of the profile of the breakwater increases with increasing the wave height. This trend was observed in all tests. The effect of the wave period was observed by plotting the initial and final profiles for tests ST5, ST6, and ST7 as shown in Figure 5.30. The figure shows that profile erosion increases with an increase in the wave period. The same trend was observed for all tests.

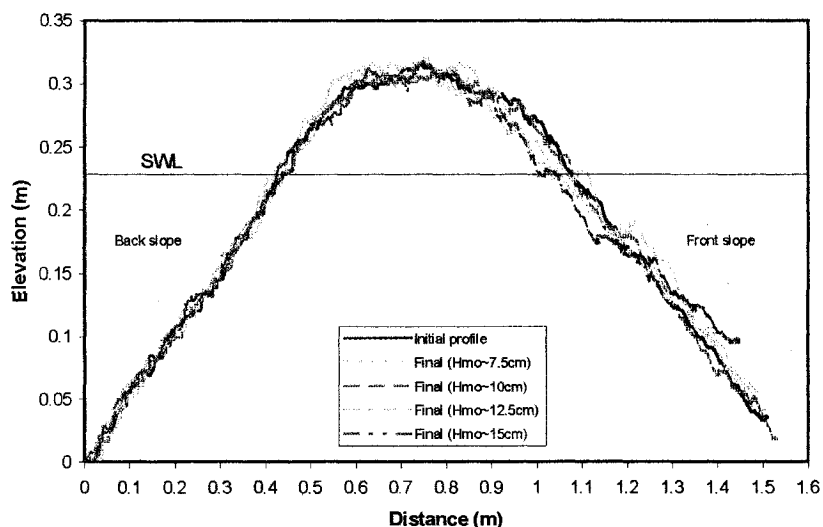


**Figure 5.29.** Influence of wave height on stability of breakwater (tests SH4, SH5, SH6, SH7, water depth = 0.23m).

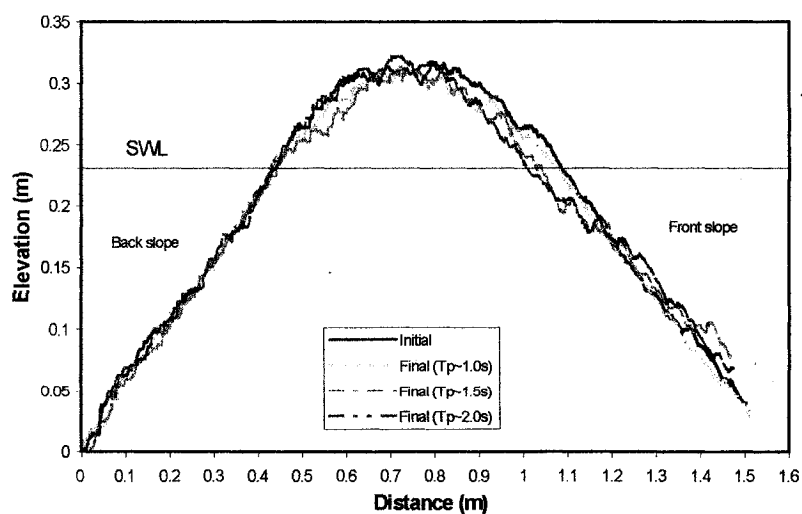


**Figure 5.30.** Influence of wave period on stability of breakwater (tests ST5, ST6, ST7, water depth  $h = 0.23\text{m}$ ).

The observed profiles of the breakwater are plotted in Figure 5.31 to evaluate the influence of water depth. This figure shows that eroded profiles were less affected by increasing the water depth. However, when the water depth was at the crest of the breakwater, the profile eroded the most and is greater than the erosion taking place for water depth either below or above the crest. Influence of grouped waves was evaluated by using Figure 5.32. Initial and final profiles from tests SG4 and SG41 were plotted together. Tests SG4 and SG41 were undertaken using waves having a groupiness factor (GF) of about 0.5 and 1.0. Plots show that an increase in the groupiness factor will result in greater erosion of the area of the profile.

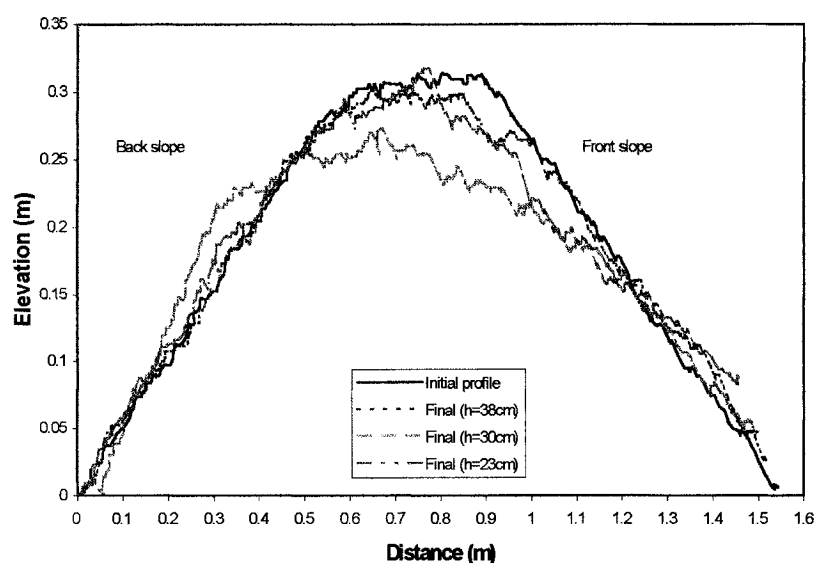


**Figure 5.31.** Influence of water depth on stability of breakwater (tests SD1, SD3, and SD4).

To assess the influence of number of waves on the damage to the structure, Figure 5.33 is plotted. The figure contains the initial and final profiles of tests SN1, SN2 and SN3. In the test series SN, the cross-section of the breakwater was profiled initially as well as after certain number of waves attacked the breakwater (3000 waves) without rebuilding the damaged profile. The final profile of test SN1 was considered as the initial profile of test SN2. The plot shows that number of waves

does significantly affect the profile due to erosion. An increase in the numbers of waves or the wave duration increases the eroded profiles. This is logical since a greater chance of occurrence of higher waves exists when a larger number of irregular waves act on the structure. The effect of  $N$  seems to be minimal on the back slope.

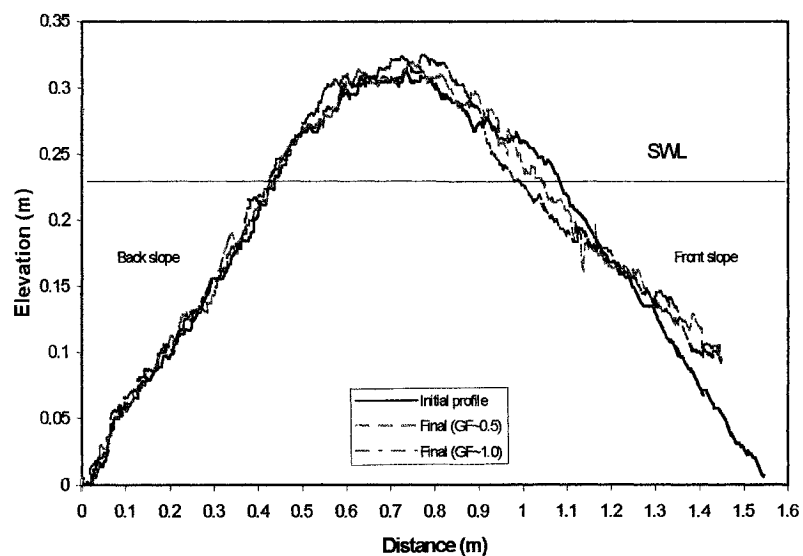


**Figure 5.32.** Influence of grouped waves on stability of breakwater (tests SG4 and SG41).

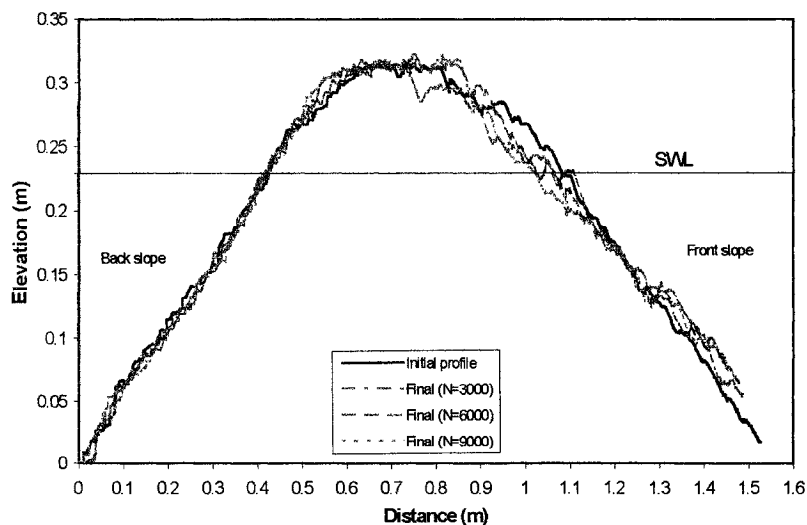


**Figure 5.33.** Influence of wave number (duration) on stability of breakwater (tests SN1, SN2 and SN3).



As described previously, wave climate consists of several wave height and wave period combinations that represent the growth and decay of prototype waves. Hence, initial and final profiles for test of SC1 to SC5 are plotted together to assess the effect of wave climate on the profile erosion as shown in Figure 5.34. The plot shows that the erosion increases significantly near the crest area and the front slope with increases in the wave height and wave period. The rate of erosion also increases with increase in the wave height and wave period.

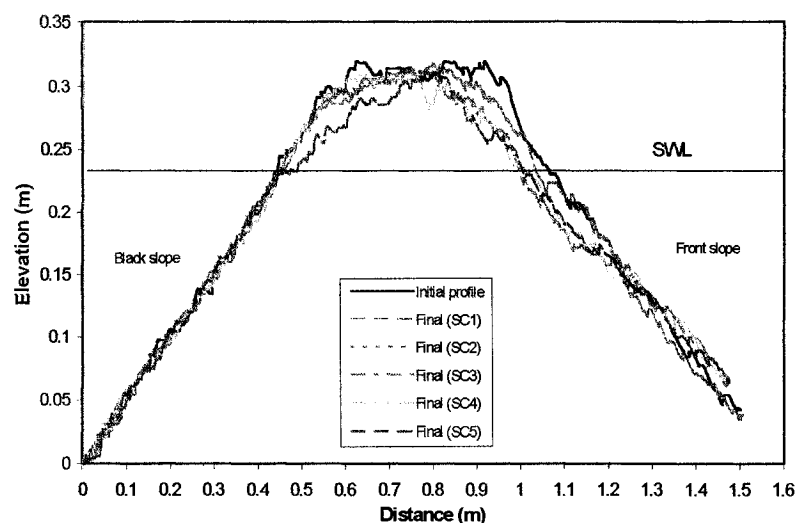


**Figure 5.34.** Influence of wave climate on stability of breakwater (tests SC1, SC2, SC3, SC4, and SC5).

Initial and final profiles from tests SD1 and SS1 are plotted to evaluate the influence of the angle of the slope of the structure on the rate of profile erosion. In test SD1 the breakwater has a slope of 1 on 2 while in test SS1 it has slope of 1 on 1. Figures 5.35 and 5.36 show that steeper slopes do have more erosion than milder slopes, particularly near the front portion of the crest.

Result from tests SH7 and SP2 are plotted together in Figure 5.37 to compare the rate of erosion between permeable core (SH7) and impermeable core (SP2). The figure shows that, in case of an impermeable core, the erosion of the profile increases, all other conditions remaining the same. This behaviour can be due to the fact that the impermeable core does not extend right up to the crest level, leaving the crest area

still exposed to the wave energy. Simultaneously, as the reflection is more intense for the impermeable case, the material eroded near the crest area and tends to slide back on the front slope. This feature is very clearly depicted in Figure 5.37.

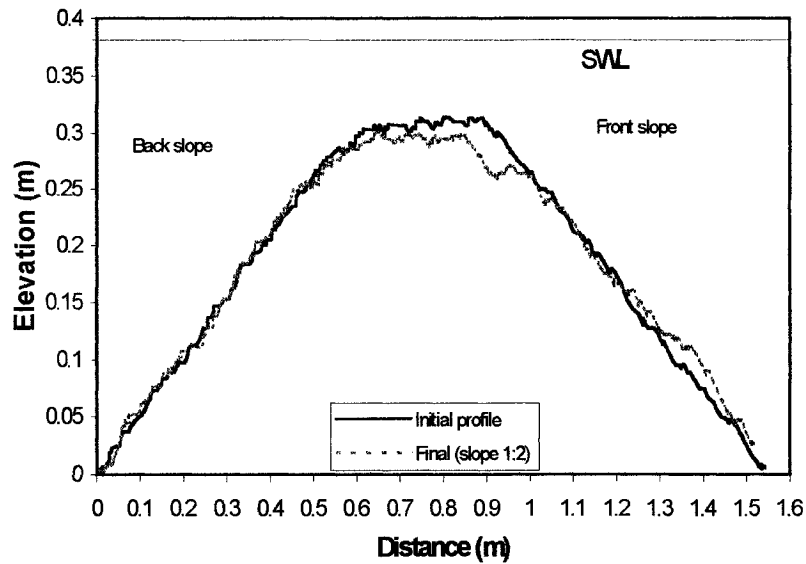


**Figure 5.35.** Influence of slope of structure on stability of breakwater (test SD1, slope 1:2).

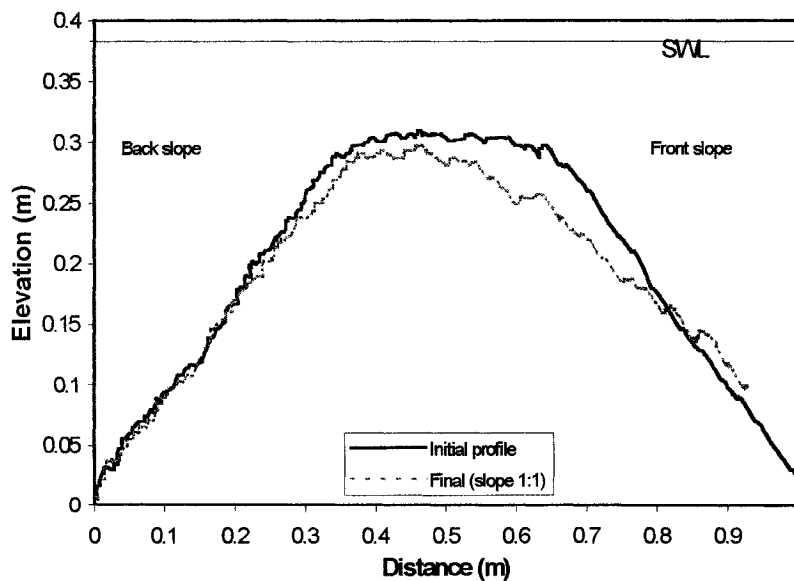


**Figure 5.36.** Influence of slope of structure on stability of breakwater (test SS1, slope 1:1).

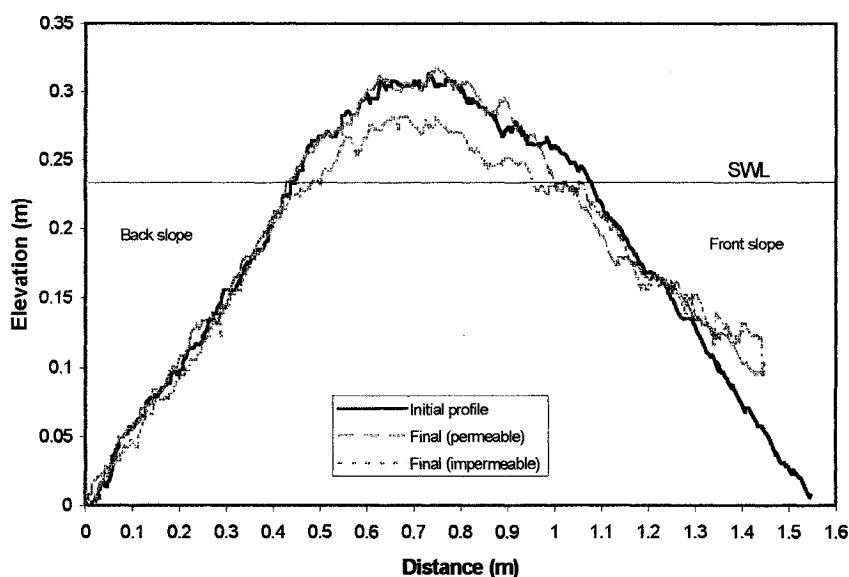


**Figure 5.37.** Influence of core permeability on stability of breakwater (tests SH7 and SP2).

## 5.5 WAVE TRANSMISSION, REFLECTION AND STABILITY

This section describes, in more detail, the influence of each variable on wave transmission and reflection processes at low crested breakwaters by considering various dimensionless variables in graphical form. Several important plots are presented and comparisons between present data and existing design equations are also presented and evaluated.

### 5.5.1 Wave Transmission

#### a. Effect of Relative Crest Height, $h_c/H_i$

It was found that transmission coefficient,  $K_t$ , is primarily influenced by the relative crest height,  $h_c/H_i$ , as shown on selected plots in section 5.4.2. Therefore, this variable is used to observe the effects of other variables. Figure 5.38 is plotted to observe the relationship between the transmission coefficients for the test series T1 as

a function of dimensionless relative crest height. Results show that use of relative crest height as the only variable gives a good amount of scatter of the data which cannot be attributed to experimental errors alone. From the figure it can also be observed that in all cases for  $-1.5 \leq h_c/H_i \leq 1.0$ , the relative crest height strongly influences  $K_t$ . The relative crest height has less influence on  $K_t$  for  $h_c/H_i \leq -1.5$  and  $h_c/H_i \geq 1.0$ , indicates that transmission is no longer influenced by the water depth. Using all of the data, a plot of the transmission coefficient against the relative crest height is obtained as shown in Figure 5.39. The result shows that data are scattered wide, but a clear trend can be observed. This indicated the influence of other independent variables, which significantly affect the transmission coefficient. It can also be observed that for  $h_c = 0$ , that is when water level is at the crest, a large spread in the value of  $K_t$  take place because of loss of influence of wave height. Therefore attempts are made to describe the relationship between the coefficient of transmission and other relevant variables.

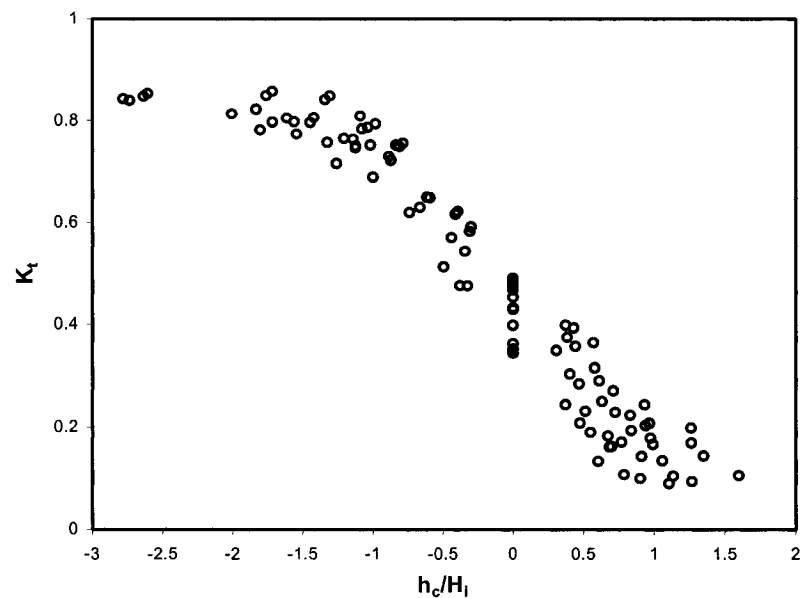


**Figure 5.38.** Wave transmission as a function of relative crest height,  $h_c/H_i$  (Test series T1).

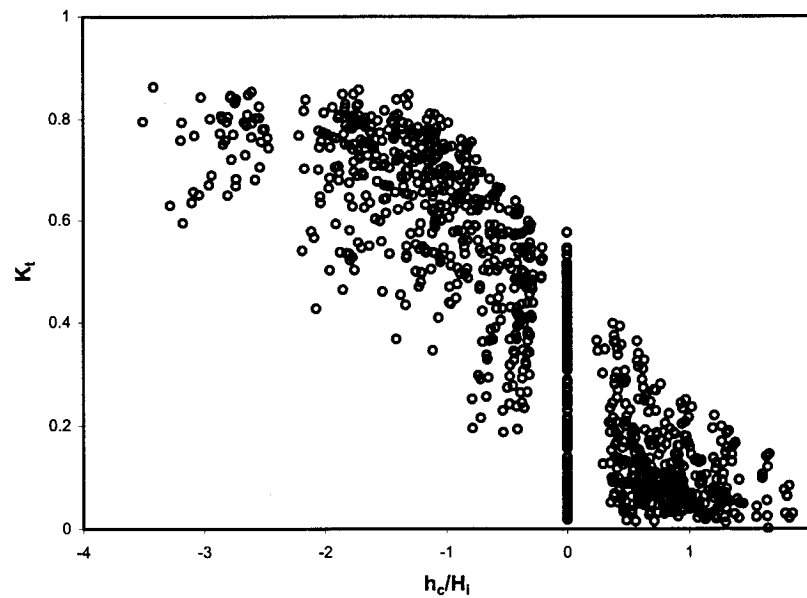


**Figure 5.39.** Wave transmission coefficients as a function of relative crest height,  $h_c/H_i$  (all test data).

An alternative form of the relative crest height was introduced by van der Meer (1991) in the form of  $h_c/D_{50}$ . The role of nominal diameter is usually found to express the wave height that attacks the structure. The dimensionless combination is known as the stability number,  $H_s/\Delta D_{50}$ . Van der Meer assumes that the nominal diameter,  $D_{50}$ , can be used to characterize both the wave height and the crest height in a dimensionless way.

Plotting the transmission coefficient against  $h_c/D_{50}$  for test series T1, Figure 5.40 is obtained. The data are grouped according to wave period,  $T_p$ . Similar trends, as previously shown in Figure 5.40 are visible, where the relative crest height strongly influences the wave transmission. It is also clearly seen that longer wave periods results in higher transmission coefficients. In the range of  $h_c/D_{50}$  between +2 and -2, the transmission coefficients increase rapidly. This range may be important for describing wave transmission process.

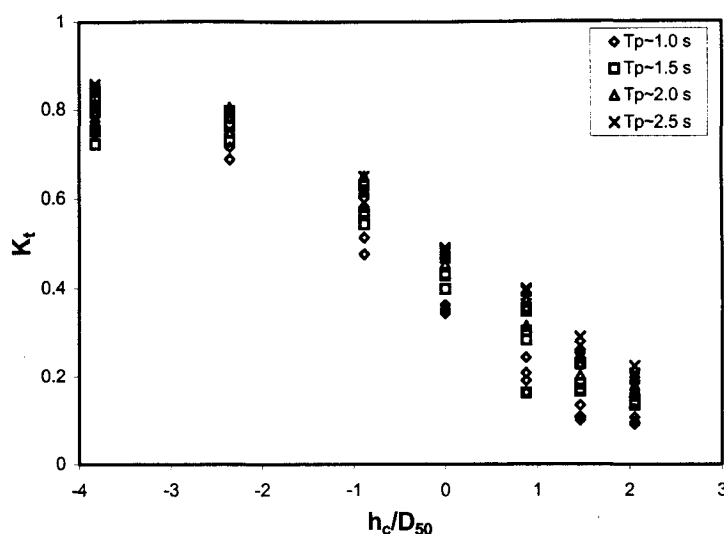


**Figure 5.40.** Wave transmission coefficients as a function of relative crest height,  $h_c/D_{50}$  for T1 test series.

#### b. Effect of Wave Steepness

The effect of wave steepness on transmission is evaluated using Figures 5.41 and 5.42. The relative crest height for different representative wave steepness,  $s_p$ , is plotted against  $K_t$ . The wave height and wavelength are combined in evaluating the representative wave steepness parameter. The representative wave steepness is the value obtained by using the wave length corresponding to local depth. A value of  $s_p < 0.02$  represents long waves, while  $s_p > 0.04$  represents short waves. Figure 5.41 shows that combination of the relative crest height,  $h_c/H_i$ , and wave steepness could represent well the influence of wave steepness on transmission. For non-submerged conditions, lower wave steepness (longer wave period) gives higher transmission than larger wave steepness values. There is no clear trend observed to the influence of the wave steepness for submerged conditions. Figure 5.42 shows that for lower wave steepness, submerged conditions yield a high wave transmission as no breaking of waves take place. Usually the value of  $s_p > 0.05$  will cause wave breaking resulting in lower transmission as shown on the plot.

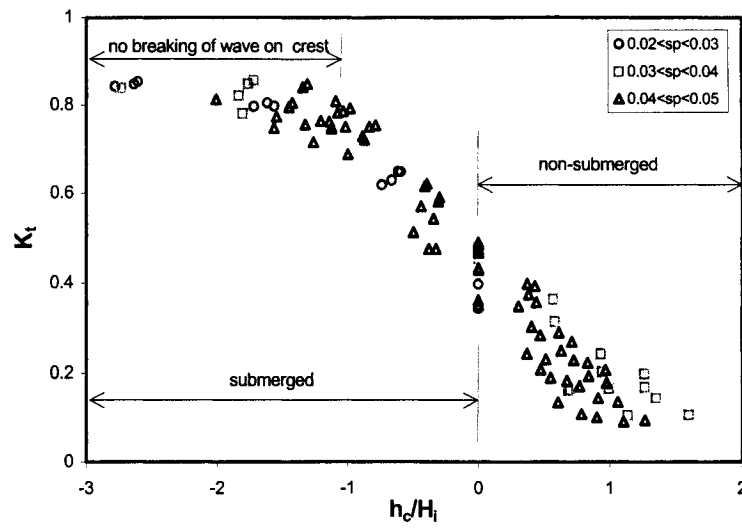


**Figure 5.41.** Effect of wave steepness related to  $h_c/H_i$  on transmission (test series T1).

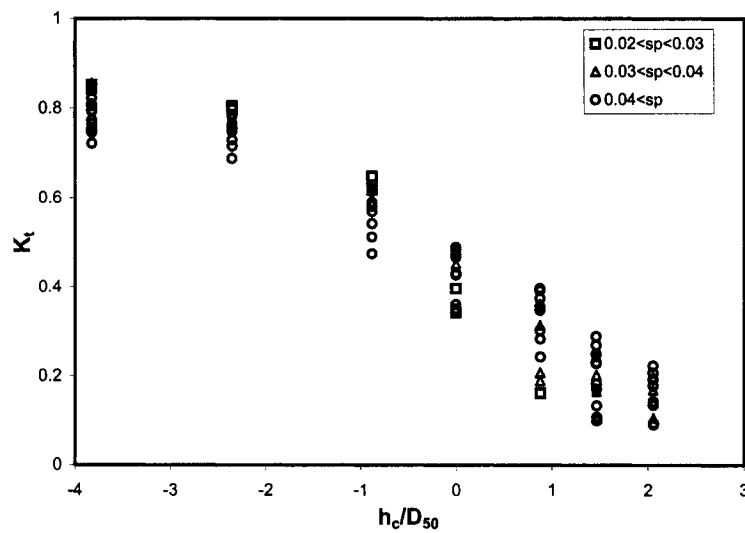


**Figure 5.42.** Effect of wave steepness related to  $h_c/D_{50}$  on transmission (test series T1).

In order to observe the effects of wave height alone, Figure 5.43 is plotted showing  $K_t$  as a function of relative crest height,  $h_c/H_i$ , for different relative wave

height,  $H_i/D_{50}$ . It can be observed that smaller relative wave height results in lower transmission for submerged conditions, whereas the magnitude of the relative wave height has insignificant effect on the transmission coefficient when the water level is below the crest of the breakwater, i.e.  $h_c/H_i > 0$ .

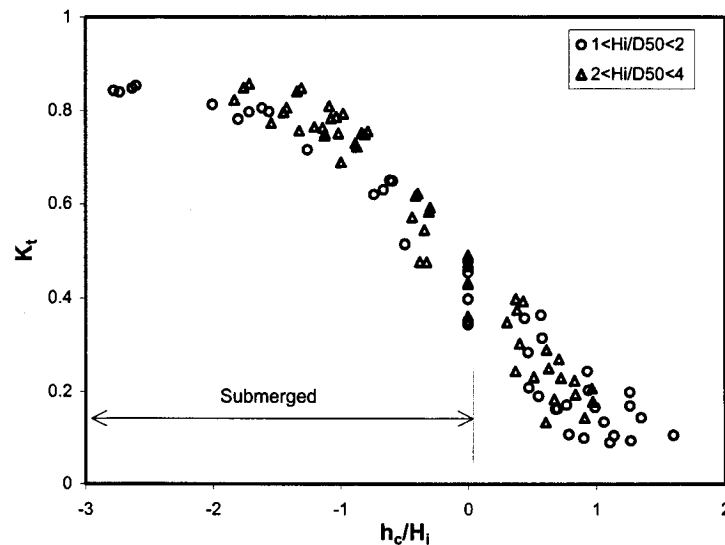


**Figure 5.43.** Effect of relative wave height on transmission (test series T1).

### c. Effect of Crest Width

The effect of the crest width on  $K_t$  is observed by plotting the transmission coefficient against the relative crest height,  $h_c/H_i$ , for different values of relative crest width,  $B/H_i$ , as shown in Figure 5.44. The results show that crest width has a significant effect on transmission. Narrower crest widths result in higher transmission. The term  $B/H_i$  can be used as an indicator of the nature of overtopping. Lower  $B/H_i$  conditions result in waves breaking into the lee of the structure, whereas, higher  $B/H_i$  conditions result in waves breaking at the crest. The first condition leads to higher transmission since a substantial amount of the wave energy is transmitted to the lee side of the breakwater while the second condition results in lower transmission as the wave energy gets dissipated over the crest. These assumptions are reasonable



for submerged conditions where water level is above the crest. For a water level below the crest, the effect of flow within the body of the structure may be an important factor in determining  $K_t$ . Hence,  $D_{50}$ , which can account for permeability of the body, crest width,  $B$ , that indicates the importance of frictional resistance and the wave length,  $L_p$ , are likely to have an important role in this case. Increasing the wavelength and permeability will increase the transmission while increasing the crest width will decrease the transmission. The combined effect of the three parameters is discussed in section g.

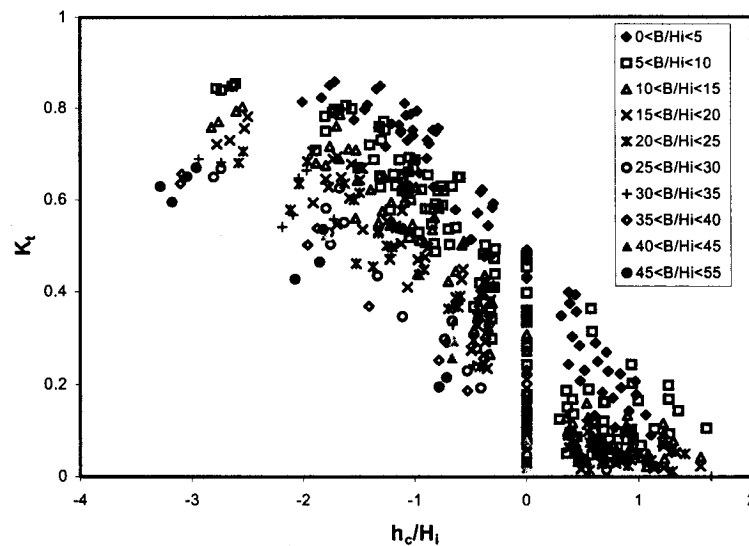


**Figure 5.44.** Effect of dimensionless crest width  $B/H_i$  on transmission (tests series T1-T6).

**d. Effect of Gradation (armour size)**

Figure 5.45 shows the effect of non-dimensional armour size,  $D_{50}/H_i$ , on wave transmission. A specific range was chosen for non-dimensional armour size for easier control. For submerged conditions, it appears that the non-dimensional armour size does not give significantly influence wave transmission. Result shows no definite trend associated with the variation in  $D_{50}/H_i$ . For non-submerged conditions, a definite trend is evident in this plot with increasing wave transmission associated with

larger dimensionless armour size. This phenomenon could be explained in physical terms by the difference in flow through the structure. For structures with a larger armour size, the water easily flows through the structure. This increases the transmission on the structure.

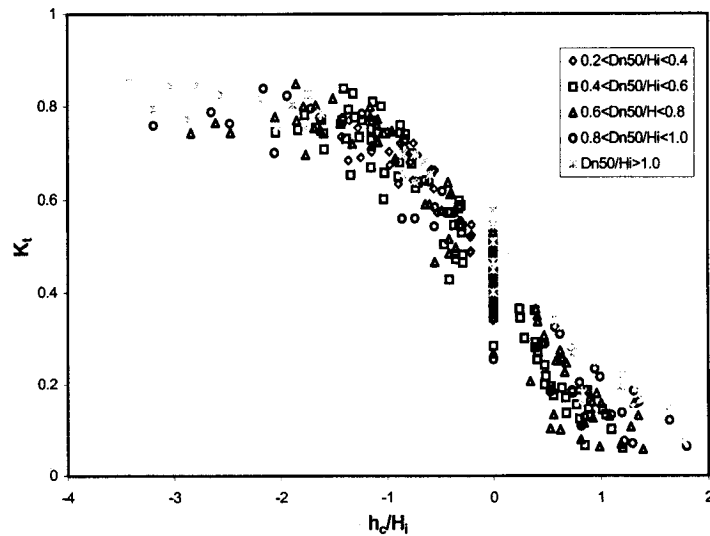


**Figure 5.45.** Effect of dimensionless armour size on transmission (tests series T12, W22 and W32).

**e. Effect of the Breakwater Slope**

Figure 5.46 shows the influence of breakwater slope on the transmission process. The plot shows that a breakwater with the steeper slope ( $\cot \alpha=1$ ) has a higher coefficient of transmission than the breakwater with milder slopes, for both submerged and non-submerged conditions, though the effect of slope is more pronounced for non-submerged breakwaters. In physical terms, this difference can be explained by the frictional effects. The energy of the waves propagating along the slope will get dissipated by surface friction. On milder slopes the flow travels longer distances against friction, wave transmission will decrease. This will be true for coarser armour as well.

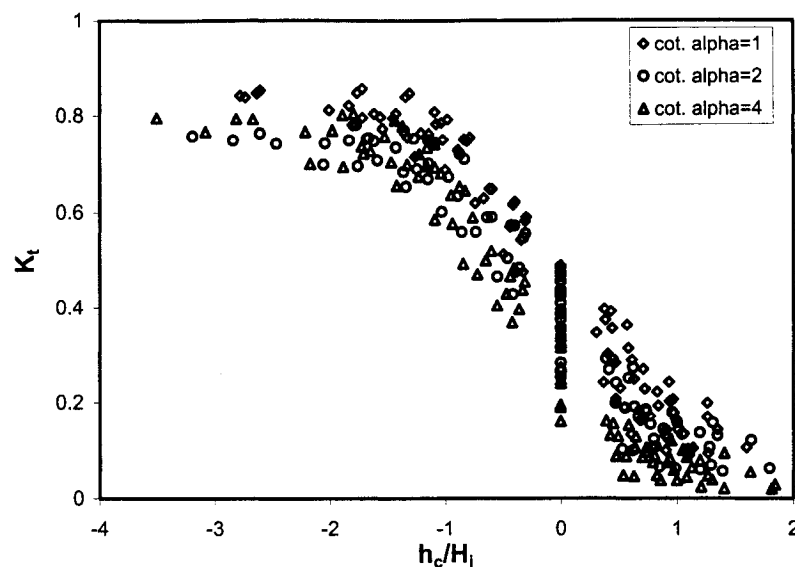


**Figure 5.46.** Effect of breakwater slope on wave transmission of breakwater (tests series T1, T12 and T14).

#### f. Effect of Core Permeability

Permeable and impermeable cores were tested to study the effect of core permeability. For the permeable condition the core comprised of crushed stones with  $D_{50} = 0.0165\text{m}$ , while for the impermeable condition, a plywood board of height 23.2 cm was placed within the core. Obviously, for impermeable submerged breakwaters, the wave is transmitted over the crest of the breakwater. For non-submerged breakwaters, where water level lies below the crest, transmission can occur just by wave overtopping. In the case of permeable core, wave transmission also occurs through the body of the structure resulting in higher values of transmission coefficient than through the impermeable structure.

The structures investigated during test series T1 and IM1 represent two versions of rubble mound that differ only in respect to the permeability of the core as considered in section 4.1.2. A comparison of the wave transmission under similar conditions during these two test series indicate that the permeable core generally gives rise to greater transmission than impermeable core. The test results are plotted

in Figure 5.47, showing that the permeable breakwater indeed has a higher transmission coefficient than the impermeable breakwater for both submerged and non-submerged conditions. The difference is more pronounced for  $h_c/H_i > -1.0$ . It can be explained that for permeable breakwater at submerged conditions, a part of the wave energy is transmitted over the crest, while the other part will be transmitted through the structure. For impermeable conditions, waves are transmitted only over the crest, resulting in lower transmission.

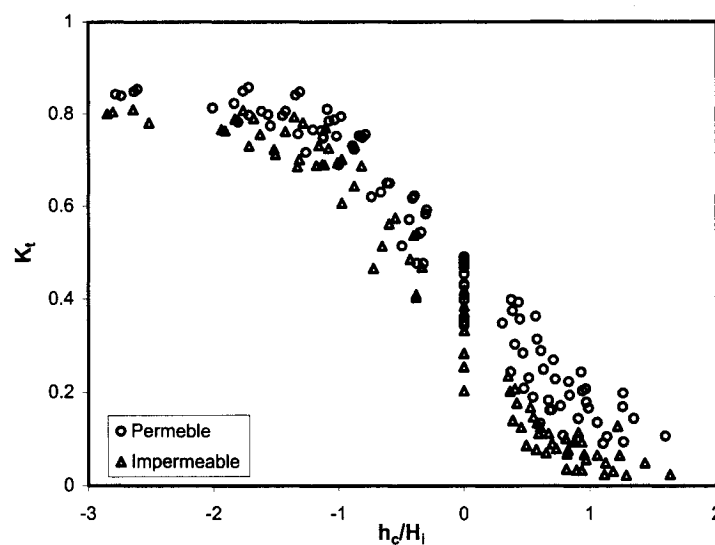


**Figure 5. 47.** Effect of core permeability on transmission (tests series T1 and IM1).

**g. Effect of Surface Friction and Internal Flow**

Considering the basic dimensionless variables as discussed previously (see Chapter 3), it is also possible that those dimensionless variables have significant influence if combined with each other to form new variables. It was mentioned previously that dissipation of wave energy by the breakwater is associated with friction on the surface and the flow within the interstices of the structure. The friction term, which is related to the wave transmission, could be represented by combining the relative crest height,  $h_c/D_{50}$ , and the relative wave height,  $H_i/B$ . In the physical

sense, surface friction is proportional to the roughness of the surface layer, hence to the diameter of the armour. The amount of energy loss is proportional to the length of the surface and the amount of energy transmitted, hence to the crest width of the breakwater, wave height and water depth.

The effective flows through the structure increase as the crest width decreases and the nominal diameter of stone increases. Larger diameters lead to increase in void volume increasing flow within the structure. The internal flow term can be represented as  $B^2/L_p D_{50}$ . Figures 5.48 and 5.49 show the influence of the surface friction and the internal flows on the relationship between  $K_t$  and the relative crest height,  $h_c/H_i$ .

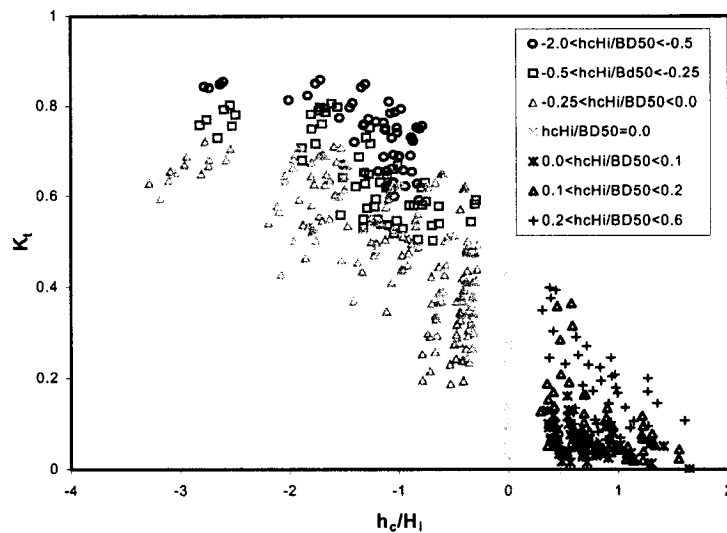


**Figure 5.48.** Effect of surface friction on transmission (tests series T1-T6).

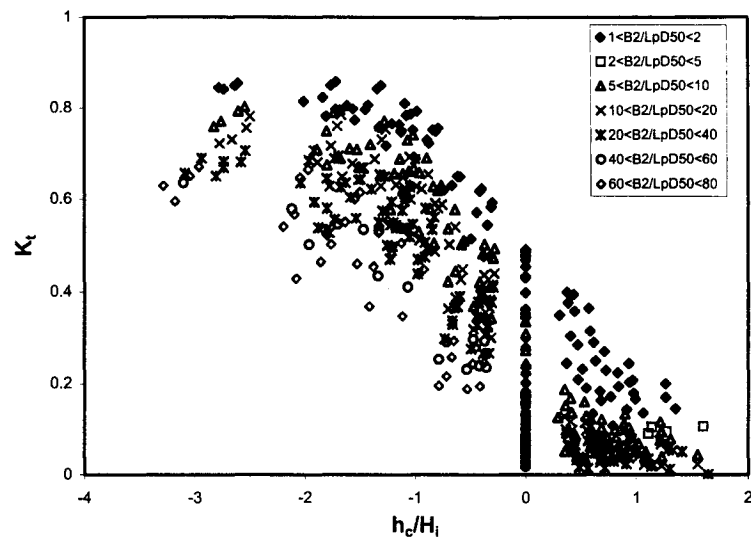


**Figure 5.49.** Effect of the internal flows on transmission (tests series T1-T6).

#### h. Comparison with Existing Design Equations

A comparison of test data with existing design equations (Ahrens 1987, van der Meer 1991, Seabrook and Hall, 1998) was made by comparing calculated  $K_t$  values with measured  $K_t$  of the test data for various crest widths. The design equation by Ahrens (1987) predicts the transmission past reef type breakwaters and is given in the following form.

$$K_t = \left\{ 1.0 + \left( \frac{h_s}{h} \right)^{C_1} \left( \frac{A_v}{hL_p} \right)^{C_2} \exp \left( C_3 \left( \frac{F}{H_{mo}} \right) + C_4 \left( \frac{A_v^{1.5}}{D_{50}^2 L_p} \right) \right) \right\}^{-1}, \text{ for } \frac{F}{H_{mo}} < 1.0 \quad [5.1]$$

where:

- $D_{50}$  = nominal diameter of breakwater material (m)
- $A_v$  = average cross section area of breakwater ( $m^2$ )
- $L_p$  = local wave length (m)
- $F$  = freeboard (i.e.  $h_c$ ) (m)

$C_1, C_2, C_3$  and  $C_4$  are the empirical coefficients 1.188, 0.261, 0.529 and 0.00551 respectively.

The reef breakwater was a homogeneous rubble mound structure designed to reshape itself to a stable profile after initial construction. The transmission equation was found to be well bounded, and in general, the trends predicted are consistent with existing theories, as shown in Figure 5.50. Results indicate that the Ahrens' equation predicts  $K_t$  relatively well for  $K_t > 0.3$ , but overestimates for lower values of  $K_t$ . Inspection of the data further indicates that lower  $K_t$  values occur for low submergence, higher wave height, shorter wave period and wider crest for the submerged conditions. For non-submerged conditions, lower  $K_t$  occurs for lower wave height, shorter wave period, wider crest and impermeable core. The discrepancy of Ahrens' equation for lower  $K_t$  probably arises due to the exclusion of permeability in the equation. However, for  $K_t > 0.3$ , Equation [5.1] can yield reliable answers.

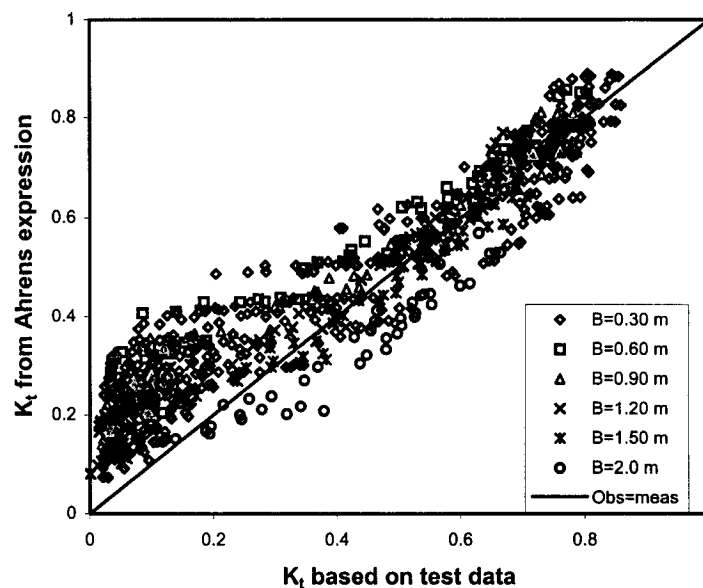


**Figure 5.50.** Comparison of Ahrens' Equation and present test data.

Van der Meer (1991) and van der Meer and Daemen (1994) have developed a design equation for wave transmission at various non-submerged and submerged breakwaters (see Eq. [2.34]). Comparison of transmission coefficient from the

present data and the ones predicted by van der Meer's equation is shown in Figure 5.51. The agreement is relatively good only for narrow crested structures. Transmission over wider crests is not well predicted, since the equation produces negative values of  $K_t$ . This is because the existing design equation proposed earlier was developed based on a limited range of breakwater configurations. In particular, crest width has not been varied over a wide range of tests.

Seabrook and Hall (1998) have developed a design equation for defining the transmission process for submerged breakwaters as presented in Eq. [2.40] of Chapter 2. The equation represents effects of wave breaking, wave overtopping, frictional losses and internal flow. Using all test data for submerged conditions, comparison of Seabrook and Hall's equation and present data was made and shown in Figure 5.52. The result indicates that the equation predicts  $K_t$  relatively well, although under certain conditions Seabrook and Hall's equation predicts  $K_t$  higher than the test data. Part of the differences maybe because the test data include the effect of varied permeability of the core and nominal diameter of armour size.

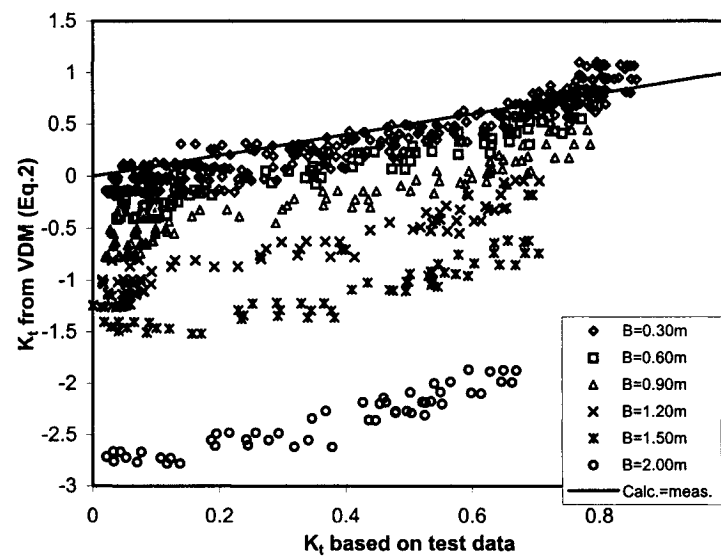


**Figure 5.51.** Comparison of van der Meer's values and present test data for various crest width.



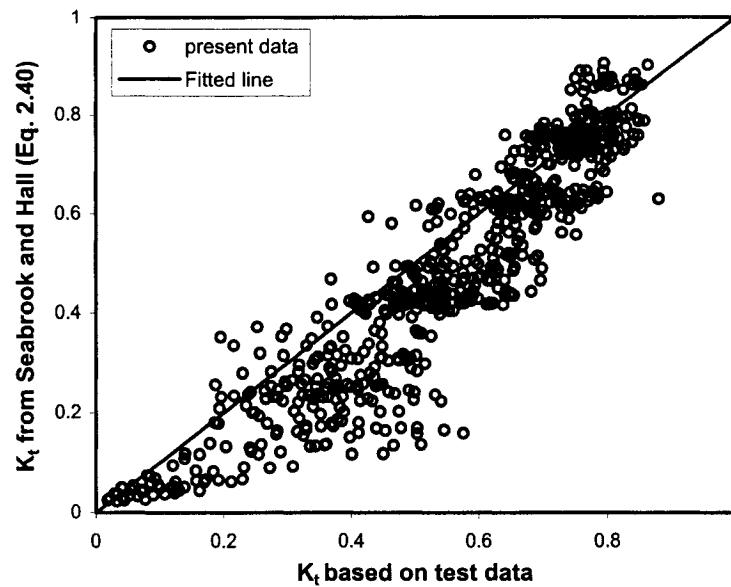


**Figure 5.52.** Comparison of Seabrook's Equation and present test data for submerged conditions.

## 5.5.2 Wave Reflection

### a. Effect of Surf Similarity Parameter

Analysis of wave reflection by the breakwater was undertaken by considering various dimensionless variables in graphical form to assess their influence on the reflection process. The surf similarity parameter,  $\xi$ , is commonly used to parameterize wave reflection. This parameter is represented by a combination of the wave height, wave period and the slope angle. The surf similarity parameter represents the type of wave breaking. There is a physical limit to the steepness of the waves,  $H/L$ . When the physical limit is exceeded, the wave breaks and dissipates its energy. Therefore, this variable was used to observe the effect of other variables.

A plot of  $K_r$  versus surf similarity parameter for a slope 1:1 as a function of water depth for test series T1 is given in Figure 5.53. The general trend of the data shows that for low values of surf similarity parameter,  $\xi$ , (i.e. in the breaking wave regime), reflection increases rapidly with  $\xi$ , whereas increase in  $\xi$  beyond 8 or so

causes no further increase in  $K_r$ . The reduction in wave energy reflection for  $\xi$  less than 8 is primarily due to larger wave transmission, surface friction and turbulence effects of the structure. From Figure 5.53, the effect of water depth is clearly visible. Increasing the water depth will decrease reflection due to a part of the wave energy being transmitted and dissipated over the crest. The zero-submergence case clearly brings out the role of submergence on  $K_r$ .

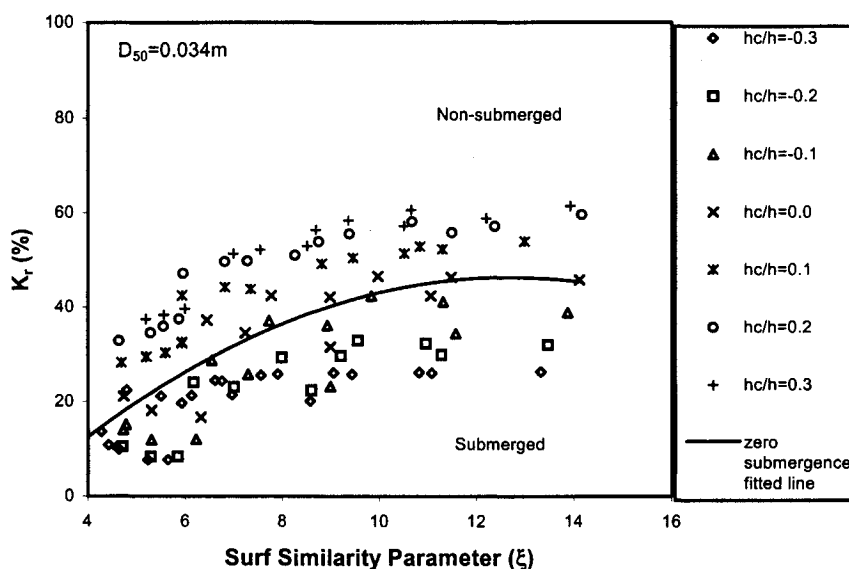


**Figure 5.53.** Effect of surf similarity on reflection for different water depths (test series T1).

#### b. Effect of Crest Width

The dependence of wave reflection on crest width is shown in Figure 5.54. The trend of the data seems to indicate that increasing the surf similarity parameter results in an increase of the wave reflection. It is also observed that the crest width does not significantly influence the wave reflection. It can be explained that when water depth lies below the crest, wave reflection is mostly influenced by the front slope while for overtopped and submerged conditions, wave transformation is mostly influenced by wave breaking and surface friction in which  $B$  has a very minor role.

That the reflection coefficient  $K_r$  depends on the surf similarity parameter and relative depth of submergence is clearly depicted in Figure 5.55 by a family of curves drawn for each submergence ratio. As  $B$  has no effect on  $K_r$ , data for different crest width are included in drawing the curves.

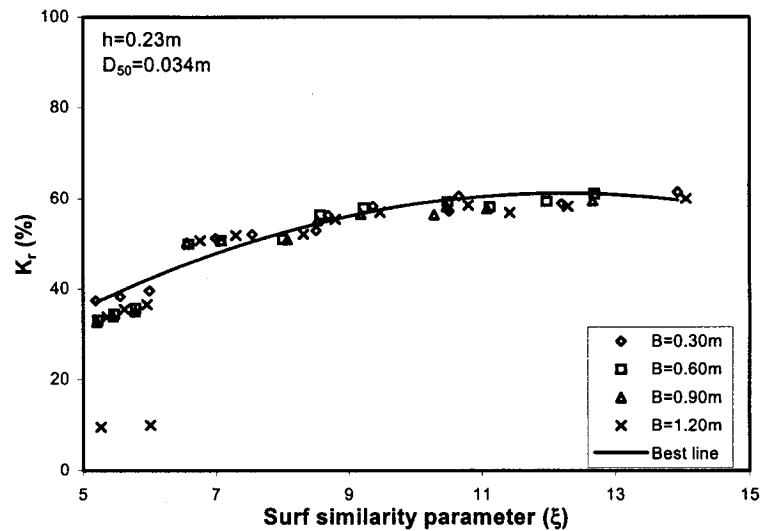


Figure 5.54. Effect of crest width on reflection (tests series T1, T2, T3 and T4).

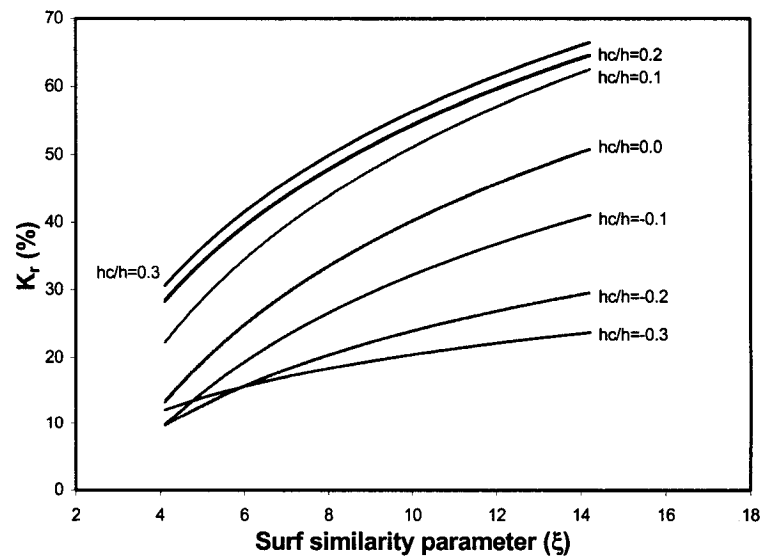


Figure 5.55. Effect of submergence on  $K_r$ - $\xi$  relationship.

**c. Effect of Armour Size**

A plot of the wave reflection coefficient against the surf similarity parameter,  $\xi$ , as a function of armour size  $D_{50}$  is shown in Figure 5.56 using the data of test series T12, W22 and W32 for a water depth of 0.23m. The surface roughness influences the amount of energy loss due to friction. Increasing the surface roughness will increase the amount of energy loss and the energy is scattered thereby decreasing wave reflection. By setting other parameters constant, increasing the slope angle ( $\cot \alpha$ ) results in the increase of the length of surface roughness, thereby decreasing wave reflection. The plot shows that armour size effect is small and may be neglected.

**d. Effect of Water Depth**

As shown in Figures 5.53 and 5.55, the effect of water depth is clearly visible. Increasing the water depth will decrease the wave reflection due to increasing wave transmission. In contrast, a decrease in water depth leads to breaking of the incident wave on the slope, therefore reduces wave reflection.

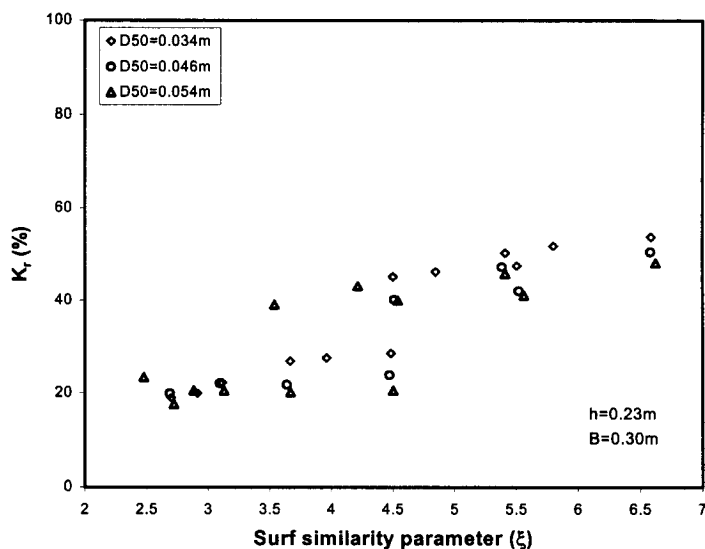


**Figure 5.56.** Effect of armour size on reflection (tests series T12, W22 and W32).

### e. Effect of Core Permeability

The role of core permeability on the reflection coefficient is shown in Figure 5.57 using data from test series T1 and IM1. It shows that permeable structures have marginally lower reflection than impermeable structures. It is observed that for a permeable structure, a part of the wave energy is transmitted and dissipated over the crest and through the body of the structure and a part of the energy is reflected by the slope. In contrast, for an impermeable core some part of the wave energy is transmitted over the crest while the rest is reflected by the slope. No energy gets transmitted or dissipated through the structure.

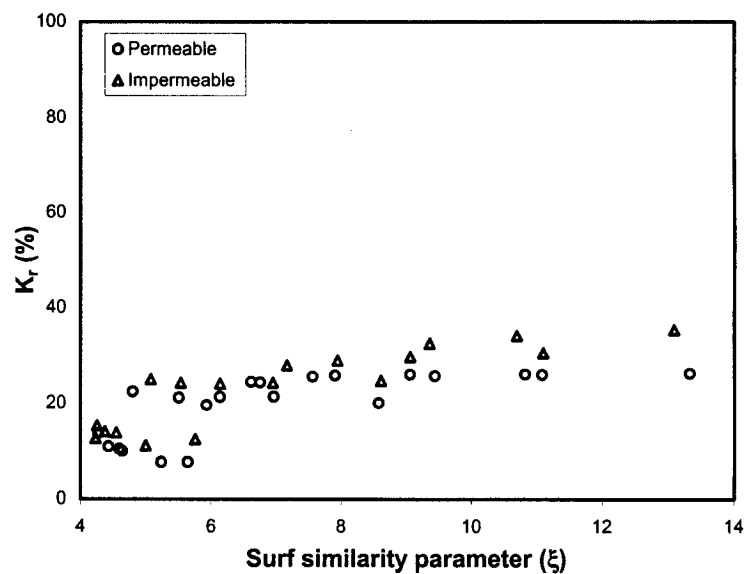


**Figure 5.57.** Effect of core permeability on reflection (tests series T1 and IM1 at  $h = 0.43\text{m}$ ).

### f. Comparison with Existing Design Equations

A comparison of the wave reflection of the test data was made using the equation proposed by Seelig and Ahrens (1981), Seelig (1983) and Allsop (1990) as presented in Eq. [2.39]. Plotting of the present test data and the existing equations is shown in Figure 5.58 as function of the surf similarity parameter. The purpose of

using the surf similarity parameter is to observe the effect of wave characteristics and structure geometry on reflection performance.

In general, the two existing equations give a higher value for the reflection coefficients than the experimental results. The equations predict relatively well the reflection coefficient for non-submerged conditions but poorly predict the values for submerged conditions. The reason for this is that the existing equations were developed using non-overtopped conditions and therefore are not meaningful for submerged conditions. The plot shows that water depth strongly influences the reflection coefficients. At lower  $\xi$ , the reflection coefficient calculated from Seelig and Ahrens (1981) and Allsop (1990) give more conservative estimates. This observation is similar to the result described by Bird et al. (1996). Further, it can be observed that the curve corresponding to zero-submergence test case yields  $K_r$  values smaller than the values of Ahrens and Allsop and Seelig for the entire range of  $\xi$  tested. However, for non-submerged cases, the present test values are in agreement with their values, specifically for  $\xi > 5$ .

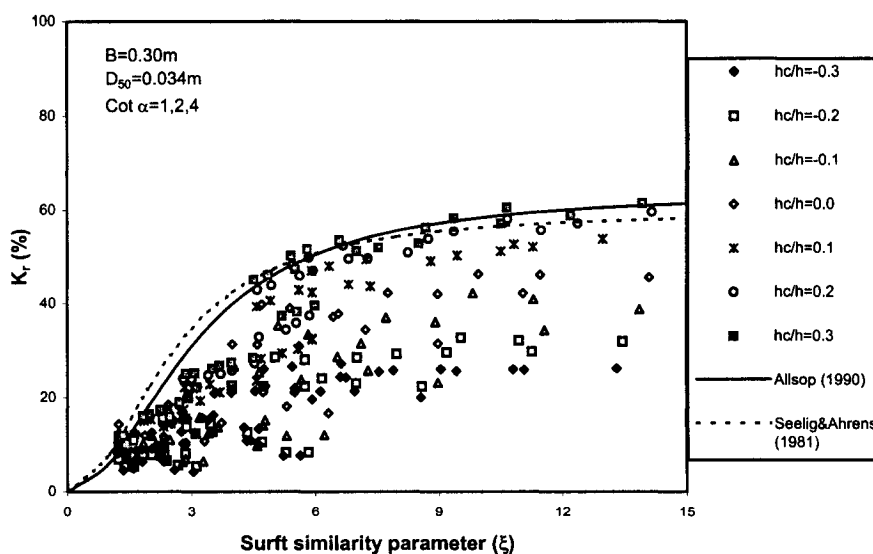


**Figure 5.58.** Comparison of Allsop's (1990) and Seelig & Ahrens' (1981) Eq. with test data.

### 5.5.3 Stability of the Breakwater

#### a. Initiation of Damage

Observation of the initiation of damage was made during the tests. The initiation of damage is defined as the condition when a wave force is just sufficient to initiate damage to an armour unit. At this condition, the driving and resisting forces acting on some units are in balance, so that few armour units with poor stability will get displaced. For the 1:1 slopes, the waves broke mostly in the form of plunging breakers. The water mass of the breaking waves impinged on the armour units and tended to move the units, which then rolled downward due to gravity. For 1:2 slopes several types of wave breaking occur, such as plunging or surging breakers. When surging breaker occurs, up-rushing water dragged armour units upward. Some of these stones were carried downward again by the returning backflow of water.

To identify initiation of damage conditions, the criterion  $S_A = 1$  is used. For this study,  $S_A$  is computed according to the expression described below.

$$S_A \begin{cases} S_N & S_N \leq 1 \\ \left(1 - \left(\frac{S_N - 1}{2}\right)\right) S_N + \left(\frac{S_N - 1}{2}\right) S & 1 < S_N < 3 \\ S & S_N \geq 3 \end{cases} \quad [5.2]$$

and

$$S_N = \frac{N_d D_{50}}{l(1 - e)} \quad [5.3]$$

where  $N_d$  is the number of stones displaced,  $l$  is the width of the test section and  $e$  is the porosity of the armour layer.  $S$  is damage parameter as represented in Eq. [2.28]. Equation [5.3] represents the volume eroded within a width of  $D_{50}$ . This expression is similar to the ones used by Vidal and Mansard (1995). It was found that the initiation

of damage level,  $S_A = 1$  corresponds to the displacement of, on average, 15 armour units from the 100 cm wide flume. The photograph for the damage level  $S_A = 1$  is shown in Figure 5.59 as an example.

The significant wave height required to initiate damage,  $H_D$ , is found by fitting a damage criterion against incident waves in the form of

$$S_A = a \left( \frac{H_i}{\Delta D_{50}} \right)^b \quad [5.4]$$

where  $a$  and  $b$  are constants.



**Figure 5.59.** Photograph of the initiation of damage ( $S_A = 1$ ).



By setting  $S_A=1$  and  $D_{50}=0.034\text{m}$ , the wave height that required to initiate damage is obtained in term of

$$H_D = \Delta D_{50} \exp\left(\frac{1}{b} \ln \frac{1}{a}\right) \quad [5.5]$$

In this case, the wave height  $H_D$  is found equal to 9.02 cm. The entire test results, corresponding to a single wave period, are used to obtain a single value of  $H_D$ . Figure 5.60 shows the damage curve of the tests SH4 - SH7 with period  $T_p = 1.5\text{s}$ .

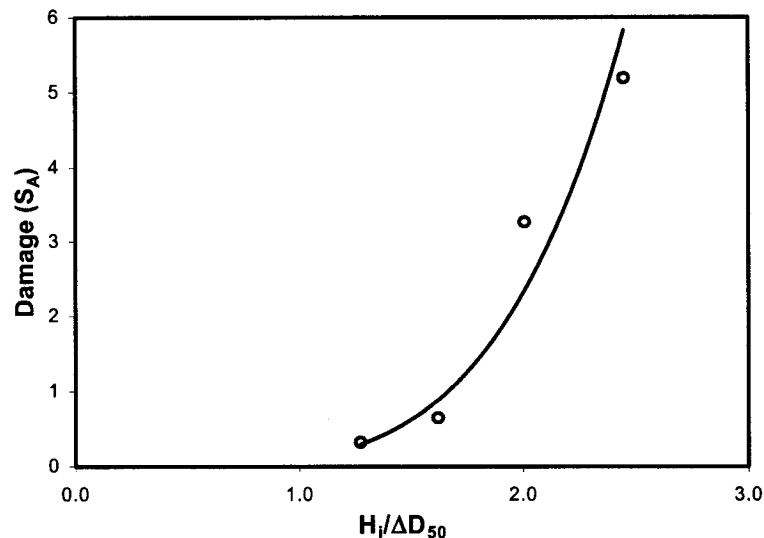


**Figure 5.60.** Damage curve (tests SH4, SH5, SH6, SH7,  $T_p \sim 1.5\text{s}$  and  $h = 0.23\text{m}$ ).

#### b. Effect of Wave Height

Generally, wave height is a dominant factor affecting the stability of armour stones. The energy of waves can be described as  $1/8 \rho g H^2$  based on the linear wave theory. When waves attack a rubble mound breakwater, the wave energy will be reflected, dissipated and transmitted depending on wave characteristics and structural geometry. Wave dissipation occurs due to flow through the body of the breakwater

and friction on the breakwater surface. The external flows (return flows) and internal flows (within the structure) can lead to damage of the armour layers. The influence of wave height on damage can be observed using Figure 5.60. It is observed that a non-linear relationship exists between the damage level and wave height. As wave height increases, the damage level increases. This indicates larger quantities of erosion at higher wave heights.

c. **Effect of Wave Period**

The effect of wave period as reflected in  $\xi$  is observed using  $H_i/\Delta D_{50} - \xi$  plot as shown in Figure 5.61. The wave period and slope of structure are incorporated in the surf similarity parameter  $\xi$  and it represents the type of wave breaking that may occur. The type of wave breaking influences the flow pattern and forces acting on the armour units, therefore influencing the stability of the structure. It is observed that for higher wave periods, resulting in a higher surf similarity parameter, lower stability of the structure occurs.

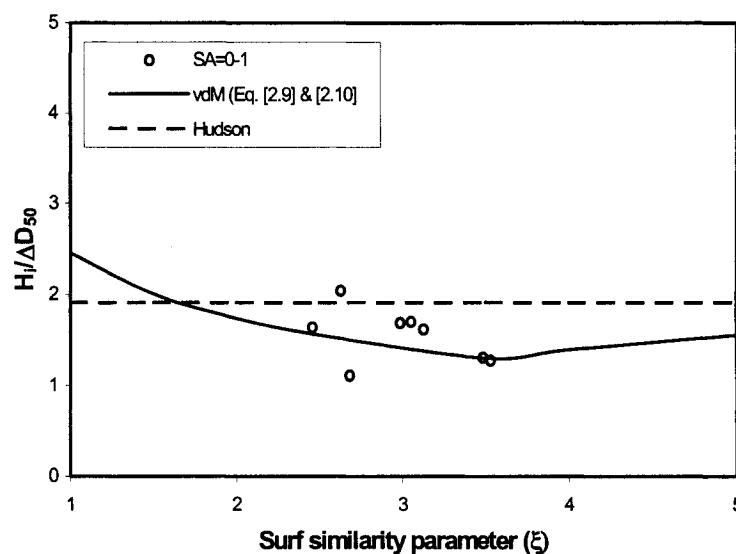


**Figure 5.61.** Effect of wave period on stability of breakwater at  $h = 0.23\text{m}$  (Test series ST).

The test data compared relatively well with the van der Meer equation for plunging waves. According to Meer, minimum stability is found near the transition zone between surging and plunging breakers (usually called collapsing breaker), which appear to give the most severe attack on the slope. Other investigators, including Losada-Giménez-Curto (1979) have identified the collapsing breaker as the critical type of wave breaking that affects stability. The design equations of van der Meer indicate that the damage increases with increasing wave periods for plunging waves, and decreases with an increase in the wave period for surging waves. In the Hudson's formula, wave period is not taken into account.

**d. Effect of Water Depth**

The effect of water depth was evaluated in this study by testing three different water levels in the flume; submerged condition ( $h = 0.38\text{m}$ ), water level at the crest ( $h = 0.30\text{m}$ ) and overtopped condition ( $h = 0.23\text{m}$ ), all depths measured from the toe of the structure. Figures 5.62 and 5.63 show the plots of the non-dimensional parameter  $H_i/\Delta D_{50}$  and surf similarity parameter,  $\xi$ , for  $S_A = 1$  and damage level  $S_A$  versus  $H_i/\Delta D_{50}$ , respectively. The stability of the structure for the submerged condition was higher than for the overtopped condition, since a certain amount of wave energy passes over the crest. Higher waves broke on the slope and crest when tested using water depth of  $0.23\text{m}$ , resulting in more damage on the slope and crest. The results from tests having the water level at the crest were more complex than the others. Wave setup occurred for the longer wave periods resulting in a drag force on the armour units in the backward direction and removing armour down the slope. When the water depth was maintained at the crest level, it was causing severe damage to the structure (not shown in the figure). It can be concluded based on Figures 5.62 and 5.63 that the influence of water depth and the corresponding freeboard (the distance between water level and the crest) on stability is significant. Figure 5.62 indicates that the design equation by van der Meer provides lower estimates, i.e. a conservative value on the stability for the water depths tested.

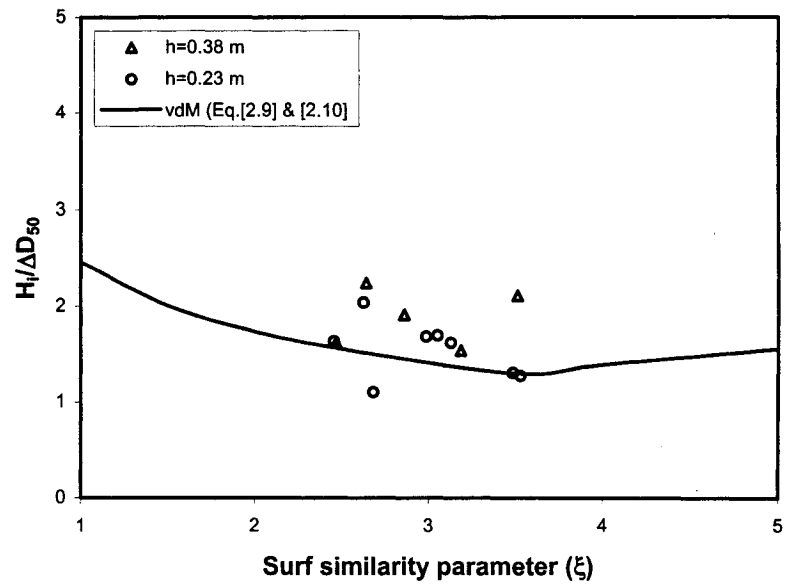


Figure 5.62. Effect of water depth at initiation of damage ( $S_A = 0 - 1$ ).

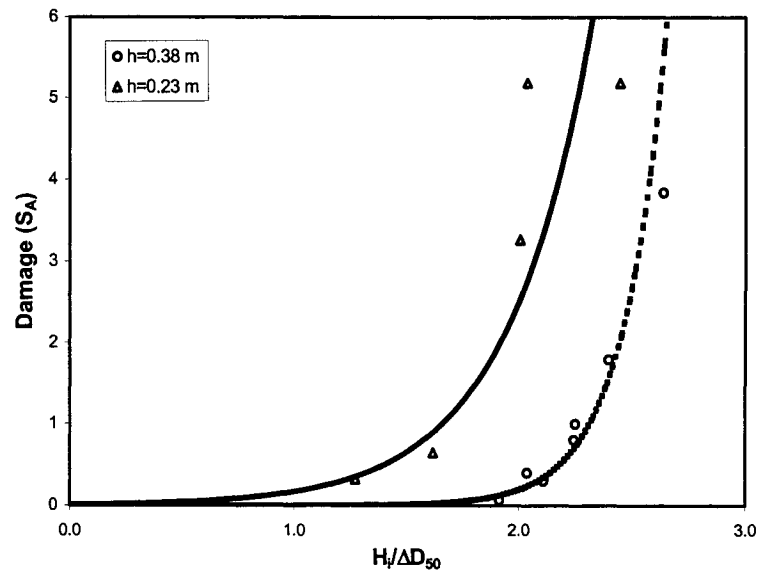
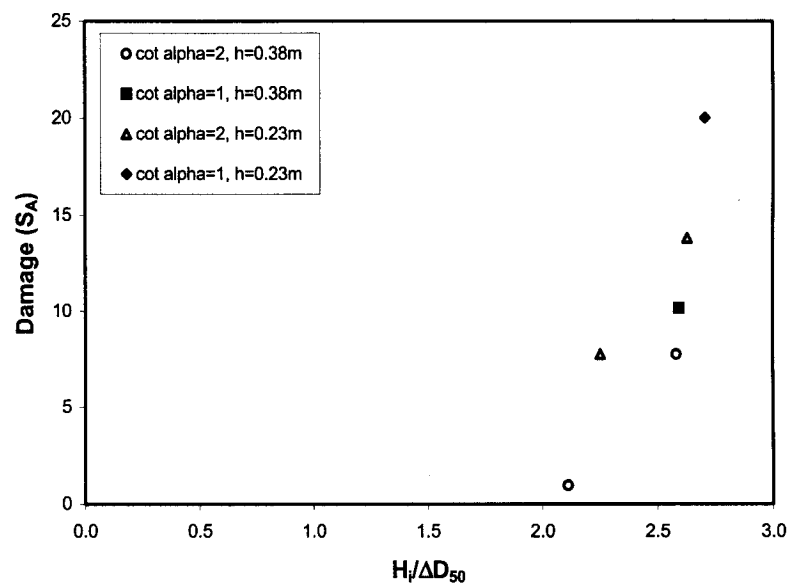


Figure 5.63. Effect of water depth on stability for  $T_p = 1.5$  sec. and  $\cot \alpha = 2.0$ .

**e. Effect of Structure Slope**

The slope angle of a breakwater will influence the type of wave breaking that occurs for a given wave condition. It will also influence the proportion of weight of stone that acts normal and tangential to the surface. When  $\alpha$  approaches the friction angle  $\phi$ , armour units become unstable.

Results from test series with similar wave periods can be compared to assess the effect of slope angle. Figure 5.64 shows the influence of slope on stability for a permeable core with  $\cot \alpha = 1$  and 2 for two different water depths. Because of limited data, only one data point of  $\cot \alpha = 1$  for each water depth can be plotted. Results indicate that for a given water depth, an increase in armour stability occurs for milder slopes.



**Figure 5.64.** Effect of slope on stability for  $T_p \sim 2.0\text{s}$  on various water depths

**f. Effect of Wave Duration**

The effect of duration of waves on breakwater damage is evaluated using the relationship that is described by van der Meer (1988). Van der Meer's design

equations show that the effect of wave durations can be described by  $S/\sqrt{N}$ , where  $N$  is number of waves attacking the breakwater. In this study, the structure was attacked by 3000 or more waves before observing the damage level, thus the modified relationship can be written as follows by considering  $S_A$  of 3000 waves as the reference.

$$\frac{S_A}{S_A(3000)} = 2[1 - \exp(-0.0003N)] \quad [5.6]$$

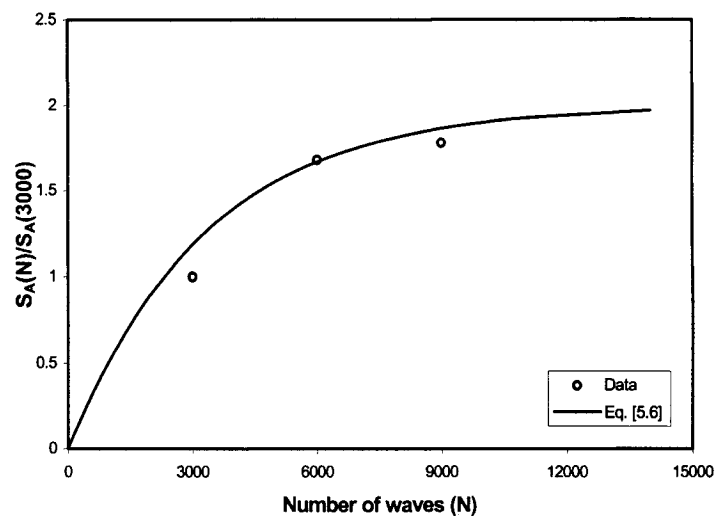
It is well known that damage of armour units depends on the intensity and duration of wave attack, among other factors. Once the armour unit reaches the critical condition (driving and resisting forces in a balanced condition), the damage will depend on the duration of waves. These unstable armour units usually move within the armour layers or along the slope. At a certain time in the duration under consideration, progress of damage will decrease until an equilibrium condition is reached. After this point, the wave duration will no longer influence the stability of armour units.

Figure 5.65 shows the relationship of damage suffered due to varying number of waves. The result shows a good agreement between the modified relationships (Eq. [5.6]) with the present data. The rate of damage initially increases rapidly, but decreases asymptotically at extended wave durations.

#### **g. Effect of Grouped Waves**

The test series were conducted with the JONSWAP spectrum and wave targets were synthesized containing grouped waves to assess the effect of wave groupiness. Results of the tests show that the effect of grouped waves on stability is significant, for  $2 < \xi < 3$ , as shown in Figure 5.66. Visual comparison of damage caused by grouped waves, represented by Groupiness Factor, GF, shows a systematic higher damage level for the higher GF. On the other hand, van der Meer (1988) found

that the influence of groupiness (corresponds to spectral shape) of waves on stability is very small and might be ignored. The influence of spectral shape was investigated using a wide and a narrow spectrum. The present study used groupiness factor, GF, to express the groupiness, where GF is square of SIWEH and SIWEH is square of smoothed surface displacement. The dependence of GF on spectral shape only if a low frequency is taken into account. The present study used narrow spectral shape for all generated waves; therefore the use of two different spectral shapes may leads to the disagreement of van der Meer's and the present results.



**Figure 5.65.** Effect of number of waves (N) on stability

#### **h. Effect of Core Permeability**

Effect of permeability on damage is observed using Figure 5.67 where damage levels for permeable and impermeable core of breakwater section are plotted against stability number. Data from test series SH, ST and SP for a wave period of 1.5s and slope with  $\cot \alpha = 2$  were plotted. Result shows that for a given water depth, armour units on permeable structures are relatively more stable than on impermeable structures. A permeable structure results in increased energy dissipation through the

core, thereby increasing the stability of the armour units and reducing the wave reflection. For a structure with an impermeable core, the flows generated by wave attack are unable to penetrate into the structure and tend to concentrate on the surface and within the armour layer causing larger forces on the armour units during run down.

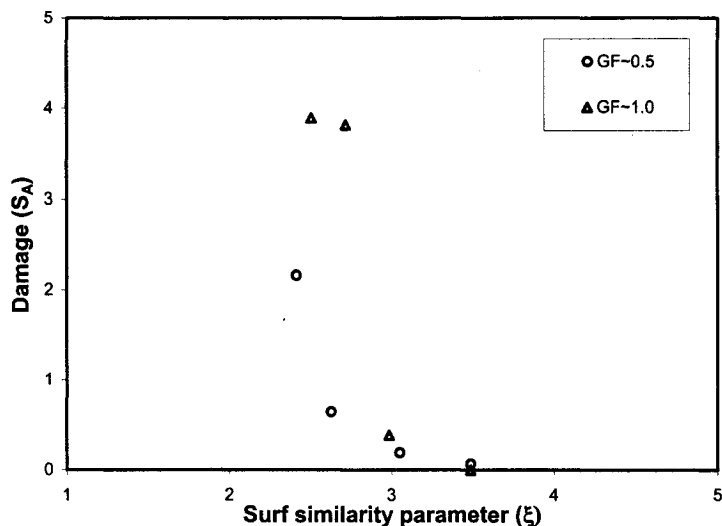


Figure 5.66. Effect of wave grouping on stability (tests series SG).

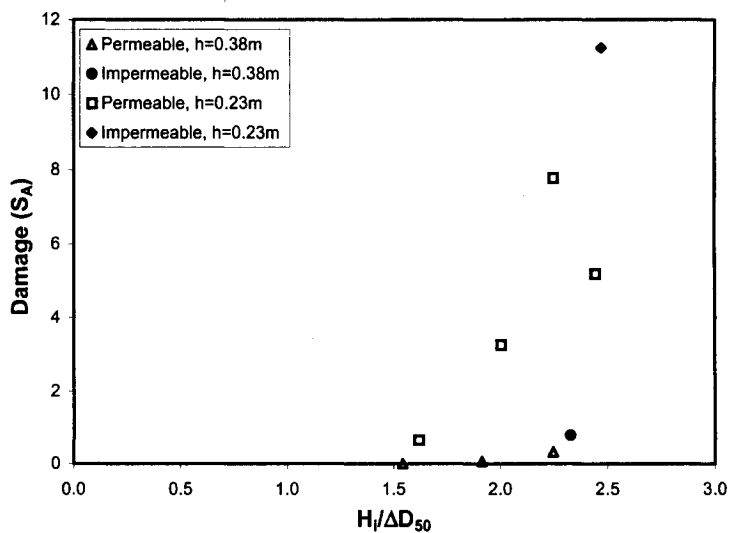


Figure 5.67. Effect of core permeability on stability for  $T_p \sim 1.5s$  at various water depths.



### i. Comparison with Existing Design Equations

A well known design formula proposed by Hudson (1959) is used in practice extensively for the stability of armour stone under wave attack and is shown in Equation [2.1]. Several modifications have been proposed related to Hudson's equation for use with irregular waves. More recently a design equation for rock armour under irregular wave attack has been proposed by van der Meer (1988). Since these equations are being widely used in practice, a comparison is made between the two.

The Hudson equation was developed for regular waves and only considers the 'no-damage' criterion. CERC (1984) presents a relation between wave height (H) and wave height of "no damage" as related to the damage level S and the  $K_D$  factor for Hudson's formula as shown in Table 5.1. The damage level S was computed according to  $S = 0.8 D\%$ , therefore the "no-damage" criterion  $S = 2$  is equivalent to 2.5% damage D,  $S = 4$  is equivalent to 5% damage etc. Using the above relation, Hudson's formula for  $S = 2$  can be expanded to relate the damage level S and significant wave height using  $H_s$ , as

$$\frac{H_s}{\Delta D_{50}} = (K_D \cot \alpha)^{1/3} S^{0.15} \quad [5.7]$$

or

$$S = K_D^{-2.22} (\cot \alpha)^{-2.22} \left( \frac{H_s}{\Delta D_{50}} \right)^{6.67} \quad [5.8]$$

**Table 5.1.** Wave height relationship for different damage levels (CERC, 1984).

Damage D (%)	H/H <sub>D=0</sub>	Damage level S
0 – 5	1.00	2
5 – 10	1.08	6
10 – 15	1.19	10
15 – 20	1.27	14
20 – 30	1.37	20
30 – 40	1.47	28
40 – 50	1.56	36

Two sets of design formulae of van der Meer's for plunging and surging waves have been developed as defined in Equations [2.9] and [2.10]. These equations were derived for non-overtopped slopes. For overtopped slopes, part of the wave energy will be transmitted over the crest and part will be destroyed on the slope resulting in an increase in the required size of armour units. For crests above the still water level, van der Meer used a reduction factor for the  $D_{50}$  as derived from Equations [2.9] and [2.10], which can be rewritten as follows.

$$\frac{H_s}{\Delta D_{50}} = 6.2\xi^{-0.5}P^{0.18}\left(\frac{S}{\sqrt{N}}\right)^{0.2}\left(1.25 - 4.8\frac{h_c}{H_s}\sqrt{\frac{S_{op}}{2\pi}}\right) \text{ for plunging waves} \quad [5.9]$$

The expanded Hudson's equation can be compared with present data to obtain Figure 5.68. The  $K_D$  factor used for the plot is  $K_D = 4$  (for non-breaking wave conditions). It can be seen that the expanded Hudson's equation under predicts for  $S > 2$  and  $h = 0.23\text{m}$  and predicts with mixed accuracy for  $h = 0.30\text{m}$ . It should be noted that the expanded Hudson's formula is derived using  $H_s$  for use with irregular waves. CERC (1984) suggests  $H_{1/10} = 1.27 H_s$  could be used as the design wave height. Use of  $H_{1/10}$  leads to larger mass of stone needed for a given wave condition by a factor of  $(1.27)^3 \times 2 = 4.1$  for the non-breaking condition. It will be a very conservative and uneconomical.

Comparison of present data with van der Meer's equation (Eq. [5.9]) for a low crest condition is shown in Figures 5.69 and Figure 5.70. It shows that the present data compare well with the existing equation.

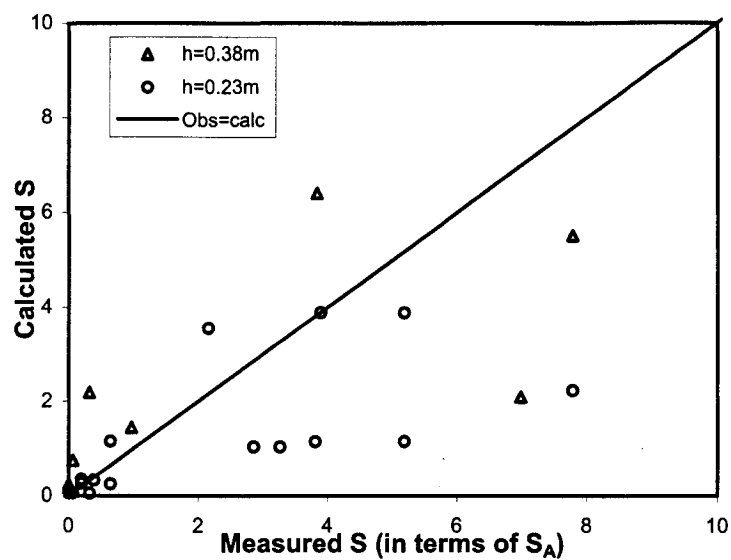


**Figure 5.68.** Comparison of the test data and Hudson's Equation for  $K_D = 4$  (non-breaking).

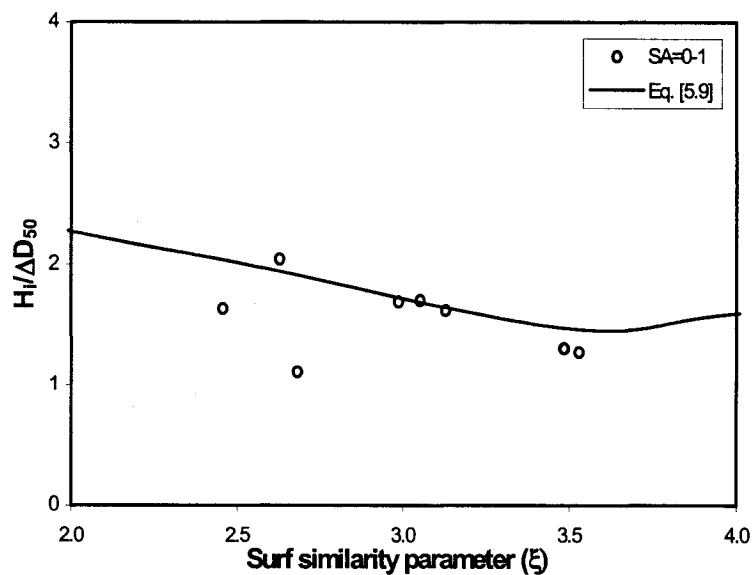


**Figure 5.69.** Comparison of the test data and van der Meer's Equation on initiation of damage ( $S_A = 0 - 1$ ) at  $h = 0.23\text{m}$ .

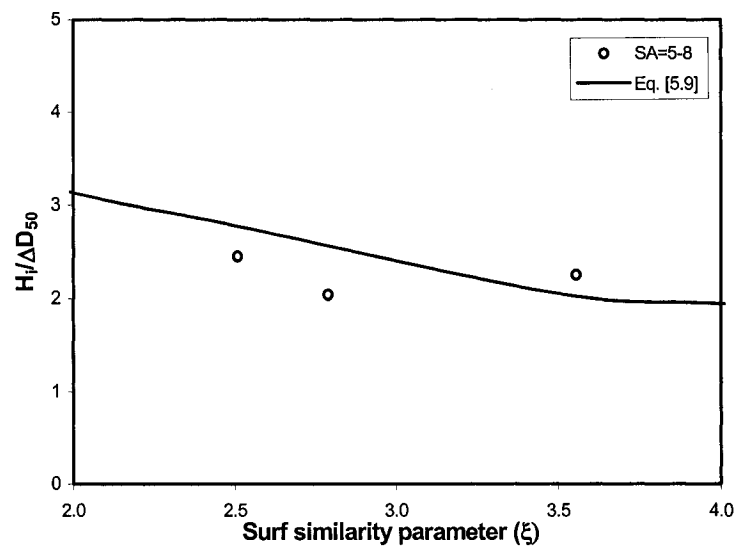


**Figure 5.70.** Comparison of the test data and van der Meer's Equation on intermediate of damage ( $S_A = 5 - 8$ ) at  $h = 0.23\text{m}$ .

## 5.6 SUMMARY

A number of investigations have been made on transmission, reflection and stability of low crested breakwaters involving a large number of variables. The experimental findings lead to the following conclusions.

The transmission coefficient is strongly influenced by water depth and wave period in most cases. Longer wave periods have higher wave transmission than shorter wave periods. Wave height also slightly influences the wave transmission for the range of variable tested. Slope of structure and core permeability has less impact on the wave transmission for the range of tests conducted. The crest width appears as one of the important parameters in this process.

The reflection coefficient is also strongly influenced by water depth and wave period. Waves with longer periods have lower wave reflection coefficients,  $K_r$ , than waves with shorter periods. Wave height also slightly influences the wave reflection. Slope of the structure and core permeability did not have a strong contribution to the

wave reflection process for the cases tested. The width of the crest also does not appear to be an important parameter in this process.

The stability of low crested breakwaters is significantly influenced by water depth and the wave period. In general, the stability of a breakwater depends upon other parameters like wave height, wave duration, front slope and core permeability.

Evaluation using dimensionless forms shows that the transmission coefficient is very dependent on the relative submergence (corresponds to water depth). The range of  $h_c/H_i$  between  $-2$  and  $+1$  is important where the transmission increases rapidly with changes in the water depth. Outside this range, the transmission increases or decreases slightly. It is also observed that the dimensionless crest width is an important parameter that affects wave transmission. A wider crest width results in a significant reduction of wave transmission compared to a narrow crest. Other variables that significantly influence wave transmission are breakwater slope ( $\cot \alpha$ ) and core permeability. Surface friction and internal flow terms also have significant influence on the process. Wave steepness,  $s_p$ , and dimensionless armour diameter were found less influential on wave transmission process.

The reflection of waves is strongly influenced by surf similarity parameter. Waves with lower  $\xi$  have lower wave reflection coefficients than ones with larger  $\xi$  values. Relative water depth is also an important variable affecting wave reflection. A clear correlation is evident between relative water depth and reflection coefficient. Lower  $K_r$  corresponds to higher relative water depths. In some cases, many of waves may be breaking so reflection is low.

The stability of low crested breakwaters can be described by the dimensionless variables such as the number of waves,  $S/\sqrt{N}$ , surf similarity parameter,  $\xi$ , slope of structure,  $\cot \alpha$ , permeability factor,  $P$ , groupiness factor,  $GF$ , and the wave height parameter,  $H_i/\Delta D_{50}$ . Number of waves has significant influence on stability. Higher number of waves results in higher damage of the profile. The surf similarity parameter describes the influence of the slope and the wave steepness. Steeper slope gives higher damage than milder slope, as well as longer wave period.

Groupiness Factor, GF, shows a systematic higher damage level for the higher GF. Evaluation of the influence of the core permeability shows that a permeable structure results in increased energy dissipation through the core, thereby increasing the stability of the armour units and reducing the wave reflection. While for impermeable core, the wave flows concentrate on the surface and within the armour layer causing larger forces on the armour units, thereby decreasing the stability. Influence of the wave height as described correctly by the wave height parameter indicates increase in erosion with increase in wave height. Prediction of stability conditions based on equations of van der Meer seems to agree with the trend observed in the model tests.

Considering the influence of the above dimensional and dimensionless variables, a model describing wave transmission and reflection for low crested breakwaters under wave attack will be developed. The following chapter will discuss the development of wave transmission and reflection models using statistical analysis based on the test data from this study.

## Chapter 6

# DEVELOPMENT OF PREDICTIVE MODELS

### 6.1 INTRODUCTION

This chapter discusses the development of empirical models for wave transmission and reflection at low crested breakwaters under wave attack based on two dimensional test data undertaken from this study. The test data was subjected to linear (Pearson) correlation test to observe the correlation of the transmission and reflection coefficients to other parameters. The Pearson correlation coefficient measures the strength of the linear relationship between two variables. Models for wave transmission and reflection were developed using statistical approach. The SYSTAT software package was used towards this objective. The procedure adopted here was to carry out the regression analysis on a number of primary parameters in order to assess their relative effects on wave transmission and reflection. In cases when the primary variables could not represent the relationship well, a number of secondary parameters were then derived on the basis of the initial analysis. The primary parameters are the dimensionless parameters derived using dimensional analysis described previously such as the relative crest height,  $h_c/H_i$ , the relative crest width,  $B/H_i$ , the wave steepness,  $H_i/L_o$ , etc. The secondary parameters are combination of primary parameters that are assumed to be important in these processes. Therefore, the development of the design equations is undertaken by assuming the wave transmission and reflection are due to the primary parameters and their combinations.

The development of the models considered here use both linear and non-linear forms of equations. A linear model was firstly used in order to determine the relationship between dependent and independent variables. In cases where wave transmission and reflection could not be described using the linear model, a non-linear model was used in order to evaluate the relative importance and relationship (direct or inverse) between independent and the dependent variables.

## **6.2 DEVELOPMENT OF THE WAVE TRANSMISSION MODEL**

### **6.2.1 General Consideration**

The considerations herein that were used in developing a relationship in this investigation include a possible range of application in the field. The qualitative results described in the previous chapter show that some of the mechanisms and variables involved in the wave transmission processes are water depth, wave breaking over the crest, wave overtopping, dissipation by friction and penetration through the structure. The wave transmission process across the breakwater can thus be described by the following dimensionless variables:

- The relative crest height,  $h_c/H_i$ , or  $h_c/D_{50}$ : It characterizes the role of water depth. These parameters are found to be the most important factors affecting the wave transmission mechanism over low crested breakwaters. A decrease in water depth will lead to wave breaking over the crest of the structure, thereby reducing transmission.
- The relative wave height,  $H_i/D_{50}$ : Wave transmission increases as the wave height decreases.
- An internal flow parameter,  $B^2/L_p D_{50}$ : The effective flow through the structure increases as the crest width decreases. Also, bigger diameters of armour stone lead to increased void volume thus increasing the flow within the structure.



- Friction over the surface of the structure: This is seen to be an important parameter affecting wave transmission on a rubble mound breakwater. The parameter  $H_{i,h_c}/BD_{50}$  reflects the role of surface friction.
- Permeability of structure represented by the grading of armour and core,  $D_{50}/D_{50c}$ : The permeability of structure is influenced by the properties of material (i.e. diameter of armour and core). An increase in the permeability factor of a material will increase wave penetration through the structure, thereby increasing wave transmission.

The aforementioned parameters above were used to assess their relative effects on wave transmission by carrying out regression analysis. The following criteria were used to assess the suitability of the equation.

- The squared multiple correlation coefficient ( $R^2$ ). This parameter is a measure of how well the equation fits the data.
- Limit values of the equation in the range of  $0.0 \leq K_t \leq 1.0$
- The residuals of the equation should be normally distributed, indicating that there are no significant trends missed.
- The equation describes relevant physical variables while minimizing the number of statistically fitted parameters.

### 6.2.2 Development of the Model

The review of the relation between  $K_t$  and some of the variables tested as shown in the previous chapter indicated that the relationship was not linear. Given the dominant effect of the relative crest height on the transmission process, this parameter was taken as the main influencing factor. Other parameters were then added iteratively to represent the influence of other physical processes. Given two conditions of core permeability (permeable and impermeable), the permeable data set was firstly used in the analysis. Once an equation of permeable condition meet the requirements, that equation will be used to fit the impermeable data set.

Considering only the relative crest height  $h_c/H_i$  or  $h_c/D_{50}$  as a parameter to represent wave transmission in the design equation, the accuracy of the predictive equation could not be achieved. The squared coefficient correlation ( $R^2$ ) for this equation was 0.746 and standard error of estimate ( $\sigma$ ) was 0.129 using  $h_c/H_i$  while  $R^2 = 0.762$  and  $\sigma = 0.125$  using  $h_c/D_{50}$ . The relative wave height terms,  $H_i/D_{50}$ , was then added to the equation resulting in higher values of the squared coefficient correlation (0.772). The form of this equation is:

$$K_t = C_1 \left( \frac{h_c}{D_{50}} \right) + C_2 \left( \frac{H_i}{D_{50}} \right) + C_3 \quad [6.1]$$

Plotting the measured and estimated values of  $K_t$  shows that a number of estimated values fall below the practical limit  $K_t = 0.0$  and a number of values above  $K_t = 1.0$ , indicating that the equation can not be used for prediction for very small and very large values of  $K_t$ . In order to improve the ability of the equation predicting  $K_t$ , the term of friction and internal flow were then added, represented by  $H_i h_c / B D_{50}$  and  $B^2 / L_p D_{50}$ , respectively. The friction term is a combination of relative wave height  $H_i / B$  and relative crest height,  $h_c / D_{50}$ . The physical significance of this term relates to increased wave energy dissipation due to friction and turbulence of the structure by increasing armour stone diameter. The effect of internal flow in term of  $B^2 / L_p D_{50}$  suggests a direct relationship between transmission coefficient and breakwater width that represents the transmission of waves through the structure. Increased armour diameter leads to increase permeability, thus enhancing transmission. Adding the terms of friction  $H_i h_c / B D_{50}$  and internal flow,  $B^2 / L_p D_{50}$ , to Equation [6.1], the  $R^2$  increases significantly to about 0.907 with standard error of about 0.075. The general form of this equation is:

$$K_t = C_1 \left( \frac{h_c}{D_{50}} \right) + C_2 \left( \frac{H_i}{D_{50}} \right) + C_3 \left( \frac{H_i h_c}{B D_{50}} \right) + C_4 \left( \frac{B^2}{L_p D_{50}} \right)^{C_5} + C_6 \quad [6.2]$$

Plotting of this equation shows relatively good fit of estimated and measured data; however, a number of estimated values still fall below  $K_t = 0.0$  indicating that this equation underestimates small values of  $K_t$ . The probability plot of residuals shows that the residuals are normally distributed, indicated by straight line of the plot. To improve the ability of the equation for predicting  $K_t$ , especially for very small values, the permeability of the structure was then introduced in terms of  $D_{50}/D_{50c}$  the friction term was modified to  $H_i h_c / D_{50}^2$ . The equation is in the following form.

$$K_t = C_1 \left( \frac{h_c}{D_{50}} \right) + C_2 \left( \frac{H_i}{D_{50}} \right) + C_3 \left( \frac{H_i h_c}{D_{50}^2} \right) + C_4 \left( \frac{B^2}{L_p D_{50}} \right)^{C_5} + C_6 \frac{D_{50}}{D_{50c}} + C_7 \quad [6.3]$$

This equation improves the squared coefficient correlation to about 0.921 and standard error of estimate to about 0.070 and provides adequate estimates  $K_t$ . The plot shows no estimate values below and above the lower and upper limits of  $K_t$ . To take into account the gradation factor of the structure for impermeable condition, Equation [6.3] was applied to fit the impermeable data set as well and a gradation factor of 1.5 is found to be appropriate. Figure 6.1 shows the estimated  $K_t$  values using Eq. [6.3] compared to the impermeable data set for  $D_{50}/D_{50c}$  of 1.5. Applying Equation [6.3] to all data set, the squared correlation coefficient is found to be 0.913 for both permeable and impermeable conditions. The resulting equation of both permeable and impermeable conditions for  $K_t$  is given in the following form.

$$K_t = -0.180 \left( \frac{h_c}{D_{50}} \right) + 0.001 \left( \frac{H_i}{D_{50}} \right) + 0.024 \left( \frac{H_i h_c}{D_{50}^2} \right) - 0.239 \left( \frac{B^2}{L_p D_{50}} \right)^{0.196} + 0.006 \frac{D_{50}}{D_{50c}} - 0.611 \quad [6.4]$$

where  $K_t$  is the transmission coefficient,  $h_c$  is the depth of submergence or freeboard,  $H_i$  is the incident wave height,  $B$  is the crest width,  $L_p$  is the local wave length,  $D_{50}$  is the nominal diameter of armour units and  $D_{50c}$  is the nominal diameter of the core.

It should be noted that several other forms and combinations of variables were tested with no significant improvement in predicting  $K_t$  for the range of observations.

### 6.2.3 Evaluation of Predictive Equation for Wave Transmission

Inspection of the statistical results for each equation above shows that the accuracy of the predictive equation is significantly improved through the addition of the variables. The improvement of the accuracy of the equation is shown by increasing the squared correlation coefficient  $R^2$ . Equation [6.4] provides a robust solution for wave transmission given the enormously wide range parameter covered by the 1058 data points. The variables in the equation have physical significance in the processes related to wave dissipation due to friction induced by structural roughness,  $H_i h_c / D_{50}^2$ , internal flow through the breakwater,  $B^2 / L_p D_{50}$ , effect of relative water depth,  $h_c / D_{50}$ , relative wave height,  $H_i / D_{50}$ , and permeability of the structure represented by gradation factor,  $D_{50} / D_{50c}$ .

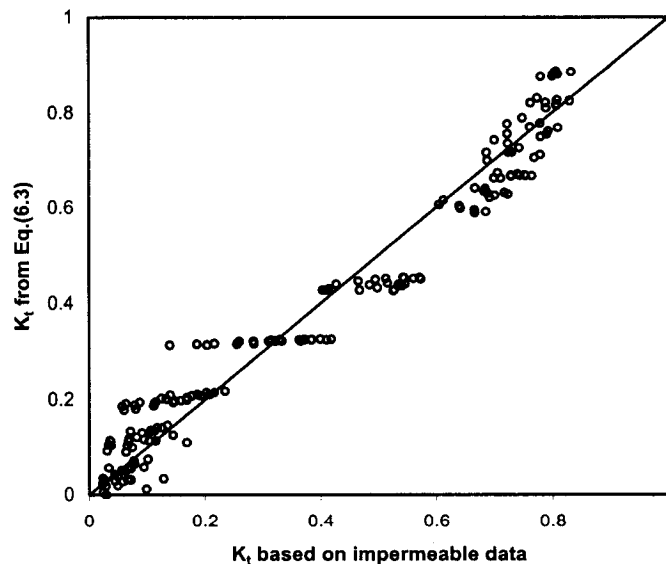


**Figure 6.1.** Estimated  $K_t$  compared to  $K_t$  based on impermeable data by applying  $D_{50}/D_{50c} = 1.5$ .

Plotting Eq. [6.4] shows a good fit between estimated and all measured data and provides adequate estimates of  $K_t$  as indicated in Figure 6.2. The plot shows that the data are distributed about the mean having a relatively tight clustering of spread. Plot of the residuals shows the distribution of the residuals follow approximately a straight line, indicating that they are normally distributed (Figure 6.3).

To evaluate, in more detail, the suitability of the equation, a sensitivity analysis was carried out. Sensitivity analysis is usually used to determine the effect of variation in the estimates. The statistical analysis for the equation provides a number of statistical measures of the equation and its parameters such as 95% upper and lower confidence interval of the parameters and approximate standard error that associated with each parameter.

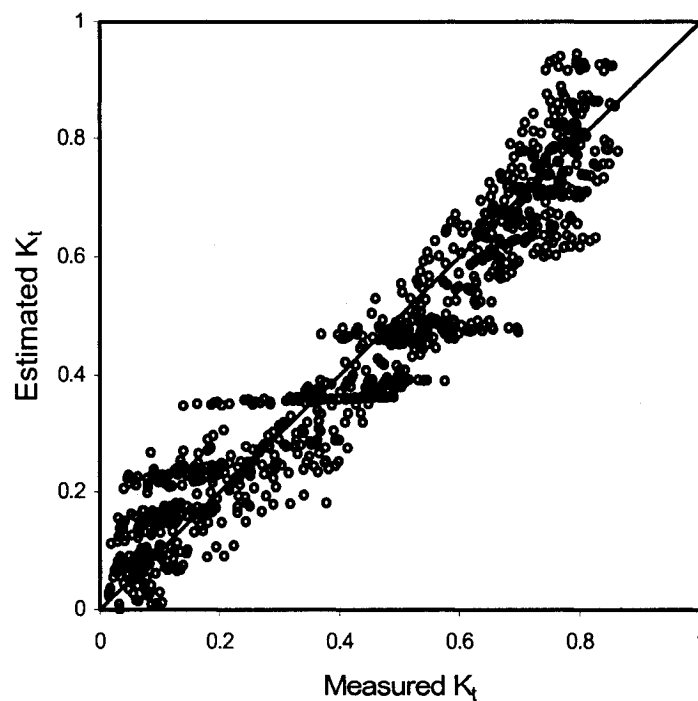


**Figure 6.2.** Estimated  $K_t$  compared to experiment data for both permeable and impermeable conditions.

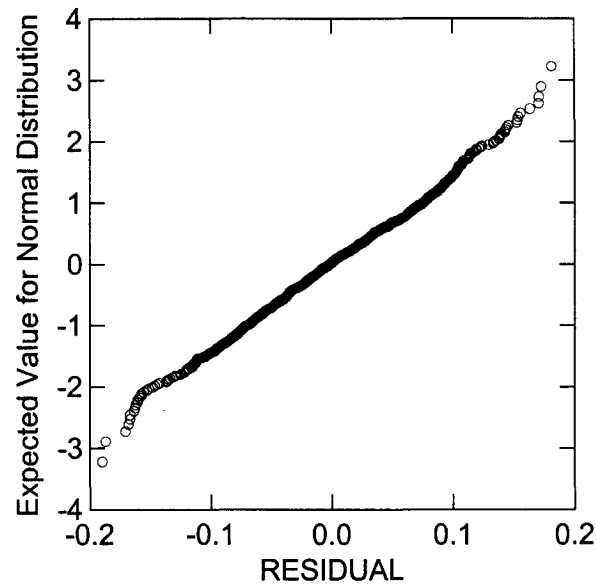


**Figure 6.3.** Normal probability of  $K_t$  residuals.

The effects of +95% of the confidence interval variation in each regression coefficient are plotted against the value calculated in equation [6.4] and presented in Figure 6.3. The values selected for the relative crest height,  $h_c/D_{50}$ , between -3.8 and 2, the relative wave height,  $H_i/D_{50}$ , between 1.15 and 4.58, the gradation factor,  $D_{50}/D_{50c}$ , between 1.5 and 3.2, the surface friction,  $H_i h_c/D_{50}^2$ , between -5 and 17, and the internal flow,  $B^2/L_p D_{50}$ , between 1.3 and 2.05. This figure shows that coefficient  $C_4$  and  $C_7$  are the most sensitive, since a small variation in the parameters produces a large variation in the response  $K_t$ . The maximum variation in the response is 18% and 16% for  $C_4$  and  $C_7$ , respectively.

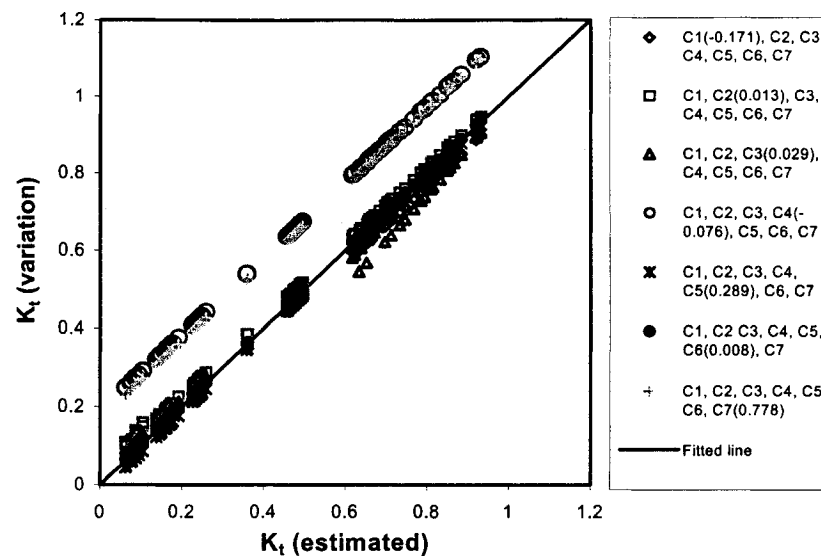


**Figure 6.4.** Sensitivity of  $K_t$  to variation of +95% confidence interval in regression coefficients.

### 6.3 DEVELOPMENT OF THE WAVE REFLECTION MODEL

Considerations similar to the development of the wave transmission model were used for developing the wave reflection equation. Wave reflection is no doubt complementary to the process of wave propagation around a structure. However, other processes like wave transmission through and over the structure, dissipation due to breaking, friction, turbulence, etc. come into picture. The process of the wave propagation can be expressed using energy balance including the processes of wave transmission, reflection and dissipation. The following equation represents the energy balance when a wave propagates to a structure.

$$E_i = E_t + E_r + E_d \quad [6.5]$$

where  $E_i$ ,  $E_t$ ,  $E_r$  and  $E_d$  are the incident, transmitted, reflected and dissipated wave energy, respectively. In this case, the dissipated wave energy is part of wave energy

remaining after subtracting the incident wave energy with transmitted and reflected energy. The equation above can be expressed as

$$1.0 = K_t^2 + K_r^2 + \text{dissipation} \quad [6.6]$$

Therefore, a solution for the reflection coefficient should follow the expression above. Since the predictive equation of the wave transmission includes the process of dissipation (see section 6.2), Equation [6.6] can be simplified in the form of

$$1.0 = K_t^2 + K_r^2 \quad [6.7]$$

Though the process of wave propagation can be expressed using an energy balance, which includes wave transmission, reflection and dissipation, efforts to develop a predictive wave reflection equation using an energy balance approach has resulted in little success. Estimate values of the reflection coefficient much higher than the observed data indicates that the amount of energy dissipated cannot be simplified by equation [6.7]. Other efforts to relate wave reflection and wave transmission resulted in a little success. Therefore, it was decided to develop independently a predictive equation similar to the wave transmission case. Thus, each of the most significant process/parameters involved in the wave reflection processes is included in the formulation.

Following the qualitative results described in the previous section, the wave reflection process can be described in terms of the following dimensionless variables:

- Surf similarity parameter,  $\xi$ : This characterizes the type of the breaking waves and associated dissipation of wave energy due to breaking.
- Amount of wave energy transmitted over and through the body of breakwater. This depends on the wave height (responsible for wave overtopping) and permeability of material (responsible for internal flow). The wave energy



transmitted could be represented by  $H_i/D_{50}$ . The crest width does not significantly contribute to wave reflection, as found in this study.

- The relative crest height,  $h_c/H_i$ , or  $h_c/D_{50}$ : These terms characterize the freeboard. The effect of decreasing water depth leads to a decrease in wave transmission over the crest of the structure. Consequently wave reflection increases.
- Permeability of structure represented by the grading of armour and core,  $D_{50}/D_{50c}$ : The permeability of structure is influenced by the properties of material (i.e. diameter of armour and core). An increase in the permeability factor of a material will increase wave penetration through the structure, thereby increasing the wave transmission and reducing the wave reflection.

### 6.3.1 Development of the Model

Investigation on the role of various parameters affecting wave reflection showed that the surf similarity parameter,  $\xi$ , and water depth were the dominant variables in this process. Therefore, these variables were taken as the main parameters for all alternative design equations. Using regression analysis, the design equation for wave reflection was developed with  $\xi$  and  $h_c/D_{50}$  as the principal variables for both permeable and impermeable data set. The gradation factor,  $D_{50}/D_{50c}$ , for impermeable condition was 1.5 as derived previously.

Applying only the surf similarity parameter,  $\xi$ , in the equation, the accuracy of predictive equation was not satisfactory. The squared correlation coefficient ( $R^2$ ) was 0.345 and standard error of estimate ( $\sigma$ ) was 0.118. Applying logarithm to the variable, the correlation coefficient increases slightly into 0.370 and reduces the standard error of estimate into 0.114. Adding term of the relative crest height,  $h_c/D_{50}$ , the predictive equation significantly improved as indicated by the squared coefficient correlation and the standard error of estimate with values of 0.706 and 0.077, respectively. The form of the equation is:

$$K_r = C_1 \log(\xi) + C_2 \left( \frac{h_c}{D_{50}} \right) + C_3 \quad [6.8]$$

In order to improve the accuracy of the equation, the multiple regression analysis was continued by adding of the transmission term,  $H_i/D_{50}$ . Inspection of the result shows the improvement of the equation. However, plotting the estimated values of this equation against the observed data shows that a number of estimated values fall below 0.0, indicating that the equation underestimates in predicting small  $K_r$ , while plotting the probability of the residual shows that the residuals normally distributed. Adding the gradation factor,  $D_{50}/D_{50c}$ , the correlation between observed and predicted reflection coefficient improved significantly. The squared coefficient correlation ( $R^2$ ) associated with this equation was 0.792 and standard error of estimate was 0.063. The fitted equation is:

$$K_r = C_1 \log \xi + C_2 \left( \frac{h_c}{D_{50}} \right) + C_3 \left( \frac{H_i}{D_{50}} \right)^{C_4} + C_5 \left( \frac{D_{50}}{D_{50c}} \right) \quad [6.9]$$

Inspection of the estimated values of this equation shows a number of the estimated values fall below 0.0, indicating that the equation cannot predict well for lower values of coefficient reflection ( $K_r \leq 10$ ). This is perhaps to be expected for higher water depth and gentler slope. Careful inspection of the data set show that the underestimated values of  $K_r$  occur in higher water depth and lower incident wave and wave period. At this condition most of incident wave energy promote to transmitted energy. The considerably under estimated values of the reflection coefficient occur under these highly transmitted conditions.

In order to minimize the negative values of the prediction, the right side of the equation was then squared resulted in significant improvement of the squared correlation coefficient. The squared correlation coefficient was 0.838 and standard

error of estimate was 0.055 and the relationship for  $K_r$  is given in the following equation.

$$K_r = \left( 0.1753 \log \xi + 0.0528 \left( \frac{h_c}{D_{50}} \right) + 0.1722 \left( \frac{H_i}{D_{50}} \right)^{0.452} + 0.0086 \left( \frac{D_{50}}{D_{50c}} \right) \right)^2 \quad [6.10]$$

A number of alternative equations that involve different variables and different mathematical forms were investigated in order to maximize the correlation between estimate values and observed data and limits of estimated  $K_r$ . All attempts to improve the predictive Equation [6.10] were less successful. It was decided therefore, Equation [6.10] above to be the alternative design equation on wave reflection.

Figure 6.5 shows the comparison between estimated values from Equation [6.10] and data of the experiment. This figure shows that the values are scattered in non-symmetrical way about the mean line. Though the equation underestimates for  $40\% < K_r < 50\%$ , overall, the equation represents  $K_r$  well in the entire range  $5\% \leq K_r \leq 100\%$ . Figure 6.6 shows the distribution of the residuals. It appears that the residuals are normally distributed indicating that there is no bias in the equation.

### 6.3.2 Evaluation of Predictive Equation for Wave Reflection

The sensitivity of the proposed equation was tested using the value of + 95% confidence interval and given in Figure 6.7. The values selected for surf similarity parameter,  $\xi$ , between 0.6 and 1.2, the relative crest height,  $h_c/D_{50}$ , between -3.8 and 2, the gradation factor between 1.5 and 3.2, and the transmission term,  $H_i/D_{50}$ , between 1.1 and 5.0. This figure shows that coefficient  $C_3$  is the most sensitive, since a small variation in the equation produces a large variation in the response  $K_r$ . However, the maximum variation in the response is about 4.8% with the average of 3%.

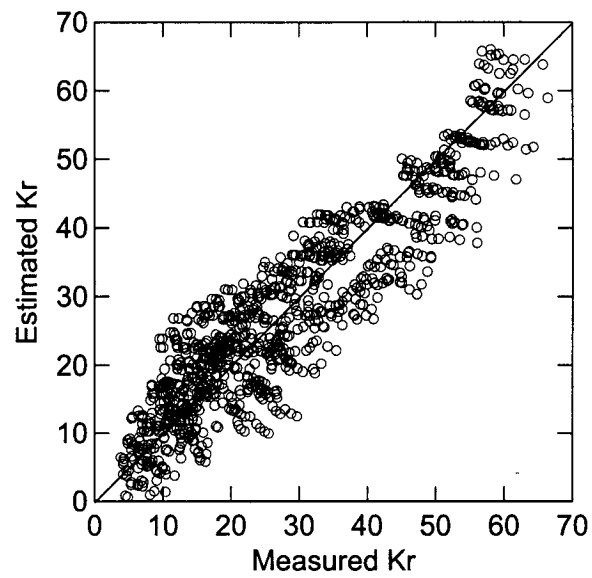


Figure 6.5. Estimated  $K_r$  compared to experiment data.

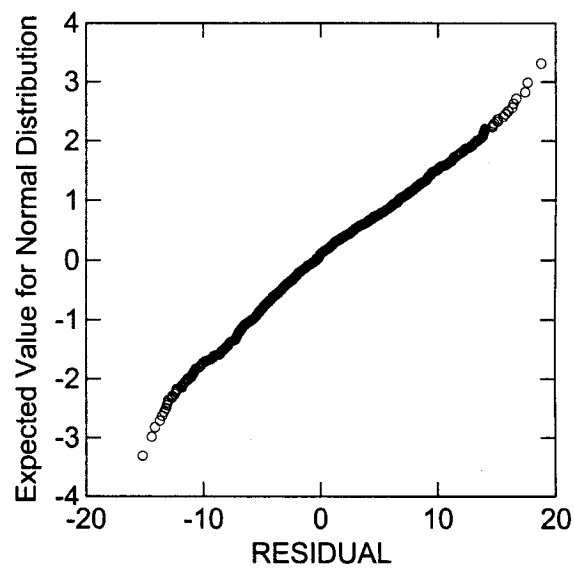
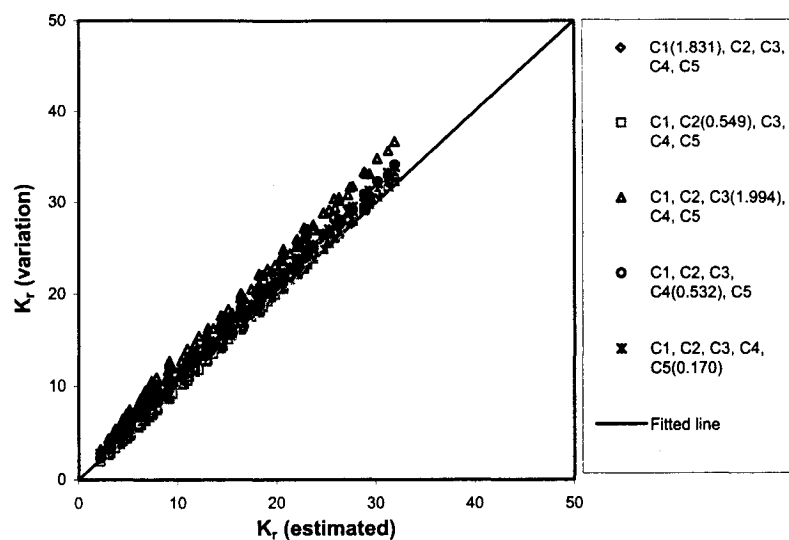


Figure 6.6. Normal probability of  $K_r$  residuals.



**Figure 6.7.** Sensitivity of  $K_r$  to variation of +95% confidence interval in regression coefficients.

#### 6.4 VALIDITY OF THE MODELS

Since the proposed equations outlined above are empirical, their use will be naturally restricted to the range of variables tested. The valid range of variables for both equations is given in Table 6.1. Higher water depths in front of the structure produce higher transmission coefficient estimates, while for reflection this condition produces lower values as expected. However, the role of other variables may not be as evident. The applicability of the wave transmission and reflection equations outside the given range may produce incorrect estimates. The range of variables tested here reflects the field conditions to a large extent. For example, Davidson et al. (1996) collected field data on the reflection performance of a rock island breakwater. The range of variables measured were  $1.18 \leq H_i/D_{50} \leq 7.28$ ,  $6.4 \leq \xi \leq 70.7$ , slope gradient = 1.23 and values of  $K_r$  were lying between 26% - 73%.

**Table 6.1.** The valid range of variables for transmission and reflection equations.

Variables	Range
$h_c/D_{50}$	-3.82 – 2.06
$H_i/D_{50}$	0.65 – 4.68
$h_c H_i/D_{50}^2$	-5.27 – 17.9
$B^2/L_p D_{50}$	0.85 – 84.34
$\xi$	1.16 – 14.54
$D_{50}/D_{50c}$ (permeable)	2.06 – 3.2
$D_{50}/D_{50c}$ (impermeable)	1.50

## 6.5 CALIBRATION OF THE MODEL

Calibration of the model was made using the 3-D test data collected by Stuart Seabrook (1997). The purpose of this calibration was to evaluate the ability of the 2-D test model to predict the 3-D test results. The interaction of wave and structure in the 3-D modeling is more complex than the 2-D modeling. The complex, three dimensional wave-structure interactions include diffraction of the wave passing by the tip of the structure. When wave travel into the breakwater, it separates the wave zone (in front of the breakwater) and the sheltered zone (behind the breakwater). There will be transfer of energy across the zone where wave crests will spill into the sheltered zone and troughs will be filled with water from the sheltered zone. This phenomenon does not occur in the 2-D tests where the test model is usually constructed across the entire width of the test flume. The objective of this study is to provide model equations that are suitable for the design purpose. Thus attempt will be made to find as to how the 2-D model parameters represent the more realistic 3-D case for design purposes.

### 6.5.1 Brief Description of Seabrook's 3-D Testing

The 3-D test was undertaken in the 3-D wave basin at QUCERL, where the basin is approximately 30m x 35m x 1.2m and equipped with a wave generator that is capable of generating regular and irregular waves. The model was constructed on the flat floor of the basin and a concrete beach was developed at the slope of 1:10 to dissipate wave energy and to minimize the reflection from the testing area. The breakwaters were constructed from stones with  $D_{50} = 0.004\text{m}$  for the core and two layers of armour with  $D_{50} = 0.037\text{m}$ . Three different crest widths were modeled during the tests.

The breakwaters were tested with incident waves at  $90^\circ$  and  $60^\circ$  to the shoreline. In order to minimize the effect of disturbances outside the testing area, wave guides were constructed perpendicular to the wave paddle, from the paddle to the beach. Eight wave probes and two velocity probes were used to measure the wave conditions. One probe was located offshore of the breakwater to define the incident waves and others were located behind the breakwater to define the wave transmission and effect of diffraction. No measurements were taken for reflected waves.

Irregular waves were used for all of the wave trains tested. The wave targets were generated from a JONSWAP spectrum with  $\alpha_p = 0.0081$  and  $\gamma = 3.3$ . The heights of waves targeted varied from 0.032m to 0.095m and the wave period ranged from 0.95s to 1.98s. All data sampling was undertaken using the GEDAP data acquisition system and was analyzed using the GEDAP data analysis package. The transmission coefficients were defined at each probe location based on the transmitted significant wave heights. The wave probe located offshore was used to define the incident wave height. A summary of Seabrook's experiments including the range of specific dimensionless variables compared to the author's data sets is summarized in Table 6.2 and the configuration of the 3-D testing can be seen in Figure 6.8 and 6.9

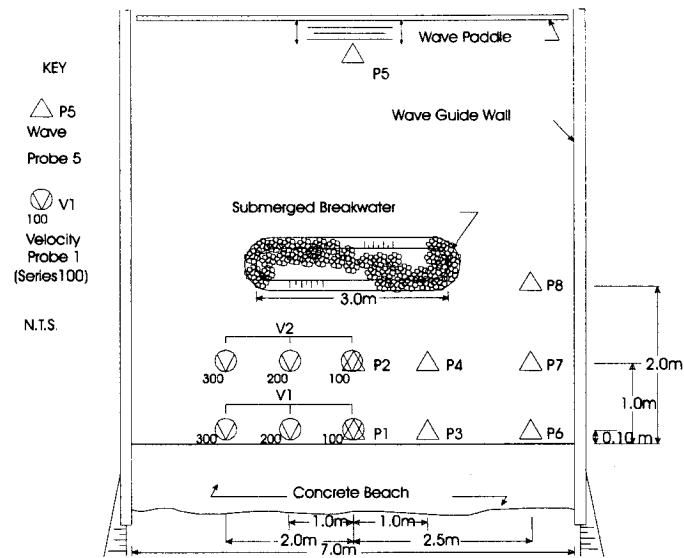


Figure 6.8. 3-D Testing set up at waves direction of 90°. (from Seabrook, 1997)

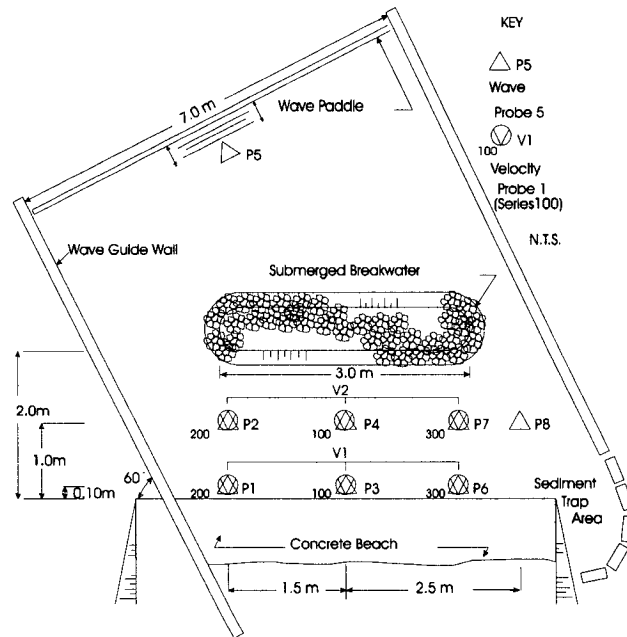


Figure 6.9. 3-D Testing set up at waves direction of 60°. (from Seabrook, 1997)



**Table 6.2.** A Summary of data sets used in calibration.

Variable	Expression	Range	
		Seabrook (1997) 3-D	Author 2-D
The relative wave height	$H_i/D_{50}$	0.58 - 2.64	0.65 - 4.68
The relative crest height	$h_c/H_i$	(-5.91) - (-0.32)	(-3.28) - 1.41
The wave steepness	$s_{op}$	0.005-0.06	0.02 - 0.09
The wave angle	$\phi_o$	60° - 90°	90°
The surf similarity parameter	$\xi$	2.66 - 9.87	1.16 - 14.54
The relative crest width	$B/H_i$	1.97 - 37.65	1.63 - 52.20
The slope angle	$\text{Cot } \alpha$	1.5	1.0 - 4.0
The permeability of the core	P	permeable	perm. - imperm.
The grading of material	$D_{50}/D_{50c}$	9.25	1.5 - 3.2

### 6.5.2 Comparison of Proposed Model and the 3-D Results

Inspection of Seabrook's data (not reported here) shows that the 3-D testing produced some transmitted waves higher than the incident waves. The possible reason of this phenomenon could be due to complex reflection and diffraction conditions around the structure.

The comparison of estimated and observed  $K_t$  values of the 3-D model data recorded by probe 2 when waves were attacking at 90° to the axis of the breakwater is shown in Figure 6.10. There is more scatter for  $K_t$  values predicted by the earlier proposed 2-D equation and the actual 3-D test results as shown in the plot. This is not surprising since the 3-D modeling conditions introduce more complex interaction between the breakwater and the waves that travel to the structure while the proposed equation did not account for the physical processes that occur in the 3-D test as described above. It is also possible that the results of the tests performed in a 3-D environment are influenced by the wave reflections from the guide walls and wave paddle and might be contributing to the discrepancies. Other comparison using data recorded by probe 4 when waves were attacking at 60° is also made as shown in Figure 6.11. The same trend as probe 2 is depicted. However, in general, the

comparisons seem fair as indicated by the squared correlation coefficients of 0.7746 for data recorded at probe 2 and 0.6655 for data recorded at probe 4.

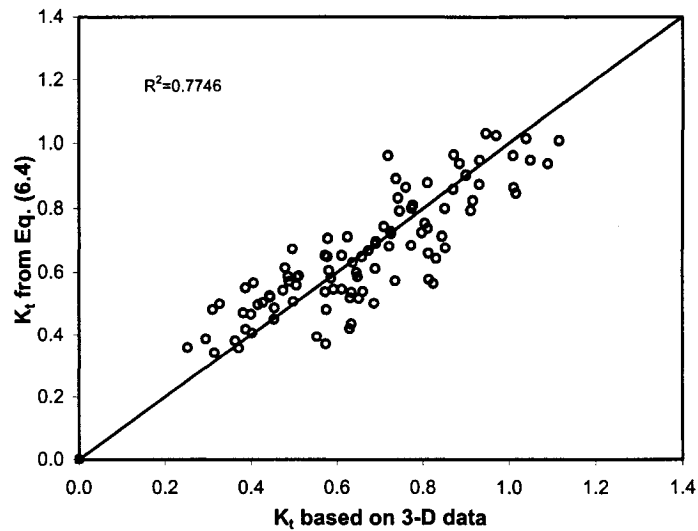


**Figure 6.10.** Comparison between 2-D equation and 3-D test results for probe 2 at  $\phi_0 = 90^\circ$ .

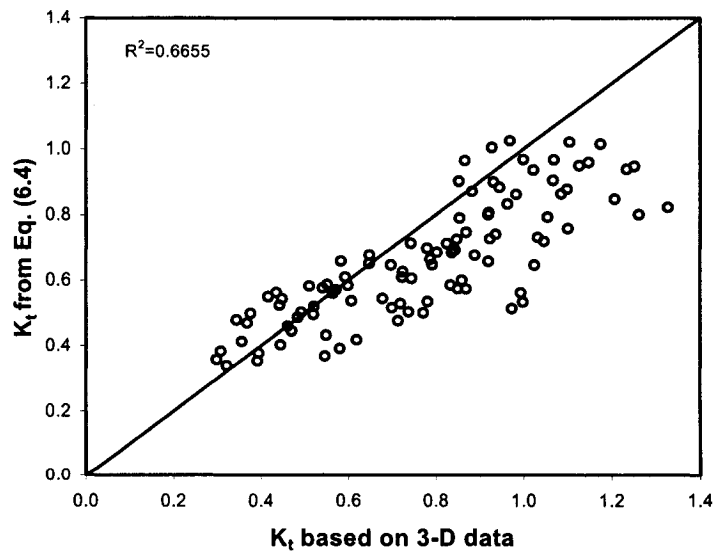


**Figure 6.11.** Comparison between 2-D equation and 3-D test results for probe 4 at  $\phi_0 = 60^\circ$ .

In order to propose equations that are applicable for 3-D test conditions, a correction for the excess energy due to diffraction of the waves, not accounted for earlier, is introduced. The height of waves behind a breakwater due to diffraction is influenced by the distance from the corner, angle from the breakwater, the incident wave direction and length. Penney and Price (1952), and Dean and Dalrymple (1984) analytically solved the diffraction problem behind a semi-infinite barrier that can be applied to the surface water wave. The analysis was based on an assumption that the barrier is impermeable. The results were given in a dimensionless diagram for incident waves approaching the barrier and can be used for preliminary calculations.

Applying the method used by Penney and Price (1952), the diffraction coefficients,  $K_d$ , were determined for the 3-D test data. The values of diffraction coefficients were converted to equivalent wave energies and wave heights so as to evaluate the relationship between the excess energies and the diffracted energies. It was found that no correlation exists between the excess energies and the diffracted energies. Figure 6.12 shows the relationship between the diffracted energies calculated from the diffraction coefficients of Penney and Price's method and the diffracted energies found from the measured data.

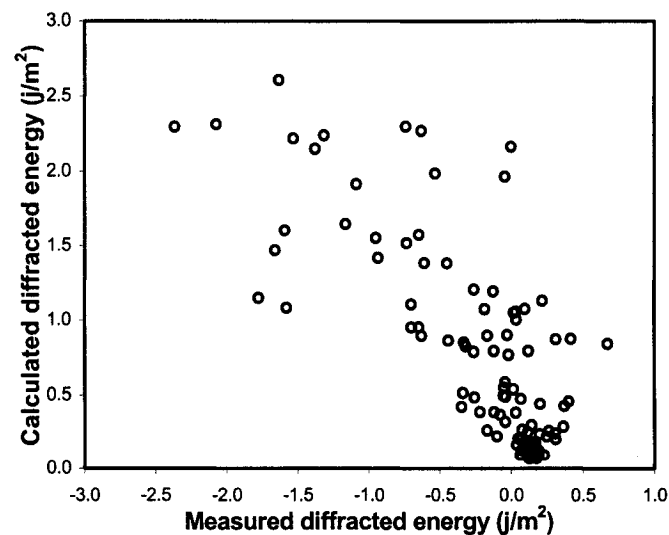


**Figure 6.12.** Comparison between diffracted energies calculated using  $K_d$  and measured data.

Consideration should be given to the fact that the diffraction coefficients calculated herein are based on the assumption that the crest of the breakwater is above the water level, while the tests performed were for submerged conditions. Another consideration is that the diffraction theory presented by Penney and Price deals only with rigid breakwaters in which the waves are completely reflected, whereas the breakwaters tested had a permeable core. These differences are expected to have a significant influence on diffraction coefficients found for the present test case using Penney and Price's method. Considering the above, it was concluded that the 2-D equation could be applied for 3-D data with caution.

To provide a better understanding and insight into the wave transmission process in the 3-D environment, it was decided therefore, to represent all processes in the three-dimensional environment accurately by developing a new model for predicting the wave transmission process. The development of the 3-D model for determining wave transmission using Seabrook's test results will be discussed in the next section.

## **6.6 DEVELOPMENT OF THE 3-D MODEL FOR $K_t$**

The development of the model was carried out using statistical analysis, similar to the development of the 2-D equations as described previously. Firstly, a correlation in the data was established by plotting the transmission coefficients against dimensional and dimensionless variables. Parameters that were found to be significantly influencing the transmission process were then used to develop the model. The parameters that are significantly affecting the transmission process are discussed below. Since most of the transmission processes in 2-D are similar to the 3-D case, only the important parameters appearing in 3-D that did not appear in the 2-D process will be discussed in this section (i.e. diffraction).

Theoretical analysis of diffraction of sea waves by breakwaters has been presented by many researchers (Penney and Price, 1952; Dean and Dalrymple, 1984; Goda, 1985). Even for a relatively simple problem, a calculation of diffraction is quite complicated. Penney and Price investigated the diffraction process of a long straight breakwater for incident waves from different directions. The problem has been solved by assuming that the height of the waves is small compared with their wave length, so that the small amplitude wave theory may be applied. The solution can be used for uniform water depth and perfectly reflecting structure. For being incident normally, the solution yields the wave crest pattern in the  $x,y$  plane and the distribution of the wave height throughout the affected area. When the incident waves approach at an angle to the breakwater, the wave pattern is in polar coordinates  $(r,\phi)$  instead of  $(x,y)$  where  $r$  is radial distance from the end and  $\phi$  is an angle from the breakwater. When waves approaching a structure of finite length, diffracted waves will occur at each end of the structure. The wave patterns can be developed by combining the results for semi-infinite structure diffraction at each end (Sorensen, 1993). Behind the structure, the height of waves will decrease and along the lines where the wave crests from each end meet, the highest waves will occur as a result of the summation of the heights of the two component waves from the individual diffraction. The effect of diffraction is usually characterized by a diffraction coefficient,  $K_d$ , where  $K_d = H_d/H_i$ ,  $H_d$  is the diffracted height at a point of interest and  $H_i$  is the incident wave height. Diffracted height at the point of interest is affected by the radial distance,  $r$ , the angle,  $\phi$ , and the incident wave direction,  $\phi_o$ . Notation for parameters affecting diffraction for oblique incidence of waves on a breakwater is shown in Figure 6.13.

For preliminary calculations, tabulated results from Wiegel (1962) for semi infinite structure summarized from Penney and Price (1952) solution can be used. Graphic plots of Wiegel's results also found in CERC (1984).

### 6.6.1 Effect of Wave Direction

The effect of wave direction in the transmission process was observed using the data from probe 2 for wave direction of  $90^\circ$  and probe 4 of wave direction of  $60^\circ$ . The two probes were placed at the same position relative to the breakwater and at same distance from the breakwater. Figure 6.14 shows the plot of transmission coefficients,  $K_t$ , against the relative crest height,  $h_c/H_i$ , for both probes 2 and 4. Plot shows that transmission coefficients from probe 2 are relatively lower than transmission coefficients of probe 4 that are in conformity with the diffraction theory. According Penney and Price (1952) and Wiegel (1962), higher waves will occur for lower wave directions.

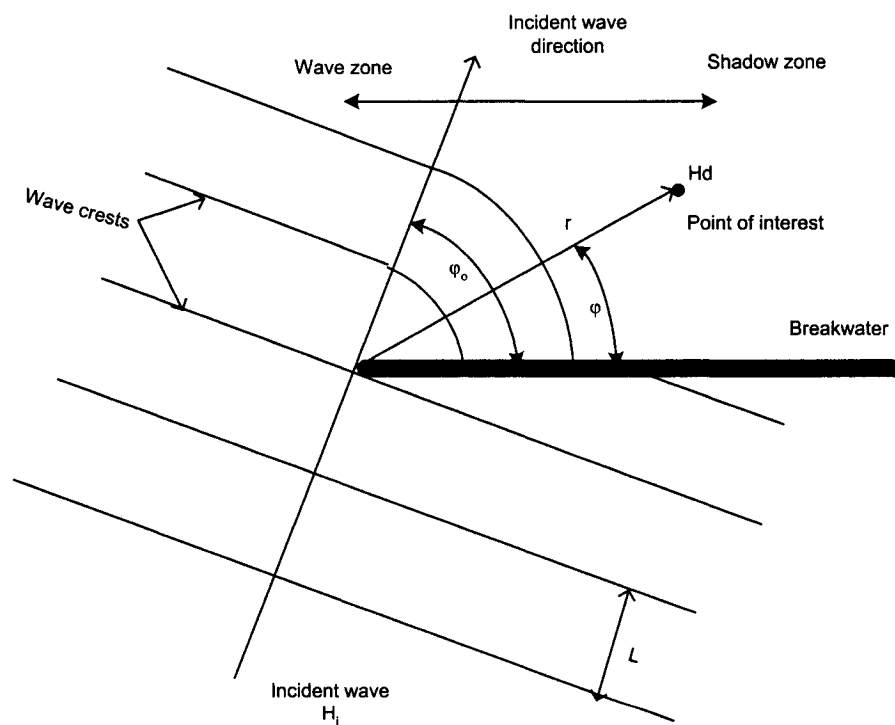


**Figure 6.13.** Wave diffraction behind a breakwater for oblique incidence of waves.

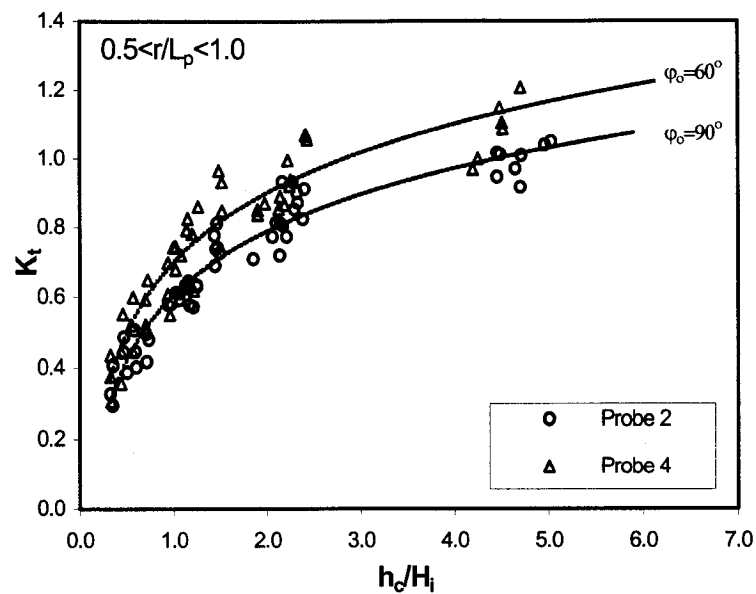


**Figure 6.14.** Effect of incident wave direction (probes 2 and 4 at the same location and distance to the breakwater).

### 6.6.2 Effect of Angle of Location from the Breakwater

In order to evaluate the effect of angle of location of a point with reference to the breakwater, Figure 6.15 is plotted. Transmission coefficients calculated from probe 2 and 4 both for  $\phi_o = 90^\circ$  wave direction are plotted against  $h_c/H_i$ . Probes 2 and 4 were located on the centerline of the breakwater at distances of 1m and 2m from the toe of the breakwater, respectively. A general trend can be observed that for higher values of the angle (probe 4), higher transmitted waves occur, agreeing with the theoretical results where for higher value of an angle yields to higher diffraction coefficients as well as transmission coefficients. Examining Figure 6.16 where transmission coefficients from probes 1 and 2 at  $90^\circ$  waves direction are plotted, results in higher transmission for greater angle  $\phi$ . Again, this confirms the diffraction theory where for greater  $\phi$ , the diffraction coefficient increases, hence higher transmission.

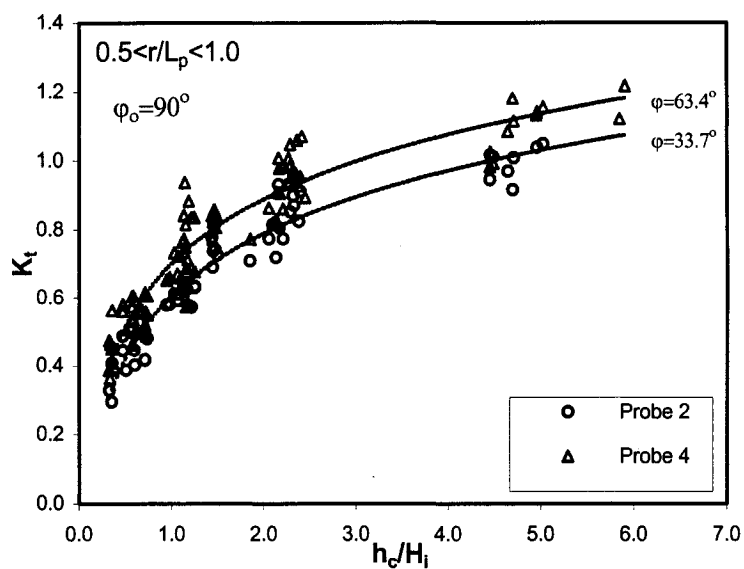


**Figure 6.15.** Effect of angle from the breakwater to the point of interest at normally incident waves (probes 2 and 4 at the same distance to the breakwater).

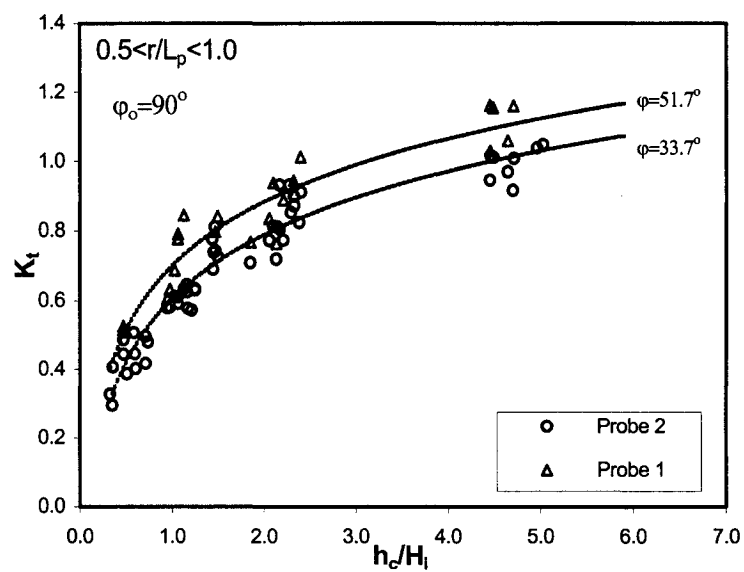


**Figure 6.16.** Effect of angle from the breakwater to the point of interest at normally incident waves (probes 1 and 2 at the center line of the breakwater).



### 6.6.3 Effect of Relative Radial Distance, $r/L_p$

Radial distance of a point of interest on leeward side of breakwater is a square root of  $x^2$  and  $y^2$ , where  $x$  is distance in  $x$  direction and  $y$  is distance in  $y$  direction from the end of breakwater. In this region the diffracted waves tend to decrease for larger distance  $x$  and  $y$  since obvious fact that the reduction becomes more effective farther away the end. Figure 6.17 shows the plot of the transmission coefficients from probe 2 at  $90^\circ$  for two different range of relative radial distance,  $r/L_p$ . It shows that the transmission coefficients for higher values of  $r/L_p$  are slightly lower than lower values of  $r/L_p$ . For a given  $\phi_0$  and  $\phi$  values, decreasing wave periods resulting in larger values of  $r/L_p$  and decreasing of diffracted waves as noted above.

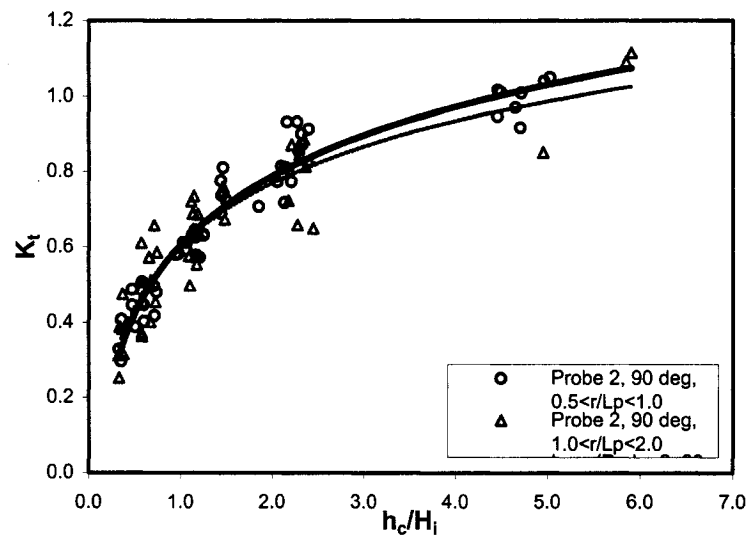


**Figure 6.17.** Effect of relative radial distance from the tip of breakwater to the point of interest at normally incident waves.

### 6.6.4 Statistical Development

Similar criteria and variables involved in the development of design equation for wave transmission in 2-D case were adopted in the development of wave transmission model for 3-D data. In addition, diffraction process that usually occurs

in 3-D tests was added. It was evaluated that the incident wave direction  $\phi_0$  and length  $L_p$ , radial distance  $r$  from the tip of the breakwater and angle  $\phi$  from the breakwater to the point of interest are all significant in influencing the diffraction process.

As previously noted, the 3-D testing produced sometimes transmission coefficients greater than 1.0. Even though this situation is possible at site specific locations under directional spectral transformation and complex reflection and diffraction conditions, it is likely that 3-D testing apparatus and analysis procedures have introduced some error into the measured  $K_t$  values (Seabrook, 1997). Therefore, any  $K_t$  value greater than one was removed from the data set before developing the model.

Regression analysis was performed within the data sets to find the fitted parameters for predicting the values of  $K_t$ . The resulting alternative design equation of the regression analysis for  $K_t$  is

$$K_t = -0.869 \exp\left(-\frac{h_c}{H_i}\right) + 1.049 \exp\left(-0.003 \frac{B}{H_i}\right) - 0.026 \frac{H_i h_c}{BD_{50}} - 0.005 \frac{B^2}{L_p D_{50}} + 0.003 \frac{h_s}{h} \times \frac{r}{L_p} \cos(\phi - \phi_0) \dots [6.16]$$

A plot of this equation, Figure 6.18 shows a relatively good fit between estimated and measured values and provides adequate answers for  $K_t$ , with the squared correlation coefficient ( $R^2$ ) equal to 0.854 and standard error of estimate ( $\sigma$ ) being 0.07. The equation shows physical process as related to depth of submergence, hence is related to wave breaking, the relative crest width,  $B/H_i$ , friction by structural roughness and length,  $H_i h_c / BD_{50}$ , the internal flow resistance parameter,  $B^2 / L_p D_{50}$ , and the diffraction process that is represented by the last term in Equation [6.16]. The normal probability plot of residuals in Figure 6.19 is almost a straight line indicating that the residuals are nearly normally distributed.

In order to evaluate the suitability of the equation, a sensitivity analysis was carried out using the value of +95% confidence interval as shown in Figure 6.20. The equation is in the form

$$K_t = C_1 \exp\left(-\frac{h_c}{H_i}\right) + C_2 \exp\left(C_3 \frac{B}{H_i}\right) + C_4 \frac{H_i h_c}{BD_{50}} + C_5 \frac{B^2}{L_p D_{50}} + C_6 \frac{h_s}{h} \times \frac{r}{L_p} \cos(\phi - \phi_o) \quad [6.17]$$

The value selected for  $h_c/H_i$  was between 0.169 and 3.125,  $B/H_i$  between 1.95 and 37.5,  $H_i h_c/BD_{50}$  between 0.02 and 1.57,  $B^2/L_p D_{50}$  between 0.29 and 20.62, and the diffraction term between 0.54 and 1.49. Result shows that coefficient  $C_2$  is the most sensitive having a minimum variation in the response of about 2.2% and maximum variation of about 4.8%, with the average value being 3.3%.

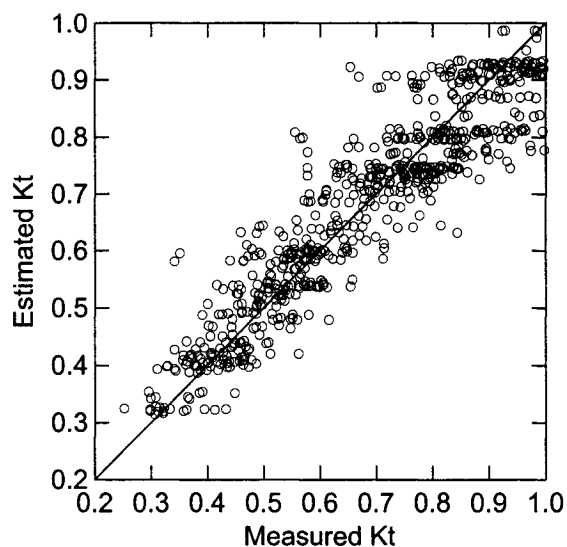


**Figure 6.18.** Estimated and measured  $K_t$  of 3-D equation.

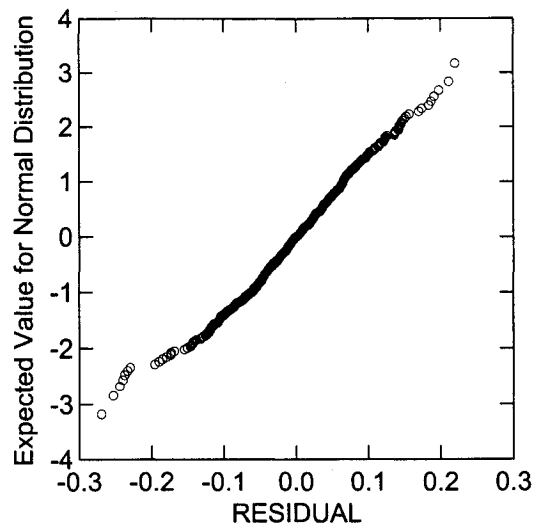


Figure 6.19. Normal probability of  $K_t$  residuals for 3-D equation.

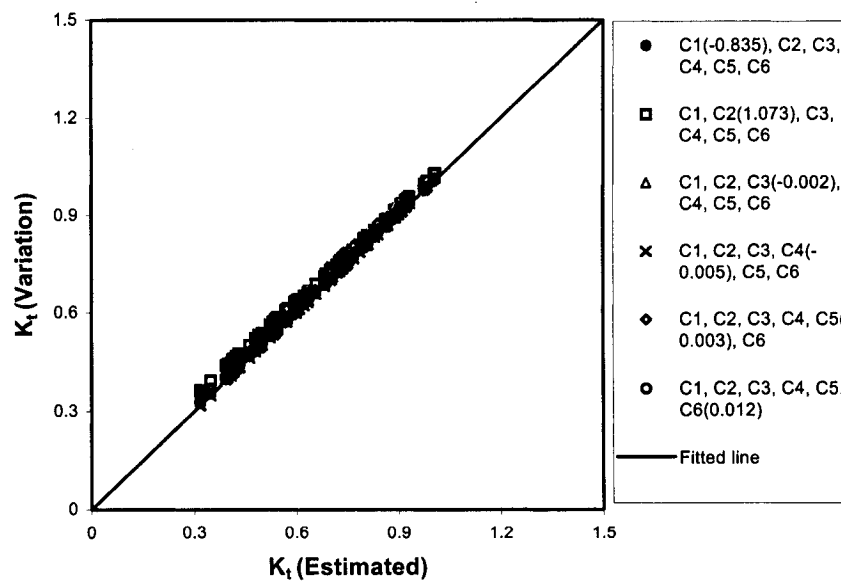
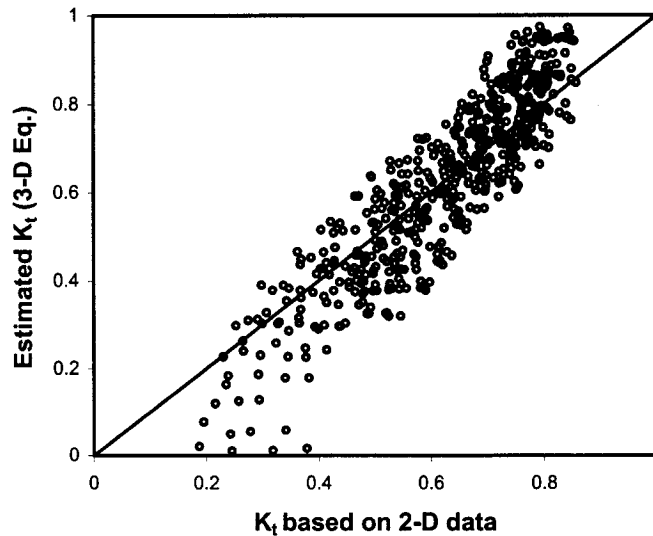


Figure 6.20. Sensitivity of  $K_t$  to variation of +95% confidence interval in regression coefficients.

The performance of 3-D equation to predict  $K_t$  was also evaluated using 2-D data. Since the 3-D equation was derived from the data set of submerged conditions, the comparison will also be made for the 2-D data set for submerged including zero submergence. Figure 6.21 shows that the 3-D equation predicts relatively well  $K_t$  values in the range of  $0.4 \leq K_t \leq 0.8$ .



**Figure 6.21.** Comparison between 3-D equation and 2-D data for submerged condition.

## 6.7 LIMITATION OF THE PROPOSED EQUATIONS

The equations developed above are based on the 2-D test data for irregular waves. The wave transmission equation includes parameters that are considered to be representing physical processes such as water depth fluctuation ( $h_c/D_{50}$ ), hence is related to wave breaking, wave overtopping ( $H_i/D_{50}$ ), dissipation due to surface friction, and transmission through the breakwater. For the wave reflection, the equation includes parameters that are physically significant in the process of energy dissipation through breaking ( $\xi$ ), impact of water depth ( $h_c/D_{50}$ ) and transmission into

and through the breakwater ( $D_{50}/D_{50c}$ ,  $H_i/D_{50}$ ). The use of the models should be restricted to the range of the variables tested. Application outside this range of variables may result in incorrect estimates.

The 2-D equation for wave transmission shows that there was a discrepancy between the equation and the 3-D test results. The effects of the diffraction and reflection in 3-D test environment should be considered when comparing 2-D and 3-D test results, whereas, the 2-D equation did not account for it. However, results show that the 2-D equation is fair enough to predict 3-D results.

An equation developed to predict  $K_t$  based on 3-D data fails to predict  $K_t$  when the water level was at or below the crest level. It should be noted that the equation was derived using 3-D testing results conducted for submerged condition; therefore the use of the equation should be for the same condition.

It is emphasized once again that the 2-D transmission and reflection models developed here need further verification or validation. However, since the equations were developed using a wide range of variables and relevant physical processes, the models may be used for preliminary designs.

## Chapter 7

# SOURCES OF ERROR

### 7.1 POSSIBLE ERRORS

In any experimental study, instrumental and human errors are the potential sources of error. It is also possible in many experimental studies, involving random materials, that errors might occur due to the variation of material properties. Therefore, the possible errors are composed of instrumental error, material variability and human error.

### 7.2 INSTRUMENTAL ERROR

The following instruments were used during the experiments.

- Wave probes.
- Electro-mechanical profiler.

The measurement of wave height in this study was conducted using capacitance type wave gauges, whose non-linearity of the electronic circuitry was less than 1% of the full scale. Under ideal conditions, the resolution is less than 1 mm (Wiegert and Edwards, 1981). The wave heights measured were in the range of 5cm to 20cm (wave targets). Therefore for the typical wave target mentioned above, the potential error was about 0.5 to 2.0%.

The mechanical profiler was used in profiling the breakwater cross section. A small wheel was attached on the rod tip so that it traveled smoothly over the surface.

In order to record as many points as possible, the profiler was dragged slowly. The profiler is capable of measuring to  $\pm 0.1$  cm that is obtained by reading the level during calibration. The error in measurement of any length by the profiler would be about one half of the size of the stone. The diameter of the armour stone being 3.4cm, the error in the profiler reading was about 1.7cm. Considering that typical measured widths were of the order of 100cm to 300cm, such an error is about 1.7% to 5.1%, relatively speaking.

### **7.3 HUMAN ERROR**

The human errors can be considered as human variability. In the case of this study, the error affects how the breakwater is built and observation recorded regarding stone motion and overall breakwater performance. For example, while building the test section, the material is compacted during building of the test model and any variation in compaction will affect the permeability of the structure. If the damaged breakwater is not loosened before building another one for test, it could affect the permeability and the movement of the stones, as natural sorting and compaction due to the earlier wave action may have occurred. There is no quantitative measurement of telling how much error could be involved in the above process. Since all tests were undertaken by the same person, the relative errors from test to test are probably minimal and assumed to have no significant effect on the results.

### **7.4 MATERIAL VARIABILITY**

The materials used were crushed stones and therefore expected to be variable in both shape and dimension. In this study, only angular stones were accepted,



therefore, they were carefully chosen and thoroughly mixed during the construction of each test section. However, the influence of material variability on the stability tests is difficult to estimate, as there are infinitely many ways in which each stone can interact with the other, resulting in different effective dimension. After each test, the cross section was rebuilt; therefore errors due to material variability were minimized.

## 7.5 REPEATABILITY

In order to get an idea of how profiles compare with each other, the tests ST6, SH6 and SN1 were compared. These tests have the same boundary conditions and were tested for the same relative water depth,  $h_c/h = 0.3$ , the incident wave height,  $H_i$ , and period,  $T_p$ , of  $\sim 12.5\text{cm}$  and  $1.5\text{s}$ , respectively. The structure had a slope of 2 and  $D_{50}$  of  $0.034\text{m}$  in each case. Measurements resulted in the following eroded areas,  $60\text{cm}^2$ ,  $56\text{cm}^2$  and  $54\text{cm}^2$  respectively for the breakwater cross-section. This gives a difference of  $6\text{cm}^2$  between the maximum and minimum and an average of  $56.7\text{cm}^2$ . Thus, error of repeatability was found to be within the range of 4.7% - 5.9%.

## Chapter 8

# CONCLUSIONS AND RECOMMENDATIONS

### 8.1 CONCLUSIONS

In this study, experiments with physical models of low crested rubble mound breakwaters have been carried out to investigate various aspects of the process of wave transmission and reflection over and through the structure. The stability of armour layer under irregular wave attack was also investigated. Different rubble mound breakwaters, including permeable and impermeable cores, slopes of the breakwater between  $\cot \alpha=1$  and 4, crest widths between 0.3m and 2.0m and different armour gradations were tested for the wave transmission and reflection in a variety of irregular wave conditions and water depths. To investigate the stability of armour units, wave conditions were also varied in grouped and non-grouped waves. The author is not aware of any previous studies in which these different quantities have been measured together.

A number of observations were made with respect to the effect of various independent variables on the transmission, reflection and stability of low crested breakwaters. The transmission of waves is very dependent on the relative submergence (corresponds to water depth) and the crest width. Other variables that significantly influence wave transmission are breakwater slope,  $\cot \alpha$ , and structure permeability, represented by  $D_{50}/D_{50c}$ . Wave steepness,  $s_p$ , and dimensionless armour diameter were found less influential on wave transmission process. The reflection of waves is strongly influenced by water depth and surf similarity parameter. Effect of crest width and armour size is less significant in influencing wave reflection. The

stability of low crested breakwaters is significantly influenced by water depth and the wave period. In general, the stability of a breakwater also depends upon other parameters like wave height, wave duration, front slope and core permeability.

With respect to the models currently available, it was found that existing design equations are unable to accurately predict wave transmission and reflection over a wide range of design conditions, especially for wide crested breakwaters. Therefore a new model for wave transmission and reflection were developed to better predict of the processes.

A predictive transmission equation was developed using dimensionless variables, which represent physical processes in the transmission phenomenon. The equation provides a robust solution given the enormously wide range of parameters and are considered to be appropriate for most feasible design conditions. The variables in the equation have physical significance in the processes related to wave dissipation due to friction induced by structural roughness,  $H_i h_c / D_{50}^2$ , internal flow through the breakwater,  $B^2 / L_p D_{50}$ , effect of relative water depth,  $h_c / D_{50}$ , relative wave height,  $H_i / D_{50}$ , and permeability of the structure represented by the gradation factor,  $D_{50} / D_{50c}$ . The proposed equation is also able to predict relatively well of the 3-D model data and may be expressed as follows.

$$K_t = -0.180 \left( \frac{h_c}{D_{50}} \right) + 0.001 \left( \frac{H_i}{D_{50}} \right) + 0.024 \left( \frac{H_i h_c}{D_{50}^2} \right) - 0.239 \left( \frac{B^2}{L_p D_{50}} \right)^{0.196} + 0.006 \frac{D_{50}}{D_{50c}} - 0.611$$

In the development of the reflection model, a predictive model was developed by considering parameters with the most influence and reflects the physical processes in the reflection phenomenon such as surf similarity,  $\xi$ , the amount of wave energy transmitted over and through the structures,  $H_i / D_{50}$ , the relative crest height,  $h_c / D_{50}$ , and structure permeability,  $D_{50} / D_{50c}$ . The equation provides good estimate with the results of 2-D data and represents  $K_r$  well for the entire small to high  $K_r$  values. The predictive reflection model may be expressed as follows.

$$K_r = \left( 0.1753 \log \xi + 0.0528 \left( \frac{h_c}{D_{50}} \right) + 0.1722 \left( \frac{H_i}{D_{50}} \right)^{0.452} + 0.0086 \left( \frac{D_{50}}{D_{50c}} \right) \right)^2$$

To provide a better understanding and insight to wave transmission process in the 3-D environment, a model for predicting wave transmission process was also developed. The equation shows physical processes related to depth of submergence,  $h_c/H_i$ , (related to wave breaking), the relative crest width,  $B/H_i$ , friction by structural roughness and length,  $H_i h_c / BD_{50}$ , the internal flow resistance parameter,  $B^2 / L_p D_{50}$ , and the diffraction process. The equation presented here provides adequate answers for  $K_t$  and predicts relatively well  $K_t$  values in the range of  $0.4 \leq K_t \leq 0.8$  using the 2-D data. The 3-D equation for transmission may be expressed as follows.

$$K_t = -0.869 \exp\left(-\frac{h_c}{H_i}\right) + 1.049 \exp\left(-0.003 \frac{B}{H_i}\right) - 0.026 \frac{H_i h_c}{BD_{50}} - 0.005 \frac{B^2}{L_p D_{50}} + 0.003 \frac{h_s}{h} \times \frac{r}{L_p} \cos(\varphi - \varphi_o)$$

The valid range of variables for transmission and reflection models for both 2-D and 3-D conditions is shown in the following table.

Variables	Range	
	2-D	3-D
$h_c/D_{50}$	-3.82 - 2.06	(-5.91) - (-0.32)
$H_i/D_{50}$	0.65 - 4.68	0.58 - 2.64
$h_c H_i / D_{50}^2$	-5.27 - 17.9	(-0.57) - (-8.17)
$B^2 / L_p D_{50}$	0.85 - 84.34	0.29 - 21.72
$\xi$	1.16 - 14.54	2.66 - 9.87
$D_{50}/D_{50c}$ (permeable)	2.06 - 3.2	9.25
$D_{50}/D_{50c}$ (impermeable)	1.50	-

## 8.2 RECOMMENDATIONS FOR FUTURE WORKS

This thesis has focused on the study of wave transmission, wave reflection and stability of rock-armour on rubble mound breakwaters in a variety of irregular

wave conditions and properties of the structures. The investigation presented here could be extended in several areas.

- Permeability of breakwater has been identified as an important parameter in the process of transmission, reflection and stability. There is a need for further investigation of this parameter, since the present investigations were focused only on two permeability conditions, in which with permeable and impermeable core.
- In real situation, location of the breakwater to the shoreline may be has significant contribution on the wave transmission due to secondary hydrodynamics impacts such as resonant long wave. This process gives the potential for local setup, hence influences the wave transmission and should be considered.
- Site-specific interactions between the breakwater and wave should be investigated using 3-D physical modeling due to complexity of this process. In addition, effect of diffraction can also be assessed with more detail.
- The performance of rubble mound breakwaters under multi directional wave action is not addressed in the present investigation. Therefore, further investigation of the effect of multi directional wave action on the breakwaters performance is necessary to determine the physical processes suggested herein.
- In this study, stability of the breakwaters was assessed by measuring the initial and final profiles and by counting the number of stones displaced before and after the wave action. More detailed investigations with regard to the relationship between the wave-induced forcing and the resulting damage of rock-armour rubble mound breakwaters should be conducted.
- Data obtained in this study could be used to calibrate an existing numerical model or to develop a new numerical model that could include a prediction of the transmission and reflection over a wide range of water depth and structural geometry.

## REFERENCES

- Abdul Khader, M.H. and Rai, S.P., 1980, A Study of Submerged Breakwaters, J. of Hydraulic Research, 18, No. 2, pp. 113-121.
- Abul-Azm, A.G., 1993, Wave Diffraction Through Submerged Breakwaters, J. of Waterway, Port, Coastal, and Ocean Eng., ASCE, Vol. 119, No. 6, pp. 587-605.
- Adam, C.B. and Sonu, C.J., 1986, Wave Transmission a cross Submerged Near Surface Breakwaters, Proc. of the 20<sup>th</sup> Coastal Engineering Conf., Taipei, Taiwan, pp.1729-1738.
- Ahrens, J.P., 1975, *Large Wave Tank Tests of Riprap Stability*, Technical Memorandum No. 51, CERC, Vicksburg, Mississippi.
- Ahrens, J.P. and McCartney, B.L., 1975, Wave Period Effect on the Stability of Riprap, Proc. of Civil Engineering in the Oceans/III, ASCE, pp1019-1034.
- Ahrens, J.P., 1984, Reef Type Breakwaters, Proc. of the 19<sup>th</sup> Coastal Engineering Conf., Houston, Texas, pp. 2648-2662.
- Ahrens, J.P. and Titus, M.F., 1985, Wave Runup Formulas for Smooth Slopes, J. of Waterway, Port, Coastal, and Ocean Eng., ASCE, Vol. 111, No. 1, pp. 128-133.
- Ahrens, J.P., 1987, *Characteristics of Reef Breakwaters*, Technical Report 87-17, CERC, Vicksburg, Mississippi.
- Ahrens, J.P., 1989, Stability of Reef Breakwater, J. of Waterway, Port, Coastal, and Ocean Eng., ASCE, Vol. 115, No. 2, pp. 221-233.
- Allsop, N.W.H., 1983, Low Crest Breakwater, Studies in Random Waves, Proc. of Coastal Structures '83, Arlington-Virginia, ASCE, pp. 94-107.
- Allsop, N.W.H, 1990, Reflection Performance of Rock Armoured Slopes in Random Waves, Proc. of the 22<sup>nd</sup> Coastal Engineering Conf., Delft, the Netherlands, pp. 1460-1472.

- Bade, P. and Kaldenhoff, H., 1980, Energy Transmission Over Breakwater-A Design Criterion?, Proc. of the 17<sup>th</sup> Coastal Engineering Conf., Sydney-Australia, pp. 1885-1897.
- Battjes, J.A., 1974, Surf Similarity, Proc. of the 14<sup>th</sup> Coastal Engineering Conf., Copenhagen-Denmark, pp. 466-480.
- Battjes, J.A. and Stive, M.J.F., 1984, Calibration and Verification of a Dissipation Model for Random Breaking Waves, Proc. of the 19<sup>th</sup> Coastal Engineering Conf., Houston, Texas, pp. 649-660.
- Beji, S. and Battjes, J.A., 1993, Experimental Investigation of Wave Propagation over a Bar, Coastal Engineering, 23, Elsevier, The Netherlands, pp. 151-162.
- Bird, P.A.D., Davidson, M.A., Ilic, S., Bullock, G.N., Chadwick, A.J., Axe, P. and Huntley, D.A., 1996, Wave Reflection, Transformation and Attenuation Characteristics of Rock Island Breakwaters, *Advances in Coastal Structures and Breakwaters*, Thomas Telford, London, pp. 93-106.
- Bremner, W.D., Foster, N., Miller, C.W. and Wallace, B.C., 1980, The Design Concept of Dual Breakwaters and Its Application to Townsville, Australia, Proc. of the 17<sup>th</sup> Coastal Engineering Conf., Sidney, Australia, pp.1898-1908.
- Brown, C.T., Blanket Theory & Low Cost Revetments, Proc. of the 16<sup>th</sup> Coastal Engineering Conf., Hamburg, Germany, pp.2510-2527.
- Bruun, P. and Gunbak, A.R., 1976, New Design Principles for Rubble Mound Structures, Proc. of the 15<sup>th</sup> Coastal Engineering Conf., Honolulu, pp.2429-2473.
- Bruun, P. and Johannesson, P., 1976, Parameters Affecting Stability of Rubblemounds, J. of Waterway, Harbours, Coastal Eng. Div. ASCE, Vol. 102, No. WW2, pp. 141-164.
- Bruun, P. and Kjelstrup, S., 1983, Design of Mound Breakwaters, Proc. of Coastal Structures '83, ASCE, New York, NY, pp. 122-139.
- Bruun, P., 1990, Discussion of 'Deterministic and Probabilistic Design of Breakwater Armour layers', J. of Waterway, Port, Coastal, and Ocean Eng., ASCE, Vol. 116, No. 4, pp. 502-504.
- Bruun, P. (ed.), 1985, *Design and Construction of Mounds for Breakwaters and Coastal Protection*, Elsevier, Amsterdam, The Netherlands.

Burcharth, H.F., 1979, The Effect of Wave Grouping on Onshore Structures, Coastal Engineering, 2, pp. 189-199.

Camfield, F.E., 1996, Natural Periods of Armour Stones, Proc. of the 25<sup>th</sup> Coastal Engineering Conf., Orlando, Florida, pp. 1583-1588.

Carstens, T., Tørum, A. and Traetteberg, A., 1966, The Stability of Rubble Mound Breakwaters Against Irregular Waves, Proc. of the 10<sup>th</sup> Coastal Engineering Conf., Tokyo, Japan, pp.958-971.

Cartwright, D.E. and Longuet-Higgins, M.S., 1956, The Statistical Distribution of the Maxima of a Random Function, Proc. R. Soc. London, Series A, pp. 212-232.

Coastal Engineering Research Center, 1977, *Shore Protection Manual*, Department of the Army, WES, Corps of Engineers, Vicksburg, Mississippi.

Coastal Engineering Research Center, 1984, *Shore Protection Manual*, Department of the Army, WES, Corps of Engineers, Vicksburg, Mississippi.

Dai, Y.B. and Kamel, A.M., 1969, *Scale effect Tests for Rubble Mound Breakwaters*, WES Research Report H-69-2, U.S. Army Corps of Engineers, Vicksburg.

Dalrymple, R.A., 1985, *Physical Modeling in Coastal Engineering*, A.A. Balkema, Rotterdam.

Dattatri, J., Raman, H. and Shankar, N.J., 1978, Performance Characteristics of Submerged Breakwater, Proc. of the 16<sup>th</sup> Coastal Engineering Conf., Hamburg, Germany, pp.2153-2171.

Davidson, M.A., Bird, P.A.D., Bullock, G.N. and Huntley, D.A., 1996a, A New Non-dimensional Number for Analysis of Wave Reflection from Rubble Mound Breakwaters, Coastal Engineering, 28, Elsevier, The Netherlands, pp. 93-120.

Davidson, M.A., Bird, P.A.D., Huntley, D.A. and Bullock, G.N., 1996b, Prediction of Wave Reflection from Rock Structures: An Integration of Field & Laboratory Data, Proc. of the 25<sup>th</sup> Coastal Engineering Conf., Orlando, Florida, pp. 2077-2086.

Dean, R.G. and Dalrymple, R.A., 1984, *Water Wave Mechanics for Engineers and Scientists*, Prentice-Hall, Englewood Cliffs, N.J.

Dick, T.M. and Brebner, A., 1968, Solid and Permeable Submerged Breakwaters, Proc. of the 11<sup>th</sup> Coastal Engineering Conf., London, England, pp. 1141-1149.



- Driscoll, A.M., Dalrymple, R.A. and Grilli, S.T., 1992, Harmonic Generation and Transmission Past a Submerged Rectangular Obstacle, Proc. of the 23<sup>rd</sup> Coastal Engineering Conf., Venice, Italy, pp.1142-1152.
- Ergin, A. and Pora, S., 1971, Irregular Wave Action on Rubble Mound Breakwaters, J. of Waterway, Harbours and Coastal Eng. Div. ASCE, Vol. 97, WW2, pp. 279-293.
- Feuillet, J. and Sabaton, M., 1980, Stability of Rubblemound Breakwaters, Proc. of the 17<sup>th</sup> Coastal Engineering Conf., Sydney-Australia, pp. 1988-2002.
- Font, J.B., 1968, The Effect of Storm Duration on Rubble Mound Breakwater Stability, Proc. of the 11<sup>th</sup> Coastal Engineering Conf., London, England, pp.779-785.
- Funke, E.R. and Mansard, E.P.D, 1980, On the Synthesis of Realistic Sea States, Proc. of the 17<sup>th</sup> Coastal Engineering Conf., Sydney-Australia, pp. 2974-2991.
- Galvin, C.J., 1968, Breaker Type Classification on Three Laboratory Beaches, J. of Geophysical Research, Vol. 73, No. 12, pp. 3651-3660.
- Goda, Y., 1970, Numerical Experiments on Wave Statistics with Spectral Simulation, *Port and Harbour Res. Inst.*, Japan, Vol. 9, No. 3.
- Goda, Y., 1974, Estimation of Wave Statistics from Spectra Information, Proc. Intl. Symp. On Ocean Wave Meas. and Anal., ASCE, Vol. 1, pp. 320-337.
- Goda, Y. and Suzuki, Y., 1976, Estimation of Incident and Reflected Waves in Random Wave Experiments, Proc. of the 15<sup>th</sup> Coastal Engineering Conf., Honolulu, Hawaii, pp.823-845.
- Goda, Y, 1985, *Random Seas and Design of Maritime Structures*, U. Tokyo Press.
- Hall, K.R. and Seabrook, S.R., 1998, Design Equation for Transmission at Submerged Rubblemound Breakwaters, J. of Coastal Research, (26), pp. 102-106.
- Hasselmann, K., Barnett, T.P., Bouws, E, Carlson, H., Cartwright, D.E., Enke, K., Ewing, J.A., Gienapp, H., Hasselmann, D.E., Krunsmann, P., Meerburg, A., Muller, P., Olbers, D.J., Richter, K., Sell, W. and Walden, H., 1973, *Measurement of Wind-Wave Growth and Swell Decay During the Joint North Sea Wave Project (JONSWAP)*, Report, Hamburg.
- Hedar, P.A., 1986, Armor Layer Stability of Rubble-Mound Breakwaters, J. of Waterway, Port, Coastal, and Ocean Eng., ASCE, Vol. 112, No. 3, pp. 343-350.

Horikawa, K. and Kuo, C.T., 1966, A Study on Wave Transformation Inside Surf Zone, Proc. of the 10<sup>th</sup> Coastal Engineering Conf., Tokyo, Japan, pp.217-233.

Hudson, R.Y., 1959, Laboratory Investigation of Rubble-Mound Breakwaters, J. of Waterways, Harbours and Coastal Eng. Div., ASCE, Vol. 85, No. WW3, pp. 93-121.

Hudson, R.Y. and Davidson, D.D., 1975, Rehabilitation of Rubble-Mound Breakwater Stability Models, Proc. on Modeling Techniques, ASCE, pp. 1603-1622.

Hughes, S.A. and Borgman, L.E., 1987, Beta-Rayleigh Distribution for shallow Water Wave Heights, Proceeding of Conference Sponsored by WW. Div. Of ASCE, Newark, DE.

Hunt, I.A., 1959, Design of Seawalls and Breakwaters, J. of Waterway, Harbors, Coastal Eng. Div. ASCE, Vol. 85, No. WW3, pp. 123-152.

Jensen, O.J. and Klinting, P., 1983, Evaluation of Scale Effects in Hydraulic Models by Analysis of Laminar and Turbulent Flows, Coastal Engineering 7, pp. 319-329.

Jensen, T., Andersen, H., Grønbech, J., Mansard, E.P.D. and Davies, M.H., 1996, Breakwater Stability under Regular and Irregular Wave Attack, Proc. of the 25<sup>th</sup> Coastal Engineering Conf., Orlando, Florida, pp.1679-1692.

Johnson, R.R., Mansard, E.P.D. and Ploeg, J., 1978, Effect of Wave Grouping on Breakwater Stability, Proc. of the 16<sup>th</sup> Coastal Engineering Conf., Hamburg, Germany, ASCE, pp. 2228-2243.

Kamphuis, J.W., 1991, Incipient Wave Breaking, Coastal Engineering, 15, pp. 185-203.

Kobayashi, N. and Wurjanto, A., 1989, Wave Overtopping on Coastal Structures, J. of Waterway, Port, Coastal, and Ocean Eng., ASCE, Vol. 115, No. 2, pp. 235-251.

Liberatore, G. and Petti, M., 1992, Wave Transformations Over a Submerged Bar: Experiments and Theoretical Interpretations, Proc. of the 23<sup>rd</sup> Coastal Engineering Conf., Venice, Italy, pp. 447-459.

Longuet-Higgins, M.S., 1975, On the Joint Distribution of wave Periods and Amplitudes of Sea waves, J. of Geophys. Res., Vol. 80, pp. 2688-2694.

- Lopez, C., Losada, M.A. and Kobayashi, N., 1998, Stability of Mound Breakwaters: Dependence on Wave Reflection, Proc. of the 26<sup>th</sup> Coastal Engineering Conf., Copenhagen, Denmark, pp. 1833-1845.
- Lording, P.T. and J.R. Scott, 1971, Armor Stability of Overtopped Breakwater, J. of Waterways, Harbours and Coastal Eng. Div., ASCE, Vol. 97, No. WW2, pp. 341-355.
- Losada, M.A. and Gimenez-Curto, L.A., 1979, The Joint Effect of the Wave Height and Period on the Stability of Rubble Mound Breakwaters Using Iribarren's Number, Coastal Engineering 3, Elsevier, The Netherlands, pp. 77-96.
- Losada, M., Kobayashi, Nobuhisa, and F.L. Martin, 1992, Armor Stability on Submerged Breakwaters, J. of Waterway, Port, Coastal, and Ocean Eng., ASCE, Vol. 118, No. 2, pp. 207-212.
- Madsen, O.S. and White, S.M., 1976, Energy Dissipation on A Rough Slope, J. of Waterway, Harbours and Coastal Eng. Div. ASCE, Vol. 102, No. WW1, pp. 31-47.
- Madsen, O.S. and White, S.M., 1976, Wave Transmission Through Trapezoidal Breakwaters, Proc. of the 15<sup>th</sup> Coastal Engineering Conf., ASCE, New York, NY, pp.2662-2676.
- Magoon, O.T., Sloan, R.L. and Foote, G.L., 1974, Damages to Coastal Structures, Proc. of the 14<sup>th</sup> Coastal Engineering Conf., Copenhagen, Denmark, pp. 1655-1659.
- Mansard, E.P.D. and Funke, E.R., 1980, The Measurement of Incident and Reflected Spectra Using a Least Squares Method, Proc. of the 17<sup>th</sup> Coastal Engineering Conf., Sidney, Australia, pp.154-172.
- Mansard, E.P.D. and Funke, E.R., 1987, *On the Reflection Analysis of Irregular Waves*, Technical Report, TR-Hy-017, National Research Council Canada.
- Mansard, E.P.D., Funke, E.R., Readshaw, J.S. and Girard, R.K., 1988, On the Transformation of Wave Statistics Due to Shoaling, Proc. of the 21st Coastal Engineering Conf., Malaga, Spain, pp. 106-120.
- Mansard, E.P.D., Davies, M.H. and Caron, O., 1996, Model Study of Reservoir Riprap Stability, Proc. of the 25<sup>th</sup> Coastal Engineering Conf., Orlando, Florida, pp. 1748-1761.
- Medina, J.R. and Hudspeth, R.T., 1990, A Review of the Analyses of Ocean Wave Groups, Coastal Engineering 14, Elsevier, The Netherlands, pp. 515-542.

Medina, J.R., Fassardi, C. and Hudspeth, R.T., 1990, Effects of Wave Groups on The Stability of Rubble Mound Breakwaters, Proc. of the 22<sup>nd</sup> Coastal Engineering Conf., Delft, The Netherlands, pp. 1552-1563.

Medina, J.R. and McDougal, W.G., 1990, Deterministic and Probabilistic Design Armour Layer (Discussion). J. of Waterway, Port, Coastal, and Ocean Eng., ASCE, Vol. 116, No. 4, pp. 508-510.

Medina, J.R., Hudspeth, R.T. and Fassardi, C., 1994, Breakwater Armor Damage Due to Wave Groups, J. of Waterway, Port, Coastal, and Ocean Eng., ASCE, Vol. 120, No. 2, pp. 179-198.

Michell, J.H., 1893, On the Highest Waves in Waters, London, Edinburgh and Dublin Phil. Magazine, 5<sup>th</sup> series, Vo. 36, pp. 430-437.

Miles, M.D., 1989, *User Guide for GEDAP Version 2.0 Wave Generation Software*, Technical Memorandum LM-HY-034, National Research Council of Canada, Ottawa.

Munk, W.H., 1949, The Solitary Wave Theory and its Application to Surf Problems, Ann. New York Acad. of Science, Vol. 51, pp. 376-424.

Muttray, M., Oumneraci, H., Zimmermann, C. and Partensky, H.W., 1992, Wave Energy Dissipation on and in Rubble Mound Structures, Proc. of the 23<sup>rd</sup> Coastal Engineering Conf., Venice-Italy, pp. 1434-1447.

Ochi, M.K., 1982, Stochastic Analysis and Probabilistic Prediction of Random Seas, Adv. Hydrosci., 13, pp. 218-375.

Penney, W.G. and Price, A.T., 1952, The Diffraction Theory of Sea Waves and the Shelter Afforded by Breakwaters, Philos. Trans. R. Soc. London, Series A, 244, pp.236-253.

Petti, M. and Ruol, P., 1991, Experimental Study on the Behaviour of Submerged Detached Breakwaters, Proc. of 3<sup>rd</sup> Coastal and Port Engineering in Developing Countries, pp. 167-179.

Petti, M. and Ruol, P., 1992, Laboratory Tests on The Interaction Between Nonlinear Long Waves and Submerged Breakwaters, Proc. of the 23<sup>rd</sup> Coastal Engineering Conf., Venice, Italy, pp.792-803.

Philips, O.M., 1958, The Equilibrium Range in the Spectrum of Wind-Generated Waves, J. of Fluid Mechanics, Vol. 4, pp.426-434.

Pierson, W.J. and Moskowitz, L., 1964, A Proposed Spectral Form for Fully Developed Wind Seas Based on the Similarity Theory of S.A. Kitagorodskii, J. of Geophysical Research, Vol. 69, pp. 5181-5196.

Pilarczyk, K.W. and R.B. Zeidler, 1996, *Offshore Breakwaters and Shore Evolution Control*, A.A. Balkema, Rotterdam.

Pina, G.G. and J.M. Valdes F. Alarcon, 1990, Experiments on Coastal Protection Submerged Breakwaters: A Way to Look at the Results, Proc. of the 22<sup>nd</sup> Coastal Engineering Conf., Delft, the Netherlands, pp.1592-1605.

Rahman, M., 1995, *Water Waves: Relating Modern Theory to Advanced Engineering Practice*, Oxford University Press, Oxford.

Raichlen, F., 1972, Discussion of Armor Stability of Overtopped Breakwater, J. of Waterway, Harbours and Coastal Eng. Div. ASCE, Vol. 98, No. WW1, pp. 273-279.

Rogan, A.J., 1968, Destruction Criteria for Rubble Mound Breakwaters, Proc. of the 11<sup>th</sup> Coastal Engineering Conf., ASCE, New York, NY, pp.761-772.

Rye, H., 1977, The Stability of Some Currently Used Wave Parameters, Coastal Engineering, 1, pp. 17-30.

Sakakiyama, T. and Kajima, R., 1996, Wave Overtopping and Stability of Armour units Under Multidirectional Waves, Proc. of the 25<sup>th</sup> Coastal Engineering Conf., Orlando, Florida, pp. 1862-1875.

Seabrook, S.R., 1997, *Investigation of the Performance of Submerged Rubblemound Breakwaters*, MSc. thesis, Queen's University, Kingston, Canada.

Seabrook, S.R. and Hall, K.R., 1998, Wave Transmission at Submerged Rubblemound Breakwaters, Proc. of the 26<sup>th</sup> Coastal Engineering Conf., Copenhagen, Denmark, pp. 2000-2013.

Seelig, W.N., 1980, *Two-dimensional Tests of Wave Transmission and Reflection Characteristics of Laboratory Breakwaters*, Technical Report, No. 80-1, CERC, Vicksburg, Miss.

Seelig, W.N. and Ahrens, J.P., 1981, *Estimation of Wave Reflection and Energy Dissipation Coefficients for Beaches, Revetments, and Breakwaters*, Technical Paper 81-1, CERC, Va.

Seelig, W.N., 1983, Wave Reflection From Coastal Structures, Proc. of Coastal Structures'83, Arlington-Virginia, ASCE, pp. 961-973.

Sigurdsson, G., 1962, Wave Forces on Breakwater Capstones, J. of Waterways, Harbours and Coastal Eng. Div., ASCE, Vol. 88, WW3, pp. 27-60.

Sleath, J.F.A., 1984, *Sea Bed Mechanics*, John Wiley & Sons, Toronto.

Smith, O.P., 1986, Cost-Effectiveness of Breakwater Cross Sections, J. of Waterway, Port, Coastal, and Ocean Eng., ASCE, Vol. 113, No. 5, pp. 447-460.

Smith, W.G., Kobayashi, N. and Kaku, S., 1992, Profile Changes of Rock Slopes by Irregular Waves, Proc. of the 23<sup>rd</sup> Coastal Engineering Conf., Venice, Italy, pp.1556-1572.

Sollitt, C.K. and Cross, R.H., 1972, Wave Transmission Through Permeable Breakwaters, Proc. of the 13<sup>th</sup> Coastal Engineering Conf., Vancouver, Canada, pp.1827-1846.

Sorensen, R.M., 1993, *Basic Wave Mechanics for Coastal and Ocean Engineers*, Wiley, New York.

Teisson, C., 1990, Statistical Approach of Duration of Extreme Storms: Consequences of Breakwater Damages, Proc. of the 22<sup>nd</sup> Coastal Engineering Conf., Delft, the Netherlands, pp. 1850-1860.

Teisson, C. and Benoit, M., 1994, Laboratory Measurement of Oblique Irregular Wave Reflection on Rubble Mound Breakwaters, Proc. of the 24th Coastal Engineering Conf., Kobe, Japan, pp. 1610-1624.

Thompson, E.F. and Vincent, C.L., 1985, Significant Wave Height for Shallow Water Design, J. of Waterways, Harbours and Coastal Eng. Div., ASCE, pp. 828-842.

Tschirky, P.A., Hall, K.R. and Turcke, D.J., 1998, Wetland Wave Attenuation and Shore Protection, Int. Water Resources Engineering Conference-Symposium on Wetlands, ASCE, pp. 598-603.

Van de Kreeke, J., 1969, Damage Function of Rubble-Mound Breakwaters, J. of Waterways, Harbours and Coastal Eng. Div., ASCE, Vol. 95, WW3, pp. 345-354.

Van der Meer, J.W. and K.W. Pilarczyk, 1984, Stability of Rubble Mound Slope under Random Wave Attack, Proc. of the 19<sup>th</sup> Coastal Engineering Conf., Houston, Texas, pp.2620-2634.

Van der Meer, J.W., 1987, Stability of Breakwater Armour Layers-Design Formulae, Coastal Engineering, 11, pp. 219-239.

Van der Meer, J.W., 1988, *Rock Slopes and Gravel Beaches under Wave Attack*, Doctoral thesis, Delft University of Technology. Also: Delft Hydraulics Communication No. 396.

Van der Meer, J.W. and K.W. Pilarczyk, 1990, Stability of Low Crested and Reef Breakwaters, Proc. of the 22<sup>nd</sup> Coastal Engineering Conf., Delft, the Netherlands, pp.1375-1387.

Van der Meer, J.W., 1991, Stability and Transmission at Low Crested Structures, Delft Hydraulics Publication No. 453.

Van der Meer, J.W. and Stam, C.J.M., 1992, Wave Runup on Smooth and Rock slopes of Coastal Structures, J. of Waterway, Port, Coastal, and Ocean Eng., ASCE, Vol. 118, No. 5, pp. 534-550.

Van der Meer, J.W., Petit, H.A.H., van den Bosch, P., Klopman, G. and Broekens, R.D., 1992, Numerical Simulation of Wave Motion on and in Coastal Structures, Proc. of the 23<sup>rd</sup> Coastal Engineering Conf., Venice, Italy, pp.1772-1784.

Van der Meer, J.W. and F.R. Daemen, 1994, Stability and Wave Transmission at Low Crested Rubble Mound Structures, J. of Waterway, Port, Coastal, and Ocean Eng., ASCE, Vol. 121, No. 1, pp. 1-19.

Van der Meer, 1995, A Review of Stability Formulas for Rock and Riprap Slopes under Wave Attack, in *River, Coastal and Shoreline Protection: Erosion Control Using Riprap and Armour stone*, ed. by C.R. Thorne et al., John Wiley & Sons.

Vidal, C., Losada, M.A. and Medina, R., 1991, Stability of Mound Breakwater's Head and Trunk, J. of Waterway, Port, Coastal, and Ocean Eng., ASCE, Vol. 117, No. 6, pp. 570-587.

Vidal, C., Losada, M.A., Medina, R., Mansard, P.D. and Pina, G.G., 1992, A Universal for The Stability of Both Low Crested and Submerged Breakwaters, Proc. of the 23<sup>rd</sup> Coastal Engineering Conf., Venice, Italy, pp.1679-1692.

Vidal, C and Mansard, E.P.D., 1995, *On the Stability of Reef Breakwaters*, Technical Report, NRC Coastal Engineering Laboratory, Canada.

Vidal, C, Losada, M.A. and Mansard, E.P.D., 1995a, Suitable Wave Height Parameter for Characterizing Breakwater Stability, *J. of Waterway, Port, Coastal, and Ocean Eng.*, ASCE, Vol. 121, No. 2, pp. 88-96.

Walker, J.R, Palmer, R.Q. and Dunham, J.W., 1975, Breakwater Back Slope Stability, *Proc. of Civil Engineering in the Oceans/III*, ASCE, New York, NY, pp. 879-898.

Weggel, R.J., 1972, Maximum Breaker Height, *J. of Waterways, Harbours and Coastal Eng. Div.*, ASCE, Vol. 98, No. 1, pp. 529-542.

Wiegel, R.L., 1962, Diffraction of Waves by a Semi-infinite Breakwater, *J. of Hydraulic Div. ASCE*, pp. 27-44.

Wiegel, R.L., 1964, *Oceanographical Engineering*, Prentice-Hall, London.

Wuryanto, A. and Kobayashi, N., 1993, Irregular wave Reflection and Runup on Permeable Slopes, *J. of Waterway, Port, Coastal, and Ocean Eng.*, ASCE, Vol. 119, No. 5, pp. 537-557.



## APPENDIX A.

### WAVE CHARACTERISTICS BASED ON LINEAR THEORY

Table A.1.

	<b>Expression</b>	<b>Deep Water (<math>h/L &gt; 1/2</math>)</b>	<b>Shallow Water (<math>h/L &lt; 1/20</math>)</b>
Velocity [m/s]	$C = \frac{L}{T} = \frac{gT}{2\pi} \tanh kh$	$C_o = \frac{gT}{2\pi}$	$C = \sqrt{gh}$
Wave length [m]	$L = CT = \frac{gT^2}{2\pi} \tanh kh$	$L_o = \frac{gT^2}{2\pi}$	$L = T\sqrt{gh}$
Energy density [j/m <sup>2</sup> ]	$E = \frac{1}{8} \rho_w g H^2$	-	-
Group velocity [m/s]	$C_G = nC$	$(C_G)_o = \frac{C_o}{2}$	$C_G = C$
Group velocity parameter	$n = \frac{1}{2} \left[ 1 + \frac{2kh}{\sinh 2kh} \right]$	$n_o = \frac{1}{2}$	$n = 1$
Wave breaking criterion	$\left( \frac{H}{L} \right)_{\max} = 0.142 \tanh kh$	$\left( \frac{H}{L} \right)_{\max} = 0.142$	$\left( \frac{H}{h} \right)_{\max} = 0.89$

## APPENDIX B

### WAVE GENERATION CHARACTERISTICS

```

REM      THIS PROGRAM GENERATES A BATCH FILE OF IRREGULAR WAVE SIGNALS
REM      FOR TRANSMISSION TESTS
REM      SILADHARMA, Oct 1999 (2-D Flume Tests)
REM      FILENAME: BATCHBLD.GBAT
REM
REM      %1 = WAVE SPECTRUM FILENAME
REM      %2 = PEAK FREQUENCY (Hz) (1/Tp) (prototype)
REM      %3 = DURATION OF SIGNAL (min)
REM      %4 = WAVE TRAIN FILENAME
REM      %5 = MODEL DEPTH (m)
REM      %6 = AMPLIFICATION FACTOR
REM      %7 = VOLTAGE SIGNAL FILENAME
REM           h = Hs (cm)
REM           t = Tp (s)
REM           d = Depth (cm)
REM      %8 = SIGNIFICANT WAVE HEIGHT IN METERS (prototype)
REM      %9 = Wave Machine Calibration Filename (compensated for servo
REM           response)
REM
REM      #PARSPEC
REM      %1      # name of first wave spectrum output file [.001]
REM      2      # type of wave spectrum (1-6) [1]
REM      %5      # water depth for wave power calculations (m) [10000.0]
REM      %2      # frequency at which spectrum peaks (Hz)
REM           # value of Phillips Alpha constant [0.0081]
REM      4      # JONSWAP spectrum option (1-4) [1]
REM           # Gamma [3.3]
REM      %8      # significant wave height (m)
REM      #END
REM
REM      #RWSYN
REM      1      # model scale factor [1.0]
REM      %3      # duration in full-scale minutes (0.1 - 218.453) [20.0]
REM           # seed option [1]
REM           # wave synthesis option [1]
REM      %1      # name of wave spectrum input file [.001]
REM      %4      # name of first wave record output file [.001]
REM      #END
REM
REM      #RWREP2
REM           # wave generation option (0 to 5) [1]
REM      %9      # name of wave machine calibration file [.001]
REM      %5      # DEPTH (model m)
REM           # wave propagation distance D (model m) [0.0]
REM           # lower cut-off frequency F1 (model Hz) [0.03]
REM           # upper cut-off frequency F2 (model Hz) [4.0]
REM           # Scale Factor [1.0]
REM      %6      # wave amplification factor [1.0]
REM      %4      # name of wave record input file [.001]
REM           # Apply spectral matching transfer function? [No]:
REM      %7      # name of wave machine control signal output file [.001]
REM      #END

```

```

REM THIS PROGRAM GENERATES A BATCH FILE OF IRREGULAR WAVE
SIGNALS CONTAINS GROUPINESS
REM SILADHARMA, March 2000 (2-D Flume Tests)
REM FILENAME: Grouping.GBAT
REM
REM %1 = WAVE SPECTRUM FILENAME
REM %2 = PEAK FREQUENCY (Hz) (1/Tp) (prototype)
REM %3 = SIGNIFICANT WAVE HEIGHT IN METERS (prototype)
REM %4 = DESIRED SIWEH
REM %5 = PEAK FREQUENCY OF THE SIWEH (1/10 OF %3)
REM %6 = RMS OF THE TIME SERIES (Hs/4) (M)
REM %7 = SYNTHESIZED WAVE TRAIN
REM %8= VOLTAGE SIGNAL FILENAME
REM h = Hs (cm)
REM t = Tp (s)
REM d = Depth (cm)
REM %9 = SIWEH OF THE SYNTHESIZED WAVE TRAIN
REM
#PARSPEC
%1 # name of first wave spectrum output file [.001]
2 # type of wave spectrum (1-6) [1]
1.33 # water depth for wave power calculations (m) [10000.0]
%2 # frequency at which spectrum peaks (Hz)
# value of Phillips Alpha constant [0.0081]
4 # JONSWAP spectrum option (1-4) [1]
# Gamma [3.3]
%3 # significant wave height (m)
#END
REM
#SYSI
%4 # name of output file [.001]
%5 # F0 (Hz)
0.2 # ZETA
300 # TN (sec)
0.5 # GF
%6 # RMS (meters)
0 # K
#END
REM
#SYW
%4 # name of input file containing SIWEH [.001]
%1 # name of input file containing variance spectral density
[.001]
%7 # name of output file containing synthesized wave train [.001]
0 # option [0]
0 # option [0]
# max number of iterations [10]
#END
REM
#RWREP2
# wave generation option (0 to 5) [1]
wmcals # name of wave machine calibration file [.001]
1.33 # DEPTH (model m)
# wave propagation distance D (model m) [0.0]

```

```
      # lower cut-off frequency F1 (model Hz) [0.05]
      # upper cut-off frequency F2 (model Hz) [2.0]
      # Scale Factor [1.0]
%10  # wave amplification factor [1.0]
%7   # name of wave record input file [.001]
      # Apply spectral matching transfer function? [No]:
%8   # name of wave machine drive signal output file [.001]
#END
REM
#SIWEH
%7   # input file containing wave heights [.001]
%9   # output file containing SIWEH [.001]
      # trend [0]
      # option [0]
      # filter (0=Bartlett, 1=envelope) [0]
      # Normalize SIWEH? [No]:
# END
```

APPENDIX C  
WAVE ANALYSIS ROUTINES

```

REM   THIS PROGRAM IS USED TO ANALYZE THE IRREGULAR WAVE DATA FOR
      TRANSMISSION TESTS
REM   ANALYSIS OF IRREGULAR WAVE DATA TO OBTAIN WAVE
      CHARACTERISTICS IN TIME AND SPECTRAL DOMAIN
REM   SILADHARMA, Oct 1999
REM   FILENAME: ANAL_IRREG.GBAT
REM
REM   %1 = INPUT DATA FILE NAME
REM   %2 = WATER DEPTH
REM   %3 = Target Spectrum Filename
REM
REM   Demultiplex the GEDAP sampling file to individual channel
      components
REM   (Generates sequential files G1.XXX for each probe, where XXX is
      the BNC Channel No)
REM
#SPLIT_DAC
%1   # name of DAC input file [.DAC]
      # GEDAP file name option [1]
0    # output data scale option [0]
#END
REM
REM   RUN STATISTICAL ANALYSIS ON INDIVIDUAL PROBE DATA
REM
#STAT1 -C10
G1.001# name of input file [.001]
#END
REM
REM   RUN ZERO-CROSSING ANALYSIS ON INDIVIDUAL PROBE DATA
REM
#ZCA -C10
g1.001# name of time series input file [.001]
      # name of primary output file [g1_ZCA.001]
%2   # depth of water (m)
no   # Use default parameters? [Yes]:
      # Is the input wave train cyclic? [Yes]:
      # Alpha (percent) [2.0]
      # TMIN (seconds) [0.0]
      # trend removal option [1]
      # output file option [1]
      # vertical asymmetry factor option [2]
#END
REM
REM   RUN VARIANCE SPECTRAL DENSITY ON INDIVIDUAL PROBE DATA
REM
#VSD -C10
g1.001# name of time series input file [.001]
      # name of spectral density output file [g1_SPEC.001]
no   # Use default parameters? [Yes]:
      # data window option [1]
      # Alpha (0.0 to 0.5) [0.0]
      # filter bandwidth in Hz (or 0.0 to specify dof instead) [0.0]
      # dof = degrees of freedom per spectral estimate [20]
      # F1 = low frequency limit (Hz) [0.0]

```

```

# F2 = high frequency limit (Hz) [Nyquist frequency]
# Generate 80% confidence interval file? [No]:
# Generate spectral parameter files? [No]:
#END
REM
REM Probe spacing routine for reflection analysis - Offshore Rack
#PRBSP
G1.001# name of first wave probe input file [.001]
REFG1.001 # yyy = name of first output file [.001]
# model scale factor [1.0]
%2 # water depth in model units (m)
Y # Use a standard probe spacing? [Yes]:
N # Use deep basin spacing? [Yes]:
#END
REM RUN CROSS SPECTRAL ANALYSIS TWICE FOR RACK 1 REFLECTION
ANALYSIS
REM
#XSPEC1
G1.001# name of x(t) input file [.001]
REFG1.001 # name of y(t) input file [.001]
CSPEC12 # name of first output file [.001]
# Use default parameters? [Yes]:
#END
#XSPEC1
G1.001 # name of x(t) input file [.001]
REFG1.002 # name of y(t) input file [.001]
CSPEC13 # name of first output file [.001]
# Use default parameters? [Yes]:
#END
REM
REM RUN REFLECTION ANALYSIS ON RACK 1
REM
#REFLA
CSPEC12 # xxx = phase lag file for probes 1 and 2 [.002]
CSPEC13 # yyy = phase lag file for probes 1 and 3 [.002]
REFLA_R1 # zzz = name of first output file [.001]
# error threshold (percent) [10]
N # Enter new Z, X12 and X13 values? [Yes]:
# threshold for coherency [0.3]
# N = length of smoothing filter [5]
# frequency 1
#END
REM
REM RUN CROSS-SPECTRAL ANALYSIS TWICE FOR RACK 2 REFLECTION
ANALYSIS
REM
REM Probe spacing routine for reflection analysis - Inshore Rack
#PRBSP
G1.006 # name of first wave probe input file [.001]
REFG2.001 # yyy = name of first output file [.001]
# model scale factor [1.0]
%2 # water depth in model units (m)
Y # Use a standard probe spacing? [Yes]:
N # Use deep basin spacing? [Yes]:

```



```

#END
REM
#XSPEC1
G1.006      # name of x(t) input file [.001]
REFG2.001  # name of y(t) input file [.001]
CSPEC67    # name of first output file [.001]
           # Use default parameters? [Yes]:

#END
#XSPEC1
G1.006      # name of x(t) input file [.001]
REFG2.002  # name of y(t) input file [.001]
CSPEC68    # name of first output file [.001]
           # Use default parameters? [Yes]:

#END
REM
REM   RUN REFLECTION ANALYSIS ON RACK 2
REM
#REFLA
CSPEC67    # xxx = phase lag file for probes 1 and 2 [.002]
CSPEC68    # yyy = phase lag file for probes 1 and 3 [.002]
REFLA_R2   # zzz = name of first output file [.001]
           # error threshold (percent) [10]
N          # Enter new Z, X12 and X13 values? [Yes]:
           # threshold for coherency [0.3]
           # N = length of smoothing filter [5]
           # frequency 1

#END
#EXPORT_V2
refla_r1   # name of input file [.001]
%3         # name of ASCII output file [.DAT]
#END
#EXPORT_V2
refla_r2   # name of input file [.001]
%4         # name of ASCII output file [.DAT]
#END
REM
REM   PLUCK DESIRED DATA AND DELETE TRANSITIONAL FILES
REM
#PLUCK
PLUCKER    # name of input Collection Worksheet [.PAR]
           # name of output Data Worksheet [PLUCKER.DAT]
           # processing mode [1]

#END
COPY OUTASCII.DAT+PLUCKER.DAT OUTASCII.DAT

```

```

REM   THIS PROGRAM IS USED TO ANALYZE THE IRREGULAR WAVE DATA FOR
      STABILITY TESTS
REM   ANALYSIS OF IRREGULAR WAVE DATA TO OBTAIN WAVE
      CHARACTERISTICS IN TIME AND SPECTRAL DOMAIN
REM   SILADHARMA, MARCH 2000
REM   FILENAME: ANAL_IRREG.GBAT
REM
REM   %1 = INPUT DATA FILE NAME
REM   %2 = WATER DEPTH
REM   %3 = Target Spectrum Filename
REM
REM   Demultiplex the GEDAP sampling file to individual channel
      components
REM   (Generates sequential files G1.XXX for each probe, where XXX is
      the BNC Channel No)
REM
#SPLIT_DAC
%1   # name of DAC input file [.DAC]
      # GEDAP file name option [1]
0    # output data scale option [0]
#END
REM
REM   RUN STATISTICAL ANALYSIS ON INDIVIDUAL PROBE DATA
REM
#STAT1 -C5
G1.001# name of input file [.001]
#END
REM
REM   RUN ZERO CROSSING ANALYSIS ON INDIVIDUAL PROBE DATA
REM
#ZCA -C5
g1.001 # name of time series input file [.001]
      # name of primary output file [g1_ZCA.001]
%2   # depth of water (m)
no   # Use default parameters? [Yes]:
      # Is the input wave train cyclic? [Yes]:
      # Alpha (percent) [2.0]
      # TMIN (seconds) [0.0]
      # trend removal option [1]
      # output file option [1]
      # vertical asymmetry factor option [2]
#END
REM
REM   RUN VARIANCE SPECTRAL DENSITY ON INDIVIDUAL PROBE DATA
REM
#VSD -C5
g1.001 # name of time series input file [.001]
      # name of spectral density output file [g1_SPEC.001]
no   # Use default parameters? [Yes]:
      # data window option [1]
      # Alpha (0.0 to 0.5) [0.0]
      # filter bandwidth in Hz (or 0.0 to specify dof instead)
      [0.0]
      # dof = degrees of freedom per spectral estimate [20]

```

```

# F1 = low frequency limit (Hz) [0.0]
# F2 = high frequency limit (Hz) [Nyquist frequency]
# Generate 80% confidence interval file? [No]:
# Generate spectral parameter files? [No]:
#END
REM
REM   Probe spacing routine for reflection analysis - Offshore Rack
REM
#PRBSP
G1.001      # name of first wave probe input file [.001]
REFG1.001   # yyy = name of first output file [.001]
            # model scale factor [1.0]
%2          # water depth in model units (m)
Y           # Use a standard probe spacing? [Yes]:
N           # Use deep basin spacing? [Yes]:
#END
REM   RUN CROSS SPECTRAL ANALYSIS TWICE FOR RACK 1 REFLECTION
      ANALYSIS
REM
#XSPEC1
G1.001      # name of x(t) input file [.001]
REFG1.001   # name of y(t) input file [.001]
CSPEC12     # name of first output file [.001]
            # Use default parameters? [Yes]:
#END
#XSPEC1
G1.001      # name of x(t) input file [.001]
REFG1.002   # name of y(t) input file [.001]
CSPEC13     # name of first output file [.001]
            # Use default parameters? [Yes]:
#END
REM
REM   RUN REFLECTION ANALYSIS ON RACK 1
REM
#REFLA
CSPEC12     # xxx = phase lag file for probes 1 and 2 [.002]
CSPEC13     # yyy = phase lag file for probes 1 and 3 [.002]
REFLA_R1    # zzz = name of first output file [.001]
            # error threshold (percent) [10]
N           # Enter new Z, X12 and X13 values? [Yes]:
            # threshold for coherency [0.3]
            # N = length of smoothing filter [5]
            # frequency 1
#END
#SIWEH
g1.001      # input file containing wave heights [.001]
siweh       # output file containing SIWEH [.001]
            # trend [0]
            # option [0]
            # filter (0=Bartlett, 1=envelope) [0]
            # Normalize SIWEH? [No]:
# END
REM   PLUCK DESIRED DATA AND DELETE TRANSITIONAL FILES
REM

```

```
#PLUCK
PLUCKER      # name of input Collection Worksheet [.PAR]
              # name of output Data Worksheet [PLUCKER.DAT]
              # processing mode [1]
#END
COPY OUTASCII.DAT+PLUCKER.DAT OUTASCII.DAT
```

**APPENDIX D**  
**PROFILE ANALYSIS ROUTINES**

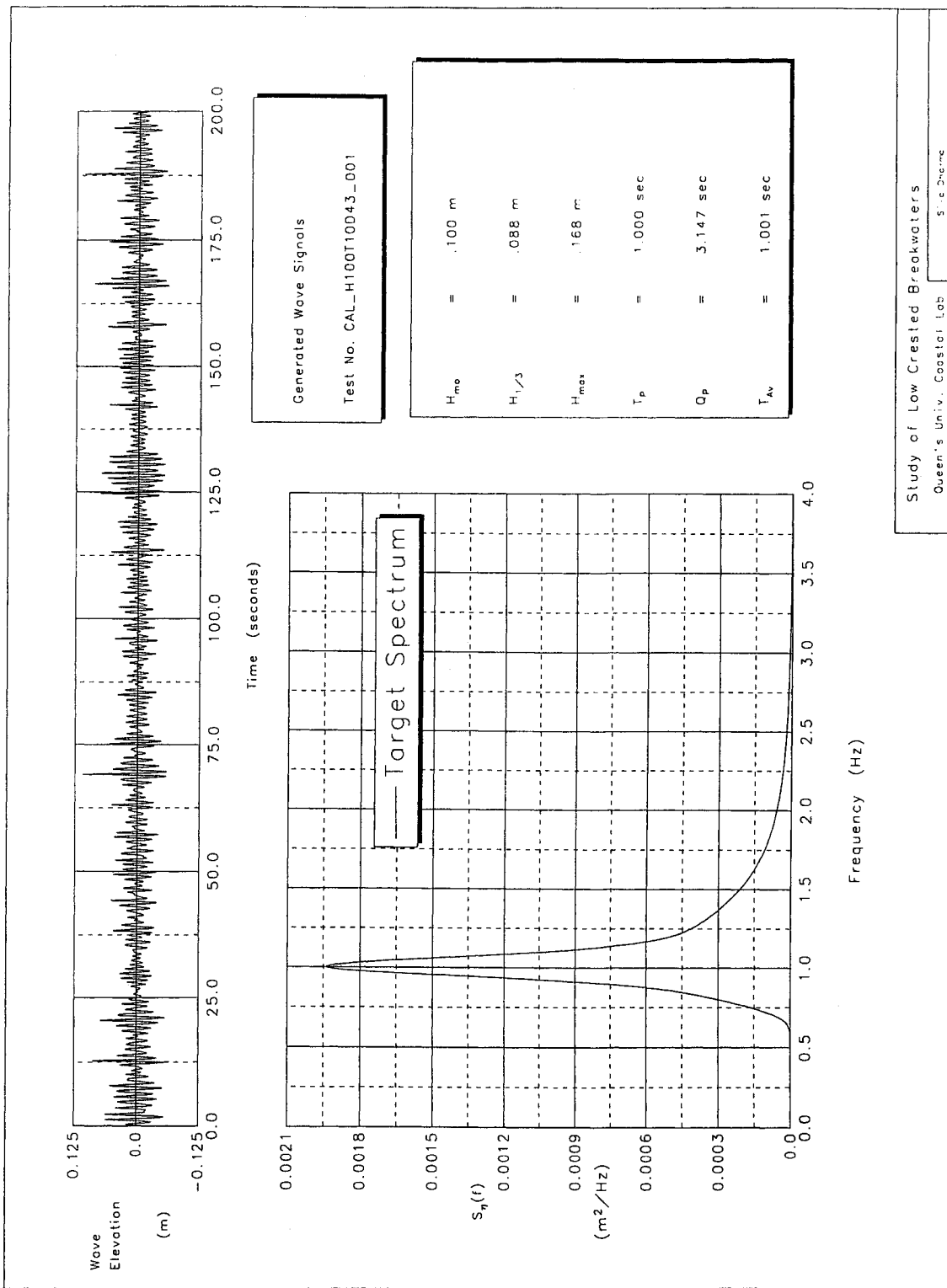
```

REM   THIS PROGRAM IS USED TO ANALYZE OF PROFILER DATA
REM   SILADHARMA, APRIL 2000
REM   FILENAME: PROFILER.GBAT
REM
REM   %1 = INPUT DATA FILE NAME
REM   %2 = OUTPUT FILE NAME
REM
#IMPORT
%1      # name of ASCII input file [.DAT]
G1      # name of GEDAP output file [G1.001]
2       # number of data columns in ASCII input file [1]
2       # conversion option [1]
y       # Is there an implicit variable such as time associated
        # with the data? [No]:
        # initial value of implicit variable [0.0]
        # step size of implicit variable [1.0]
        # name of implicit variable [Time]
        # units of implicit variable [seconds]
R       # name of data in column 1 [Channel 1]
m       # units of data in column 1
theta   # name of data in column 2 [Channel 2]
rad     # units of data in column 2
#END
#HEADER
G1.002  # name of GEDAP data file to be modified [.001]
set DAS_HSCL 1.000
exit
#END
#HEADER
G1.001  # name of GEDAP data file to be modified [.001]
set DAS_HSCL 1.000
exit
#END
#MERGE_BW
G1.002  # name of Theta data input file [.001]
G1.001  # name of r data input file [.001]
%2      # name of output file [.001]
1.235   # LENGTH OF PROFILER ROD IN M (MODEL)
0       # SHIFT OF ORIGIN FROM CENTRELINE -M(MODEL)
-0.246  # HORIZONTAL OFFSET ADJUSTMENT FOR PLOTS, M (PROT)
0.958   # ELEVATION OF TOP OF BEAM ABOVE DATUM, M (MODEL)
1.      # SENSE: +1 UNLESS PROFILER TURNED AROUND
#END
#EXPORT_V2
%2      # name of input file [.001]
%3      # name of ASCII output file [.DAT]
#END

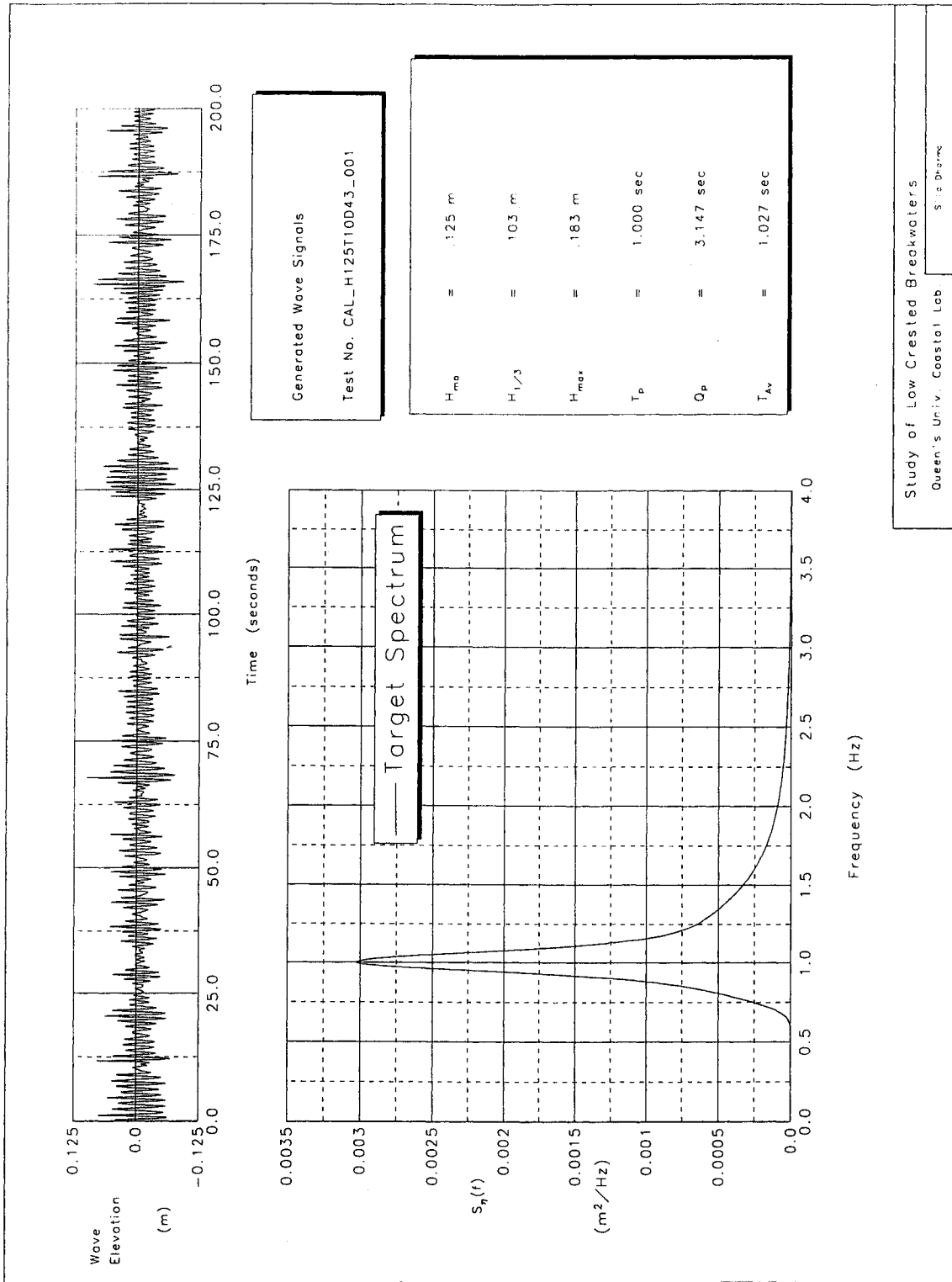
```

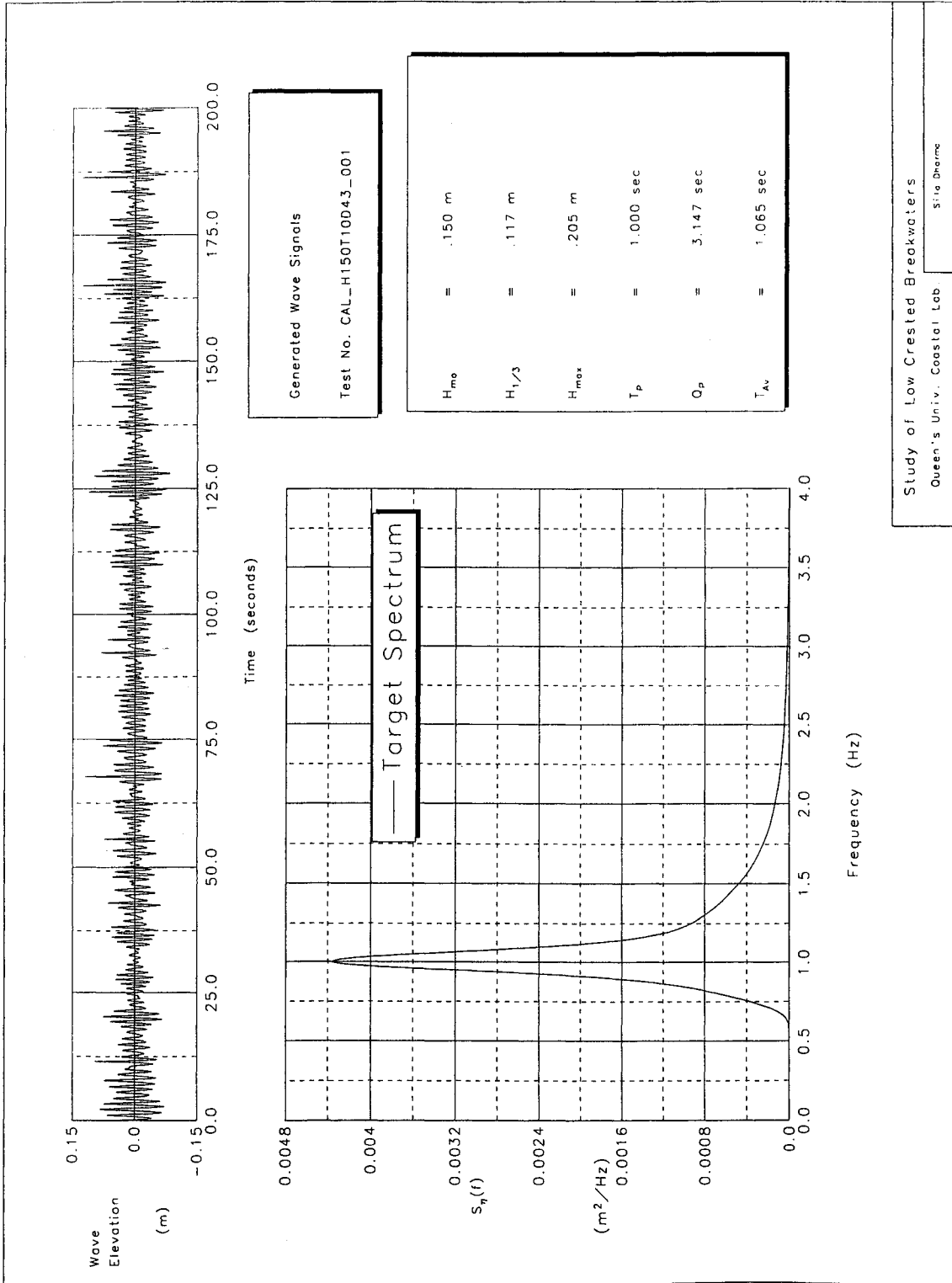
## APPENDIX E

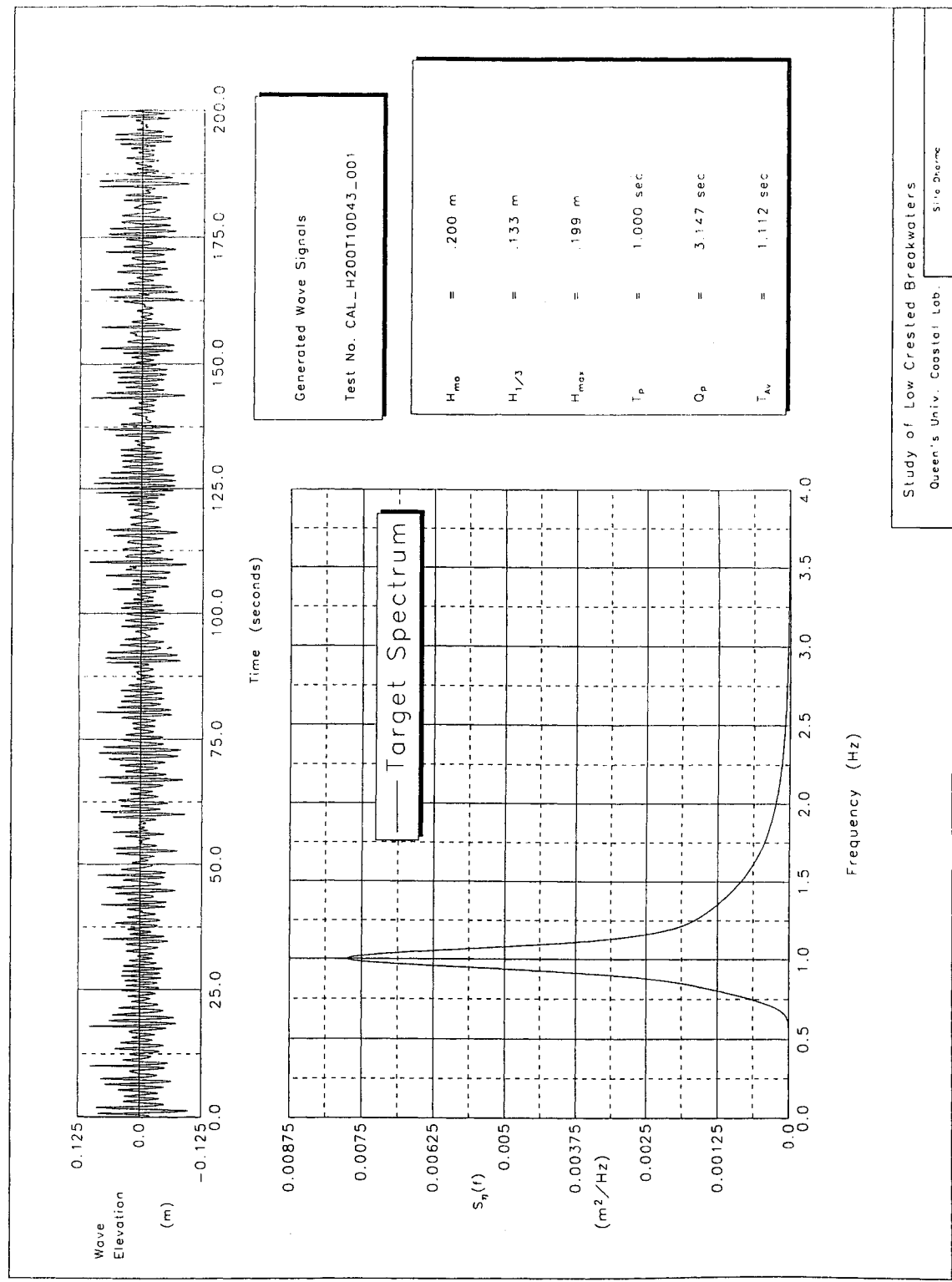
### WAVE GENERATION CHARACTERISTICS

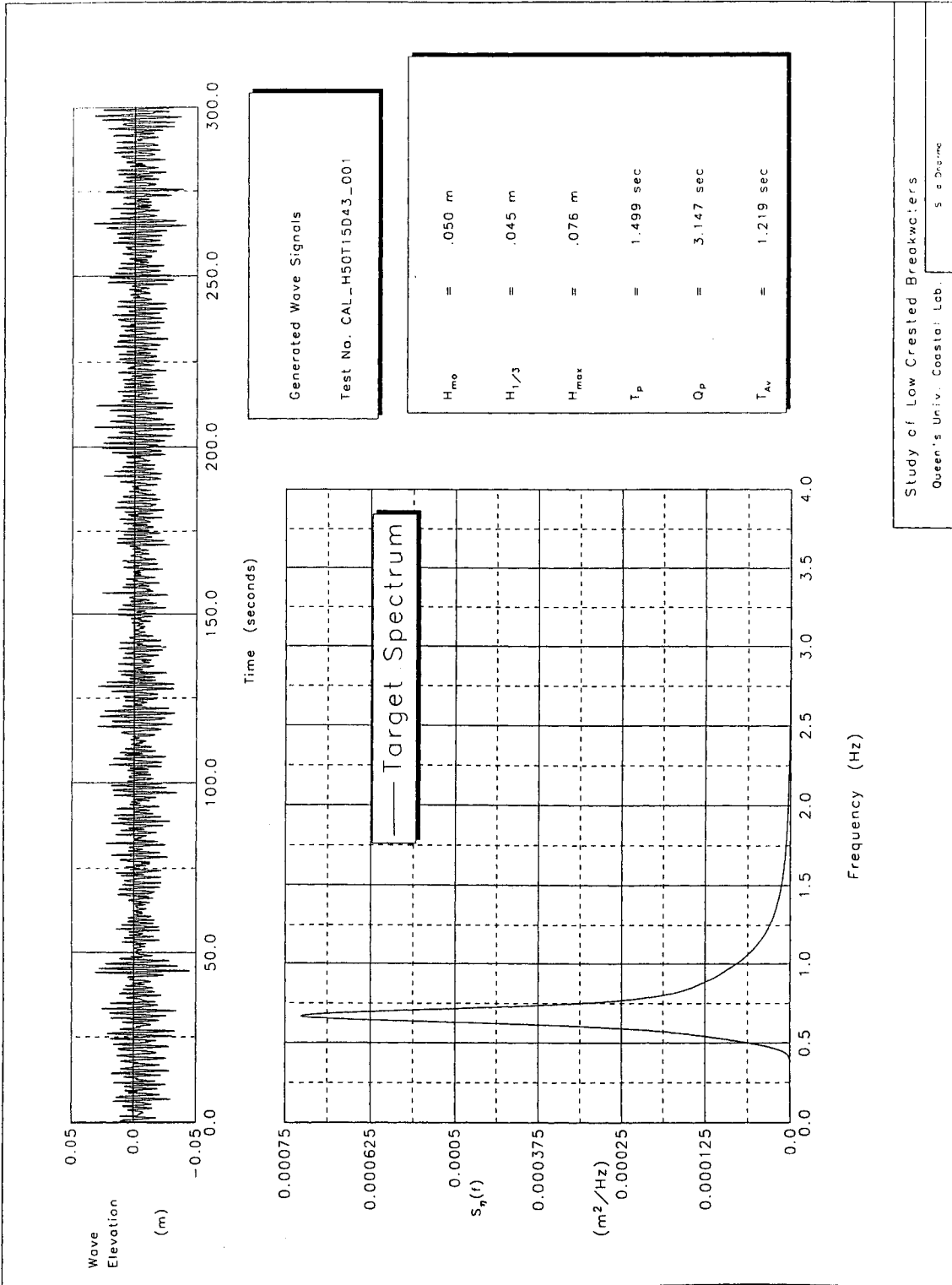


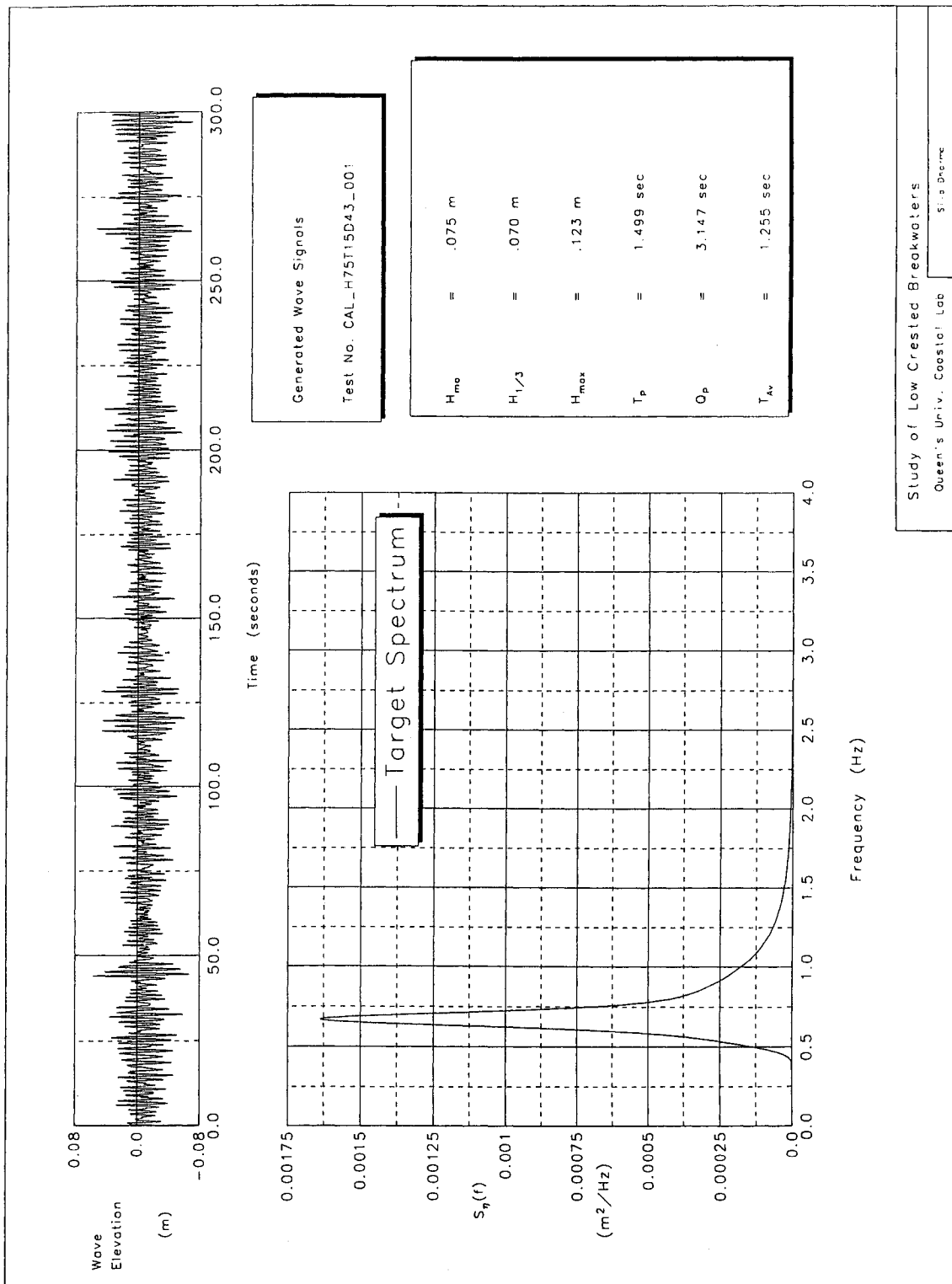


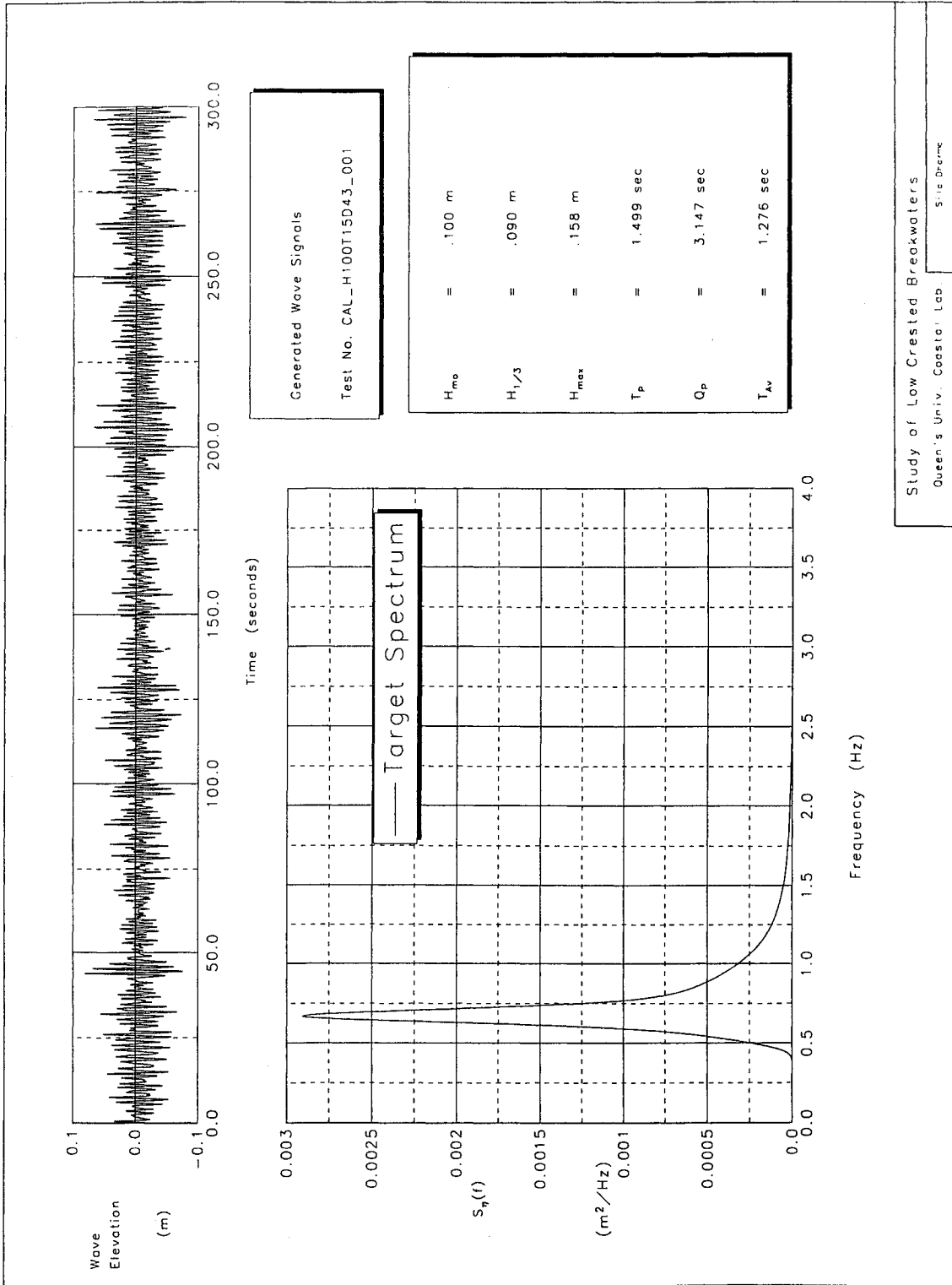


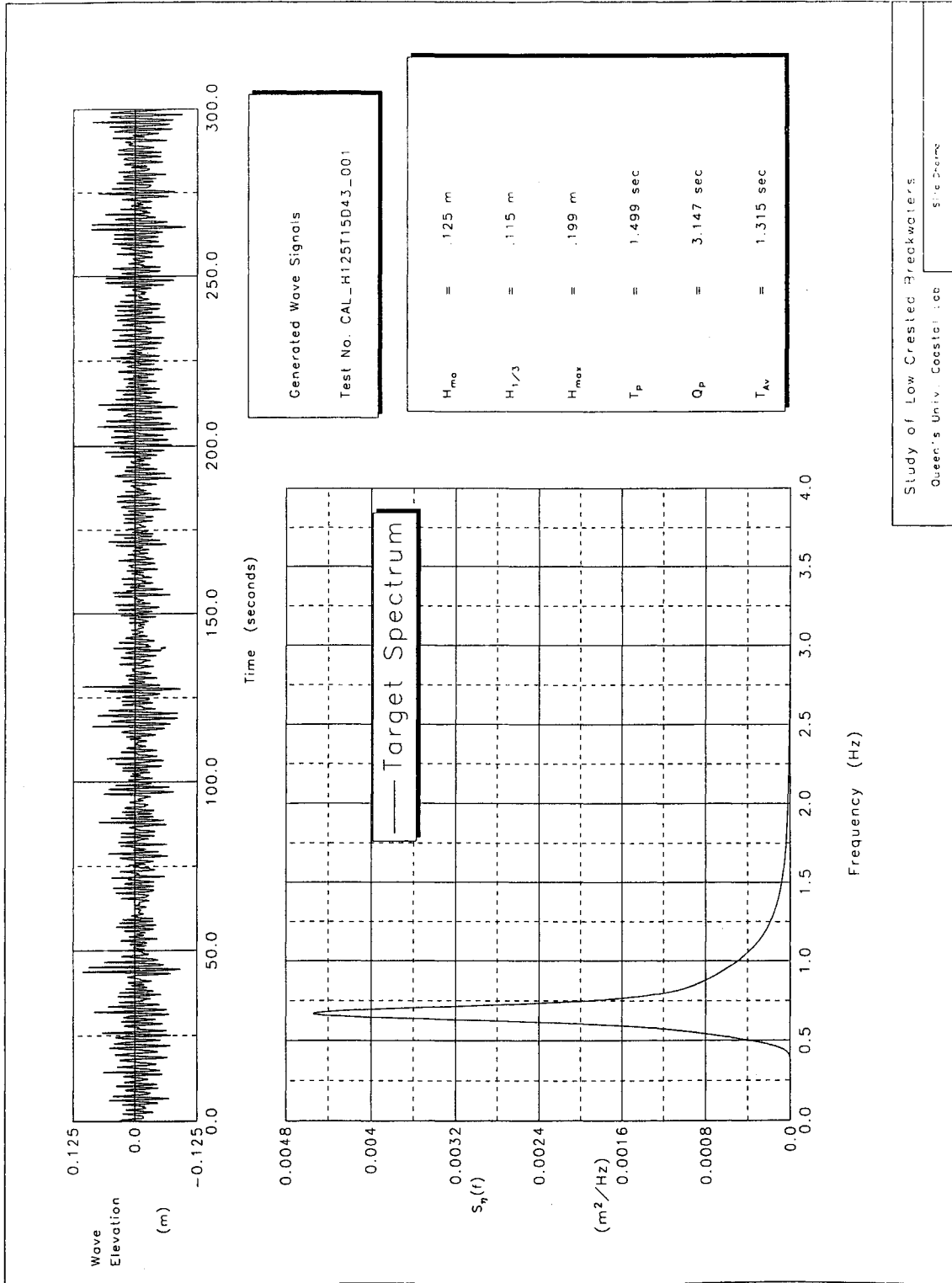


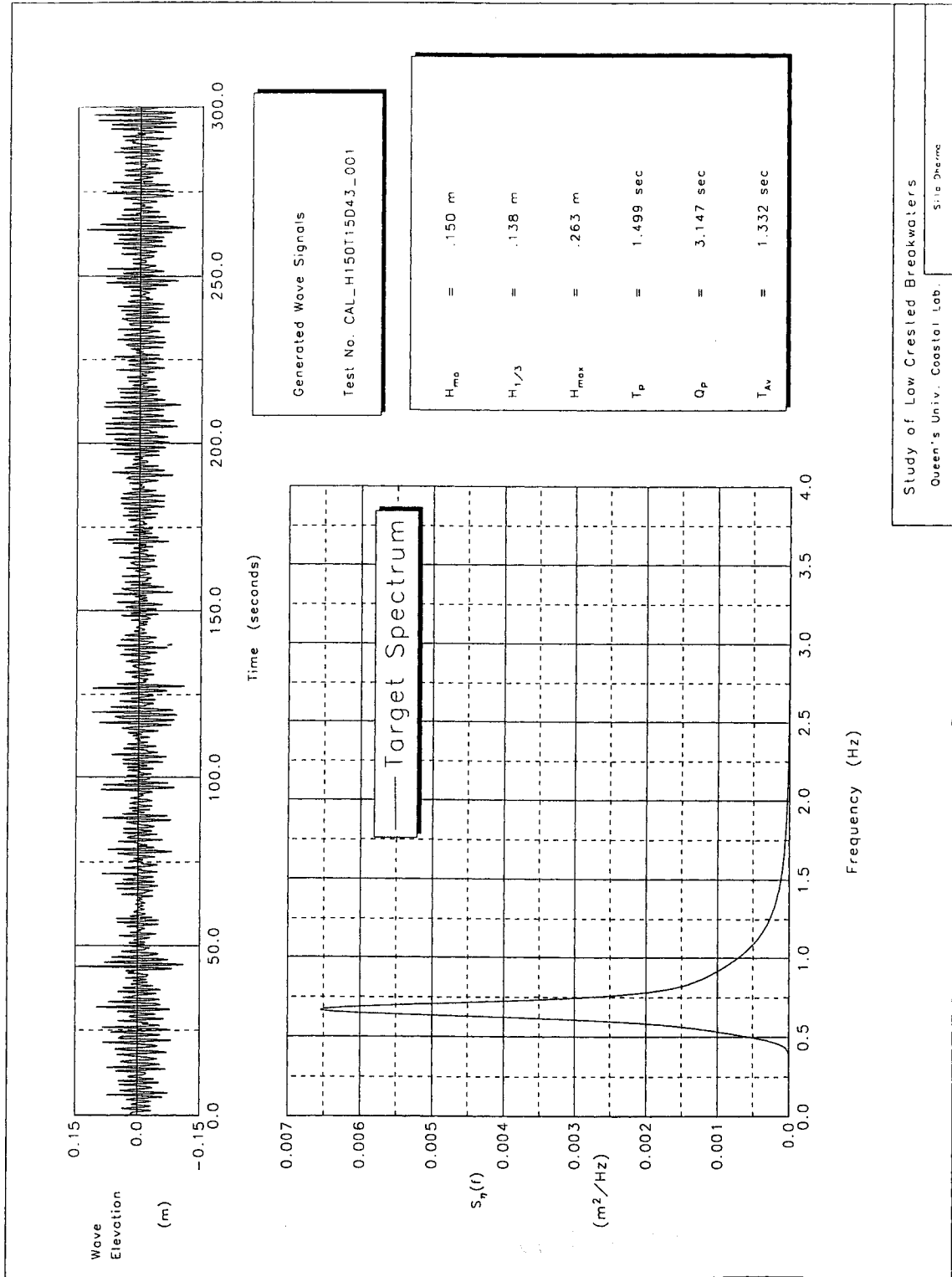




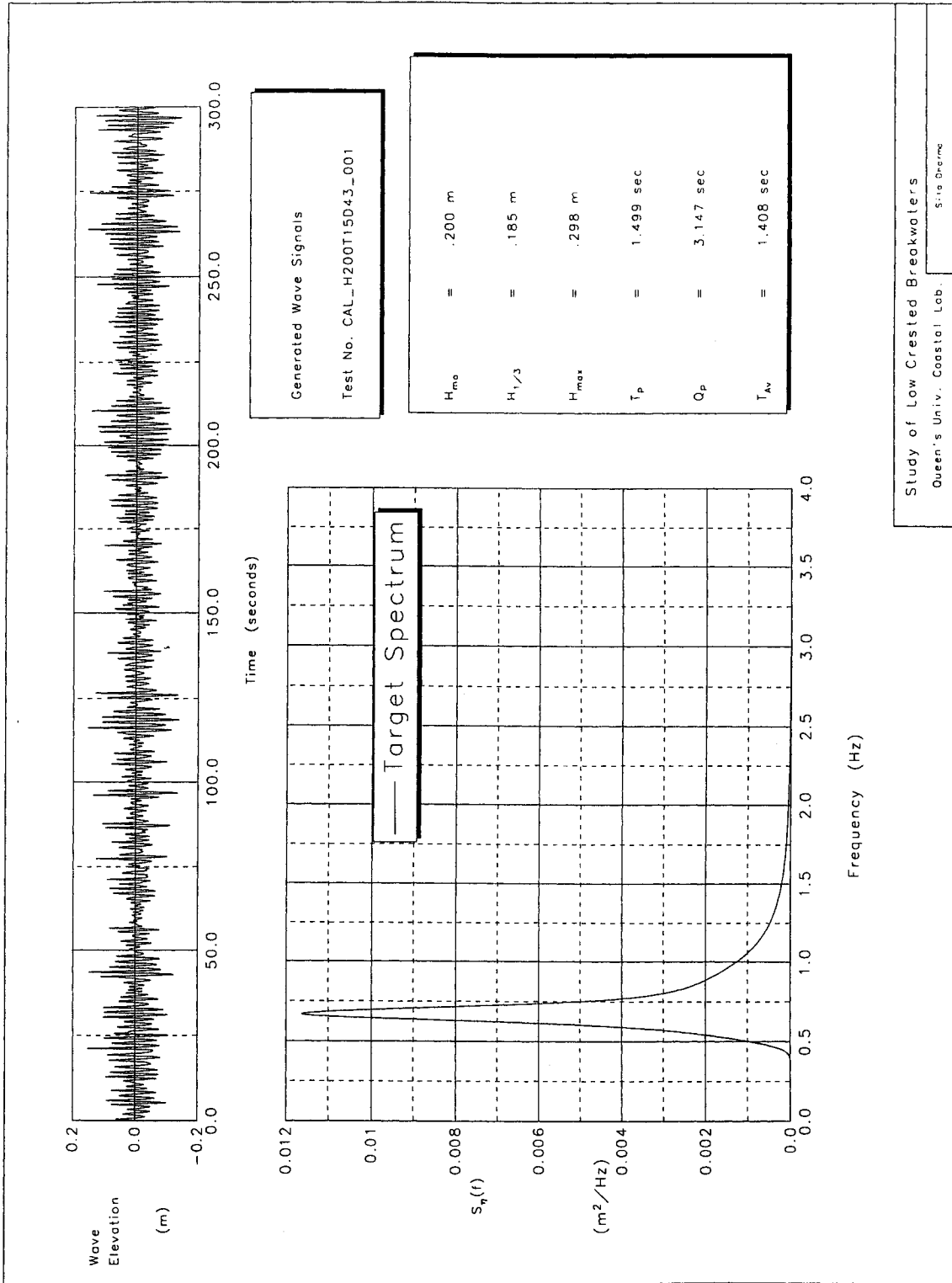


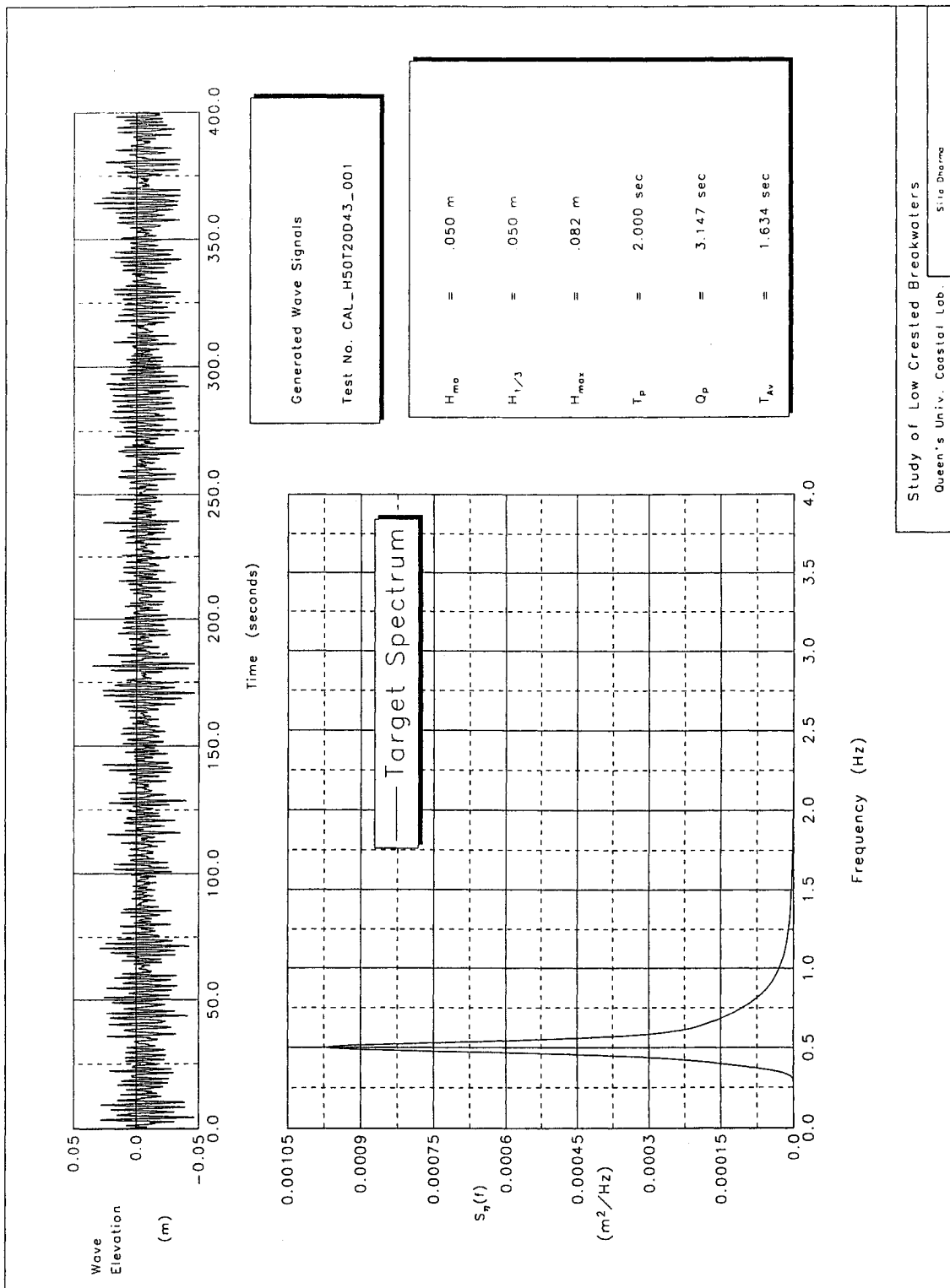


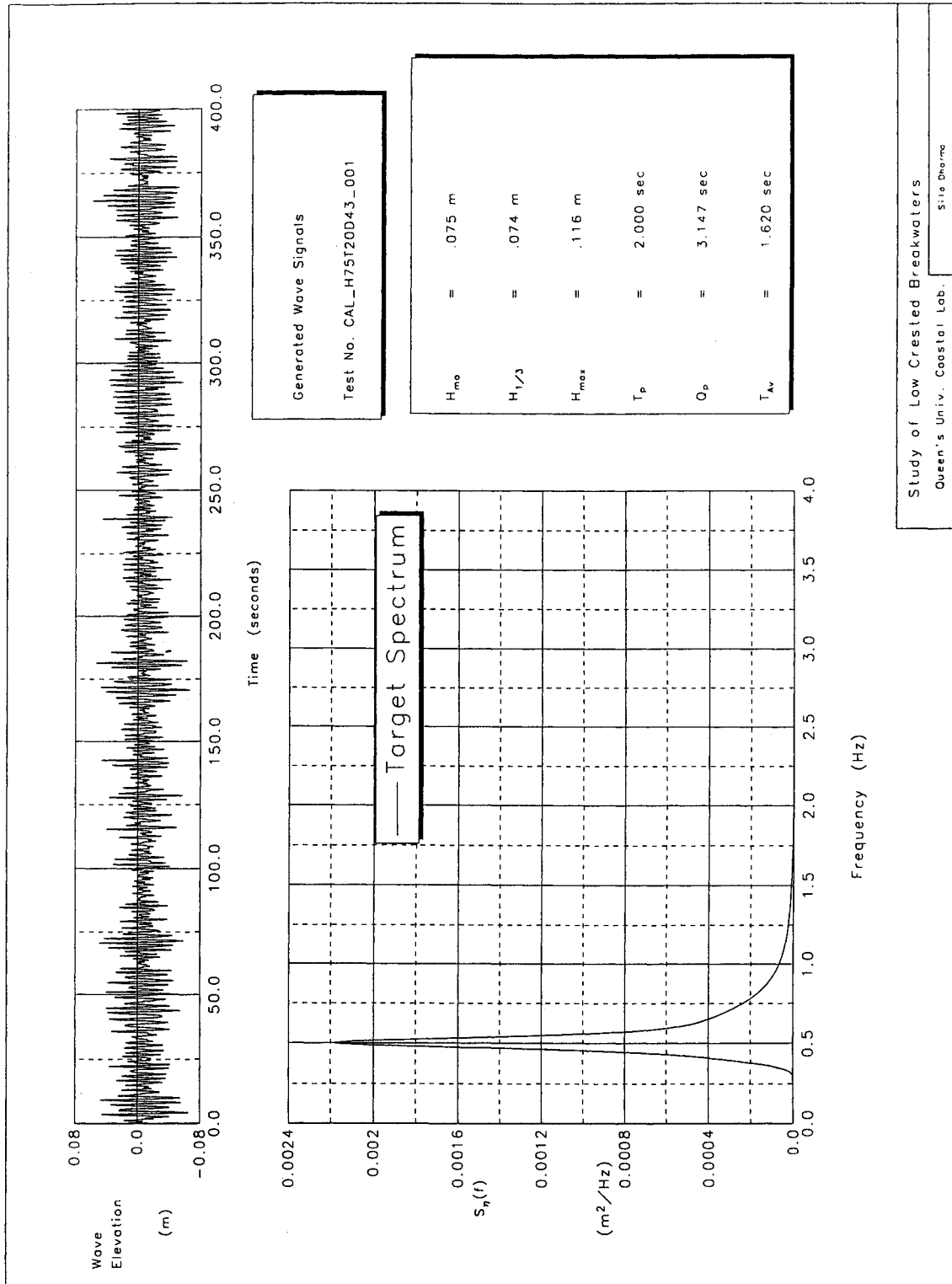


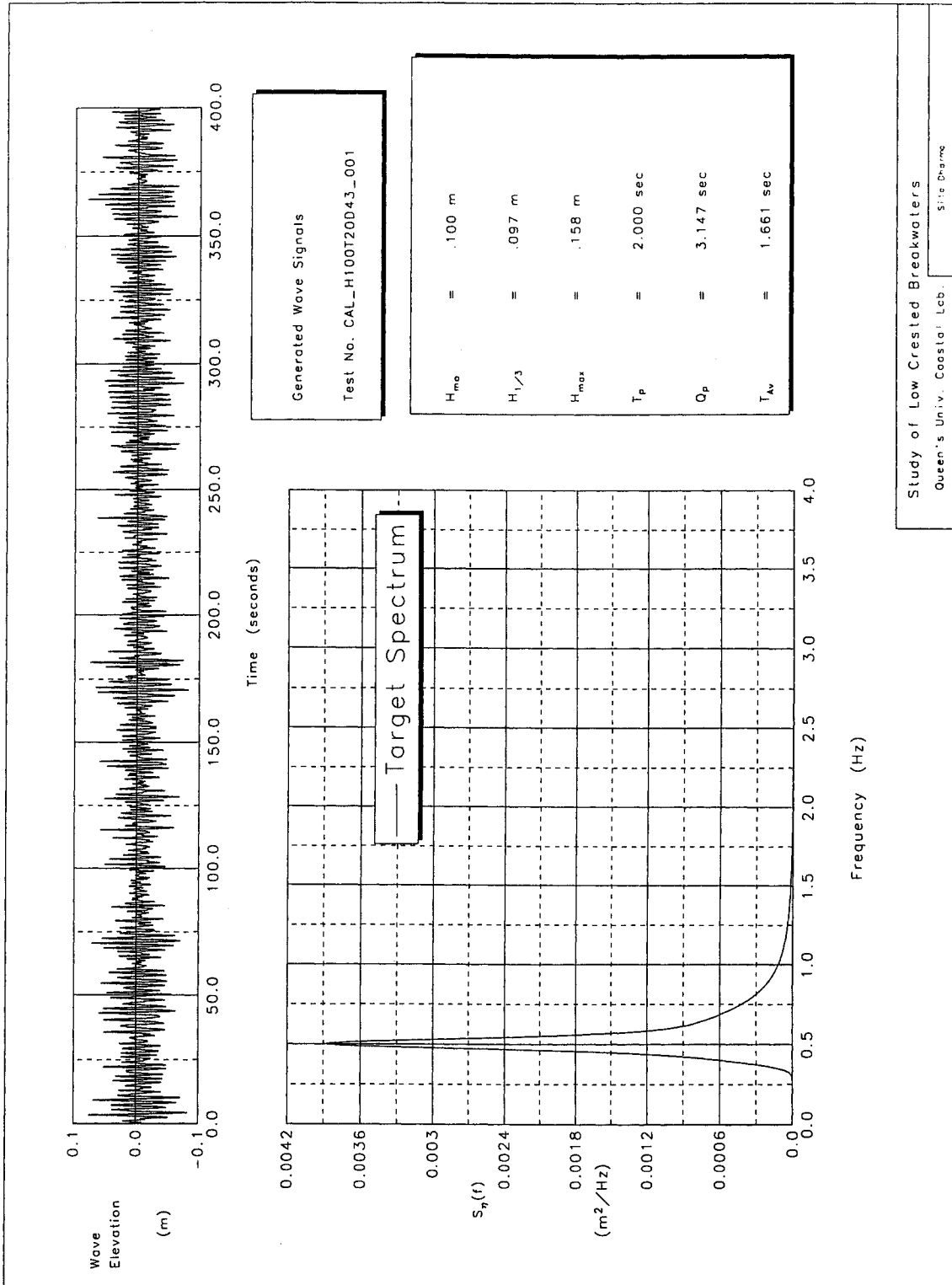


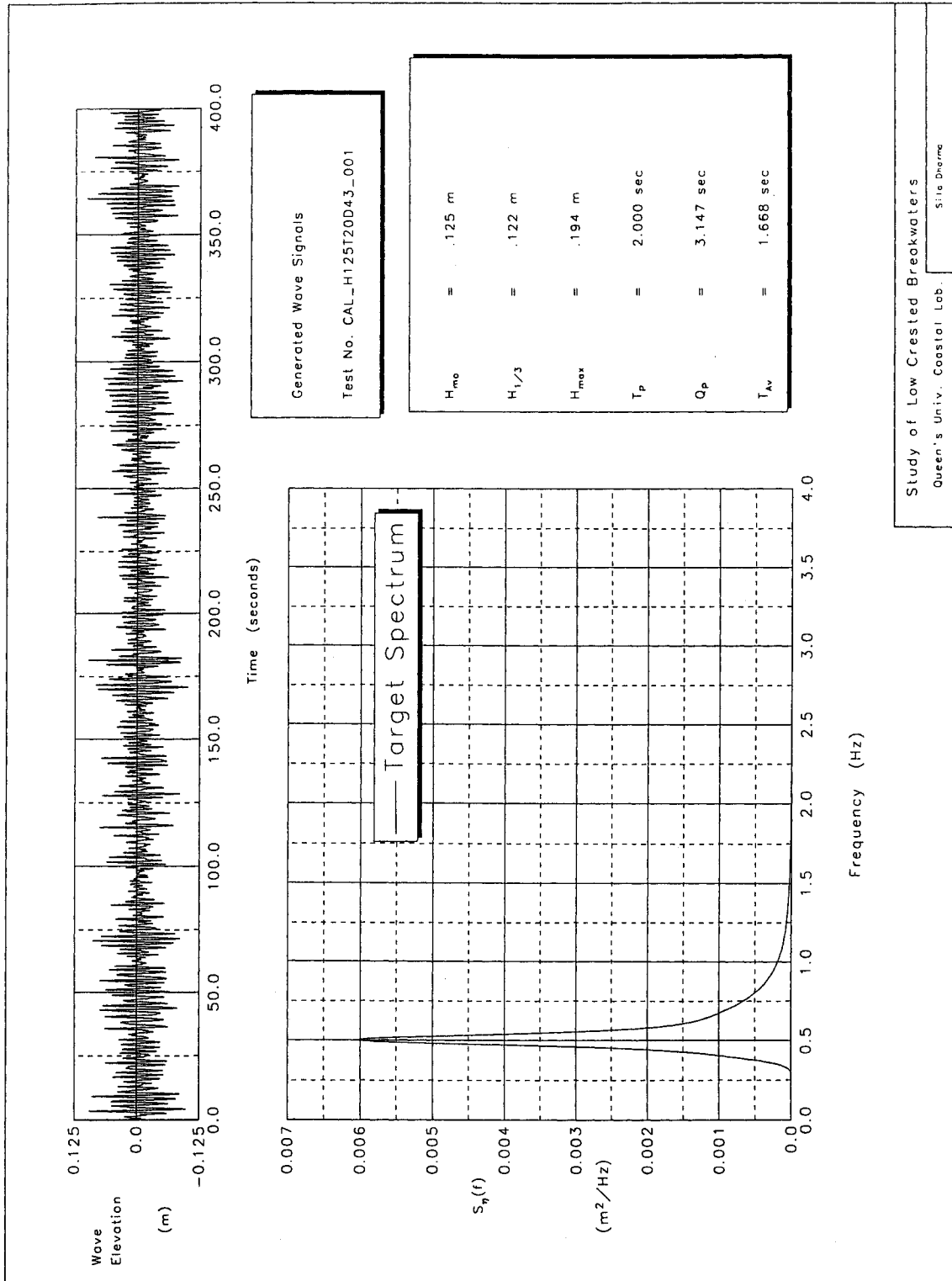


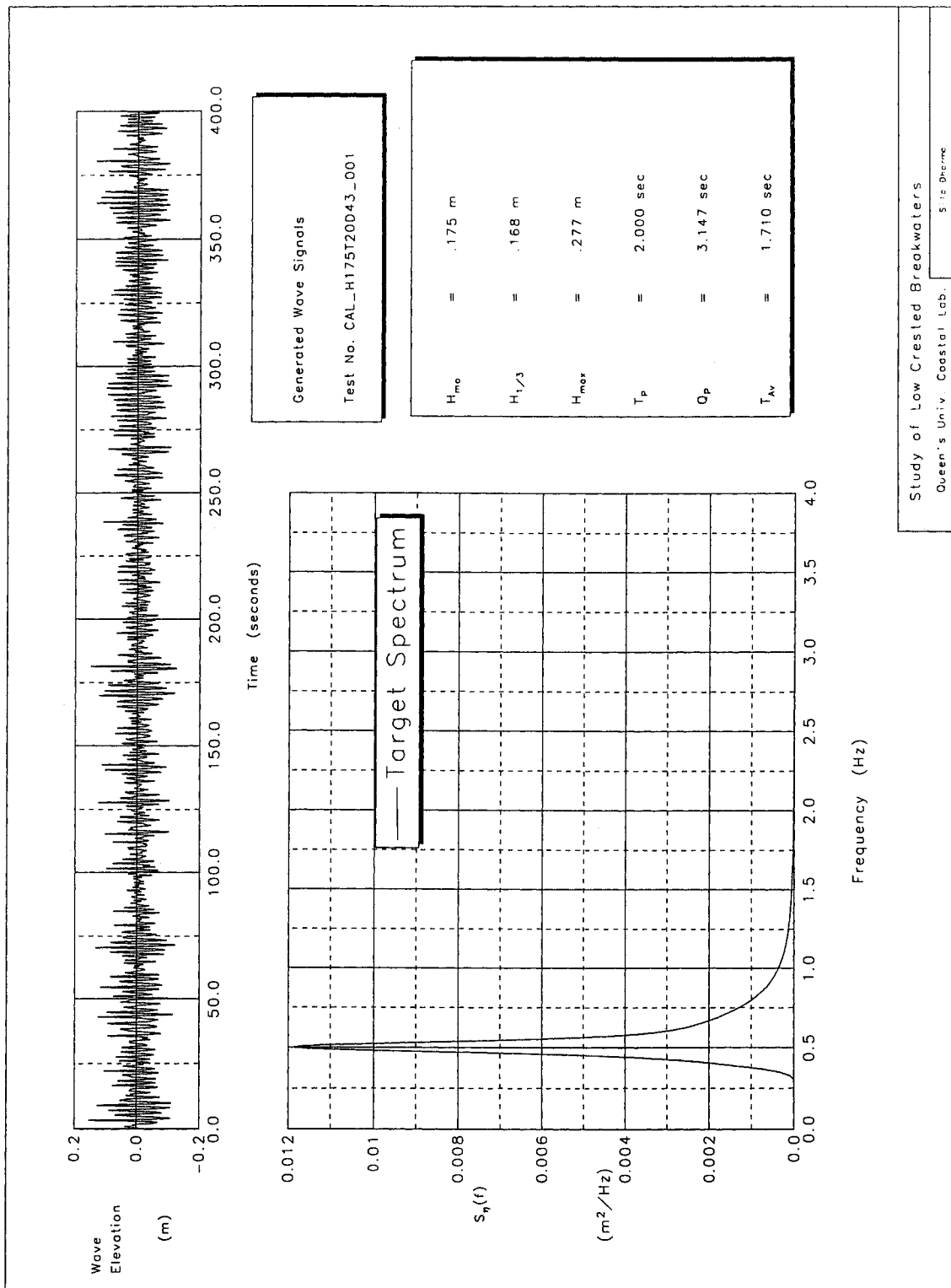


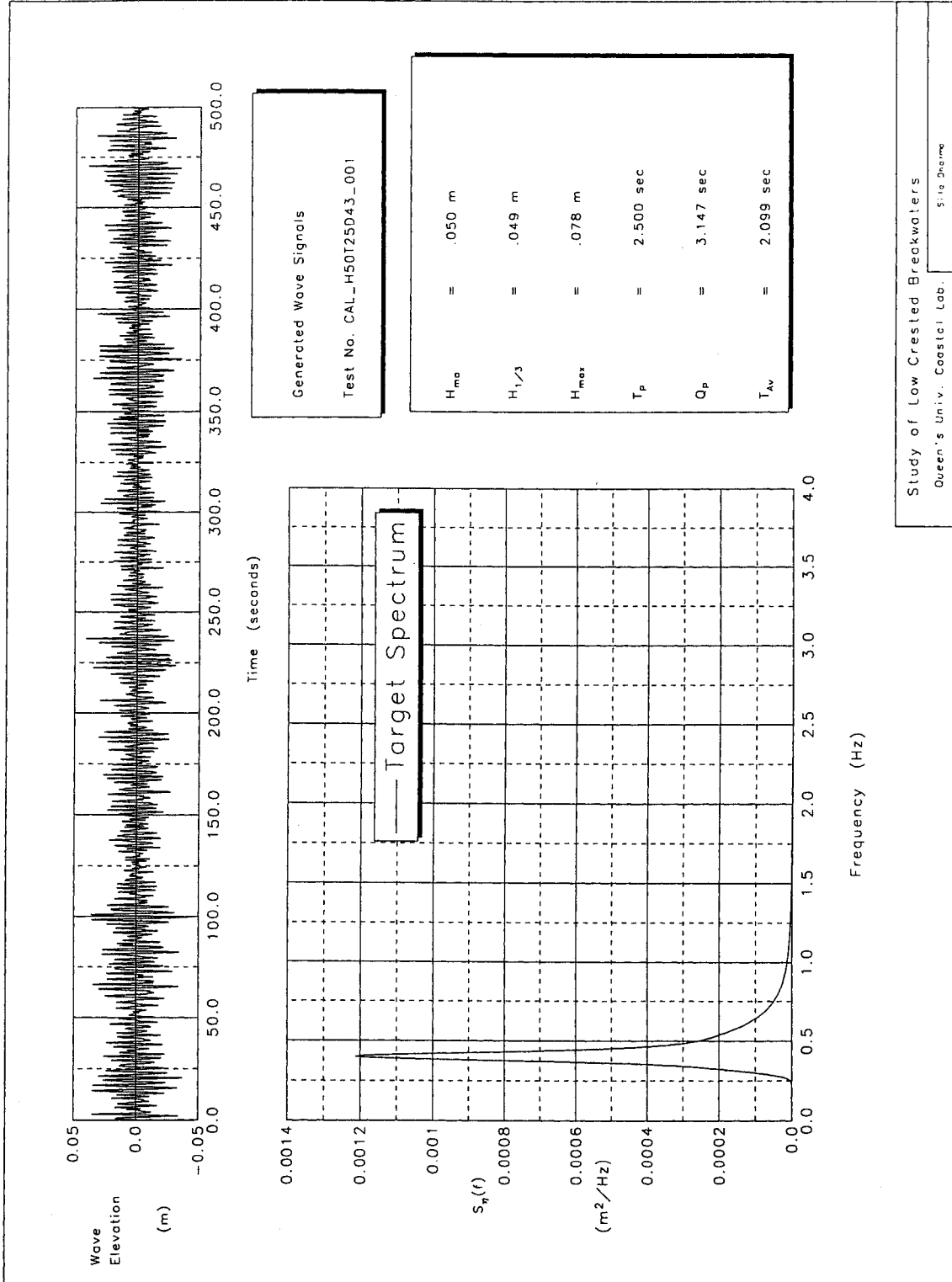


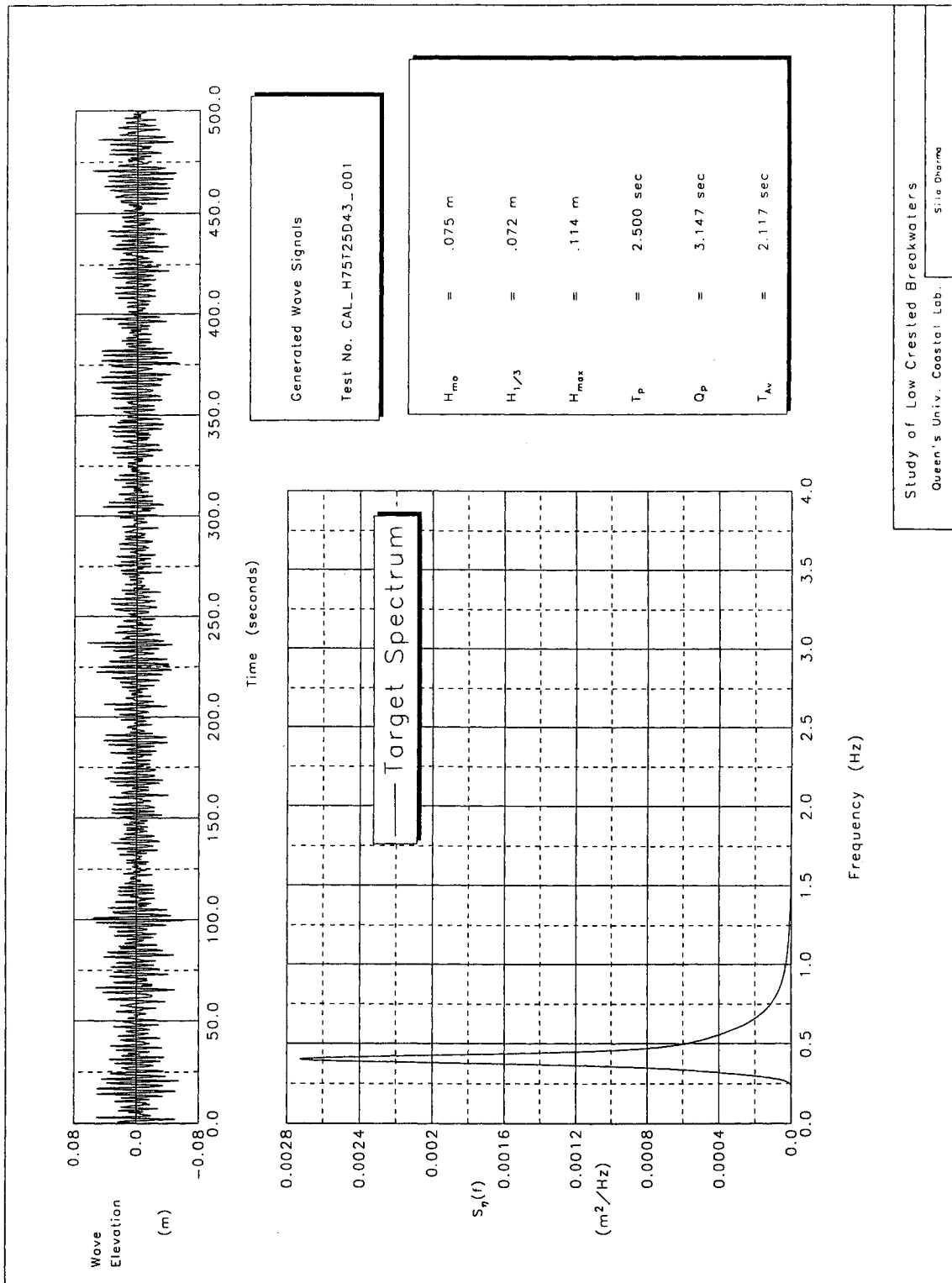




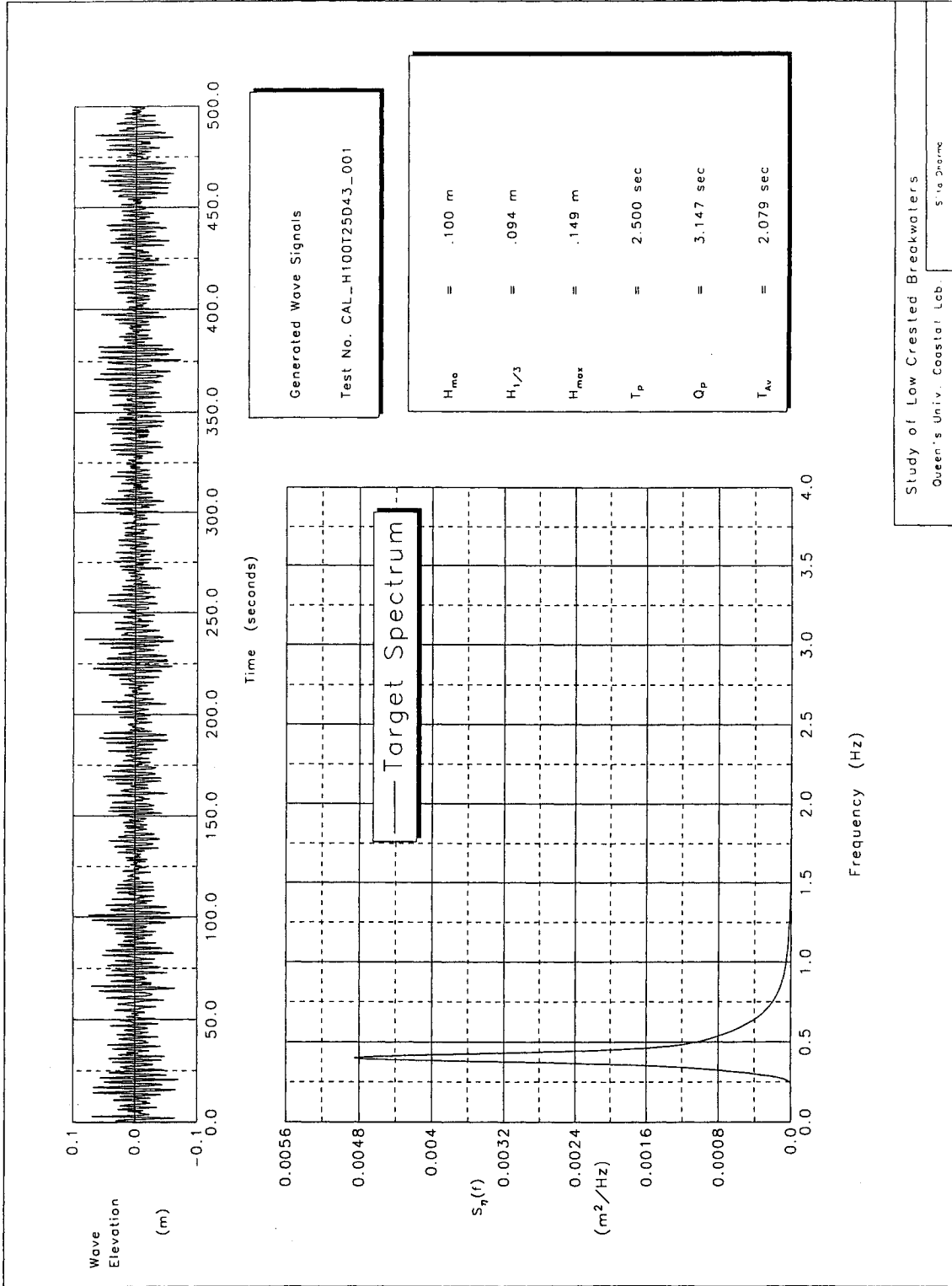


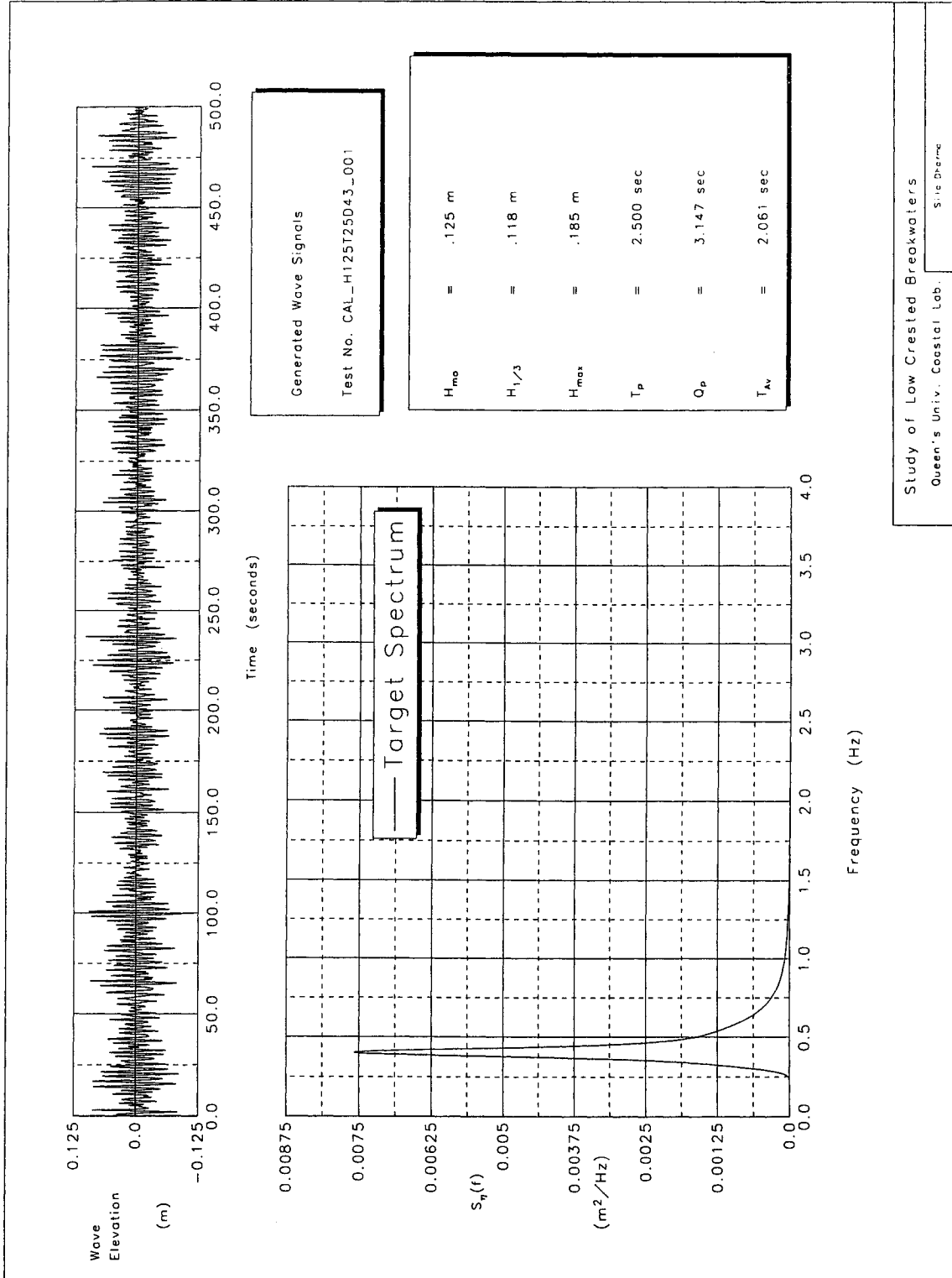


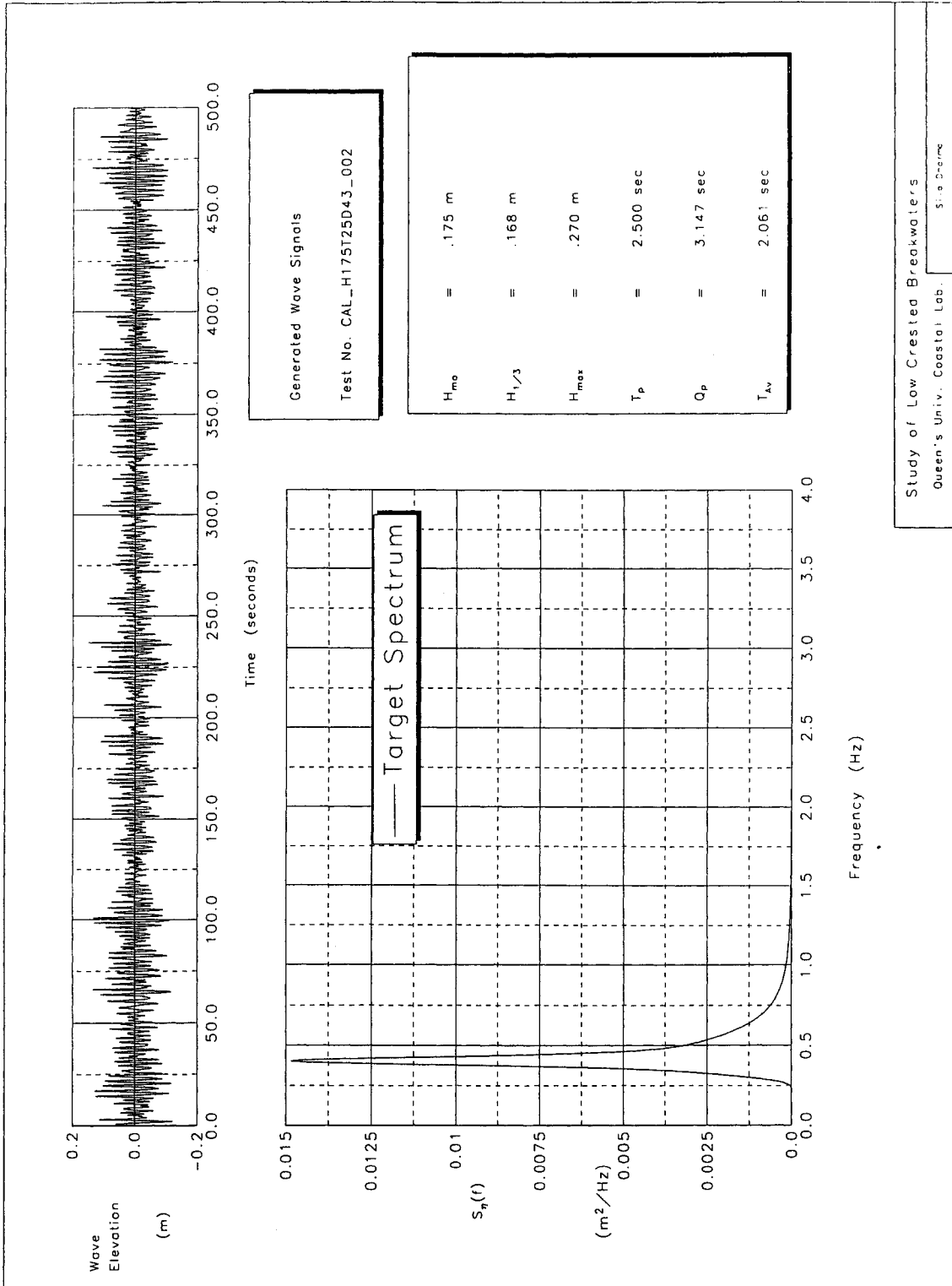




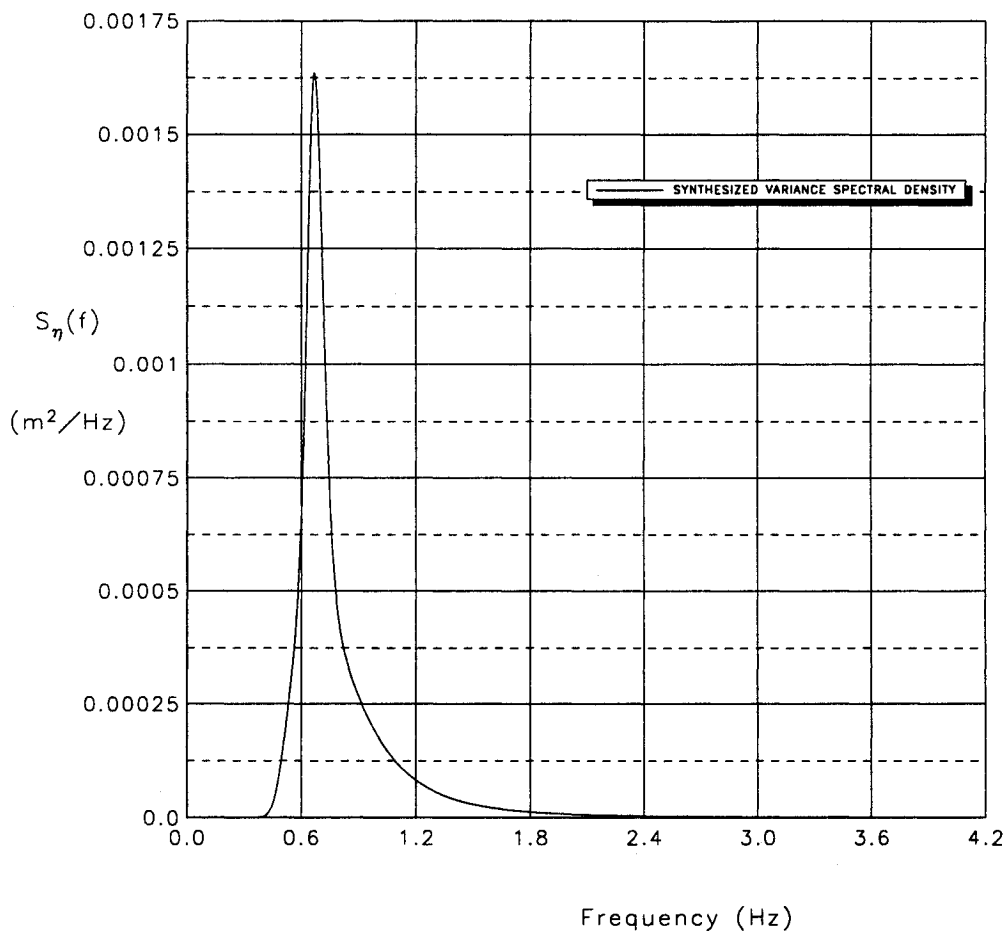
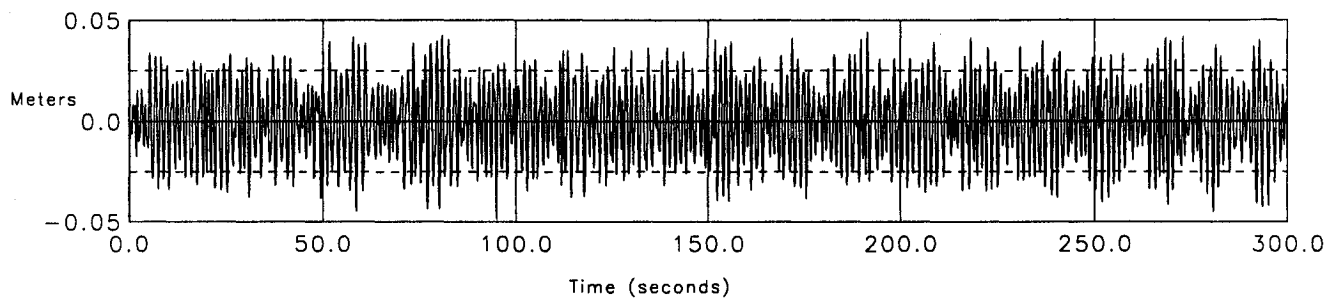
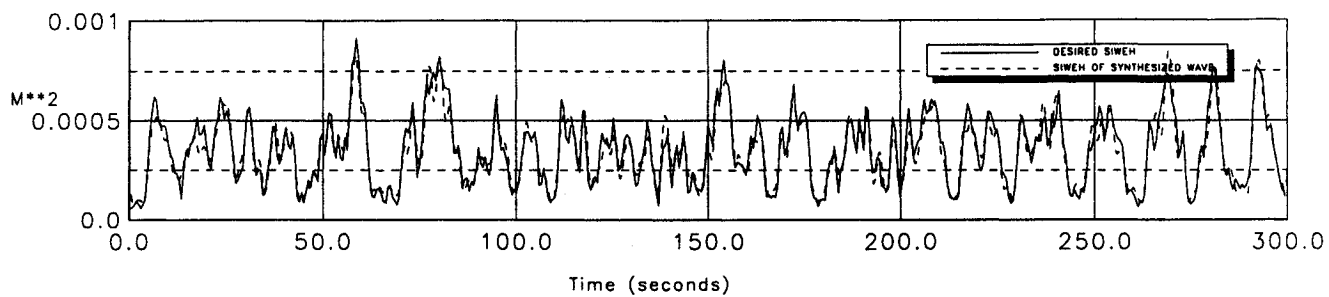






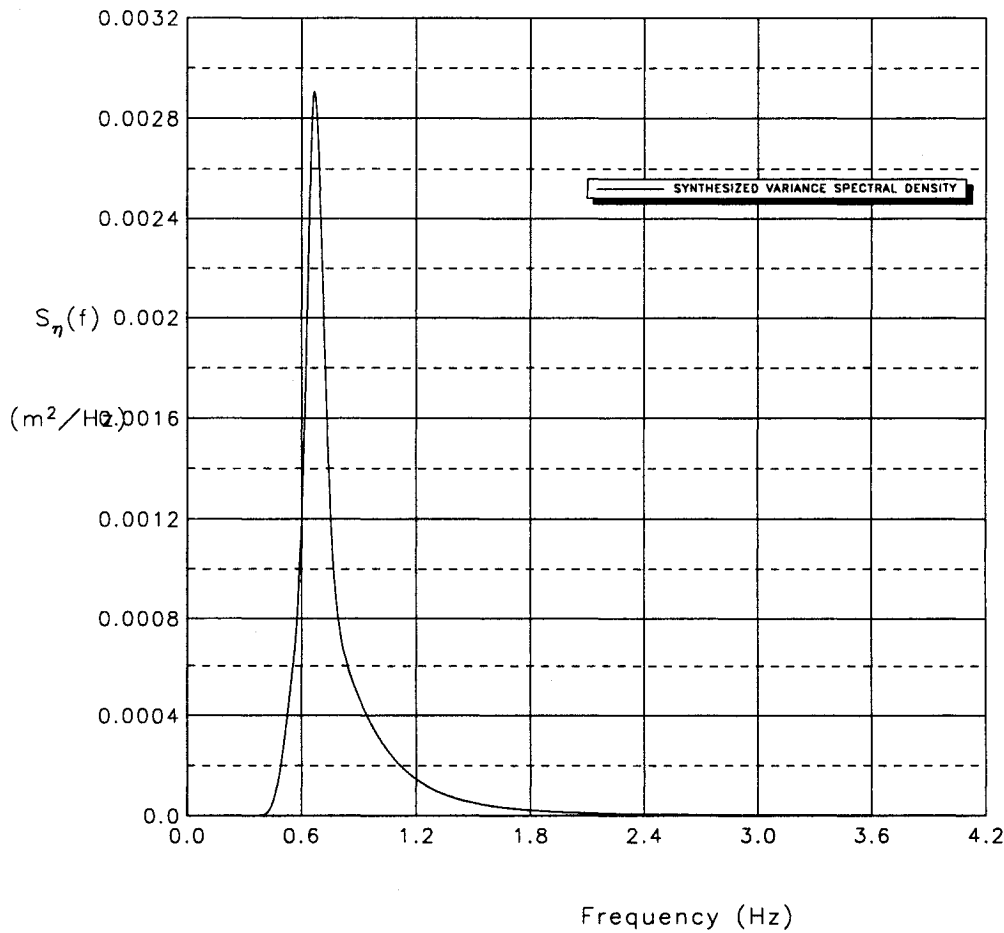
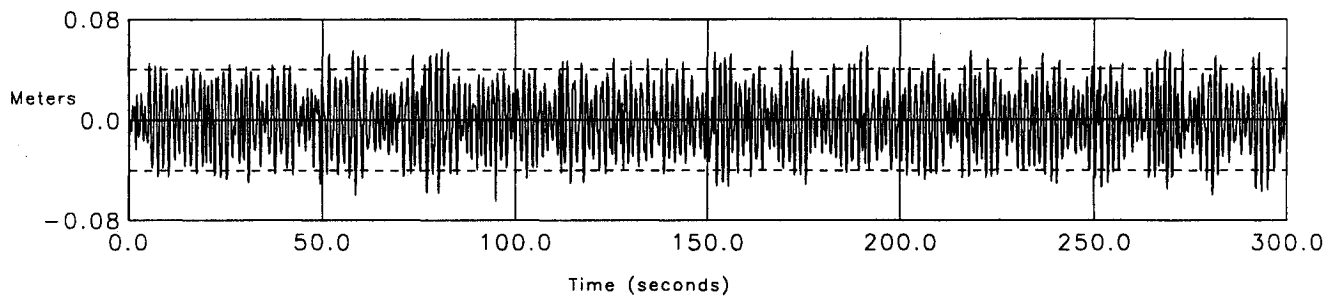
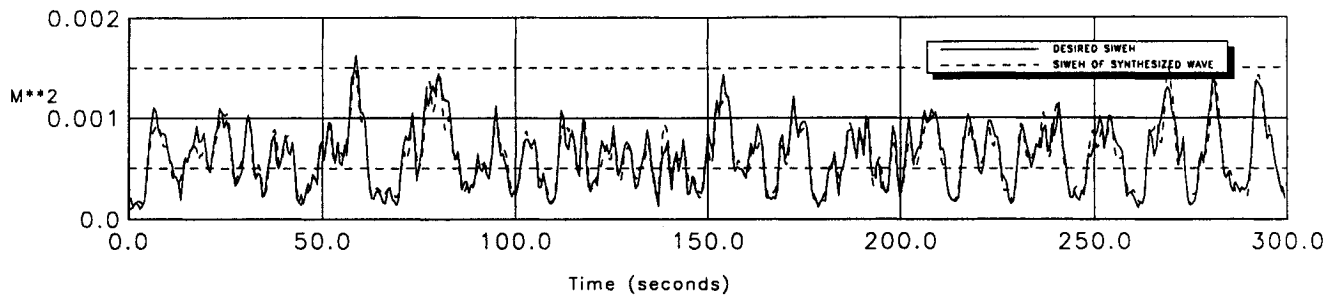


# SYNTHESIS OF A GROUPED WAVE



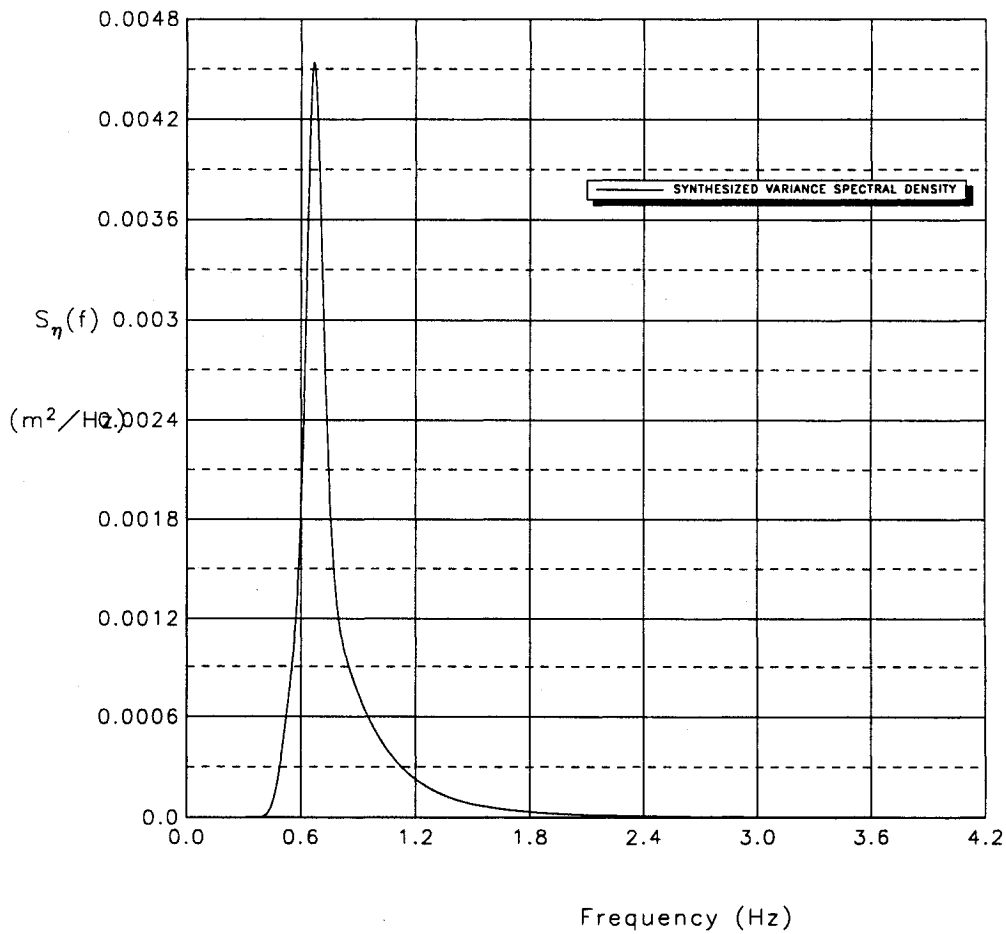
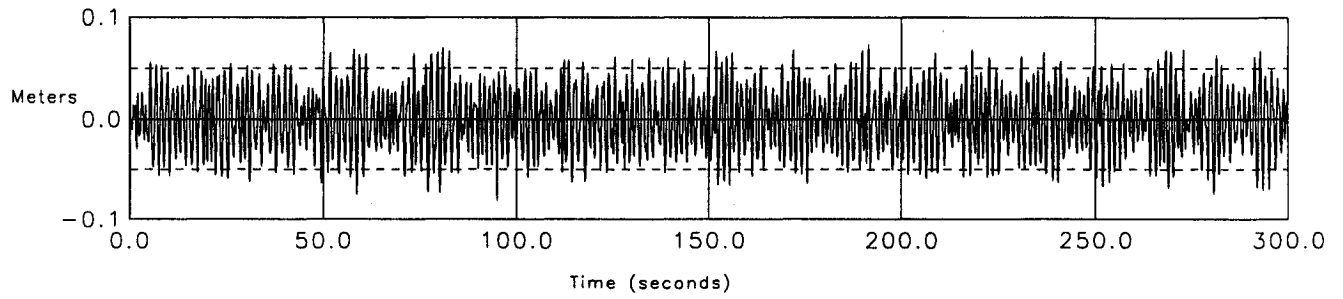
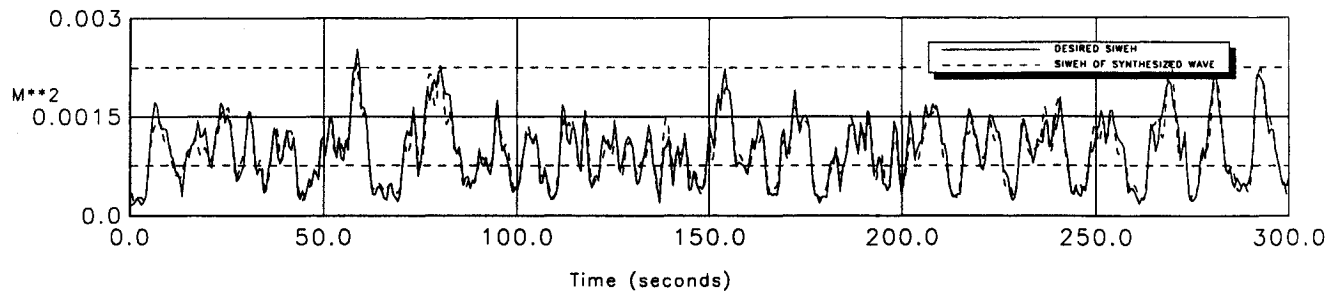
$H_{mo} = .075 \text{ m}$   
 $T_p = 1.499 \text{ sec.}$   
 $ZETA = .200$   
 $GF = .460$

# SYNTHESIS OF A GROUPED WAVE



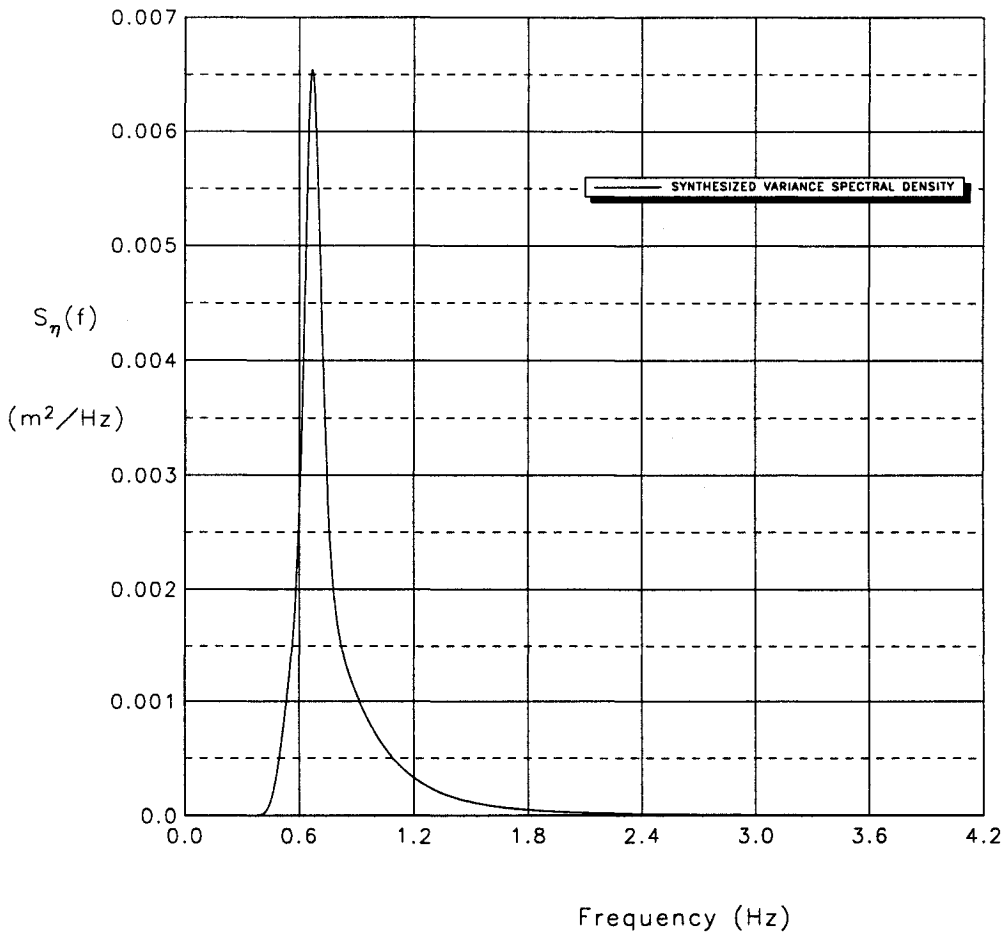
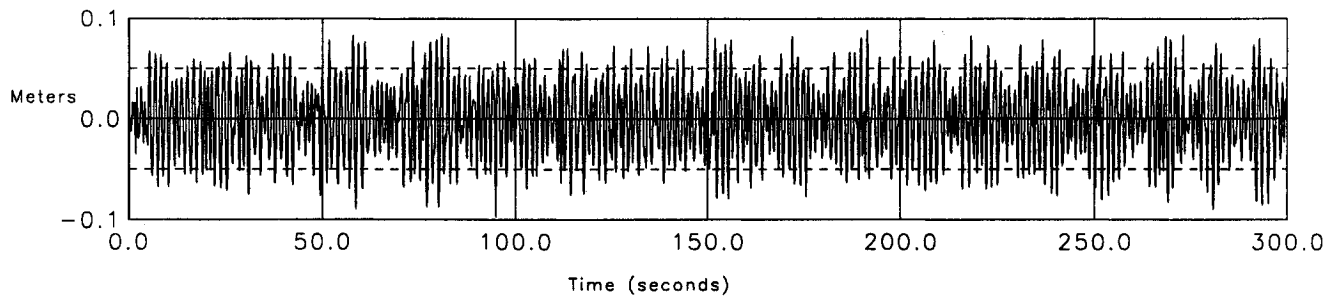
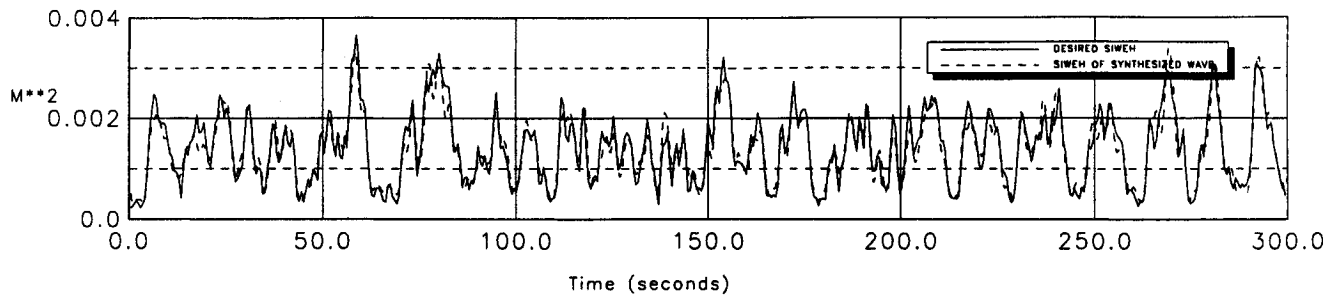
$H_{mo} = .100 \text{ m}$   
 $T_p = 1.499 \text{ sec.}$   
 $ZETA = .200$   
 $GF = .460$

# SYNTHESIS OF A GROUPED WAVE



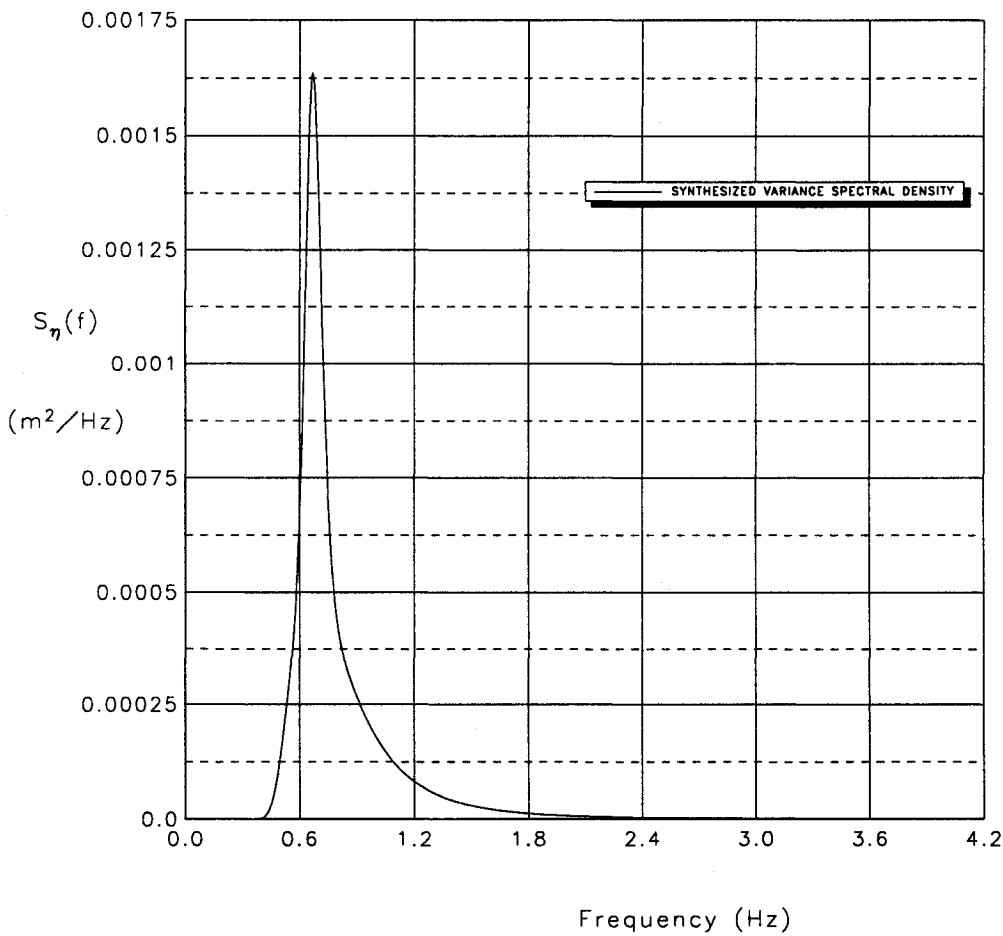
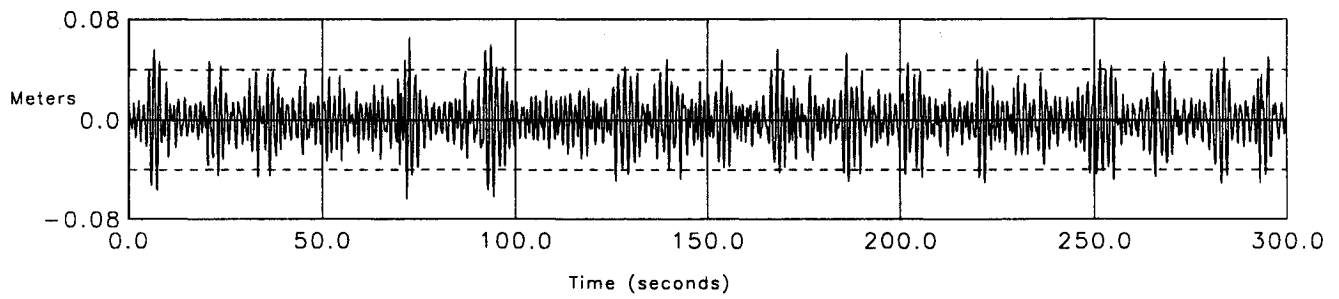
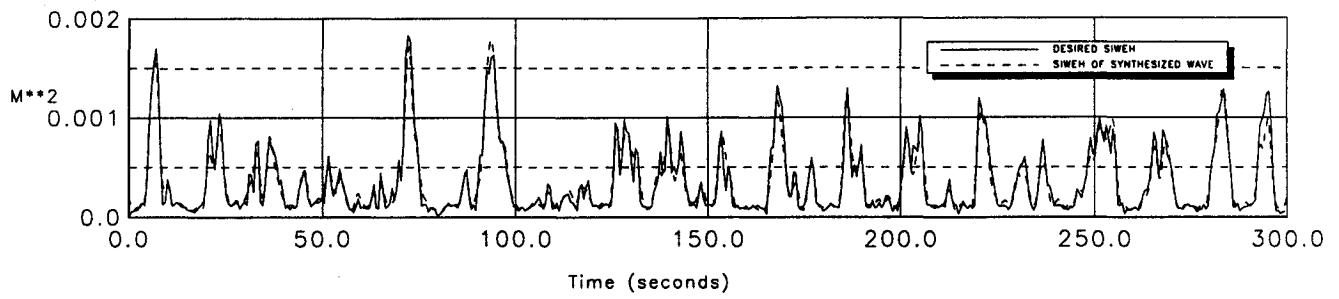
$H_{mo} = .125 \text{ m}$   
 $T_p = 1.499 \text{ sec.}$   
 $ZETA = .200$   
 $GF = .460$

# SYNTHESIS OF A GROUPED WAVE



$H_{mo} = .150 \text{ m}$   
 $T_p = 1.499 \text{ sec.}$   
 $ZETA = .200$   
 $GF = .460$

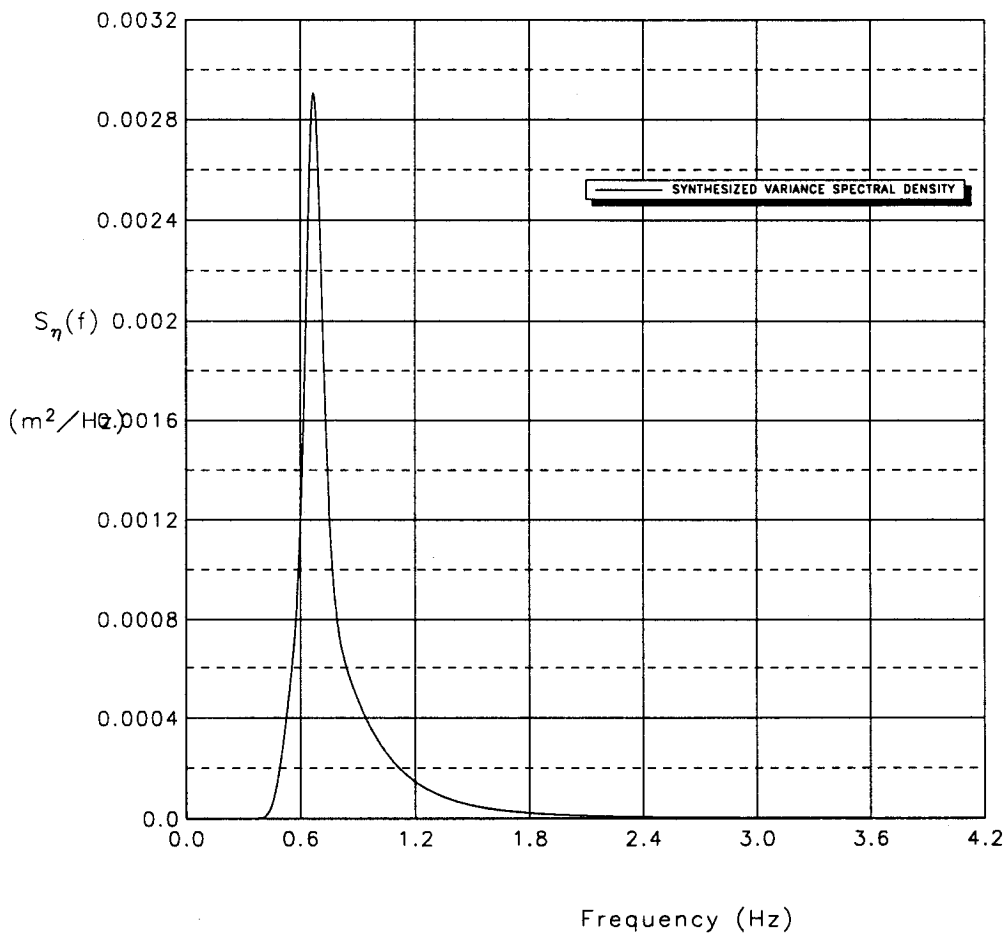
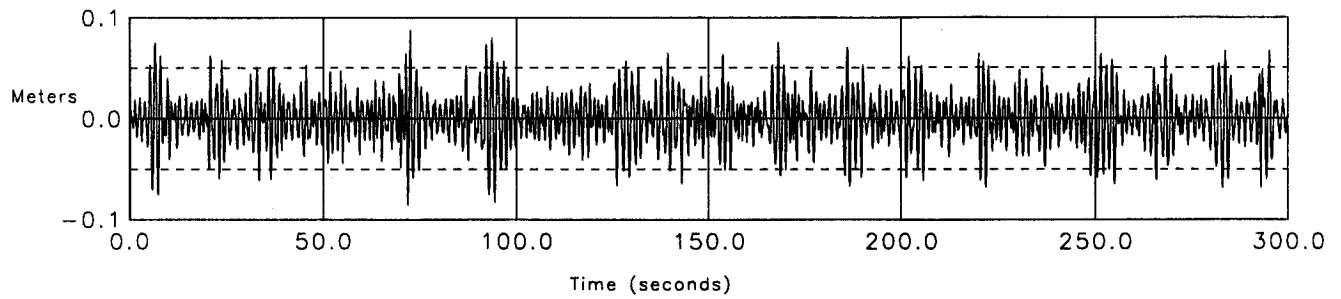
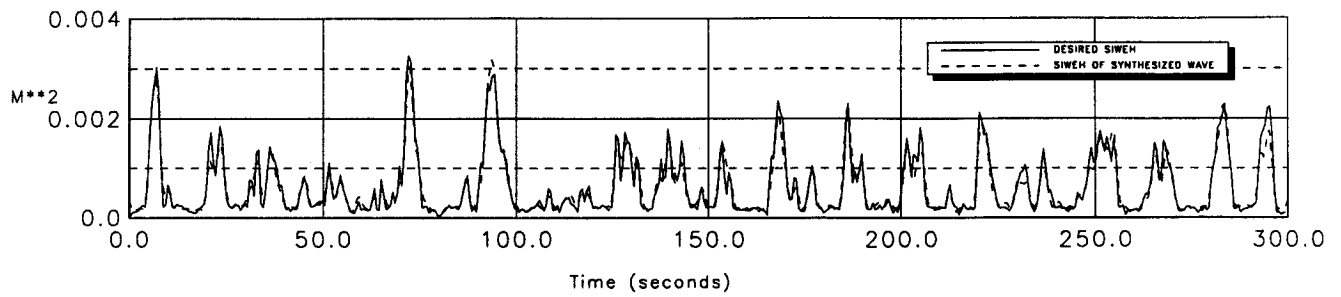
# SYNTHESIS OF A GROUPED WAVE



$H_{mo} = .075 \text{ m}$   
 $T_p = 1.499 \text{ sec.}$   
 $ZETA = .200$   
 $GF = .911$

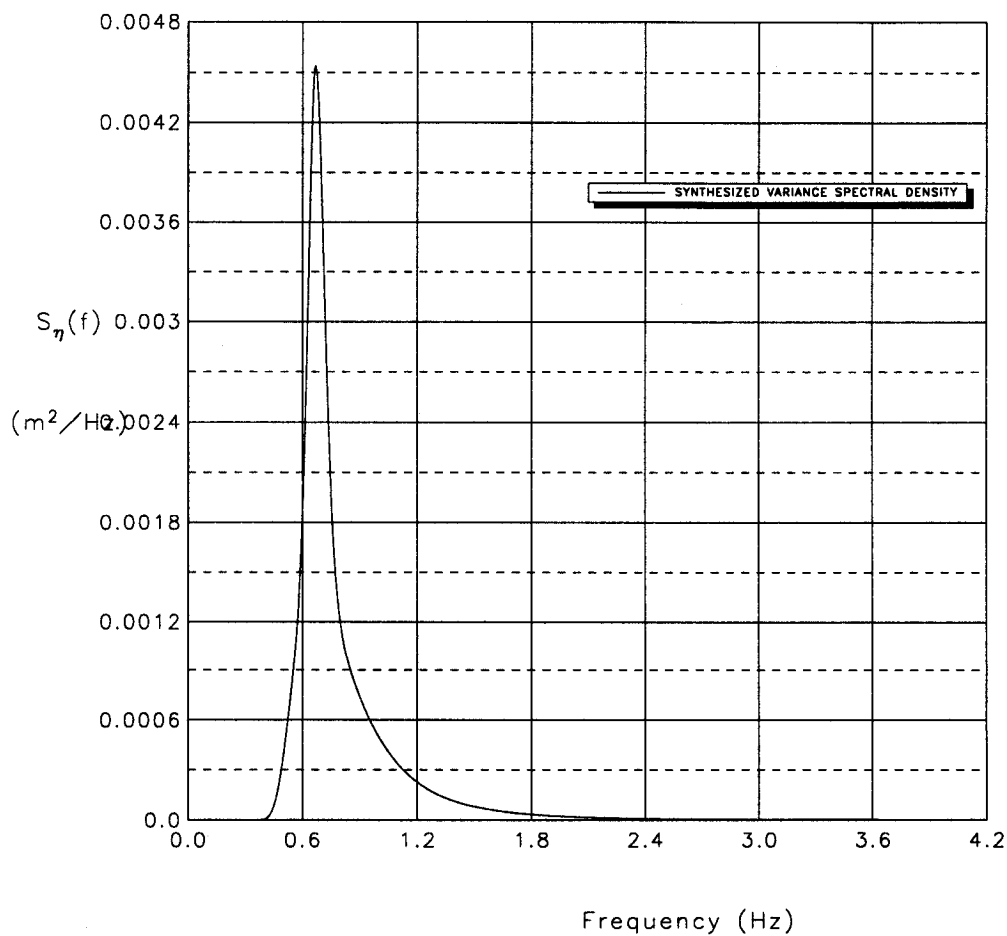
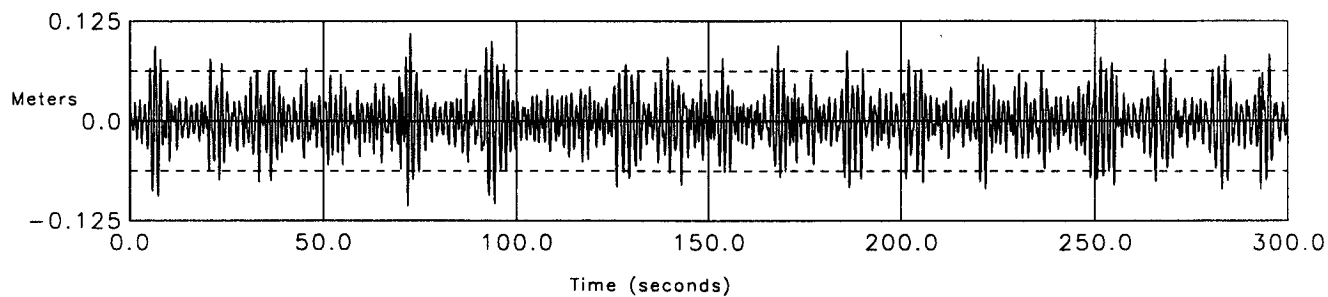
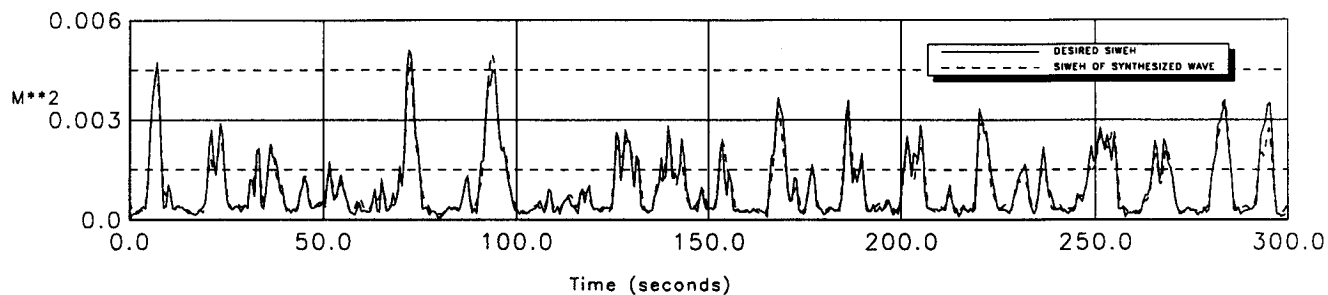


# SYNTHESIS OF A GROUPED WAVE



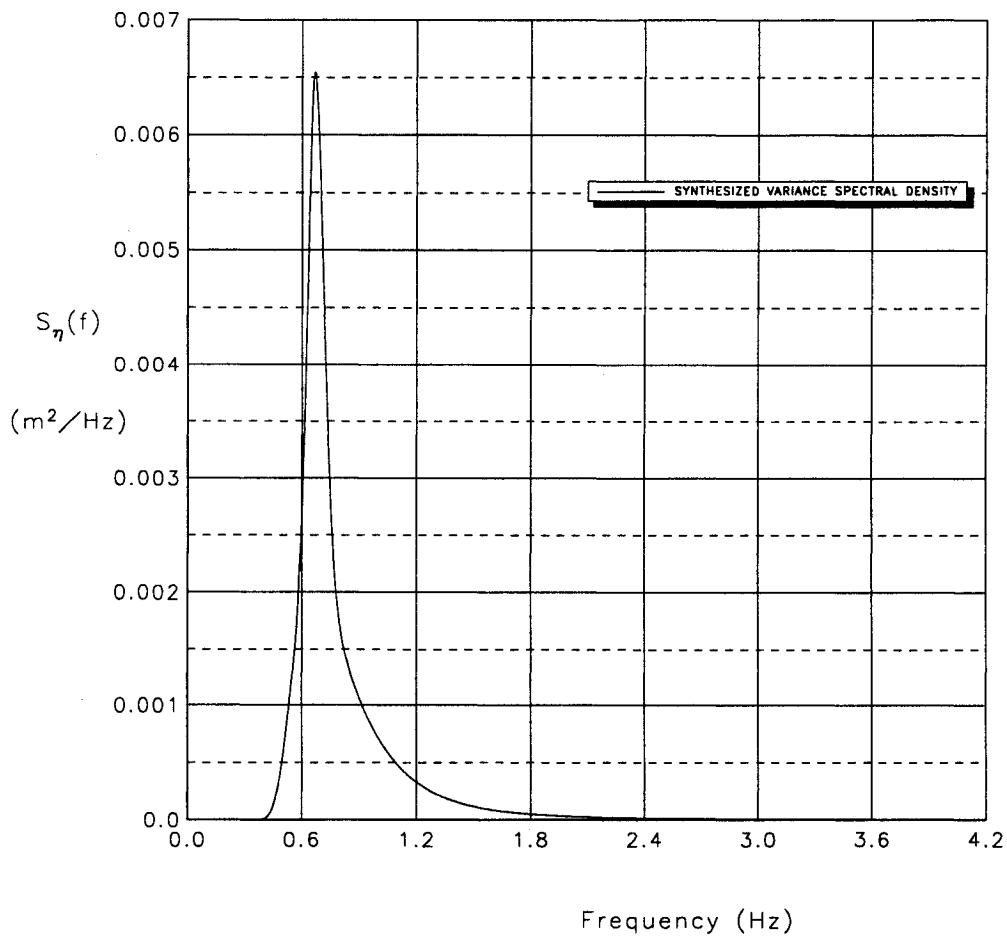
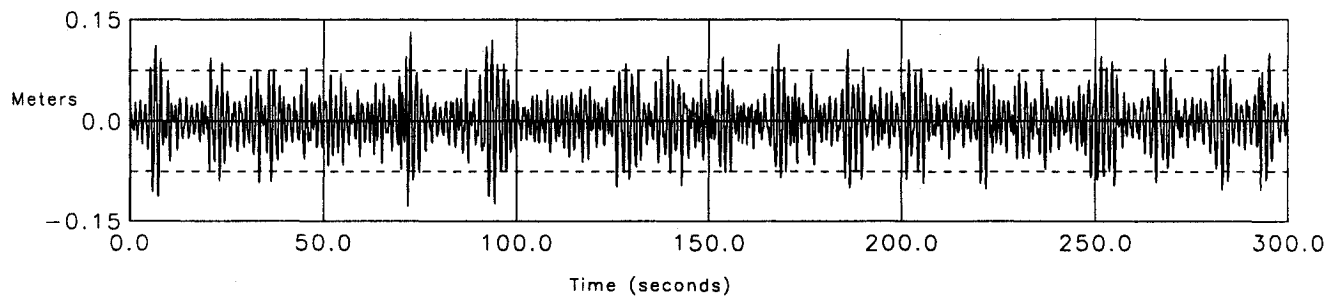
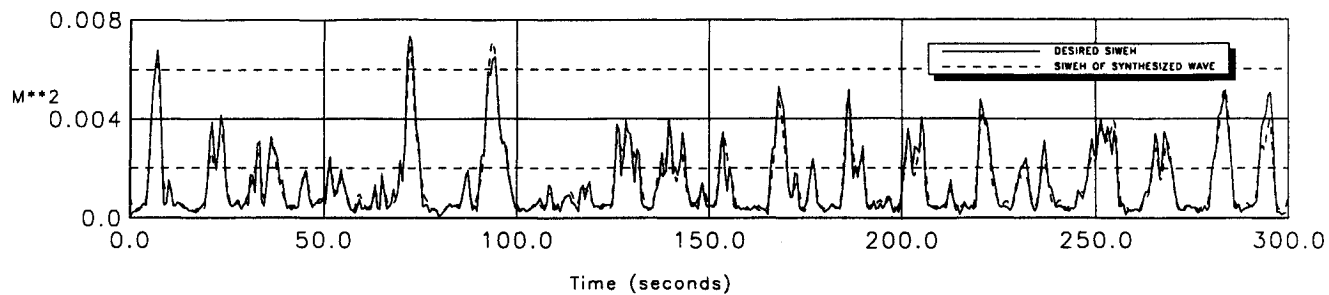
$H_{m0} = .100 \text{ m}$   
 $T_p = 1.499 \text{ sec.}$   
 $ZETA = .200$   
 $GF = .911$

# SYNTHESIS OF A GROUPED WAVE



$H_{mo} = .125 \text{ m}$   
 $T_p = 1.499 \text{ sec.}$   
 $ZETA = .200$   
 $GF = .911$

## SYNTHESIS OF A GROUPED WAVE



$$\begin{aligned}
 H_{mo} &= .150 \text{ m} \\
 T_p &= 1.499 \text{ sec.} \\
 ZETA &= .200 \\
 GF &= .911
 \end{aligned}$$

## APPENDIX F

### BOUNDARY CONDITIONS FOR TRANSMISSION AND STABILITY TESTS

Table F.1. Conditions for Transmission Tests

Test #	Test Series	H <sub>i</sub> (m)	T <sub>oil</sub> (s)	H <sub>l</sub> (m)	K <sub>t</sub>	K <sub>c</sub> (%)	B (m)	h (m)	h <sub>b</sub> (m)	D <sub>50</sub> (m)	Cota	L <sub>c</sub> (m)	s <sub>op</sub>	ξ
1	T1	0.0475	0.985	0.0399	0.840	7.710	0.3	0.43	0.3	0.034	1	1.514	0.0324	5.5575
2	T1	0.0648	1.067	0.0527	0.814	7.693	0.3	0.43	0.3	0.034	1	1.777	0.0419	4.8843
3	T1	0.0843	1.067	0.0652	0.774	10.456	0.3	0.43	0.3	0.034	1	1.777	0.0545	4.283
4	T1	0.0982	1.164	0.0743	0.757	10.024	0.3	0.43	0.3	0.034	1	2.115	0.0606	4.0634
5	T1	0.1078	1.164	0.0825	0.765	10.957	0.3	0.43	0.3	0.034	1	2.115	0.0665	3.8771
6	T1	0.1158	1.164	0.087	0.751	13.731	0.3	0.43	0.3	0.034	1	2.115	0.0715	3.7409
7	T1	0.1156	1.164	0.0864	0.747	13.704	0.3	0.43	0.3	0.034	1	2.115	0.0713	3.7442
8	T1	0.0468	1.484	0.0395	0.844	20.086	0.3	0.43	0.3	0.034	1	3.440	0.0262	6.176
9	T1	0.0709	1.484	0.0584	0.823	21.425	0.3	0.43	0.3	0.034	1	3.440	0.0398	5.0152
10	T1	0.0914	1.484	0.0737	0.807	21.328	0.3	0.43	0.3	0.034	1	3.440	0.0512	4.4175
11	T1	0.0898	1.422	0.0716	0.797	19.641	0.3	0.43	0.3	0.034	1	3.160	0.051	4.4263
12	T1	0.1279	1.575	0.0961	0.752	21.173	0.3	0.43	0.3	0.034	1	3.877	0.0705	3.7665
13	T1	0.1493	1.484	0.1079	0.722	22.480	0.3	0.43	0.3	0.034	1	3.440	0.0837	3.4567
14	T1	0.0494	1.969	0.0419	0.849	25.975	0.3	0.43	0.3	0.034	1	6.058	0.026	6.2064
15	T1	0.0739	1.969	0.0628	0.850	26.033	0.3	0.43	0.3	0.034	1	6.058	0.0388	5.0742
16	T1	0.0969	1.969	0.0816	0.842	25.843	0.3	0.43	0.3	0.034	1	6.058	0.051	4.4288
17	T1	0.1194	2.09	0.0967	0.810	25.593	0.3	0.43	0.3	0.034	1	6.822	0.0622	4.0094
18	T1	0.1328	1.969	0.1054	0.794	24.370	0.3	0.43	0.3	0.034	1	6.058	0.0698	3.7842
19	T1	0.1558	2.09	0.1172	0.752	24.491	0.3	0.43	0.3	0.034	1	6.822	0.0812	3.5093
20	T1	0.0499	2.381	0.0426	0.854	26.283	0.3	0.43	0.3	0.034	1	8.859	0.0256	6.2514
21	T1	0.0757	2.381	0.065	0.858	26.074	0.3	0.43	0.3	0.034	1	8.859	0.0388	5.0742
22	T1	0.0995	2.381	0.0845	0.849	25.709	0.3	0.43	0.3	0.034	1	8.859	0.051	4.4263
23	T1	0.0444	0.985	0.0347	0.782	8.445	0.3	0.38	0.3	0.034	1	1.514	0.0309	5.6912
24	T1	0.0635	1.067	0.0455	0.716	8.421	0.3	0.38	0.3	0.034	1	1.777	0.0422	4.8675
25	T1	0.0802	1.067	0.0553	0.689	10.627	0.3	0.38	0.3	0.034	1	1.777	0.0533	4.3299
26	T1	0.0466	1.484	0.0371	0.797	22.430	0.3	0.38	0.3	0.034	1	3.440	0.0273	6.0527
27	T1	0.0702	1.484	0.0536	0.764	23.132	0.3	0.38	0.3	0.034	1	3.440	0.0411	4.9297
28	T1	0.0904	1.484	0.066	0.730	24.137	0.3	0.38	0.3	0.034	1	3.440	0.053	4.3452
29	T1	0.0495	2.008	0.0399	0.806	29.840	0.3	0.38	0.3	0.034	1	6.297	0.0274	6.0427
30	T1	0.0744	2.008	0.0583	0.784	29.632	0.3	0.38	0.3	0.034	1	6.297	0.0411	4.9315
31	T1	0.0988	2.008	0.074	0.749	29.325	0.3	0.38	0.3	0.034	1	6.297	0.0546	4.2789
32	T1	0.0512	2.438	0.0409	0.798	32.022	0.3	0.38	0.3	0.034	1	9.286	0.0277	6.008
33	T1	0.0774	2.438	0.0609	0.787	32.233	0.3	0.38	0.3	0.034	1	9.286	0.0419	4.8866
34	T1	0.1018	2.438	0.077	0.756	32.854	0.3	0.38	0.3	0.034	1	9.286	0.0551	4.2603
35	T1	0.0406	1.004	0.0252	0.620	12.052	0.3	0.33	0.3	0.034	1	1.574	0.0288	5.8896
36	T1	0.0605	1.045	0.0311	0.514	11.954	0.3	0.33	0.3	0.034	1	1.706	0.0421	4.8733
37	T1	0.0793	1.067	0.0378	0.476	14.151	0.3	0.33	0.3	0.034	1	1.777	0.0546	4.2778
38	T1	0.0923	1.164	0.044	0.476	15.249	0.3	0.33	0.3	0.034	1	2.115	0.0613	4.0374
39	T1	0.0452	1.528	0.0285	0.630	23.142	0.3	0.33	0.3	0.034	1	3.649	0.0277	6.0052
40	T1	0.0686	1.528	0.0392	0.571	25.797	0.3	0.33	0.3	0.034	1	3.649	0.0421	4.8728
41	T1	0.0878	1.552	0.0477	0.544	28.731	0.3	0.33	0.3	0.034	1	3.760	0.0537	4.3143
42	T1	0.0489	2.048	0.0318	0.650	34.303	0.3	0.33	0.3	0.034	1	6.552	0.0287	5.9042
43	T1	0.0731	1.932	0.0451	0.617	36.062	0.3	0.33	0.3	0.034	1	5.831	0.0432	4.8119
44	T1	0.0978	1.932	0.057	0.583	37.052	0.3	0.33	0.3	0.034	1	5.831	0.0578	4.1605
45	T1	0.0506	2.498	0.0329	0.649	38.813	0.3	0.33	0.3	0.034	1	9.744	0.0292	5.8536
46	T1	0.0762	2.498	0.0474	0.622	40.988	0.3	0.33	0.3	0.034	1	9.744	0.0439	4.7719
47	T1	0.1008	2.498	0.0596	0.592	42.266	0.3	0.33	0.3	0.034	1	9.744	0.0581	4.1494
48	T1	0.0394	1.004	0.0135	0.344	16.725	0.3	0.3	0.3	0.034	1	1.574	0.0286	5.9116
49	T1	0.0604	1.045	0.0213	0.352	18.175	0.3	0.3	0.3	0.034	1	1.706	0.0431	4.8141
50	T1	0.0791	1.067	0.0287	0.362	21.203	0.3	0.3	0.3	0.034	1	1.777	0.056	4.2246
51	T1	0.0451	1.528	0.018	0.398	31.487	0.3	0.3	0.3	0.034	1	3.649	0.0288	5.8929
52	T1	0.0697	1.528	0.0302	0.433	34.495	0.3	0.3	0.3	0.034	1	3.649	0.0445	4.7412
53	T1	0.0906	1.552	0.0389	0.429	37.210	0.3	0.3	0.3	0.034	1	3.760	0.0576	4.1658
54	T1	0.0496	1.969	0.0225	0.454	42.252	0.3	0.3	0.3	0.034	1	6.058	0.0305	5.7272
55	T1	0.0751	1.969	0.0352	0.468	42.051	0.3	0.3	0.3	0.034	1	6.058	0.0462	4.6544
56	T1	0.1004	1.969	0.0477	0.475	42.361	0.3	0.3	0.3	0.034	1	6.058	0.0617	4.0264
57	T1	0.0514	2.56	0.0246	0.478	45.702	0.3	0.3	0.3	0.034	1	10.237	0.0309	5.6853
58	T1	0.0778	2.56	0.0382	0.491	46.214	0.3	0.3	0.3	0.034	1	10.237	0.0468	4.6225
59	T1	0.103	2.56	0.05	0.485	46.419	0.3	0.3	0.3	0.034	1	10.237	0.062	4.0177
60	T1	0.0429	0.985	0.007	0.164	32.302	0.3	0.27	0.3	0.034	1	1.514	0.0324	5.5536
61	T1	0.0545	1.045	0.0104	0.191	30.329	0.3	0.27	0.3	0.034	1	1.706	0.0401	4.9911
62	T1	0.063	1.045	0.0132	0.209	29.477	0.3	0.27	0.3	0.034	1	1.706	0.0464	4.6416
63	T1	0.0807	1.067	0.0197	0.244	28.307	0.3	0.27	0.3	0.034	1	1.777	0.059	4.1167
64	T1	0.0438	0.994	0.0071	0.163	32.538	0.3	0.27	0.3	0.034	1	1.544	0.033	5.5089
65	T1	0.0638	1.484	0.0182	0.285	43.746	0.3	0.27	0.3	0.034	1	3.440	0.0427	4.839
66	T1	0.074	1.484	0.0225	0.304	44.186	0.3	0.27	0.3	0.034	1	3.440	0.0495	4.4924
67	T1	0.0977	1.484	0.0341	0.349	42.435	0.3	0.27	0.3	0.034	1	3.440	0.0654	3.9108
68	T1	0.0516	1.969	0.0163	0.315	52.774	0.3	0.27	0.3	0.034	1	6.058	0.0332	5.4849
69	T1	0.0677	1.969	0.0242	0.358	50.414	0.3	0.27	0.3	0.034	1	6.058	0.0436	4.7864
70	T1	0.078	1.969	0.0293	0.376	49.130	0.3	0.27	0.3	0.034	1	6.058	0.0503	4.4604
71	T1	0.0525	2.381	0.0191	0.364	53.901	0.3	0.27	0.3	0.034	1	8.859	0.0333	5.4784
72	T1	0.0694	2.381	0.0273	0.394	52.213	0.3	0.27	0.3	0.034	1	8.859	0.044	4.7647

Table F.1. Conditions for Transmission Tests (cont'd)

Test #	Test Series	H <sub>i</sub> (m)	T <sub>90</sub> (s)	H <sub>t</sub> (m)	K <sub>i</sub>	K <sub>r</sub> (%)	B (m)	h (m)	h <sub>s</sub> (m)	D <sub>50</sub> (m)	Cotα	L <sub>c</sub> (m)	s <sub>op</sub>	ξ
73	T1	0.0801	2.381	0.032	0.399	51.297	0.3	0.27	0.3	0.034	1	8.859	0.0509	4.4337
74	T1	0.044	0.985	0.0046	0.106	37.479	0.3	0.25	0.3	0.034	1	1.514	0.034	5.426
75	T1	0.0554	1.045	0.0056	0.101	35.926	0.3	0.25	0.3	0.034	1	1.706	0.0418	4.8907
76	T1	0.0635	1.067	0.0069	0.109	34.521	0.3	0.25	0.3	0.034	1	1.777	0.0476	4.5838
77	T1	0.0824	1.067	0.0111	0.135	32.923	0.3	0.25	0.3	0.034	1	1.777	0.0618	4.0239
78	T1	0.0504	1.484	0.0084	0.167	50.996	0.3	0.25	0.3	0.034	1	3.440	0.0349	5.3565
79	T1	0.065	1.484	0.0112	0.172	49.730	0.3	0.25	0.3	0.034	1	3.440	0.0449	4.7199
80	T1	0.0742	1.484	0.0136	0.184	49.610	0.3	0.25	0.3	0.034	1	3.440	0.0513	4.4172
81	T1	0.0971	1.484	0.0225	0.231	47.092	0.3	0.25	0.3	0.034	1	3.440	0.0671	3.8612
82	T1	0.0532	1.969	0.0108	0.204	58.088	0.3	0.25	0.3	0.034	1	6.058	0.0355	5.3075
83	T1	0.0688	1.969	0.0158	0.230	55.528	0.3	0.25	0.3	0.034	1	6.058	0.0459	4.6656
84	T1	0.0791	1.969	0.0198	0.250	53.884	0.3	0.25	0.3	0.034	1	6.058	0.0528	4.3523
85	T1	0.0537	2.626	0.0131	0.244	59.605	0.3	0.25	0.3	0.034	1	10.769	0.0351	5.3353
86	T1	0.0703	2.626	0.019	0.271	57.168	0.3	0.25	0.3	0.034	1	10.769	0.046	4.6612
87	T1	0.0815	2.626	0.0237	0.290	55.734	0.3	0.25	0.3	0.034	1	10.769	0.0534	4.3289
88	T1	0.0438	1.004	0.0047	0.107	39.620	0.3	0.23	0.3	0.034	1	1.574	0.0344	5.3882
89	T1	0.0552	1.045	0.0052	0.095	38.329	0.3	0.23	0.3	0.034	1	1.706	0.0428	4.8329
90	T1	0.0633	1.045	0.0058	0.091	37.439	0.3	0.23	0.3	0.034	1	1.706	0.0491	4.5127
91	T1	0.0519	1.552	0.0075	0.145	52.944	0.3	0.23	0.3	0.034	1	3.760	0.0369	5.2057
92	T1	0.0661	1.552	0.009	0.136	52.132	0.3	0.23	0.3	0.034	1	3.760	0.047	4.6139
93	T1	0.0769	1.552	0.0111	0.144	51.291	0.3	0.23	0.3	0.034	1	3.760	0.0547	4.2772
94	T1	0.0554	2.008	0.0094	0.170	60.591	0.3	0.23	0.3	0.034	1	6.297	0.0384	5.1045
95	T1	0.0718	2.008	0.0129	0.179	58.293	0.3	0.23	0.3	0.034	1	6.297	0.0497	4.4855
96	T1	0.0834	2.008	0.0162	0.194	56.326	0.3	0.23	0.3	0.034	1	6.297	0.0577	4.1629
97	T1	0.0555	2.626	0.0111	0.199	61.429	0.3	0.23	0.3	0.034	1	10.769	0.0378	5.1444
98	T1	0.0723	2.626	0.015	0.208	58.857	0.3	0.23	0.3	0.034	1	10.769	0.0493	4.505
99	T1	0.0841	2.438	0.0188	0.224	57.166	0.3	0.23	0.3	0.034	1	9.286	0.0575	4.1707
100	T2	0.0461	0.985	0.0349	0.759	9.534	0.6	0.43	0.3	0.034	1	1.514	0.0314	5.6455
101	T2	0.0689	1.067	0.0487	0.708	10.423	0.6	0.43	0.3	0.034	1	1.777	0.0445	4.7382
102	T2	0.0862	1.067	0.0578	0.670	13.256	0.6	0.43	0.3	0.034	1	1.777	0.0558	4.2344
103	T2	0.099	1.164	0.0645	0.652	14.210	0.6	0.43	0.3	0.034	1	2.115	0.061	4.0472
104	T2	0.1094	1.164	0.0717	0.656	13.509	0.6	0.43	0.3	0.034	1	2.115	0.0675	3.8503
105	T2	0.1171	1.219	0.0768	0.656	14.377	0.6	0.43	0.3	0.034	1	2.321	0.0706	3.7625
106	T2	0.1242	1.164	0.0784	0.631	15.075	0.6	0.43	0.3	0.034	1	2.115	0.0766	3.6123
107	T2	0.0471	1.484	0.0363	0.770	13.055	0.6	0.43	0.3	0.034	1	3.440	0.0264	6.1526
108	T2	0.0723	1.484	0.0542	0.750	12.671	0.6	0.43	0.3	0.034	1	3.440	0.0405	4.9686
109	T2	0.0925	1.484	0.0666	0.720	12.935	0.6	0.43	0.3	0.034	1	3.440	0.0519	4.391
110	T2	0.1143	1.484	0.0786	0.687	14.450	0.6	0.43	0.3	0.034	1	3.440	0.0641	3.9507
111	T2	0.1356	1.484	0.0892	0.658	15.150	0.6	0.43	0.3	0.034	1	3.440	0.076	3.6267
112	T2	0.1559	1.484	0.0979	0.628	17.795	0.6	0.43	0.3	0.034	1	3.440	0.0874	3.3822
113	T2	0.05	1.969	0.0396	0.793	20.544	0.6	0.43	0.3	0.034	1	6.058	0.0263	6.1686
114	T2	0.075	1.969	0.0592	0.790	19.711	0.6	0.43	0.3	0.034	1	6.058	0.0394	5.0369
115	T2	0.0988	1.969	0.0751	0.760	19.580	0.6	0.43	0.3	0.034	1	6.058	0.052	4.3867
116	T2	0.1221	1.969	0.089	0.729	19.876	0.6	0.43	0.3	0.034	1	6.058	0.0642	3.9457
117	T2	0.1457	1.969	0.1005	0.690	20.984	0.6	0.43	0.3	0.034	1	6.058	0.0766	3.6128
118	T2	0.0511	2.438	0.041	0.803	27.026	0.6	0.43	0.3	0.034	1	9.286	0.0261	6.1841
119	T2	0.0774	2.438	0.0616	0.796	26.773	0.6	0.43	0.3	0.034	1	9.286	0.0396	5.0261
120	T2	0.102	2.438	0.0787	0.771	27.167	0.6	0.43	0.3	0.034	1	9.286	0.0522	4.3783
121	T2	0.1282	2.438	0.095	0.741	27.659	0.6	0.43	0.3	0.034	1	9.286	0.0656	3.905
122	T2	0.0445	0.985	0.0301	0.675	10.164	0.6	0.38	0.3	0.034	1	1.514	0.031	5.682
123	T2	0.0655	1.045	0.0378	0.577	9.935	0.6	0.38	0.3	0.034	1	1.706	0.044	4.767
124	T2	0.083	1.067	0.0439	0.529	10.753	0.6	0.38	0.3	0.034	1	1.777	0.0552	4.2568
125	T2	0.0968	1.164	0.0489	0.505	12.813	0.6	0.38	0.3	0.034	1	2.115	0.0617	4.0262
126	T2	0.0477	1.484	0.0329	0.690	15.949	0.6	0.38	0.3	0.034	1	3.440	0.0279	5.9838
127	T2	0.072	1.484	0.0445	0.619	16.765	0.6	0.38	0.3	0.034	1	3.440	0.0422	4.8697
128	T2	0.0927	1.484	0.0537	0.580	16.261	0.6	0.38	0.3	0.034	1	3.440	0.0543	4.291
129	T2	0.1144	1.484	0.0613	0.536	19.462	0.6	0.38	0.3	0.034	1	3.440	0.067	3.8621
130	T2	0.0502	1.969	0.0357	0.711	19.652	0.6	0.38	0.3	0.034	1	6.058	0.0278	5.9935
131	T2	0.0758	1.969	0.0501	0.661	20.518	0.6	0.38	0.3	0.034	1	6.058	0.042	4.878
132	T2	0.101	1.969	0.0626	0.619	22.559	0.6	0.38	0.3	0.034	1	6.058	0.056	4.2258
133	T2	0.1257	1.969	0.0726	0.578	24.459	0.6	0.38	0.3	0.034	1	6.058	0.0697	3.7889
134	T2	0.0524	2.498	0.0371	0.709	27.192	0.6	0.38	0.3	0.034	1	9.744	0.0283	5.9447
135	T2	0.0792	2.498	0.0529	0.669	30.304	0.6	0.38	0.3	0.034	1	9.744	0.0427	4.8371
136	T2	0.1051	2.498	0.0662	0.630	32.987	0.6	0.38	0.3	0.034	1	9.744	0.0567	4.1985
137	T2	0.0428	0.985	0.0181	0.423	9.684	0.6	0.33	0.3	0.034	1	1.514	0.0307	5.71
138	T2	0.0636	1.045	0.0234	0.368	9.505	0.6	0.33	0.3	0.034	1	1.706	0.0442	4.7539
139	T2	0.082	1.067	0.0285	0.348	11.081	0.6	0.33	0.3	0.034	1	1.777	0.0565	4.2066
140	T2	0.0963	1.164	0.033	0.343	11.574	0.6	0.33	0.3	0.034	1	2.115	0.064	3.9536
141	T2	0.0473	1.484	0.021	0.445	21.537	0.6	0.33	0.3	0.034	1	3.440	0.0292	5.8473
142	T2	0.0719	1.484	0.0302	0.420	22.766	0.6	0.33	0.3	0.034	1	3.440	0.0444	4.7454
143	T2	0.0922	1.484	0.0378	0.410	26.555	0.6	0.33	0.3	0.034	1	3.440	0.057	4.1898
144	T2	0.0518	1.969	0.026	0.502	27.284	0.6	0.33	0.3	0.034	1	6.058	0.0305	5.7253

Table F.1. Conditions for Transmission Tests (cont'd)

Test #	Test Series	H <sub>i</sub> (m)	T <sub>pl</sub> (s)	H <sub>1</sub> (m)	K <sub>1</sub>	K <sub>2</sub> (%)	B (m)	h (m)	h <sub>a</sub> (m)	D <sub>50</sub> (m)	Cotα	L <sub>o</sub> (m)	s <sub>op</sub>	ξ
145	T2	0.0778	1.932	0.0374	0.482	30.630	0.6	0.33	0.3	0.034	1	5.831	0.0459	4.6662
146	T2	0.1032	1.932	0.0488	0.472	32.441	0.6	0.33	0.3	0.034	1	5.831	0.061	4.0495
147	T2	0.0535	2.498	0.0273	0.509	32.641	0.6	0.33	0.3	0.034	1	9.744	0.0308	5.6943
148	T2	0.081	2.498	0.0407	0.502	36.008	0.6	0.33	0.3	0.034	1	9.744	0.0467	4.6278
149	T2	0.107	2.498	0.0528	0.493	38.838	0.6	0.33	0.3	0.034	1	9.744	0.0617	4.0267
150	T2	0.0417	1.004	0.0035	0.085	14.268	0.6	0.3	0.3	0.034	1	1.574	0.0303	5.7451
151	T2	0.0631	1.045	0.0088	0.139	15.045	0.6	0.3	0.3	0.034	1	1.706	0.0451	4.7114
152	T2	0.0826	1.067	0.0148	0.179	17.181	0.6	0.3	0.3	0.034	1	1.777	0.0585	4.1342
153	T2	0.0478	1.528	0.0088	0.184	30.236	0.6	0.3	0.3	0.034	1	3.649	0.0305	5.7259
154	T2	0.0731	1.528	0.0178	0.244	31.518	0.6	0.3	0.3	0.034	1	3.649	0.0466	4.6326
155	T2	0.094	1.552	0.0266	0.283	33.851	0.6	0.3	0.3	0.034	1	3.760	0.0598	4.0903
156	T2	0.0521	1.969	0.0142	0.273	41.340	0.6	0.3	0.3	0.034	1	6.058	0.032	5.5863
157	T2	0.0785	1.932	0.0263	0.336	40.854	0.6	0.3	0.3	0.034	1	5.831	0.0484	4.5474
158	T2	0.1046	1.932	0.0369	0.353	40.945	0.6	0.3	0.3	0.034	1	5.831	0.0644	3.9392
159	T2	0.0537	2.56	0.0166	0.309	45.260	0.6	0.3	0.3	0.034	1	10.237	0.0323	5.5658
160	T2	0.0809	2.56	0.0292	0.361	45.851	0.6	0.3	0.3	0.034	1	10.237	0.0487	4.5333
161	T2	0.0443	0.985	0.0015	0.034	28.322	0.6	0.27	0.3	0.034	1	1.514	0.0335	5.4663
162	T2	0.0564	1.045	0.002	0.036	26.341	0.6	0.27	0.3	0.034	1	1.706	0.0415	4.9077
163	T2	0.065	1.067	0.0027	0.041	24.755	0.6	0.27	0.3	0.034	1	1.777	0.0475	4.589
164	T2	0.0842	1.067	0.0044	0.052	25.009	0.6	0.27	0.3	0.034	1	1.777	0.0615	4.0308
165	T2	0.0509	1.484	0.0046	0.090	43.332	0.6	0.27	0.3	0.034	1	3.440	0.0341	5.4163
166	T2	0.0669	1.484	0.0059	0.088	42.640	0.6	0.27	0.3	0.034	1	3.440	0.0448	4.727
167	T2	0.0777	1.484	0.0075	0.097	42.877	0.6	0.27	0.3	0.034	1	3.440	0.052	4.3851
168	T2	0.1028	1.484	0.013	0.126	41.230	0.6	0.27	0.3	0.034	1	3.440	0.0688	3.8124
169	T2	0.0549	1.969	0.0071	0.130	53.885	0.6	0.27	0.3	0.034	1	6.058	0.0354	5.3145
170	T2	0.072	1.969	0.0099	0.137	51.495	0.6	0.27	0.3	0.034	1	6.058	0.0464	4.6428
171	T2	0.083	1.969	0.0127	0.153	50.051	0.6	0.27	0.3	0.034	1	6.058	0.0535	4.3231
172	T2	0.0562	2.381	0.009	0.160	56.949	0.6	0.27	0.3	0.034	1	8.859	0.0356	5.2964
173	T2	0.0738	2.381	0.0125	0.169	54.764	0.6	0.27	0.3	0.034	1	8.859	0.0468	4.6206
174	T2	0.0852	2.381	0.016	0.188	53.735	0.6	0.27	0.3	0.034	1	8.859	0.0541	4.2995
175	T2	0.0462	0.985	0.0023	0.050	33.477	0.6	0.25	0.3	0.034	1	1.514	0.0357	5.2948
176	T2	0.0585	1.045	0.0027	0.047	31.247	0.6	0.25	0.3	0.034	1	1.706	0.0441	4.7607
177	T2	0.0672	1.067	0.0031	0.047	30.831	0.6	0.25	0.3	0.034	1	1.777	0.0503	4.4566
178	T2	0.086	1.067	0.0042	0.049	29.162	0.6	0.25	0.3	0.034	1	1.777	0.0645	3.9386
179	T2	0.0527	1.484	0.0049	0.093	47.628	0.6	0.25	0.3	0.034	1	3.440	0.0364	5.2409
180	T2	0.0679	1.484	0.0056	0.083	47.580	0.6	0.25	0.3	0.034	1	3.440	0.0469	4.6153
181	T2	0.0777	1.484	0.0062	0.079	47.371	0.6	0.25	0.3	0.034	1	3.440	0.0537	4.3145
182	T2	0.0563	1.969	0.0063	0.113	56.869	0.6	0.25	0.3	0.034	1	6.058	0.0375	5.1609
183	T2	0.0729	1.969	0.0075	0.103	54.849	0.6	0.25	0.3	0.034	1	6.058	0.0487	4.5337
184	T2	0.0839	1.969	0.0083	0.099	53.562	0.6	0.25	0.3	0.034	1	6.058	0.056	4.2254
185	T2	0.0558	2.381	0.0075	0.134	59.805	0.6	0.25	0.3	0.034	1	8.859	0.0367	5.2208
186	T2	0.0729	2.381	0.0089	0.122	57.908	0.6	0.25	0.3	0.034	1	8.859	0.0479	4.5668
187	T2	0.0849	2.381	0.0105	0.123	56.920	0.6	0.25	0.3	0.034	1	8.859	0.0559	4.2296
188	T2	0.0452	0.985	0.002	0.044	35.695	0.6	0.23	0.3	0.034	1	1.514	0.0358	5.2852
189	T2	0.0571	1.045	0.0023	0.040	34.494	0.6	0.23	0.3	0.034	1	1.706	0.0443	4.7517
190	T2	0.0652	1.067	0.0025	0.038	33.150	0.6	0.23	0.3	0.034	1	1.777	0.0503	4.4602
191	T2	0.0537	1.484	0.0042	0.078	51.079	0.6	0.23	0.3	0.034	1	3.440	0.0384	5.1031
192	T2	0.0688	1.484	0.0047	0.069	50.790	0.6	0.23	0.3	0.034	1	3.440	0.0492	4.5079
193	T2	0.0793	1.484	0.0051	0.064	49.983	0.6	0.23	0.3	0.034	1	3.440	0.0568	4.1977
194	T2	0.0572	2.008	0.0055	0.096	59.300	0.6	0.23	0.3	0.034	1	6.297	0.0396	5.0235
195	T2	0.074	2.008	0.0063	0.086	57.929	0.6	0.23	0.3	0.034	1	6.297	0.0512	4.4197
196	T2	0.0857	2.008	0.0071	0.082	56.403	0.6	0.23	0.3	0.034	1	6.297	0.0593	4.1059
197	T2	0.0577	2.438	0.0067	0.117	60.989	0.6	0.23	0.3	0.034	1	9.286	0.0394	5.0368
198	T2	0.0751	2.626	0.0078	0.104	59.315	0.6	0.23	0.3	0.034	1	10.769	0.0511	4.4217
199	T2	0.0871	2.626	0.0087	0.100	58.126	0.6	0.23	0.3	0.034	1	10.769	0.0593	4.1056
200	T3	0.0469	1.045	0.0338	0.721	7.680	0.9	0.43	0.3	0.034	1	1.706	0.0307	5.7064
201	T3	0.069	1.067	0.0469	0.680	8.294	0.9	0.43	0.3	0.034	1	1.777	0.0446	4.7343
202	T3	0.086	1.067	0.0552	0.642	10.842	0.9	0.43	0.3	0.034	1	1.777	0.0556	4.2407
203	T3	0.0994	1.164	0.0624	0.628	11.833	0.9	0.43	0.3	0.034	1	2.115	0.0613	4.0392
204	T3	0.111	1.164	0.0701	0.631	11.414	0.9	0.43	0.3	0.034	1	2.115	0.0685	3.8216
205	T3	0.1188	1.191	0.074	0.623	12.976	0.9	0.43	0.3	0.034	1	2.215	0.0724	3.7154
206	T3	0.125	1.164	0.0749	0.599	13.513	0.9	0.43	0.3	0.034	1	2.115	0.0771	3.6018
207	T3	0.0489	1.484	0.0357	0.730	15.323	0.9	0.43	0.3	0.034	1	3.440	0.0274	6.0393
208	T3	0.0738	1.484	0.0529	0.717	16.056	0.9	0.43	0.3	0.034	1	3.440	0.0414	4.9155
209	T3	0.0952	1.484	0.0655	0.688	15.377	0.9	0.43	0.3	0.034	1	3.440	0.0534	4.3277
210	T3	0.1174	1.484	0.076	0.647	15.845	0.9	0.43	0.3	0.034	1	3.440	0.0658	3.8984
211	T3	0.1383	1.484	0.0861	0.622	17.053	0.9	0.43	0.3	0.034	1	3.440	0.0775	3.5913
212	T3	0.1592	1.484	0.0941	0.591	17.898	0.9	0.43	0.3	0.034	1	3.440	0.0892	3.3477
213	T3	0.0515	1.969	0.0389	0.756	12.157	0.9	0.43	0.3	0.034	1	6.058	0.0271	6.0787
214	T3	0.0764	1.969	0.0581	0.760	12.062	0.9	0.43	0.3	0.034	1	6.058	0.0402	4.9882
215	T3	0.1001	1.969	0.0731	0.730	12.299	0.9	0.43	0.3	0.034	1	6.058	0.0526	4.3583
216	T3	0.1241	1.969	0.0859	0.692	13.393	0.9	0.43	0.3	0.034	1	6.058	0.0653	3.9146

Table F.1. Conditions for Transmission Tests (cont'd)

Test #	Test Series	H <sub>i</sub> (m)	T <sub>pl</sub> (s)	H <sub>t</sub> (m)	K <sub>i</sub>	K <sub>c</sub> (%)	B (m)	h (m)	h <sub>s</sub> (m)	D <sub>50</sub> (m)	Cota	L <sub>o</sub> (m)	s <sub>op</sub>	ξ
217	T3	0.1477	1.969	0.0966	0.654	15.251	0.9	0.43	0.3	0.034	1	6.058	0.0777	3.5881
218	T3	0.0521	2.438	0.0407	0.781	17.560	0.9	0.43	0.3	0.034	1	9.286	0.0266	6.1258
219	T3	0.0779	2.438	0.0613	0.786	17.983	0.9	0.43	0.3	0.034	1	9.286	0.0399	5.0077
220	T3	0.1027	2.438	0.0773	0.752	20.070	0.9	0.43	0.3	0.034	1	9.286	0.0525	4.3624
221	T3	0.1301	2.438	0.0894	0.687	21.716	0.9	0.43	0.3	0.034	1	9.286	0.0666	3.8757
222	T3	0.0451	0.985	0.0283	0.627	8.739	0.9	0.38	0.3	0.034	1	1.514	0.0314	5.6431
223	T3	0.0655	1.045	0.0356	0.544	8.371	0.9	0.38	0.3	0.034	1	1.706	0.044	4.766
224	T3	0.0834	1.067	0.0427	0.512	10.471	0.9	0.38	0.3	0.034	1	1.777	0.0554	4.2472
225	T3	0.0977	1.164	0.0476	0.487	10.264	0.9	0.38	0.3	0.034	1	2.115	0.0623	4.0062
226	T3	0.0482	1.484	0.0313	0.649	19.191	0.9	0.38	0.3	0.034	1	3.440	0.0283	5.9492
227	T3	0.0731	1.484	0.0435	0.595	19.144	0.9	0.38	0.3	0.034	1	3.440	0.0428	4.8314
228	T3	0.0943	1.484	0.0516	0.548	18.626	0.9	0.38	0.3	0.034	1	3.440	0.0552	4.2549
229	T3	0.116	1.484	0.0583	0.502	21.293	0.9	0.38	0.3	0.034	1	3.440	0.068	3.8356
230	T3	0.0511	1.969	0.0346	0.678	16.113	0.9	0.38	0.3	0.034	1	6.058	0.0283	5.9444
231	T3	0.0766	1.969	0.0479	0.626	16.568	0.9	0.38	0.3	0.034	1	6.058	0.0425	4.8533
232	T3	0.1016	1.969	0.059	0.581	18.359	0.9	0.38	0.3	0.034	1	6.058	0.0563	4.215
233	T3	0.1261	1.969	0.068	0.539	21.010	0.9	0.38	0.3	0.034	1	6.058	0.0699	3.7831
234	T3	0.0539	2.438	0.036	0.669	19.154	0.9	0.38	0.3	0.034	1	9.286	0.0291	5.8579
235	T3	0.081	2.438	0.0509	0.628	21.829	0.9	0.38	0.3	0.034	1	9.286	0.0438	4.778
236	T3	0.1063	2.438	0.0626	0.588	24.562	0.9	0.38	0.3	0.034	1	9.286	0.0575	4.1691
237	T3	0.0429	0.985	0.0156	0.363	10.079	0.9	0.33	0.3	0.034	1	1.514	0.0307	5.704
238	T3	0.0637	1.045	0.0203	0.318	9.914	0.9	0.33	0.3	0.034	1	1.706	0.0443	4.7513
239	T3	0.0821	1.067	0.0252	0.307	11.598	0.9	0.33	0.3	0.034	1	1.777	0.0566	4.2034
240	T3	0.0959	1.164	0.0287	0.300	12.333	0.9	0.33	0.3	0.034	1	2.115	0.0637	3.961
241	T3	0.0476	1.484	0.0184	0.387	22.012	0.9	0.33	0.3	0.034	1	3.440	0.0294	5.8323
242	T3	0.072	1.484	0.0266	0.369	23.933	0.9	0.33	0.3	0.034	1	3.440	0.0445	4.7392
243	T3	0.0922	1.484	0.0336	0.365	27.273	0.9	0.33	0.3	0.034	1	3.440	0.057	4.1898
244	T3	0.0514	2.008	0.022	0.427	29.006	0.9	0.33	0.3	0.034	1	6.297	0.0302	5.7531
245	T3	0.0772	1.932	0.032	0.415	31.619	0.9	0.33	0.3	0.034	1	5.831	0.0456	4.6823
246	T3	0.1028	1.932	0.0421	0.410	32.999	0.9	0.33	0.3	0.034	1	5.831	0.0607	4.0592
247	T3	0.0528	2.498	0.0237	0.449	30.570	0.9	0.33	0.3	0.034	1	9.744	0.0304	5.7321
248	T3	0.0799	2.498	0.0349	0.436	34.104	0.9	0.33	0.3	0.034	1	9.744	0.0461	4.6591
249	T3	0.1058	2.498	0.0464	0.439	36.963	0.9	0.33	0.3	0.034	1	9.744	0.0609	4.0509
250	T3	0.042	0.985	0.0017	0.040	16.896	0.9	0.3	0.3	0.034	1	1.514	0.0308	5.6972
251	T3	0.0632	1.045	0.0051	0.080	16.039	0.9	0.3	0.3	0.034	1	1.706	0.0451	4.7064
252	T3	0.0825	1.067	0.0099	0.121	17.815	0.9	0.3	0.3	0.034	1	1.777	0.0584	4.1379
253	T3	0.0469	1.463	0.0046	0.098	30.030	0.9	0.3	0.3	0.034	1	3.343	0.0302	5.7566
254	T3	0.0734	1.484	0.0115	0.157	33.247	0.9	0.3	0.3	0.034	1	3.440	0.0471	4.6071
255	T3	0.0526	1.969	0.0089	0.169	42.015	0.9	0.3	0.3	0.034	1	6.058	0.0324	5.559
256	T3	0.0792	1.969	0.0184	0.232	40.681	0.9	0.3	0.3	0.034	1	6.058	0.0487	4.5315
257	T3	0.0535	2.56	0.0113	0.212	45.395	0.9	0.3	0.3	0.034	1	10.237	0.0322	5.5765
258	T3	0.1076	2.56	0.0312	0.290	45.079	0.9	0.3	0.3	0.034	1	10.237	0.0647	3.9309
259	T3	0.0446	0.985	0.0012	0.028	29.974	0.9	0.27	0.3	0.034	1	1.514	0.0337	5.4482
260	T3	0.0566	1.045	0.0017	0.030	27.426	0.9	0.27	0.3	0.034	1	1.706	0.0417	4.8981
261	T3	0.0652	1.067	0.0022	0.034	25.602	0.9	0.27	0.3	0.034	1	1.777	0.0476	4.5814
262	T3	0.0507	1.484	0.0035	0.070	43.143	0.9	0.27	0.3	0.034	1	3.440	0.034	5.4272
263	T3	0.0665	1.484	0.0044	0.066	42.305	0.9	0.27	0.3	0.034	1	3.440	0.0445	4.7392
264	T3	0.0775	1.484	0.0053	0.068	42.170	0.9	0.27	0.3	0.034	1	3.440	0.0519	4.389
265	T3	0.0547	1.969	0.0054	0.099	52.460	0.9	0.27	0.3	0.034	1	6.058	0.0352	5.3268
266	T3	0.0714	1.969	0.007	0.099	50.009	0.9	0.27	0.3	0.034	1	6.058	0.046	4.6605
267	T3	0.0824	1.969	0.0082	0.099	48.700	0.9	0.27	0.3	0.034	1	6.058	0.0531	4.3394
268	T3	0.0558	2.381	0.0064	0.115	55.017	0.9	0.27	0.3	0.034	1	8.859	0.0354	5.3157
269	T3	0.0735	2.381	0.0087	0.118	52.819	0.9	0.27	0.3	0.034	1	8.859	0.0467	4.629
270	T3	0.0854	2.381	0.011	0.129	51.861	0.9	0.27	0.3	0.034	1	8.859	0.0542	4.2955
271	T3	0.0465	0.985	0.0016	0.034	33.801	0.9	0.25	0.3	0.034	1	1.514	0.0359	5.2798
272	T3	0.0591	1.045	0.0019	0.033	31.536	0.9	0.25	0.3	0.034	1	1.706	0.0446	4.7331
273	T3	0.0673	1.045	0.0022	0.032	31.417	0.9	0.25	0.3	0.034	1	1.706	0.0508	4.4378
274	T3	0.0452	1.056	0.0016	0.036	34.594	0.9	0.25	0.3	0.034	1	1.741	0.034	5.4267
275	T3	0.0669	1.528	0.004	0.060	47.014	0.9	0.25	0.3	0.034	1	3.649	0.046	4.6633
276	T3	0.0771	1.528	0.0043	0.055	47.567	0.9	0.25	0.3	0.034	1	3.649	0.053	4.343
277	T3	0.0558	1.969	0.0053	0.096	56.502	0.9	0.25	0.3	0.034	1	6.058	0.0372	5.1818
278	T3	0.0725	1.969	0.0056	0.077	54.545	0.9	0.25	0.3	0.034	1	6.058	0.0484	4.5476
279	T3	0.0833	1.969	0.0061	0.074	53.152	0.9	0.25	0.3	0.034	1	6.058	0.0556	4.2403
280	T3	0.057	2.626	0.0053	0.093	59.209	0.9	0.25	0.3	0.034	1	10.769	0.0373	5.178
281	T3	0.0743	2.626	0.0062	0.083	57.332	0.9	0.25	0.3	0.034	1	10.769	0.0486	4.5355
282	T3	0.0863	2.626	0.0074	0.085	56.325	0.9	0.25	0.3	0.034	1	10.769	0.0565	4.2063
283	T3	0.0453	0.985	0.0011	0.023	34.988	0.9	0.23	0.3	0.034	1	1.514	0.0359	5.2805
284	T3	0.0573	1.045	0.0011	0.020	33.885	0.9	0.23	0.3	0.034	1	1.706	0.0445	4.742
285	T3	0.0656	1.067	0.0014	0.022	32.659	0.9	0.23	0.3	0.034	1	1.777	0.0505	4.4483
286	T3	0.0527	1.484	0.0028	0.053	50.960	0.9	0.23	0.3	0.034	1	3.440	0.0377	5.147
287	T3	0.0686	1.484	0.0029	0.043	50.718	0.9	0.23	0.3	0.034	1	3.440	0.0491	4.5131
288	T3	0.08	1.484	0.0032	0.040	50.309	0.9	0.23	0.3	0.034	1	3.440	0.0572	4.1801



Table F.1. Conditions for Transmission Tests (cont'd)

Test #	Test Series	H <sub>i</sub> (m)	T <sub>pi</sub> (s)	H <sub>r</sub> (m)	K <sub>i</sub>	K <sub>r</sub> (%)	B (m)	h (m)	h <sub>s</sub> (m)	D <sub>50</sub> (m)	Cota	L <sub>o</sub> (m)	s <sub>op</sub>	ξ
289	T3	0.0574	2.008	0.0039	0.067	58.146	0.9	0.23	0.3	0.034	1	6.297	0.0398	5.0156
290	T3	0.0747	2.008	0.0042	0.057	56.568	0.9	0.23	0.3	0.034	1	6.297	0.0517	4.398
291	T3	0.0866	2.008	0.0049	0.056	55.157	0.9	0.23	0.3	0.034	1	6.297	0.0599	4.0853
292	T3	0.0579	2.438	0.0044	0.075	59.393	0.9	0.23	0.3	0.034	1	9.286	0.0396	5.0266
293	T3	0.0756	2.438	0.0049	0.065	57.728	0.9	0.23	0.3	0.034	1	9.286	0.0517	4.3976
294	T3	0.0878	2.438	0.0053	0.060	56.434	0.9	0.23	0.3	0.034	1	9.286	0.06	4.0825
295	T4	0.0464	0.985	0.0301	0.650	7.994	1.2	0.43	0.3	0.034	1	1.514	0.0316	5.6273
296	T4	0.068	1.067	0.0404	0.593	8.081	1.2	0.43	0.3	0.034	1	1.777	0.044	4.7669
297	T4	0.0848	1.067	0.0474	0.559	11.086	1.2	0.43	0.3	0.034	1	1.777	0.0549	4.2694
298	T4	0.098	1.164	0.0539	0.549	11.095	1.2	0.43	0.3	0.034	1	2.115	0.0605	4.0666
299	T4	0.1088	1.164	0.0598	0.549	10.959	1.2	0.43	0.3	0.034	1	2.115	0.0671	3.86
300	T4	0.1173	1.249	0.0631	0.538	11.710	1.2	0.43	0.3	0.034	1	2.436	0.07	3.779
301	T4	0.124	1.249	0.0642	0.518	13.834	1.2	0.43	0.3	0.034	1	2.436	0.074	3.676
302	T4	0.0475	1.484	0.0317	0.668	16.999	1.2	0.43	0.3	0.034	1	3.440	0.0266	6.1288
303	T4	0.0723	1.484	0.0466	0.645	17.472	1.2	0.43	0.3	0.034	1	3.440	0.0405	4.9673
304	T4	0.0932	1.484	0.0579	0.622	17.122	1.2	0.43	0.3	0.034	1	3.440	0.0522	4.3751
305	T4	0.0504	1.969	0.0343	0.681	17.358	1.2	0.43	0.3	0.034	1	6.058	0.0265	6.1409
306	T4	0.0751	1.969	0.0518	0.689	16.914	1.2	0.43	0.3	0.034	1	6.058	0.0395	5.0304
307	T4	0.0988	1.969	0.0645	0.654	16.840	1.2	0.43	0.3	0.034	1	6.058	0.0519	4.3881
308	T4	0.1216	1.969	0.0747	0.614	16.834	1.2	0.43	0.3	0.034	1	6.058	0.0639	3.9546
309	T4	0.1441	1.969	0.0836	0.580	17.531	1.2	0.43	0.3	0.034	1	6.058	0.0758	3.6326
310	T4	0.0512	2.438	0.0361	0.706	14.999	1.2	0.43	0.3	0.034	1	9.286	0.0262	6.1778
311	T4	0.0768	2.438	0.0533	0.694	16.459	1.2	0.43	0.3	0.034	1	9.286	0.0393	5.0435
312	T4	0.1021	2.438	0.0663	0.649	17.788	1.2	0.43	0.3	0.034	1	9.286	0.0522	4.375
313	T4	0.0451	0.985	0.0238	0.528	9.756	1.2	0.38	0.3	0.034	1	1.514	0.0314	5.6441
314	T4	0.0653	1.045	0.0307	0.470	9.461	1.2	0.38	0.3	0.034	1	1.706	0.0439	4.7742
315	T4	0.0821	1.067	0.036	0.439	10.935	1.2	0.38	0.3	0.034	1	1.777	0.0546	4.2808
316	T4	0.0446	1.422	0.0259	0.581	18.254	1.2	0.38	0.3	0.034	1	3.160	0.0264	6.1527
317	T4	0.0683	1.528	0.0371	0.543	18.616	1.2	0.38	0.3	0.034	1	3.649	0.0397	5.0172
318	T4	0.088	1.484	0.0446	0.507	19.353	1.2	0.38	0.3	0.034	1	3.440	0.0516	4.404
319	T4	0.0478	1.969	0.0299	0.625	22.767	1.2	0.38	0.3	0.034	1	6.058	0.0265	6.1448
320	T4	0.0718	1.969	0.0413	0.576	22.736	1.2	0.38	0.3	0.034	1	6.058	0.0398	5.014
321	T4	0.0949	1.969	0.0507	0.535	23.417	1.2	0.38	0.3	0.034	1	6.058	0.0526	4.3608
322	T4	0.0491	2.438	0.0312	0.635	20.186	1.2	0.38	0.3	0.034	1	9.286	0.0266	6.1348
323	T4	0.0737	2.438	0.0445	0.603	23.674	1.2	0.38	0.3	0.034	1	9.286	0.0399	5.0078
324	T4	0.0971	2.438	0.0545	0.561	26.023	1.2	0.38	0.3	0.034	1	9.286	0.0525	4.3633
325	T4	0.0409	0.985	0.0122	0.299	12.203	1.2	0.33	0.3	0.034	1	1.514	0.0293	5.8424
326	T4	0.0607	1.045	0.0167	0.275	11.776	1.2	0.33	0.3	0.034	1	1.706	0.0422	4.8673
327	T4	0.0778	1.067	0.0206	0.265	13.600	1.2	0.33	0.3	0.034	1	1.777	0.0536	4.319
328	T4	0.0913	1.164	0.0243	0.266	13.506	1.2	0.33	0.3	0.034	1	2.115	0.0606	4.0608
329	T4	0.045	1.484	0.0152	0.338	23.906	1.2	0.33	0.3	0.034	1	3.440	0.0278	5.9946
330	T4	0.0683	1.484	0.0224	0.328	25.944	1.2	0.33	0.3	0.034	1	3.440	0.0422	4.8658
331	T4	0.0872	1.484	0.0283	0.324	28.864	1.2	0.33	0.3	0.034	1	3.440	0.0539	4.3075
332	T4	0.0489	2.008	0.018	0.368	31.080	1.2	0.33	0.3	0.034	1	6.297	0.0287	5.8999
333	T4	0.0733	1.932	0.0289	0.394	33.298	1.2	0.33	0.3	0.034	1	5.831	0.0433	4.8058
334	T4	0.0973	2.008	0.0366	0.376	35.127	1.2	0.33	0.3	0.034	1	6.297	0.0572	4.1811
335	T4	0.0504	2.498	0.0197	0.391	33.639	1.2	0.33	0.3	0.034	1	9.744	0.029	5.8672
336	T4	0.0764	2.498	0.0305	0.400	36.716	1.2	0.33	0.3	0.034	1	9.744	0.044	4.7676
337	T4	0.1008	2.498	0.0418	0.414	38.821	1.2	0.33	0.3	0.034	1	9.744	0.0581	4.1494
338	T4	0.0399	0.985	0.0012	0.030	17.344	1.2	0.3	0.3	0.034	1	1.514	0.0293	5.8434
339	T4	0.0601	1.045	0.0035	0.058	17.473	1.2	0.3	0.3	0.034	1	1.706	0.0429	4.8275
340	T4	0.0782	1.067	0.0073	0.093	18.299	1.2	0.3	0.3	0.034	1	1.777	0.0554	4.2494
341	T4	0.0457	1.484	0.0033	0.073	33.143	1.2	0.3	0.3	0.034	1	3.440	0.0293	5.8388
342	T4	0.07	1.484	0.0087	0.125	34.435	1.2	0.3	0.3	0.034	1	3.440	0.0449	4.7206
343	T4	0.05	1.969	0.0065	0.130	42.363	1.2	0.3	0.3	0.034	1	6.058	0.0307	5.7027
344	T4	0.0754	1.969	0.0145	0.192	41.369	1.2	0.3	0.3	0.034	1	6.058	0.0463	4.6462
345	T4	0.0507	2.56	0.0082	0.162	45.711	1.2	0.3	0.3	0.034	1	10.237	0.0305	5.7265
346	T4	0.0771	2.56	0.0177	0.230	45.924	1.2	0.3	0.3	0.034	1	10.237	0.0464	4.6438
347	T4	0.0421	1.045	0.0006	0.015	31.121	1.2	0.27	0.3	0.034	1	1.706	0.031	5.6792
348	T4	0.0535	1.045	0.0008	0.015	28.986	1.2	0.27	0.3	0.034	1	1.706	0.0394	5.0348
349	T4	0.0619	1.067	0.0011	0.017	27.726	1.2	0.27	0.3	0.034	1	1.777	0.0452	4.7016
350	T4	0.0475	1.484	0.0023	0.048	45.202	1.2	0.27	0.3	0.034	1	3.440	0.0318	5.6071
351	T4	0.0621	1.484	0.0025	0.040	44.459	1.2	0.27	0.3	0.034	1	3.440	0.0416	4.9048
352	T4	0.0727	1.484	0.0038	0.052	44.237	1.2	0.27	0.3	0.034	1	3.440	0.0487	4.533
353	T4	0.0516	1.969	0.0032	0.062	53.375	1.2	0.27	0.3	0.034	1	6.058	0.0333	5.4833
354	T4	0.0681	1.969	0.004	0.058	51.240	1.2	0.27	0.3	0.034	1	6.058	0.0439	4.773
355	T4	0.0784	1.969	0.005	0.064	49.867	1.2	0.27	0.3	0.034	1	6.058	0.0505	4.4498
356	T4	0.0532	2.381	0.004	0.075	55.899	1.2	0.27	0.3	0.034	1	8.859	0.0337	5.4439
357	T4	0.0698	2.381	0.0054	0.077	53.807	1.2	0.27	0.3	0.034	1	8.859	0.0443	4.7508
358	T4	0.0808	2.381	0.0074	0.092	52.916	1.2	0.27	0.3	0.034	1	8.859	0.0513	4.4155
359	T4	0.0438	0.985	0.0011	0.024	35.349	1.2	0.25	0.3	0.034	1	1.514	0.0338	5.4384
360	T4	0.0552	1.045	0.0013	0.024	33.327	1.2	0.25	0.3	0.034	1	1.706	0.0417	4.8999

Table F.1. Conditions for Transmission Tests (cont'd)

Test #	Test Series	H <sub>i</sub> (m)	T <sub>pl</sub> (s)	H <sub>t</sub> (m)	K <sub>i</sub>	K <sub>r</sub> (%)	B (m)	h (m)	h <sub>s</sub> (m)	D <sub>50</sub> (m)	Cota	L <sub>c</sub> (m)	s <sub>op</sub>	ξ
361	T4	0.063	1.067	0.0019	0.030	32.277	1.2	0.25	0.3	0.034	1	1.777	0.0472	4.6043
362	T4	0.0493	1.484	0.0026	0.053	49.050	1.2	0.25	0.3	0.034	1	3.440	0.0341	5.4166
363	T4	0.0638	1.484	0.003	0.046	48.662	1.2	0.25	0.3	0.034	1	3.440	0.0441	4.7634
364	T4	0.0723	1.484	0.0036	0.049	48.770	1.2	0.25	0.3	0.034	1	3.440	0.05	4.4732
365	T4	0.0524	1.969	0.0042	0.079	57.112	1.2	0.25	0.3	0.034	1	6.058	0.035	5.3479
366	T4	0.068	1.969	0.0044	0.065	55.254	1.2	0.25	0.3	0.034	1	6.058	0.0454	4.693
367	T4	0.0783	1.969	0.0043	0.055	53.946	1.2	0.25	0.3	0.034	1	6.058	0.0522	4.3759
368	T4	0.0532	2.626	0.0043	0.081	59.112	1.2	0.25	0.3	0.034	1	10.769	0.0348	5.3574
369	T4	0.0695	2.626	0.0048	0.069	57.210	1.2	0.25	0.3	0.034	1	10.769	0.0455	4.69
370	T4	0.0806	2.626	0.0055	0.068	55.883	1.2	0.25	0.3	0.034	1	10.769	0.0528	4.3534
371	T4	0.0426	0.985	4E-05	0.001	36.527	1.2	0.23	0.3	0.034	1	1.514	0.0338	5.4415
372	T4	0.054	1.045	0.0007	0.013	35.502	1.2	0.23	0.3	0.034	1	1.706	0.0419	4.8877
373	T4	0.0618	1.067	0.0012	0.019	33.837	1.2	0.23	0.3	0.034	1	1.777	0.0476	4.5825
374	T4	0.0497	1.484	0.0025	0.051	52.174	1.2	0.23	0.3	0.034	1	3.440	0.0356	5.3017
375	T4	0.0645	1.484	0.002	0.031	51.899	1.2	0.23	0.3	0.034	1	3.440	0.0462	4.6528
376	T4	0.0753	1.484	0.0028	0.037	50.743	1.2	0.23	0.3	0.034	1	3.440	0.0539	4.308
377	T4	0.054	2.008	0.0032	0.060	58.526	1.2	0.23	0.3	0.034	1	6.297	0.0374	5.1723
378	T4	0.0702	2.008	0.0035	0.049	56.965	1.2	0.23	0.3	0.034	1	6.297	0.0486	4.536
379	T4	0.0814	2.008	0.0035	0.044	55.470	1.2	0.23	0.3	0.034	1	6.297	0.0563	4.214
380	T4	0.0545	2.626	0.003	0.055	59.985	1.2	0.23	0.3	0.034	1	10.769	0.0371	5.19
381	T4	0.0713	2.626	0.0037	0.052	58.204	1.2	0.23	0.3	0.034	1	10.769	0.0485	4.539
382	T4	0.0825	2.626	0.0038	0.046	56.860	1.2	0.23	0.3	0.034	1	10.769	0.0562	4.2179
383	T5	0.0419	0.985	0.0266	0.635	9.991	1.5	0.43	0.3	0.034	1	1.514	0.0285	5.9186
384	T5	0.0615	1.045	0.0356	0.579	9.590	1.5	0.43	0.3	0.034	1	1.706	0.0403	4.9829
385	T5	0.0765	1.067	0.0418	0.546	12.443	1.5	0.43	0.3	0.034	1	1.777	0.0495	4.4949
386	T5	0.0886	1.067	0.0474	0.535	13.844	1.5	0.43	0.3	0.034	1	1.777	0.0573	4.1772
387	T5	0.098	1.164	0.0521	0.531	14.257	1.5	0.43	0.3	0.034	1	2.115	0.0605	4.0662
388	T5	0.0421	1.484	0.0276	0.656	15.294	1.5	0.43	0.3	0.034	1	3.440	0.0236	6.5108
389	T5	0.0638	1.484	0.0405	0.635	15.341	1.5	0.43	0.3	0.034	1	3.440	0.0358	5.2865
390	T5	0.0821	1.484	0.0495	0.603	15.562	1.5	0.43	0.3	0.034	1	3.440	0.046	4.6614
391	T5	0.1006	1.484	0.0578	0.574	16.471	1.5	0.43	0.3	0.034	1	3.440	0.0564	4.21
392	T5	0.1191	1.484	0.0638	0.536	17.890	1.5	0.43	0.3	0.034	1	3.440	0.0668	3.8698
393	T5	0.0442	1.969	0.0305	0.689	17.366	1.5	0.43	0.3	0.034	1	6.058	0.0233	6.5556
394	T5	0.0663	1.969	0.0453	0.684	18.071	1.5	0.43	0.3	0.034	1	6.058	0.0349	5.3564
395	T5	0.087	1.969	0.056	0.643	18.119	1.5	0.43	0.3	0.034	1	6.058	0.0458	4.6739
396	T5	0.1074	1.969	0.0638	0.594	18.147	1.5	0.43	0.3	0.034	1	6.058	0.0565	4.2081
397	T5	0.1274	1.969	0.0696	0.546	19.370	1.5	0.43	0.3	0.034	1	6.058	0.067	3.8632
398	T5	0.0475	2.381	0.0324	0.682	20.756	1.5	0.43	0.3	0.034	1	8.859	0.0244	6.4054
399	T5	0.0679	2.381	0.0479	0.705	18.286	1.5	0.43	0.3	0.034	1	8.859	0.0348	5.3591
400	T5	0.0886	2.438	0.0592	0.669	18.640	1.5	0.43	0.3	0.034	1	9.286	0.0453	4.6973
401	T5	0.0408	0.985	0.0205	0.502	11.222	1.5	0.38	0.3	0.034	1	1.514	0.0284	5.9362
402	T5	0.0599	1.045	0.026	0.435	9.964	1.5	0.38	0.3	0.034	1	1.706	0.0402	4.9855
403	T5	0.0751	1.067	0.0308	0.410	10.182	1.5	0.38	0.3	0.034	1	1.777	0.0499	4.4763
404	T5	0.0426	1.484	0.0229	0.538	19.455	1.5	0.38	0.3	0.034	1	3.440	0.025	6.3263
405	T5	0.0639	1.484	0.0319	0.500	19.788	1.5	0.38	0.3	0.034	1	3.440	0.0375	5.1673
406	T5	0.0822	1.484	0.0386	0.470	19.120	1.5	0.38	0.3	0.034	1	3.440	0.0482	4.5555
407	T5	0.0444	1.969	0.0238	0.535	21.492	1.5	0.38	0.3	0.034	1	6.058	0.0246	6.3713
408	T5	0.0666	1.969	0.0331	0.497	22.027	1.5	0.38	0.3	0.034	1	6.058	0.0369	5.2061
409	T5	0.0879	1.969	0.0417	0.475	23.332	1.5	0.38	0.3	0.034	1	6.058	0.0487	4.5302
410	T5	0.0463	2.438	0.0258	0.557	22.901	1.5	0.38	0.3	0.034	1	9.286	0.0251	6.3157
411	T5	0.0686	2.438	0.0369	0.537	26.403	1.5	0.38	0.3	0.034	1	9.286	0.0371	5.1917
412	T5	0.0905	2.438	0.0449	0.496	28.108	1.5	0.38	0.3	0.034	1	9.286	0.049	4.5181
413	T5	0.0382	0.985	0.0097	0.253	13.017	1.5	0.33	0.3	0.034	1	1.514	0.0274	6.0448
414	T5	0.0563	1.045	0.013	0.230	11.938	1.5	0.33	0.3	0.034	1	1.706	0.0392	5.051
415	T5	0.0717	1.067	0.0171	0.239	11.793	1.5	0.33	0.3	0.034	1	1.777	0.0494	4.5003
416	T5	0.0846	1.164	0.0199	0.235	13.602	1.5	0.33	0.3	0.034	1	2.115	0.0562	4.217
417	T5	0.0419	1.484	0.0122	0.291	24.165	1.5	0.33	0.3	0.034	1	3.440	0.0259	6.2131
418	T5	0.0633	1.484	0.0188	0.296	25.801	1.5	0.33	0.3	0.034	1	3.440	0.0391	5.0576
419	T5	0.0808	1.484	0.0237	0.293	28.603	1.5	0.33	0.3	0.034	1	3.440	0.0499	4.4763
420	T5	0.0454	2.008	0.015	0.330	29.231	1.5	0.33	0.3	0.034	1	6.297	0.0267	6.1184
421	T5	0.0678	1.932	0.0234	0.345	32.286	1.5	0.33	0.3	0.034	1	5.831	0.0401	4.9958
422	T5	0.0899	1.932	0.0306	0.340	34.220	1.5	0.33	0.3	0.034	1	5.831	0.0531	4.3385
423	T5	0.0467	2.498	0.0171	0.368	31.520	1.5	0.33	0.3	0.034	1	9.744	0.0269	6.097
424	T5	0.0702	2.498	0.0265	0.377	35.310	1.5	0.33	0.3	0.034	1	9.744	0.0405	4.972
425	T5	0.0925	2.498	0.0354	0.382	38.081	1.5	0.33	0.3	0.034	1	9.744	0.0533	4.3304
426	T5	0.035	0.985	0.0006	0.018	16.185	1.5	0.3	0.3	0.034	1	1.514	0.0257	6.2428
427	T5	0.0526	1.045	0.0015	0.029	16.362	1.5	0.3	0.3	0.034	1	1.706	0.0375	5.1607
428	T5	0.0685	1.067	0.0028	0.041	21.091	1.5	0.3	0.3	0.034	1	1.777	0.0485	4.5416
429	T5	0.0423	1.484	0.0018	0.041	34.841	1.5	0.3	0.3	0.034	1	3.440	0.0272	6.0681
430	T5	0.065	1.484	0.0035	0.054	35.357	1.5	0.3	0.3	0.034	1	3.440	0.0417	4.8969
431	T5	0.0837	1.484	0.0072	0.085	36.521	1.5	0.3	0.3	0.034	1	3.440	0.0537	4.3155
432	T5	0.0464	1.969	0.003	0.065	43.431	1.5	0.3	0.3	0.034	1	6.058	0.0285	5.9198

Table F.1. Conditions for Transmission Tests (cont'd)

Test #	Test Series	H <sub>i</sub> (m)	T <sub>pi</sub> (s)	H <sub>r</sub> (m)	K <sub>t</sub>	K <sub>c</sub> (%)	B (m)	h (m)	h <sub>s</sub> (m)	D <sub>50</sub> (m)	Cota	L <sub>o</sub> (m)	s <sub>oo</sub>	ξ
433	T5	0.0696	1.969	0.007	0.101	42.424	1.5	0.3	0.3	0.034	1	6.058	0.0428	4.8358
434	T5	0.0925	1.969	0.0145	0.157	41.758	1.5	0.3	0.3	0.034	1	6.058	0.0569	4.1936
435	T5	0.0491	2.56	0.0044	0.089	48.257	1.5	0.3	0.3	0.034	1	10.237	0.0295	5.8177
436	T5	0.0736	2.56	0.0089	0.121	48.004	1.5	0.3	0.3	0.034	1	10.237	0.0442	4.7546
437	T5	0.0957	2.56	0.0165	0.172	47.314	1.5	0.3	0.3	0.034	1	10.237	0.0576	4.1674
438	T6	0.0396	0.985	0.0249	0.629	9.397	2	0.43	0.3	0.034	1	1.514	0.027	6.0878
439	T6	0.0594	1.045	0.0321	0.541	9.117	2	0.43	0.3	0.034	1	1.706	0.0389	5.0707
440	T6	0.074	1.067	0.0372	0.503	12.724	2	0.43	0.3	0.034	1	1.777	0.0479	4.5712
441	T6	0.0852	1.164	0.0392	0.461	12.539	2	0.43	0.3	0.034	1	2.115	0.0525	4.3629
442	T6	0.0945	1.164	0.0429	0.455	11.711	2	0.43	0.3	0.034	1	2.115	0.0583	4.1429
443	T6	0.0409	1.484	0.0244	0.595	16.424	2	0.43	0.3	0.034	1	3.440	0.0229	6.6022
444	T6	0.0622	1.484	0.0352	0.566	16.634	2	0.43	0.3	0.034	1	3.440	0.0348	5.3572
445	T6	0.0796	1.484	0.0438	0.551	16.483	2	0.43	0.3	0.034	1	3.440	0.0446	4.7343
446	T6	0.0979	1.484	0.0516	0.527	17.137	2	0.43	0.3	0.034	1	3.440	0.0549	4.2681
447	T6	0.1157	1.484	0.0583	0.504	18.275	2	0.43	0.3	0.034	1	3.440	0.0648	3.9273
448	T6	0.0427	1.969	0.0278	0.650	13.882	2	0.43	0.3	0.034	1	6.058	0.0225	6.6706
449	T6	0.0637	1.969	0.0412	0.647	14.890	2	0.43	0.3	0.034	1	6.058	0.0335	5.4633
450	T6	0.0841	1.969	0.0504	0.599	15.461	2	0.43	0.3	0.034	1	6.058	0.0442	4.7542
451	T6	0.104	1.969	0.0575	0.553	15.926	2	0.43	0.3	0.034	1	6.058	0.0547	4.2758
452	T6	0.1237	1.969	0.065	0.526	17.624	2	0.43	0.3	0.034	1	6.058	0.0651	3.9202
453	T6	0.0439	2.438	0.0294	0.670	19.727	2	0.43	0.3	0.034	1	9.286	0.0225	6.6713
454	T6	0.0661	2.438	0.0439	0.664	19.902	2	0.43	0.3	0.034	1	9.286	0.0338	5.4384
455	T6	0.0869	2.438	0.0534	0.615	20.646	2	0.43	0.3	0.034	1	9.286	0.0445	4.7415
456	T6	0.0386	0.985	0.0165	0.428	11.160	2	0.38	0.3	0.034	1	1.514	0.0268	6.1057
457	T6	0.0566	1.045	0.0209	0.369	9.864	2	0.38	0.3	0.034	1	1.706	0.0381	5.1263
458	T6	0.0719	1.067	0.0249	0.347	10.341	2	0.38	0.3	0.034	1	1.777	0.0478	4.5755
459	T6	0.0432	1.484	0.02	0.464	18.500	2	0.38	0.3	0.034	1	3.440	0.0253	6.2888
460	T6	0.0661	1.484	0.0317	0.479	15.197	2	0.38	0.3	0.034	1	3.440	0.0387	5.0807
461	T6	0.0831	1.484	0.0363	0.437	19.008	2	0.38	0.3	0.034	1	3.440	0.0487	4.5308
462	T6	0.0446	1.969	0.0233	0.522	18.779	2	0.38	0.3	0.034	1	6.058	0.0247	6.3601
463	T6	0.0661	1.969	0.0317	0.480	19.893	2	0.38	0.3	0.034	1	6.058	0.0366	5.2241
464	T6	0.087	1.969	0.039	0.448	21.363	2	0.38	0.3	0.034	1	6.058	0.0482	4.553
465	T6	0.0439	2.438	0.0235	0.535	19.584	2	0.38	0.3	0.034	1	9.286	0.0237	6.489
466	T6	0.0663	2.438	0.033	0.497	24.581	2	0.38	0.3	0.034	1	9.286	0.0359	5.2785
467	T6	0.0383	0.985	0.0075	0.196	13.238	2	0.33	0.3	0.034	1	1.514	0.0275	6.0336
468	T6	0.0567	1.045	0.0106	0.188	12.152	2	0.33	0.3	0.034	1	1.706	0.0395	5.0341
469	T6	0.0731	1.067	0.0141	0.194	13.610	2	0.33	0.3	0.034	1	1.777	0.0503	4.4567
470	T6	0.042	1.484	0.0091	0.216	24.110	2	0.33	0.3	0.034	1	3.440	0.0259	6.2105
471	T6	0.0629	1.484	0.0153	0.243	25.971	2	0.33	0.3	0.034	1	3.440	0.0389	5.0732
472	T6	0.0802	1.484	0.0197	0.246	28.518	2	0.33	0.3	0.034	1	3.440	0.0496	4.4914
473	T6	0.0449	2.008	0.0116	0.258	29.524	2	0.33	0.3	0.034	1	6.297	0.0264	6.1552
474	T6	0.067	1.932	0.0186	0.278	32.207	2	0.33	0.3	0.034	1	5.831	0.0396	5.0275
475	T6	0.0887	1.932	0.0283	0.319	33.755	2	0.33	0.3	0.034	1	5.831	0.0524	4.3694
476	T6	0.0461	2.498	0.0136	0.294	31.636	2	0.33	0.3	0.034	1	9.744	0.0266	6.1356
477	T6	0.0694	2.498	0.0237	0.341	35.108	2	0.33	0.3	0.034	1	9.744	0.04	5.0024
478	T6	0.0915	2.498	0.0346	0.379	37.825	2	0.33	0.3	0.034	1	9.744	0.0527	4.3546
479	T6	0.0532	1.045	0.0012	0.022	14.987	2	0.3	0.3	0.034	1	1.706	0.038	5.1314
480	T6	0.0692	1.067	0.0023	0.034	18.060	2	0.3	0.3	0.034	1	1.777	0.049	4.5178
481	T6	0.0423	1.484	0.0014	0.033	33.471	2	0.3	0.3	0.034	1	3.440	0.0271	6.0704
482	T6	0.0649	1.484	0.0034	0.053	34.235	2	0.3	0.3	0.034	1	3.440	0.0416	4.9024
483	T6	0.0837	1.484	0.0059	0.071	35.495	2	0.3	0.3	0.034	1	3.440	0.0537	4.3142
484	T6	0.0461	1.969	0.002	0.044	42.424	2	0.3	0.3	0.034	1	6.058	0.0284	5.9381
485	T6	0.0694	1.969	0.0075	0.108	41.578	2	0.3	0.3	0.034	1	6.058	0.0426	4.843
486	T6	0.0927	1.969	0.0109	0.118	40.234	2	0.3	0.3	0.034	1	6.058	0.057	4.1893
487	T6	0.0489	2.56	0.0038	0.077	46.569	2	0.3	0.3	0.034	1	10.237	0.0294	5.8338
488	T6	0.0737	2.56	0.0091	0.123	46.926	2	0.3	0.3	0.034	1	10.237	0.0443	4.751
489	T6	0.0963	2.56	0.0133	0.138	45.904	2	0.3	0.3	0.034	1	10.237	0.0579	4.156
490	T12	0.0407	0.985	0.0309	0.759	4.204	0.3	0.43	0.3	0.034	2	1.514	0.0277	3.0029
491	T12	0.0636	1.045	0.0474	0.745	4.683	0.3	0.43	0.3	0.034	2	1.706	0.0417	2.4493
492	T12	0.0818	1.067	0.058	0.709	6.389	0.3	0.43	0.3	0.034	2	1.777	0.0529	2.1732
493	T12	0.0955	1.067	0.0654	0.685	9.927	0.3	0.43	0.3	0.034	2	1.777	0.0618	2.0111
494	T12	0.1047	1.164	0.0723	0.691	8.496	0.3	0.43	0.3	0.034	2	2.115	0.0646	1.9675
495	T12	0.0458	1.484	0.0344	0.751	10.878	0.3	0.43	0.3	0.034	2	3.440	0.0256	3.1221
496	T12	0.071	1.484	0.0533	0.751	12.447	0.3	0.43	0.3	0.034	2	3.440	0.0398	2.5071
497	T12	0.0913	1.484	0.0672	0.736	12.555	0.3	0.43	0.3	0.034	2	3.440	0.0512	2.2106
498	T12	0.1139	1.484	0.08	0.703	12.766	0.3	0.43	0.3	0.034	2	3.440	0.0638	1.9788
499	T12	0.1341	1.484	0.0904	0.675	14.544	0.3	0.43	0.3	0.034	2	3.440	0.0751	1.824
500	T12	0.0498	1.969	0.0381	0.765	22.046	0.3	0.43	0.3	0.034	2	6.058	0.0262	3.0883
501	T12	0.0734	1.969	0.0574	0.783	21.473	0.3	0.43	0.3	0.034	2	6.058	0.0386	2.5451
502	T12	0.0962	1.969	0.0741	0.770	21.124	0.3	0.43	0.3	0.034	2	6.058	0.0506	2.2227
503	T12	0.1196	1.969	0.0893	0.746	20.980	0.3	0.43	0.3	0.034	2	6.058	0.0629	1.9937
504	T12	0.0527	2.438	0.0392	0.744	27.247	0.3	0.43	0.3	0.034	2	9.286	0.027	3.0448

Table F.1. Conditions for Transmission Tests (cont'd)

Test #	Test Series	H <sub>i</sub> (m)	T <sub>pi</sub> (s)	H <sub>i</sub> (m)	K <sub>t</sub>	K <sub>r</sub> (%)	B (m)	h (m)	h <sub>a</sub> (m)	D <sub>50</sub> (m)	Cotα	L <sub>o</sub> (m)	s <sub>op</sub>	ξ
505	T12	0.0782	2.438	0.0591	0.755	26.646	0.3	0.43	0.3	0.034	2	9.286	0.04	2.5001
506	T12	0.1025	2.438	0.0773	0.754	26.133	0.3	0.43	0.3	0.034	2	9.286	0.0524	2.1839
507	T12	0.039	0.985	0.0273	0.701	5.403	0.3	0.38	0.3	0.034	2	1.514	0.0271	3.0368
508	T12	0.0598	1.045	0.0391	0.654	5.745	0.3	0.38	0.3	0.034	2	1.706	0.0402	2.4949
509	T12	0.0777	1.067	0.0468	0.602	6.633	0.3	0.38	0.3	0.034	2	1.777	0.0517	2.2
510	T12	0.0455	1.484	0.0317	0.697	12.668	0.3	0.38	0.3	0.034	2	3.440	0.0266	3.063
511	T12	0.0696	1.484	0.0467	0.670	12.763	0.3	0.38	0.3	0.034	2	3.440	0.0408	2.4752
512	T12	0.0899	1.484	0.0571	0.635	12.377	0.3	0.38	0.3	0.034	2	3.440	0.0527	2.178
513	T12	0.0476	2.008	0.0359	0.754	22.448	0.3	0.38	0.3	0.034	2	6.297	0.0263	3.0815
514	T12	0.0699	2.008	0.0525	0.751	22.499	0.3	0.38	0.3	0.034	2	6.297	0.0386	2.5437
515	T12	0.092	1.932	0.0664	0.722	22.619	0.3	0.38	0.3	0.034	2	5.831	0.0511	2.2114
516	T12	0.0494	2.498	0.037	0.749	28.589	0.3	0.38	0.3	0.034	2	9.744	0.0267	3.0609
517	T12	0.0735	2.498	0.0546	0.743	28.068	0.3	0.38	0.3	0.034	2	9.744	0.0397	2.5094
518	T12	0.0963	2.498	0.0686	0.712	28.629	0.3	0.38	0.3	0.034	2	9.744	0.052	2.1922
519	T12	0.035	0.985	0.0196	0.560	6.471	0.3	0.33	0.3	0.034	2	1.514	0.0251	3.1553
520	T12	0.0547	1.045	0.0255	0.467	6.411	0.3	0.33	0.3	0.034	2	1.706	0.0381	2.5632
521	T12	0.0725	1.067	0.0311	0.429	10.986	0.3	0.33	0.3	0.034	2	1.777	0.05	2.2367
522	T12	0.0408	1.484	0.0229	0.561	9.845	0.3	0.33	0.3	0.034	2	3.440	0.0252	3.1483
523	T12	0.0649	1.484	0.0328	0.505	13.748	0.3	0.33	0.3	0.034	2	3.440	0.0401	2.4967
524	T12	0.0841	1.484	0.0408	0.485	15.786	0.3	0.33	0.3	0.034	2	3.440	0.052	2.1934
525	T12	0.0472	1.969	0.0279	0.591	23.885	0.3	0.33	0.3	0.034	2	6.058	0.0278	2.999
526	T12	0.0703	1.969	0.0404	0.574	25.408	0.3	0.33	0.3	0.034	2	6.058	0.0414	2.4565
527	T12	0.0932	1.969	0.0511	0.548	26.734	0.3	0.33	0.3	0.034	2	6.058	0.0549	2.1335
528	T12	0.0504	2.56	0.0298	0.591	31.544	0.3	0.33	0.3	0.034	2	10.237	0.029	2.9363
529	T12	0.075	2.56	0.043	0.573	33.445	0.3	0.33	0.3	0.034	2	10.237	0.0431	2.4072
530	T12	0.0983	2.56	0.0547	0.557	35.386	0.3	0.33	0.3	0.034	2	10.237	0.0565	2.1027
531	T12	0.0345	0.985	0.0088	0.255	10.753	0.3	0.3	0.3	0.034	2	1.514	0.0253	3.1411
532	T12	0.0542	1.045	0.0146	0.268	10.203	0.3	0.3	0.3	0.034	2	1.706	0.0387	2.5411
533	T12	0.0725	1.067	0.0206	0.285	15.030	0.3	0.3	0.3	0.034	2	1.777	0.0513	2.2074
534	T12	0.0402	1.484	0.0144	0.359	13.465	0.3	0.3	0.3	0.034	2	3.440	0.0258	3.1152
535	T12	0.062	1.484	0.0241	0.388	14.603	0.3	0.3	0.3	0.034	2	3.440	0.0398	2.5073
536	T12	0.081	1.484	0.0305	0.377	15.711	0.3	0.3	0.3	0.034	2	3.440	0.052	2.1932
537	T12	0.048	1.969	0.0198	0.412	30.929	0.3	0.3	0.3	0.034	2	6.058	0.0295	2.9099
538	T12	0.0715	1.969	0.0305	0.426	31.317	0.3	0.3	0.3	0.034	2	6.058	0.044	2.3848
539	T12	0.095	1.969	0.0415	0.437	31.391	0.3	0.3	0.3	0.034	2	6.058	0.0584	2.0693
540	T12	0.0513	2.381	0.0226	0.440	37.850	0.3	0.3	0.3	0.034	2	8.859	0.031	2.8394
541	T12	0.0763	2.381	0.035	0.459	39.064	0.3	0.3	0.3	0.034	2	8.859	0.0461	2.3286
542	T12	0.0999	2.381	0.0458	0.458	39.836	0.3	0.3	0.3	0.034	2	8.859	0.0604	2.0349
543	T12	0.0367	0.985	0.004	0.109	19.338	0.3	0.27	0.3	0.034	2	1.514	0.0277	3.0037
544	T12	0.0482	0.985	0.0049	0.101	17.407	0.3	0.27	0.3	0.034	2	1.514	0.0364	2.6205
545	T12	0.0566	1.045	0.0059	0.103	15.921	0.3	0.27	0.3	0.034	2	1.706	0.0417	2.4486
546	T12	0.0409	1.484	0.0076	0.186	23.601	0.3	0.27	0.3	0.034	2	3.440	0.0274	3.0223
547	T12	0.0539	1.484	0.0102	0.190	21.909	0.3	0.27	0.3	0.034	2	3.440	0.0361	2.6321
548	T12	0.0631	1.484	0.0126	0.200	21.189	0.3	0.27	0.3	0.034	2	3.440	0.0422	2.4329
549	T12	0.0482	1.969	0.0132	0.275	42.951	0.3	0.27	0.3	0.034	2	6.058	0.031	2.8376
550	T12	0.0627	1.969	0.0152	0.243	40.712	0.3	0.27	0.3	0.034	2	6.058	0.0404	2.4871
551	T12	0.0723	1.969	0.0196	0.271	39.421	0.3	0.27	0.3	0.034	2	6.058	0.0466	2.3163
552	T12	0.0513	2.626	0.013	0.252	49.478	0.3	0.27	0.3	0.034	2	10.769	0.0324	2.7778
553	T12	0.0668	2.626	0.0194	0.291	48.043	0.3	0.27	0.3	0.034	2	10.769	0.0421	2.4357
554	T12	0.0769	2.626	0.0225	0.293	47.058	0.3	0.27	0.3	0.034	2	10.769	0.0485	2.2703
555	T12	0.0387	0.985	0.0027	0.070	22.229	0.3	0.25	0.3	0.034	2	1.514	0.0298	2.8941
556	T12	0.0507	1.045	0.0032	0.063	20.287	0.3	0.25	0.3	0.034	2	1.706	0.0383	2.5562
557	T12	0.0589	1.045	0.0039	0.066	18.503	0.3	0.25	0.3	0.034	2	1.706	0.0445	2.3709
558	T12	0.0418	1.484	0.0058	0.138	27.371	0.3	0.25	0.3	0.034	2	3.440	0.0289	2.9428
559	T12	0.0541	1.484	0.0068	0.126	25.856	0.3	0.25	0.3	0.034	2	3.440	0.0374	2.5864
560	T12	0.0624	1.484	0.0078	0.125	25.107	0.3	0.25	0.3	0.034	2	3.440	0.0431	2.4078
561	T12	0.0498	2.008	0.0079	0.159	45.993	0.3	0.25	0.3	0.034	2	6.297	0.0332	2.7441
562	T12	0.0647	2.008	0.0101	0.156	43.945	0.3	0.25	0.3	0.034	2	6.297	0.0431	2.4087
563	T12	0.0745	2.008	0.0127	0.171	42.915	0.3	0.25	0.3	0.034	2	6.297	0.0496	2.2441
564	T12	0.052	2.438	0.0094	0.181	52.430	0.3	0.25	0.3	0.034	2	9.286	0.0342	2.7039
565	T12	0.0679	2.438	0.0124	0.182	49.911	0.3	0.25	0.3	0.034	2	9.286	0.0446	2.3669
566	T12	0.0785	2.438	0.0151	0.192	48.238	0.3	0.25	0.3	0.034	2	9.286	0.0516	2.2015
567	T12	0.039	0.985	0.0025	0.064	22.172	0.3	0.23	0.3	0.034	2	1.514	0.0309	2.846
568	T12	0.0503	1.045	0.0029	0.058	19.945	0.3	0.23	0.3	0.034	2	1.706	0.039	2.5318
569	T12	0.0584	1.045	0.0035	0.061	18.985	0.3	0.23	0.3	0.034	2	1.706	0.0453	2.35
570	T12	0.0427	1.484	0.0052	0.121	28.555	0.3	0.23	0.3	0.034	2	3.440	0.0306	2.8596
571	T12	0.0547	1.484	0.0059	0.107	27.527	0.3	0.23	0.3	0.034	2	3.440	0.0392	2.5268
572	T12	0.0639	1.484	0.0065	0.102	26.875	0.3	0.23	0.3	0.034	2	3.440	0.0457	2.3381
573	T12	0.0519	2.008	0.0068	0.132	47.461	0.3	0.23	0.3	0.034	2	6.297	0.0359	2.6375
574	T12	0.067	2.008	0.009	0.134	46.129	0.3	0.23	0.3	0.034	2	6.297	0.0464	2.3223
575	T12	0.0777	2.008	0.0103	0.133	45.108	0.3	0.23	0.3	0.034	2	6.297	0.0538	2.1563
576	T12	0.0535	2.438	0.0085	0.159	53.655	0.3	0.23	0.3	0.034	2	9.286	0.0366	2.6142

Table F.1. Conditions for Transmission Tests (cont'd)

Test #	Test Series	H <sub>i</sub> (m)	T <sub>pl</sub> (s)	H <sub>i</sub> (m)	K <sub>i</sub>	K <sub>c</sub> (%)	B (m)	h (m)	h <sub>s</sub> (m)	D <sub>50</sub> (m)	Cota	L <sub>o</sub> (m)	s <sub>op</sub>	ξ
577	T12	0.069	2.438	0.01	0.145	51.722	0.3	0.23	0.3	0.034	2	9.286	0.0472	2.3024
578	T12	0.0793	2.438	0.0116	0.146	50.255	0.3	0.23	0.3	0.034	2	9.286	0.0542	2.1479
579	T14	0.0371	0.985	0.0295	0.796	4.886	0.3	0.43	0.3	0.034	4	1.514	0.0253	1.5727
580	T14	0.0587	1.045	0.0451	0.768	4.540	0.3	0.43	0.3	0.034	4	1.706	0.0385	1.2748
581	T14	0.0761	1.067	0.055	0.723	8.150	0.3	0.43	0.3	0.034	4	1.777	0.0492	1.1269
582	T14	0.0888	1.164	0.0626	0.705	10.403	0.3	0.43	0.3	0.034	4	2.115	0.0548	1.0684
583	T14	0.098	1.164	0.0686	0.700	8.754	0.3	0.43	0.3	0.034	4	2.115	0.0605	1.0167
584	T14	0.0422	1.484	0.0324	0.768	7.044	0.3	0.43	0.3	0.034	4	3.440	0.0237	1.6256
585	T14	0.0657	1.484	0.0506	0.771	6.381	0.3	0.43	0.3	0.034	4	3.440	0.0368	1.3029
586	T14	0.0853	1.484	0.0647	0.758	6.381	0.3	0.43	0.3	0.034	4	3.440	0.0478	1.1431
587	T14	0.1065	1.484	0.0768	0.722	7.166	0.3	0.43	0.3	0.034	4	3.440	0.0597	1.0234
588	T14	0.1258	1.484	0.0857	0.681	9.134	0.3	0.43	0.3	0.034	4	3.440	0.0705	0.9416
589	T14	0.0462	1.969	0.0367	0.795	10.472	0.3	0.43	0.3	0.034	4	6.058	0.0243	1.6038
590	T14	0.0688	1.969	0.0553	0.803	9.528	0.3	0.43	0.3	0.034	4	6.058	0.0362	1.3142
591	T14	0.0908	1.969	0.072	0.793	9.157	0.3	0.43	0.3	0.034	4	6.058	0.0478	1.144
592	T14	0.1126	1.932	0.0828	0.736	9.013	0.3	0.43	0.3	0.034	4	5.831	0.0594	1.0257
593	T14	0.0487	2.498	0.0387	0.795	16.286	0.3	0.43	0.3	0.034	4	9.744	0.0249	1.5855
594	T14	0.0725	2.498	0.0584	0.806	15.502	0.3	0.43	0.3	0.034	4	9.744	0.037	1.3
595	T14	0.0951	2.498	0.0743	0.781	15.480	0.3	0.43	0.3	0.034	4	9.744	0.0486	1.1346
596	T14	0.1194	2.498	0.0887	0.742	16.404	0.3	0.43	0.3	0.034	4	9.744	0.061	1.0125
597	T14	0.0369	0.985	0.0259	0.703	5.367	0.3	0.38	0.3	0.034	4	1.514	0.0257	1.5605
598	T14	0.0564	1.045	0.037	0.656	5.391	0.3	0.38	0.3	0.034	4	1.706	0.0379	1.2835
599	T14	0.0734	1.067	0.043	0.586	6.886	0.3	0.38	0.3	0.034	4	1.777	0.0488	1.1319
600	T14	0.0854	1.164	0.0493	0.577	11.742	0.3	0.38	0.3	0.034	4	2.115	0.0544	1.0718
601	T14	0.0425	1.484	0.0296	0.695	7.706	0.3	0.38	0.3	0.034	4	3.440	0.0249	1.5839
602	T14	0.065	1.484	0.0439	0.675	7.940	0.3	0.38	0.3	0.034	4	3.440	0.0381	1.2806
603	T14	0.0845	1.484	0.0538	0.637	7.764	0.3	0.38	0.3	0.034	4	3.440	0.0495	1.1233
604	T14	0.1052	1.484	0.0621	0.590	9.377	0.3	0.38	0.3	0.034	4	3.440	0.0616	1.007
605	T14	0.0464	1.969	0.0343	0.739	8.221	0.3	0.38	0.3	0.034	4	6.058	0.0257	1.5586
606	T14	0.0692	1.969	0.0482	0.697	7.731	0.3	0.38	0.3	0.034	4	6.058	0.0384	1.2766
607	T14	0.0915	1.969	0.0599	0.654	7.845	0.3	0.38	0.3	0.034	4	6.058	0.0507	1.1099
608	T14	0.0486	2.438	0.0354	0.729	14.397	0.3	0.38	0.3	0.034	4	9.286	0.0263	1.5417
609	T14	0.0736	2.498	0.0511	0.694	13.812	0.3	0.38	0.3	0.034	4	9.744	0.0398	1.2538
610	T14	0.0967	2.438	0.0625	0.646	14.891	0.3	0.38	0.3	0.034	4	9.286	0.0523	1.0929
611	T14	0.0355	0.985	0.0175	0.494	6.906	0.3	0.33	0.3	0.034	4	1.514	0.0254	1.5675
612	T14	0.0546	1.045	0.0221	0.405	7.126	0.3	0.33	0.3	0.034	4	1.706	0.038	1.2832
613	T14	0.0715	1.067	0.0264	0.370	12.691	0.3	0.33	0.3	0.034	4	1.777	0.0493	1.1263
614	T14	0.0416	1.484	0.0196	0.472	10.162	0.3	0.33	0.3	0.034	4	3.440	0.0257	1.5584
615	T14	0.0641	1.484	0.0276	0.430	10.239	0.3	0.33	0.3	0.034	4	3.440	0.0396	1.2558
616	T14	0.0833	1.484	0.0331	0.397	12.591	0.3	0.33	0.3	0.034	4	3.440	0.0515	1.1019
617	T14	0.0463	1.969	0.0232	0.501	7.071	0.3	0.33	0.3	0.034	4	6.058	0.0273	1.5133
618	T14	0.069	1.969	0.0323	0.467	9.708	0.3	0.33	0.3	0.034	4	6.058	0.0407	1.2396
619	T14	0.0913	1.969	0.04	0.438	11.900	0.3	0.33	0.3	0.034	4	6.058	0.0538	1.0777
620	T14	0.0499	2.438	0.026	0.520	12.375	0.3	0.33	0.3	0.034	4	9.286	0.0288	1.4726
621	T14	0.0742	2.438	0.0358	0.483	15.521	0.3	0.33	0.3	0.034	4	9.286	0.0428	1.2082
622	T14	0.097	2.438	0.0442	0.456	17.419	0.3	0.33	0.3	0.034	4	9.286	0.056	1.0564
623	T14	0.0344	0.985	0.0056	0.163	8.745	0.3	0.3	0.3	0.034	4	1.514	0.0252	1.574
624	T14	0.0543	1.045	0.0104	0.192	8.337	0.3	0.3	0.3	0.034	4	1.706	0.0388	1.2692
625	T14	0.0725	1.067	0.0143	0.197	14.360	0.3	0.3	0.3	0.034	4	1.777	0.0513	1.1035
626	T14	0.0386	1.463	0.0093	0.242	11.745	0.3	0.3	0.3	0.034	4	3.343	0.0248	1.5869
627	T14	0.0617	1.484	0.0153	0.249	11.965	0.3	0.3	0.3	0.034	4	3.440	0.0396	1.2564
628	T14	0.0804	1.484	0.0221	0.275	12.405	0.3	0.3	0.3	0.034	4	3.440	0.0516	1.101
629	T14	0.0463	1.969	0.015	0.325	10.040	0.3	0.3	0.3	0.034	4	6.058	0.0285	1.4821
630	T14	0.0689	1.969	0.0219	0.317	11.362	0.3	0.3	0.3	0.034	4	6.058	0.0423	1.2152
631	T14	0.0915	1.969	0.029	0.317	12.549	0.3	0.3	0.3	0.034	4	6.058	0.0562	1.0544
632	T14	0.0502	2.438	0.0166	0.329	15.224	0.3	0.3	0.3	0.034	4	9.286	0.0303	1.4359
633	T14	0.0746	2.438	0.0258	0.346	17.052	0.3	0.3	0.3	0.034	4	9.286	0.045	1.178
634	T14	0.0976	2.438	0.0332	0.340	18.447	0.3	0.3	0.3	0.034	4	9.286	0.0589	1.0302
635	T14	0.0363	0.985	0.0018	0.049	12.093	0.3	0.27	0.3	0.034	4	1.514	0.0274	1.5103
636	T14	0.0477	1.045	0.0022	0.046	10.781	0.3	0.27	0.3	0.034	4	1.706	0.0352	1.3333
637	T14	0.0558	1.045	0.0027	0.048	10.285	0.3	0.27	0.3	0.034	4	1.706	0.0411	1.2328
638	T14	0.0405	1.484	0.004	0.098	16.425	0.3	0.27	0.3	0.034	4	3.440	0.0271	1.5183
639	T14	0.0534	1.484	0.0048	0.090	15.378	0.3	0.27	0.3	0.034	4	3.440	0.0358	1.322
640	T14	0.0628	1.484	0.0057	0.090	15.069	0.3	0.27	0.3	0.034	4	3.440	0.042	1.2192
641	T14	0.0463	1.969	0.006	0.130	15.611	0.3	0.27	0.3	0.034	4	6.058	0.0299	1.4469
642	T14	0.0608	1.969	0.0079	0.131	14.469	0.3	0.27	0.3	0.034	4	6.058	0.0392	1.2632
643	T14	0.0702	1.969	0.0094	0.134	13.843	0.3	0.27	0.3	0.034	4	6.058	0.0453	1.1752
644	T14	0.0511	2.498	0.0079	0.154	22.865	0.3	0.27	0.3	0.034	4	9.744	0.0324	1.3897
645	T14	0.0662	2.498	0.0104	0.158	21.997	0.3	0.27	0.3	0.034	4	9.744	0.0419	1.2216
646	T14	0.0762	2.498	0.0125	0.164	22.181	0.3	0.27	0.3	0.034	4	9.744	0.0482	1.1387
647	T14	0.0384	0.985	0.0015	0.040	10.790	0.3	0.25	0.3	0.034	4	1.514	0.0297	1.4516
648	T14	0.05	1.045	0.0019	0.038	9.583	0.3	0.25	0.3	0.034	4	1.706	0.0378	1.2864

Table F.1. Conditions for Transmission Tests (cont'd)

Test #	Test Series	H <sub>i</sub> (m)	T <sub>91</sub> (s)	H <sub>t</sub> (m)	K <sub>t</sub>	K <sub>r</sub> (%)	B (m)	h (m)	h <sub>s</sub> (m)	D <sub>50</sub> (m)	Cotα	L <sub>o</sub> (m)	s <sub>op</sub>	ξ
649	T14	0.0583	1.045	0.0023	0.039	10.262	0.3	0.25	0.3	0.034	4	1.706	0.044	1.1916
650	T14	0.0418	1.484	0.0033	0.080	16.609	0.3	0.25	0.3	0.034	4	3.440	0.0289	1.4717
651	T14	0.0546	1.484	0.0041	0.076	15.835	0.3	0.25	0.3	0.034	4	3.440	0.0377	1.2872
652	T14	0.0632	1.484	0.0048	0.076	15.566	0.3	0.25	0.3	0.034	4	3.440	0.0437	1.1962
653	T14	0.0476	1.969	0.0049	0.102	15.887	0.3	0.25	0.3	0.034	4	6.058	0.0318	1.4024
654	T14	0.0619	1.969	0.0056	0.090	14.959	0.3	0.25	0.3	0.034	4	6.058	0.0413	1.2302
655	T14	0.0712	1.969	0.0062	0.087	14.561	0.3	0.25	0.3	0.034	4	6.058	0.0475	1.1467
656	T14	0.0525	2.498	0.0064	0.121	24.871	0.3	0.25	0.3	0.034	4	9.744	0.0345	1.3468
657	T14	0.0678	2.498	0.0072	0.107	23.957	0.3	0.25	0.3	0.034	4	9.744	0.0445	1.1853
658	T14	0.0779	2.498	0.0084	0.107	24.030	0.3	0.25	0.3	0.034	4	9.744	0.0511	1.1057
659	T14	0.0386	0.985	0.0008	0.021	10.720	0.3	0.23	0.3	0.034	4	1.514	0.0305	1.4306
660	T14	0.0498	1.045	0.0011	0.021	10.465	0.3	0.23	0.3	0.034	4	1.706	0.0386	1.2717
661	T14	0.058	1.045	0.0014	0.025	11.946	0.3	0.23	0.3	0.034	4	1.706	0.045	1.1785
662	T14	0.0429	1.484	0.0024	0.055	17.419	0.3	0.23	0.3	0.034	4	3.440	0.0307	1.4266
663	T14	0.0553	1.484	0.0027	0.049	16.502	0.3	0.23	0.3	0.034	4	3.440	0.0396	1.2562
664	T14	0.0648	1.484	0.0029	0.045	16.103	0.3	0.23	0.3	0.034	4	3.440	0.0463	1.1613
665	T14	0.038	0.994	0.0011	0.029	10.973	0.3	0.23	0.3	0.034	4	1.544	0.03	1.4433
666	T14	0.0622	1.969	0.0041	0.065	15.958	0.3	0.23	0.3	0.034	4	6.058	0.0431	1.2042
667	T14	0.072	1.969	0.0043	0.060	15.712	0.3	0.23	0.3	0.034	4	6.058	0.0499	1.1191
668	T14	0.0497	2.498	0.0047	0.095	26.241	0.3	0.23	0.3	0.034	4	9.744	0.034	1.3565
669	T14	0.0646	2.498	0.0056	0.087	25.228	0.3	0.23	0.3	0.034	4	9.744	0.0441	1.1906
670	T14	0.0746	2.498	0.0063	0.084	25.139	0.3	0.23	0.3	0.034	4	9.744	0.0509	1.1079
671	IM1	0.0457	0.985	0.0366	0.801	12.461	0.3	0.43	0.3	0.034	1	1.514	0.0311	5.67
672	IM1	0.0682	1.045	0.0521	0.763	11.183	0.3	0.43	0.3	0.034	1	1.706	0.0447	4.7309
673	IM1	0.0859	1.067	0.0621	0.723	13.858	0.3	0.43	0.3	0.034	1	1.777	0.0556	4.2416
674	IM1	0.0991	1.067	0.0695	0.701	12.649	0.3	0.43	0.3	0.034	1	1.777	0.0641	3.9487
675	IM1	0.1105	1.164	0.076	0.687	14.105	0.3	0.43	0.3	0.034	1	2.115	0.0682	3.8302
676	IM1	0.1168	1.164	0.0805	0.689	15.368	0.3	0.43	0.3	0.034	1	2.115	0.072	3.7256
677	IM1	0.0464	1.484	0.0373	0.805	24.704	0.3	0.43	0.3	0.034	1	3.440	0.026	6.2009
678	IM1	0.0712	1.484	0.0562	0.789	24.321	0.3	0.43	0.3	0.034	1	3.440	0.0399	5.0059
679	IM1	0.0912	1.484	0.0695	0.762	24.094	0.3	0.43	0.3	0.034	1	3.440	0.0511	4.4223
680	IM1	0.1122	1.484	0.0821	0.731	24.303	0.3	0.43	0.3	0.034	1	3.440	0.0629	3.9867
681	IM1	0.1335	1.484	0.0935	0.701	25.028	0.3	0.43	0.3	0.034	1	3.440	0.0748	3.6556
682	IM1	0.0492	1.969	0.0398	0.810	30.543	0.3	0.43	0.3	0.034	1	6.058	0.0259	6.2155
683	IM1	0.0738	1.969	0.0596	0.808	29.743	0.3	0.43	0.3	0.034	1	6.058	0.0388	5.076
684	IM1	0.096	1.969	0.0762	0.794	28.975	0.3	0.43	0.3	0.034	1	6.058	0.0505	4.506
685	IM1	0.1179	1.969	0.0908	0.770	27.967	0.3	0.43	0.3	0.034	1	6.058	0.062	4.0161
686	IM1	0.0517	2.381	0.0403	0.780	35.463	0.3	0.43	0.3	0.034	1	8.859	0.0265	6.141
687	IM1	0.0775	2.381	0.0612	0.790	34.170	0.3	0.43	0.3	0.034	1	8.859	0.0397	5.0167
688	IM1	0.1012	2.381	0.079	0.781	32.546	0.3	0.43	0.3	0.034	1	8.859	0.0519	4.39
689	IM1	0.0413	0.985	0.0317	0.766	11.467	0.3	0.38	0.3	0.034	1	1.514	0.0288	5.8959
690	IM1	0.0603	1.067	0.0413	0.686	10.904	0.3	0.38	0.3	0.034	1	1.777	0.0401	4.9959
691	IM1	0.0821	1.067	0.0497	0.606	13.823	0.3	0.38	0.3	0.034	1	1.777	0.0546	4.2811
692	IM1	0.0467	1.484	0.0341	0.730	27.663	0.3	0.38	0.3	0.034	1	3.440	0.0274	6.0445
693	IM1	0.0708	1.484	0.0488	0.689	27.331	0.3	0.38	0.3	0.034	1	3.440	0.0415	4.9097
694	IM1	0.0914	1.484	0.0587	0.642	27.210	0.3	0.38	0.3	0.034	1	3.440	0.0536	4.321
695	IM1	0.0492	1.969	0.0371	0.755	32.813	0.3	0.38	0.3	0.034	1	6.058	0.0273	6.0568
696	IM1	0.0741	2.008	0.0537	0.725	32.526	0.3	0.38	0.3	0.034	1	6.297	0.0409	4.9423
697	IM1	0.098	2.008	0.0673	0.687	32.815	0.3	0.38	0.3	0.034	1	6.297	0.0542	4.2971
698	IM1	0.0532	2.438	0.0379	0.712	39.613	0.3	0.38	0.3	0.034	1	9.286	0.0288	5.8925
699	IM1	0.0794	2.438	0.0551	0.693	38.412	0.3	0.38	0.3	0.034	1	9.286	0.043	4.8244
700	IM1	0.0415	0.985	0.0193	0.466	17.796	0.3	0.33	0.3	0.034	1	1.514	0.0297	5.7981
701	IM1	0.0785	1.067	0.0321	0.409	18.301	0.3	0.33	0.3	0.034	1	1.777	0.0541	4.3006
702	IM1	0.0785	1.067	0.0317	0.404	18.445	0.3	0.33	0.3	0.034	1	1.777	0.0541	4.3003
703	IM1	0.046	1.484	0.0236	0.514	31.347	0.3	0.33	0.3	0.034	1	3.440	0.0284	5.9332
704	IM1	0.0697	1.484	0.0338	0.485	33.648	0.3	0.33	0.3	0.034	1	3.440	0.0431	4.8171
705	IM1	0.0895	1.484	0.0419	0.468	36.388	0.3	0.33	0.3	0.034	1	3.440	0.0553	4.2531
706	IM1	0.0501	1.932	0.0281	0.561	40.440	0.3	0.33	0.3	0.034	1	5.831	0.0296	5.814
707	IM1	0.0752	1.932	0.0403	0.537	41.467	0.3	0.33	0.3	0.034	1	5.831	0.0444	4.745
708	IM1	0.0546	2.498	0.0314	0.574	48.767	0.3	0.33	0.3	0.034	1	9.744	0.0315	5.6363
709	IM1	0.0803	2.498	0.0435	0.541	48.362	0.3	0.33	0.3	0.034	1	9.744	0.0463	4.6478
710	IM1	0.0394	0.985	0.008	0.204	24.869	0.3	0.3	0.3	0.034	1	1.514	0.0289	5.884
711	IM1	0.0594	1.045	0.0152	0.256	22.695	0.3	0.3	0.3	0.034	1	1.706	0.0424	4.8558
712	IM1	0.0777	1.067	0.0222	0.285	23.648	0.3	0.3	0.3	0.034	1	1.777	0.055	4.2632
713	IM1	0.0492	1.484	0.014	0.284	43.440	0.3	0.3	0.3	0.034	1	3.440	0.0315	5.6312
714	IM1	0.0738	1.484	0.0246	0.334	42.632	0.3	0.3	0.3	0.034	1	3.440	0.0474	4.5944
715	IM1	0.0942	1.484	0.0345	0.366	42.007	0.3	0.3	0.3	0.034	1	3.440	0.0605	4.0672
716	IM1	0.0524	2.048	0.0195	0.372	49.999	0.3	0.3	0.3	0.034	1	6.552	0.032	5.5859
717	IM1	0.078	1.969	0.032	0.411	47.280	0.3	0.3	0.3	0.034	1	6.058	0.048	4.5664
718	IM1	0.0557	2.56	0.0215	0.385	55.375	0.3	0.3	0.3	0.034	1	10.237	0.0335	5.462
719	IM1	0.0825	2.56	0.0346	0.419	54.276	0.3	0.3	0.3	0.034	1	10.237	0.0496	4.4894
720	IM1	0.0409	0.985	0.0033	0.080	34.182	0.3	0.27	0.3	0.034	1	1.514	0.0309	5.6883

Table F.1. Conditions for Transmission Tests (cont'd)

Test #	Test Series	H <sub>i</sub> (m)	T <sub>pl</sub> (s)	H <sub>t</sub> (m)	K <sub>i</sub>	K <sub>r</sub> (%)	B (m)	h (m)	h <sub>s</sub> (m)	D <sub>50</sub> (m)	Cotα	L <sub>o</sub> (m)	s <sub>op</sub>	ξ
721	IM1	0.0522	1.045	0.0041	0.078	32.441	0.3	0.27	0.3	0.034	1	1.706	0.0384	5.1015
722	IM1	0.0604	1.067	0.0053	0.087	31.342	0.3	0.27	0.3	0.034	1	1.777	0.0442	4.7584
723	IM1	0.0504	1.484	0.0057	0.113	53.868	0.3	0.27	0.3	0.034	1	3.440	0.0337	5.4451
724	IM1	0.0659	1.484	0.0082	0.125	52.779	0.3	0.27	0.3	0.034	1	3.440	0.0441	4.7606
725	IM1	0.077	1.484	0.0108	0.140	52.433	0.3	0.27	0.3	0.034	1	3.440	0.0516	4.4042
726	IM1	0.0541	1.969	0.008	0.148	61.766	0.3	0.27	0.3	0.034	1	6.058	0.0349	5.355
727	IM1	0.0711	1.969	0.0126	0.177	58.546	0.3	0.27	0.3	0.034	1	6.058	0.0458	4.6706
728	IM1	0.082	1.969	0.0166	0.203	56.568	0.3	0.27	0.3	0.034	1	6.058	0.0529	4.3493
729	IM1	0.0566	2.381	0.0095	0.169	64.302	0.3	0.27	0.3	0.034	1	8.859	0.0359	5.2772
730	IM1	0.0741	2.381	0.0154	0.208	61.338	0.3	0.27	0.3	0.034	1	8.859	0.047	4.6108
731	IM1	0.0853	2.381	0.02	0.235	59.933	0.3	0.27	0.3	0.034	1	8.859	0.0541	4.2986
732	IM1	0.0422	0.985	0.0013	0.031	36.370	0.3	0.25	0.3	0.034	1	1.514	0.0326	5.5386
733	IM1	0.0534	1.045	0.0018	0.033	35.637	0.3	0.25	0.3	0.034	1	1.706	0.0403	4.9828
734	IM1	0.0615	1.067	0.0022	0.036	34.663	0.3	0.25	0.3	0.034	1	1.777	0.0461	4.6578
735	IM1	0.0472	1.484	0.0031	0.066	52.422	0.3	0.25	0.3	0.034	1	3.440	0.0326	5.5349
736	IM1	0.0611	1.484	0.0042	0.069	52.400	0.3	0.25	0.3	0.034	1	3.440	0.0422	4.8669
737	IM1	0.0767	1.484	0.0054	0.071	55.147	0.3	0.25	0.3	0.034	1	3.440	0.053	4.3439
738	IM1	0.0549	1.969	0.0063	0.115	63.236	0.3	0.25	0.3	0.034	1	6.058	0.0366	5.2267
739	IM1	0.0714	1.969	0.0065	0.091	60.569	0.3	0.25	0.3	0.034	1	6.058	0.0476	4.5818
740	IM1	0.082	1.969	0.0103	0.126	58.780	0.3	0.25	0.3	0.034	1	6.058	0.0548	4.2736
741	IM1	0.0568	2.626	0.0054	0.095	66.416	0.3	0.25	0.3	0.034	1	10.769	0.0372	5.1667
742	IM1	0.0742	2.626	0.0084	0.113	63.561	0.3	0.25	0.3	0.034	1	10.769	0.0486	4.5361
743	IM1	0.0858	2.626	0.0116	0.135	62.084	0.3	0.25	0.3	0.034	1	10.769	0.0562	4.2194
744	IM1	0.0428	0.985	0.001	0.024	36.482	0.3	0.23	0.3	0.034	1	1.514	0.0339	5.4297
745	IM1	0.0544	1.045	0.0013	0.023	36.525	0.3	0.23	0.3	0.034	1	1.706	0.0422	4.8689
746	IM1	0.0628	1.045	0.0015	0.024	36.213	0.3	0.23	0.3	0.034	1	1.706	0.0487	4.5313
747	IM1	0.0783	1.067	0.0026	0.034	34.261	0.3	0.23	0.3	0.034	1	1.777	0.0603	4.0718
748	IM1	0.0487	1.484	0.0024	0.049	52.144	0.3	0.23	0.3	0.034	1	3.440	0.0349	5.3541
749	IM1	0.0622	1.484	0.0031	0.049	52.022	0.3	0.23	0.3	0.034	1	3.440	0.0445	4.7384
750	IM1	0.0722	1.484	0.0041	0.056	51.252	0.3	0.23	0.3	0.034	1	3.440	0.0517	4.3977
751	IM1	0.0566	2.008	0.0037	0.066	63.066	0.3	0.23	0.3	0.034	1	6.297	0.0392	5.0515
752	IM1	0.0732	2.008	0.0049	0.067	61.072	0.3	0.23	0.3	0.034	1	6.297	0.0507	4.4415
753	IM1	0.0847	2.008	0.0065	0.077	59.205	0.3	0.23	0.3	0.034	1	6.297	0.0586	4.1305
754	IM1	0.0573	2.626	0.0074	0.128	65.708	0.3	0.23	0.3	0.034	1	10.769	0.039	5.0607
755	IM1	0.0747	2.626	0.0071	0.094	63.096	0.3	0.23	0.3	0.034	1	10.769	0.0509	4.4327
756	IM1	0.0864	2.438	0.0088	0.101	61.350	0.3	0.23	0.3	0.034	1	9.286	0.0591	4.1137
757	IM2	0.0441	0.985	0.0353	0.801	4.709	0.3	0.43	0.3	0.034	2	1.514	0.03	2.8855
758	IM2	0.0646	1.067	0.05	0.775	4.983	0.3	0.43	0.3	0.034	2	1.777	0.0418	2.4464
759	IM2	0.081	1.067	0.0607	0.749	10.392	0.3	0.43	0.3	0.034	2	1.777	0.0524	2.1844
760	IM2	0.094	1.067	0.068	0.723	10.001	0.3	0.43	0.3	0.034	2	1.777	0.0608	2.0271
761	IM2	0.1029	1.164	0.0746	0.724	8.272	0.3	0.43	0.3	0.034	2	2.115	0.0635	1.9842
762	IM2	0.1102	1.164	0.08	0.726	7.701	0.3	0.43	0.3	0.034	2	2.115	0.068	1.9174
763	IM2	0.0455	1.484	0.0367	0.807	15.153	0.3	0.43	0.3	0.034	2	3.440	0.0255	3.1314
764	IM2	0.0691	1.484	0.0559	0.809	15.248	0.3	0.43	0.3	0.034	2	3.440	0.0387	2.541
765	IM2	0.0883	1.484	0.0689	0.780	14.730	0.3	0.43	0.3	0.034	2	3.440	0.0495	2.247
766	IM2	0.1086	1.484	0.0808	0.744	15.733	0.3	0.43	0.3	0.034	2	3.440	0.0609	2.0264
767	IM2	0.1294	1.484	0.0915	0.707	16.593	0.3	0.43	0.3	0.034	2	3.440	0.0725	1.8568
768	IM2	0.0474	1.969	0.0395	0.833	25.532	0.3	0.43	0.3	0.034	2	6.058	0.0249	3.1672
769	IM2	0.0711	1.969	0.059	0.830	24.953	0.3	0.43	0.3	0.034	2	6.058	0.0374	2.5864
770	IM2	0.0933	1.969	0.0756	0.810	24.284	0.3	0.43	0.3	0.034	2	6.058	0.0491	2.2571
771	IM2	0.1155	1.969	0.0901	0.780	23.759	0.3	0.43	0.3	0.034	2	6.058	0.0607	2.0287
772	IM2	0.0505	2.438	0.0405	0.802	29.700	0.3	0.43	0.3	0.034	2	9.286	0.0258	3.1107
773	IM2	0.0757	2.438	0.0612	0.808	28.842	0.3	0.43	0.3	0.034	2	9.286	0.0387	2.5407
774	IM2	0.0993	2.438	0.0785	0.791	27.978	0.3	0.43	0.3	0.034	2	9.286	0.0508	2.2187
775	IM2	0.0409	0.985	0.0305	0.745	6.372	0.3	0.38	0.3	0.034	2	1.514	0.0285	2.9634
776	IM2	0.0593	1.045	0.0396	0.668	6.412	0.3	0.38	0.3	0.034	2	1.706	0.0398	2.505
777	IM2	0.0757	1.067	0.0464	0.613	9.164	0.3	0.38	0.3	0.034	2	1.777	0.0503	2.2295
778	IM2	0.0452	1.484	0.0335	0.741	15.081	0.3	0.38	0.3	0.034	2	3.440	0.0265	3.0713
779	IM2	0.0683	1.484	0.0467	0.684	14.419	0.3	0.38	0.3	0.034	2	3.440	0.04	2.4998
780	IM2	0.0878	1.484	0.0563	0.641	14.453	0.3	0.38	0.3	0.034	2	3.440	0.0515	2.2038
781	IM2	0.0483	2.008	0.0364	0.753	26.657	0.3	0.38	0.3	0.034	2	6.297	0.0267	3.0603
782	IM2	0.0721	2.008	0.0518	0.719	26.447	0.3	0.38	0.3	0.034	2	6.297	0.0399	2.5045
783	IM2	0.0953	1.932	0.0636	0.667	26.754	0.3	0.38	0.3	0.034	2	5.831	0.053	2.1725
784	IM2	0.0508	2.498	0.0371	0.730	32.334	0.3	0.38	0.3	0.034	2	9.744	0.0274	3.02
785	IM2	0.0765	2.498	0.0537	0.702	32.071	0.3	0.38	0.3	0.034	2	9.744	0.0413	2.4609
786	IM2	0.1002	2.498	0.0669	0.667	33.269	0.3	0.38	0.3	0.034	2	9.744	0.0541	2.1493
787	IM2	0.0358	0.985	0.0177	0.495	8.204	0.3	0.33	0.3	0.034	2	1.514	0.0257	3.1214
788	IM2	0.0561	1.045	0.024	0.428	8.441	0.3	0.33	0.3	0.034	2	1.706	0.039	2.5318
789	IM2	0.0741	1.067	0.0307	0.414	13.058	0.3	0.33	0.3	0.034	2	1.777	0.051	2.2134
790	IM2	0.0418	1.484	0.0227	0.543	13.814	0.3	0.33	0.3	0.034	2	3.440	0.0258	3.112
791	IM2	0.0631	1.484	0.0326	0.516	16.551	0.3	0.33	0.3	0.034	2	3.440	0.039	2.5316
792	IM2	0.0806	1.484	0.0402	0.499	16.485	0.3	0.33	0.3	0.034	2	3.440	0.0498	2.2407



Table F.1. Conditions for Transmission Tests (cont'd)

Test #	Test Series	H <sub>i</sub> (m)	T <sub>pl</sub> (s)	H <sub>t</sub> (m)	K <sub>t</sub>	K <sub>c</sub> (%)	B (m)	h (m)	h <sub>s</sub> (m)	D <sub>50</sub> (m)	Cotα	L <sub>o</sub> (m)	s <sub>op</sub>	ξ
793	IM2	0.0474	1.969	0.0271	0.572	31.084	0.3	0.33	0.3	0.034	2	6.058	0.0279	2.992
794	IM2	0.0705	1.969	0.0385	0.547	31.575	0.3	0.33	0.3	0.034	2	6.058	0.0415	2.4532
795	IM2	0.0932	1.969	0.0492	0.528	32.035	0.3	0.33	0.3	0.034	2	6.058	0.055	2.133
796	IM2	0.0505	2.56	0.0275	0.545	38.503	0.3	0.33	0.3	0.034	2	10.237	0.029	2.9348
797	IM2	0.075	2.56	0.0401	0.535	39.854	0.3	0.33	0.3	0.034	2	10.237	0.0431	2.4077
798	IM2	0.0981	2.56	0.0517	0.526	40.637	0.3	0.33	0.3	0.034	2	10.237	0.0564	2.1046
799	IM2	0.0346	0.985	0.0048	0.139	17.740	0.3	0.3	0.3	0.034	2	1.514	0.0254	3.1357
800	IM2	0.0547	1.045	0.0102	0.186	15.512	0.3	0.3	0.3	0.034	2	1.706	0.0391	2.53
801	IM2	0.0734	1.067	0.0159	0.217	18.738	0.3	0.3	0.3	0.034	2	1.777	0.052	2.1933
802	IM2	0.0407	1.484	0.0106	0.259	22.514	0.3	0.3	0.3	0.034	2	3.440	0.0261	3.0948
803	IM2	0.0626	1.484	0.0195	0.311	20.978	0.3	0.3	0.3	0.034	2	3.440	0.0401	2.4955
804	IM2	0.0819	1.484	0.0264	0.322	20.703	0.3	0.3	0.3	0.034	2	3.440	0.0525	2.1813
805	IM2	0.0487	1.969	0.0154	0.316	40.929	0.3	0.3	0.3	0.034	2	6.058	0.0299	2.8892
806	IM2	0.0725	1.969	0.0264	0.364	38.151	0.3	0.3	0.3	0.034	2	6.058	0.0446	2.3677
807	IM2	0.0963	1.969	0.037	0.384	36.338	0.3	0.3	0.3	0.034	2	6.058	0.0592	2.055
808	IM2	0.0523	2.381	0.0172	0.329	47.292	0.3	0.3	0.3	0.034	2	8.859	0.0316	2.8113
809	IM2	0.0778	2.381	0.0289	0.372	46.184	0.3	0.3	0.3	0.034	2	8.859	0.047	2.3064
810	IM2	0.1017	2.381	0.0407	0.400	45.078	0.3	0.3	0.3	0.034	2	8.859	0.0615	2.0169
811	IM2	0.037	0.985	0.0022	0.060	20.919	0.3	0.27	0.3	0.034	2	1.514	0.0279	2.9919
812	IM2	0.0483	1.045	0.0027	0.057	18.747	0.3	0.27	0.3	0.034	2	1.706	0.0356	2.6512
813	IM2	0.0569	1.045	0.0036	0.063	17.670	0.3	0.27	0.3	0.034	2	1.706	0.0419	2.4424
814	IM2	0.0416	1.484	0.0046	0.111	28.036	0.3	0.27	0.3	0.034	2	3.440	0.0279	2.9957
815	IM2	0.0549	1.484	0.0063	0.115	26.274	0.3	0.27	0.3	0.034	2	3.440	0.0368	2.6079
816	IM2	0.0643	1.484	0.0086	0.133	25.326	0.3	0.27	0.3	0.034	2	3.440	0.043	2.41
817	IM2	0.0497	1.969	0.0072	0.145	47.944	0.3	0.27	0.3	0.034	2	6.058	0.032	2.7941
818	IM2	0.0653	1.969	0.0111	0.169	44.803	0.3	0.27	0.3	0.034	2	6.058	0.0421	2.4374
819	IM2	0.0756	1.969	0.0141	0.187	43.181	0.3	0.27	0.3	0.034	2	6.058	0.0487	2.2654
820	IM2	0.0538	2.626	0.0085	0.159	56.101	0.3	0.27	0.3	0.034	2	10.769	0.0339	2.714
821	IM2	0.0698	2.626	0.0135	0.193	53.544	0.3	0.27	0.3	0.034	2	10.769	0.044	2.3827
822	IM2	0.0801	2.626	0.0173	0.216	52.066	0.3	0.27	0.3	0.034	2	10.769	0.0506	2.2237
823	IM2	0.0398	0.985	0.0025	0.063	21.477	0.3	0.25	0.3	0.034	2	1.514	0.0308	2.851
824	IM2	0.0522	1.045	0.002	0.038	19.948	0.3	0.25	0.3	0.034	2	1.706	0.0394	2.5189
825	IM2	0.0606	1.045	0.0022	0.037	18.934	0.3	0.25	0.3	0.034	2	1.706	0.0458	2.3376
826	IM2	0.0432	1.484	0.0032	0.074	29.458	0.3	0.25	0.3	0.034	2	3.440	0.0298	2.8943
827	IM2	0.0561	1.484	0.0038	0.068	28.199	0.3	0.25	0.3	0.034	2	3.440	0.0387	2.5402
828	IM2	0.0643	1.484	0.0053	0.082	27.583	0.3	0.25	0.3	0.034	2	3.440	0.0444	2.3727
829	IM2	0.0514	2.008	0.0087	0.169	49.327	0.3	0.25	0.3	0.034	2	6.297	0.0343	2.7013
830	IM2	0.0666	2.008	0.0096	0.145	47.355	0.3	0.25	0.3	0.034	2	6.297	0.0443	2.3743
831	IM2	0.0767	2.008	0.0081	0.106	46.159	0.3	0.25	0.3	0.034	2	6.297	0.0511	2.2118
832	IM2	0.0543	2.438	0.0056	0.104	56.020	0.3	0.25	0.3	0.034	2	9.286	0.0357	2.6458
833	IM2	0.0703	2.438	0.0072	0.103	54.051	0.3	0.25	0.3	0.034	2	9.286	0.0462	2.3261
834	IM2	0.0813	2.438	0.0095	0.117	52.180	0.3	0.25	0.3	0.034	2	9.286	0.0534	2.1638
835	IM2	0.0393	0.985	0.0012	0.029	21.281	0.3	0.23	0.3	0.034	2	1.514	0.0311	2.835
836	IM2	0.051	1.045	0.0015	0.029	19.821	0.3	0.23	0.3	0.034	2	1.706	0.0396	2.5132
837	IM2	0.0597	1.045	0.0016	0.027	18.875	0.3	0.23	0.3	0.034	2	1.706	0.0463	2.3227
838	IM2	0.0439	1.484	0.0043	0.099	29.013	0.3	0.23	0.3	0.034	2	3.440	0.0314	2.8211
839	IM2	0.0561	1.484	0.0025	0.045	28.275	0.3	0.23	0.3	0.034	2	3.440	0.0401	2.4961
840	IM2	0.0654	1.484	0.0029	0.044	27.962	0.3	0.23	0.3	0.034	2	3.440	0.0468	2.3106
841	IM2	0.0534	2.008	0.0031	0.058	49.093	0.3	0.23	0.3	0.034	2	6.297	0.037	2.6004
842	IM2	0.069	2.008	0.0043	0.062	47.868	0.3	0.23	0.3	0.034	2	6.297	0.0477	2.2884
843	IM2	0.0799	2.008	0.0062	0.078	47.013	0.3	0.23	0.3	0.034	2	6.297	0.0553	2.126
844	IM2	0.0557	2.438	0.004	0.072	55.897	0.3	0.23	0.3	0.034	2	9.286	0.0381	2.5616
845	IM2	0.0723	2.438	0.0052	0.072	54.254	0.3	0.23	0.3	0.034	2	9.286	0.0494	2.2499
846	IM2	0.0832	2.438	0.0065	0.078	52.542	0.3	0.23	0.3	0.034	2	9.286	0.0568	2.0972
847	W22	0.0408	0.985	0.0324	0.794	4.192	0.3	0.43	0.3	0.046	2	1.514	0.0278	2.9984
848	W22	0.0635	1.045	0.0494	0.778	4.244	0.3	0.43	0.3	0.046	2	1.706	0.0416	2.4523
849	W22	0.0817	1.067	0.0607	0.743	5.792	0.3	0.43	0.3	0.046	2	1.777	0.0529	2.1747
850	W22	0.0941	1.164	0.0689	0.732	6.470	0.3	0.43	0.3	0.046	2	2.115	0.0581	2.0751
851	W22	0.1035	1.164	0.0761	0.735	7.675	0.3	0.43	0.3	0.046	2	2.115	0.0639	1.9785
852	W22	0.1199	1.249	0.0869	0.725	6.428	0.3	0.43	0.3	0.046	2	2.436	0.0715	1.8692
853	W22	0.0454	1.484	0.035	0.772	12.700	0.3	0.43	0.3	0.046	2	3.440	0.0254	3.1358
854	W22	0.0705	1.484	0.0543	0.771	13.833	0.3	0.43	0.3	0.046	2	3.440	0.0395	2.5151
855	W22	0.0909	1.484	0.0694	0.763	13.730	0.3	0.43	0.3	0.046	2	3.440	0.051	2.2145
856	W22	0.1133	1.484	0.0827	0.730	13.937	0.3	0.43	0.3	0.046	2	3.440	0.0635	1.9836
857	W22	0.1335	1.484	0.0939	0.703	15.938	0.3	0.43	0.3	0.046	2	3.440	0.0748	1.8277
858	W22	0.1731	1.484	0.1111	0.642	18.123	0.3	0.43	0.3	0.046	2	3.440	0.097	1.6052
859	W22	0.0491	1.969	0.0387	0.788	22.833	0.3	0.43	0.3	0.046	2	6.058	0.0258	3.1125
860	W22	0.073	1.969	0.0585	0.801	22.116	0.3	0.43	0.3	0.046	2	6.058	0.0384	2.5513
861	W22	0.0958	1.969	0.0761	0.794	21.476	0.3	0.43	0.3	0.046	2	6.058	0.0504	2.2274
862	W22	0.1188	1.969	0.0914	0.769	21.000	0.3	0.43	0.3	0.046	2	6.058	0.0625	2.0006
863	W22	0.163	1.969	0.1138	0.698	21.263	0.3	0.43	0.3	0.046	2	6.058	0.0857	1.7076
864	W22	0.0525	2.438	0.0401	0.764	26.806	0.3	0.43	0.3	0.046	2	9.286	0.0269	3.0502



Table F.1. Conditions for Transmission Tests (cont'd)

Test #	Test Series	H <sub>i</sub> (m)	T <sub>pi</sub> (s)	H <sub>i</sub> (m)	K <sub>r</sub>	K <sub>r</sub> (%)	B (m)	h (m)	h <sub>a</sub> (m)	D <sub>50</sub> (m)	Cotα	L <sub>c</sub> (m)	s <sub>op</sub>	ξ
865	W22	0.0806	2.438	0.0622	0.772	25.679	0.3	0.43	0.3	0.046	2	9.286	0.0412	2.4629
866	W22	0.1057	2.438	0.0816	0.772	25.132	0.3	0.43	0.3	0.046	2	9.286	0.0541	2.1504
867	W22	0.1319	2.438	0.0983	0.745	24.568	0.3	0.43	0.3	0.046	2	9.286	0.0675	1.925
868	W22	0.1841	2.438	0.1281	0.696	24.616	0.3	0.43	0.3	0.046	2	9.286	0.0942	1.6291
869	W22	0.0394	0.985	0.0299	0.758	4.900	0.3	0.38	0.3	0.046	2	1.514	0.0274	3.019
870	W22	0.0605	1.024	0.0436	0.720	5.478	0.3	0.38	0.3	0.046	2	1.638	0.0411	2.4656
871	W22	0.0783	1.164	0.0516	0.659	6.914	0.3	0.38	0.3	0.046	2	2.115	0.0499	2.2386
872	W22	0.0898	1.164	0.0584	0.650	7.254	0.3	0.38	0.3	0.046	2	2.115	0.0572	2.0897
873	W22	0.1096	1.164	0.0686	0.626	9.058	0.3	0.38	0.3	0.046	2	2.115	0.0698	1.8921
874	W22	0.0455	1.463	0.0342	0.752	13.415	0.3	0.38	0.3	0.046	2	3.343	0.0267	3.0578
875	W22	0.0701	1.463	0.0502	0.716	13.124	0.3	0.38	0.3	0.046	2	3.343	0.0412	2.4623
876	W22	0.091	1.463	0.062	0.681	13.638	0.3	0.38	0.3	0.046	2	3.343	0.0535	2.161
877	W22	0.1131	1.463	0.0723	0.639	14.490	0.3	0.38	0.3	0.046	2	3.343	0.0666	1.9381
878	W22	0.1527	1.484	0.0875	0.573	18.788	0.3	0.38	0.3	0.046	2	3.440	0.0895	1.6713
879	W22	0.0468	2.008	0.0372	0.796	24.181	0.3	0.38	0.3	0.046	2	6.297	0.0258	3.1102
880	W22	0.0694	2.008	0.054	0.779	23.601	0.3	0.38	0.3	0.046	2	6.297	0.0383	2.5536
881	W22	0.0917	1.932	0.0682	0.744	23.098	0.3	0.38	0.3	0.046	2	5.831	0.051	2.2147
882	W22	0.1392	1.932	0.0911	0.655	24.142	0.3	0.38	0.3	0.046	2	5.831	0.0773	1.7979
883	W22	0.0492	2.498	0.0382	0.776	28.831	0.3	0.38	0.3	0.046	2	9.744	0.0266	3.0674
884	W22	0.0733	2.498	0.0559	0.762	28.297	0.3	0.38	0.3	0.046	2	9.744	0.0396	2.5125
885	W22	0.0963	2.498	0.0703	0.730	28.396	0.3	0.38	0.3	0.046	2	9.744	0.052	2.1922
886	W22	0.1453	2.498	0.1279	0.880	29.416	0.3	0.38	0.3	0.046	2	9.744	0.0785	1.7851
887	W22	0.0352	0.985	0.0231	0.656	7.014	0.3	0.33	0.3	0.046	2	1.514	0.0252	3.1466
888	W22	0.0544	1.045	0.0296	0.544	7.027	0.3	0.33	0.3	0.046	2	1.706	0.0378	2.5705
889	W22	0.0725	1.067	0.0352	0.485	12.748	0.3	0.33	0.3	0.046	2	1.777	0.0499	2.2376
890	W22	0.0849	1.164	0.0402	0.473	14.386	0.3	0.33	0.3	0.046	2	2.115	0.0564	2.1051
891	W22	0.1046	1.191	0.0487	0.466	11.678	0.3	0.33	0.3	0.046	2	2.215	0.0689	1.9047
892	W22	0.0406	1.484	0.026	0.640	10.505	0.3	0.33	0.3	0.046	2	3.440	0.0251	3.1578
893	W22	0.0621	1.484	0.0359	0.577	11.392	0.3	0.33	0.3	0.046	2	3.440	0.0384	2.5521
894	W22	0.0806	1.484	0.0441	0.547	13.692	0.3	0.33	0.3	0.046	2	3.440	0.0498	2.2402
895	W22	0.1004	1.484	0.0533	0.531	13.583	0.3	0.33	0.3	0.046	2	3.440	0.0621	2.0071
896	W22	0.1409	1.484	0.0686	0.487	15.811	0.3	0.33	0.3	0.046	2	3.440	0.0871	1.6942
897	W22	0.0467	1.969	0.03	0.643	25.329	0.3	0.33	0.3	0.046	2	6.058	0.0275	3.0144
898	W22	0.0697	1.969	0.0427	0.613	25.763	0.3	0.33	0.3	0.046	2	6.058	0.041	2.4679
899	W22	0.0923	1.969	0.0538	0.583	25.871	0.3	0.33	0.3	0.046	2	6.058	0.0544	2.1441
900	W22	0.1398	1.969	0.073	0.522	27.216	0.3	0.33	0.3	0.046	2	6.058	0.0824	1.7418
901	W22	0.0502	2.56	0.0322	0.641	31.518	0.3	0.33	0.3	0.046	2	10.237	0.0289	2.9421
902	W22	0.0745	2.56	0.0457	0.613	32.354	0.3	0.33	0.3	0.046	2	10.237	0.0429	2.4145
903	W22	0.0975	2.381	0.0573	0.588	33.722	0.3	0.33	0.3	0.046	2	8.859	0.0564	2.1054
904	W22	0.1467	2.381	0.0802	0.547	35.622	0.3	0.33	0.3	0.046	2	8.859	0.0849	1.7164
905	W22	0.0344	0.985	0.0138	0.401	8.224	0.3	0.3	0.3	0.046	2	1.514	0.0252	3.1474
906	W22	0.0543	1.045	0.0201	0.370	8.678	0.3	0.3	0.3	0.046	2	1.706	0.0388	2.5386
907	W22	0.0724	1.067	0.0258	0.356	13.734	0.3	0.3	0.3	0.046	2	1.777	0.0513	2.2082
908	W22	0.0858	1.164	0.0298	0.347	15.934	0.3	0.3	0.3	0.046	2	2.115	0.0588	2.0623
909	W22	0.1042	1.164	0.0379	0.364	12.128	0.3	0.3	0.3	0.046	2	2.115	0.0714	1.8712
910	W22	0.0401	1.484	0.0187	0.467	11.093	0.3	0.3	0.3	0.046	2	3.440	0.0257	3.1166
911	W22	0.0621	1.484	0.0277	0.445	12.635	0.3	0.3	0.3	0.046	2	3.440	0.0399	2.5045
912	W22	0.0814	1.484	0.0361	0.444	13.922	0.3	0.3	0.3	0.046	2	3.440	0.0522	2.1878
913	W22	0.1024	1.484	0.0457	0.446	14.929	0.3	0.3	0.3	0.046	2	3.440	0.0657	1.9505
914	W22	0.1434	1.484	0.0601	0.419	17.105	0.3	0.3	0.3	0.046	2	3.440	0.092	1.6483
915	W22	0.0476	1.969	0.024	0.504	27.233	0.3	0.3	0.3	0.046	2	6.058	0.0292	2.9245
916	W22	0.071	1.969	0.0353	0.498	27.602	0.3	0.3	0.3	0.046	2	6.058	0.0436	2.3943
917	W22	0.0943	1.969	0.0465	0.494	27.585	0.3	0.3	0.3	0.046	2	6.058	0.0579	2.0771
918	W22	0.1431	1.969	0.0647	0.452	28.562	0.3	0.3	0.3	0.046	2	6.058	0.088	1.686
919	W22	0.0514	2.381	0.0259	0.504	34.489	0.3	0.3	0.3	0.046	2	8.859	0.031	2.8377
920	W22	0.0764	2.381	0.0381	0.499	35.774	0.3	0.3	0.3	0.046	2	8.859	0.0462	2.3272
921	W22	0.1	2.381	0.0488	0.488	36.377	0.3	0.3	0.3	0.046	2	8.859	0.0604	2.0337
922	W22	0.1502	2.381	0.0708	0.471	38.942	0.3	0.3	0.3	0.046	2	8.859	0.0907	1.6598
923	W22	0.037	0.985	0.0061	0.164	16.276	0.3	0.27	0.3	0.046	2	1.514	0.0279	2.9908
924	W22	0.0568	1.045	0.0104	0.184	14.375	0.3	0.27	0.3	0.046	2	1.706	0.0418	2.4447
925	W22	0.0414	1.484	0.0111	0.269	23.036	0.3	0.27	0.3	0.046	2	3.440	0.0277	3.0037
926	W22	0.0636	1.484	0.0195	0.307	19.851	0.3	0.27	0.3	0.046	2	3.440	0.0426	2.4239
927	W22	0.0484	1.969	0.015	0.311	39.354	0.3	0.27	0.3	0.046	2	6.058	0.0312	2.8315
928	W22	0.0732	1.969	0.0256	0.350	35.943	0.3	0.27	0.3	0.046	2	6.058	0.0471	2.3027
929	W22	0.0522	2.626	0.017	0.326	46.256	0.3	0.27	0.3	0.046	2	10.769	0.0329	2.7549
930	W22	0.0778	2.626	0.0283	0.363	43.837	0.3	0.27	0.3	0.046	2	10.769	0.0491	2.2558
931	W22	0.0392	0.985	0.0051	0.129	22.747	0.3	0.25	0.3	0.046	2	1.514	0.0302	2.8758
932	W22	0.0592	1.045	0.0069	0.116	17.974	0.3	0.25	0.3	0.046	2	1.706	0.0447	2.3652
933	W22	0.042	1.484	0.0082	0.196	24.930	0.3	0.25	0.3	0.046	2	3.440	0.029	2.9347
934	W22	0.0635	1.484	0.012	0.188	21.625	0.3	0.25	0.3	0.046	2	3.440	0.0439	2.3865
935	W22	0.0503	2.008	0.0109	0.217	41.479	0.3	0.25	0.3	0.046	2	6.297	0.0335	2.7311
936	W22	0.0751	2.008	0.017	0.227	38.154	0.3	0.25	0.3	0.046	2	6.297	0.0501	2.2348

Table F.1. Conditions for Transmission Tests (cont'd)

Test #	Test Series	H <sub>i</sub> (m)	T <sub>pi</sub> (s)	H <sub>t</sub> (m)	K <sub>i</sub>	K <sub>c</sub> (%)	B (m)	h (m)	h <sub>s</sub> (m)	D <sub>50</sub> (m)	Cota	L <sub>o</sub> (m)	s <sub>op</sub>	ξ
937	W22	0.0529	2.438	0.0124	0.234	49.337	0.3	0.25	0.3	0.046	2	9.286	0.0348	2.6813
938	W22	0.0793	2.438	0.0199	0.251	44.793	0.3	0.25	0.3	0.046	2	9.286	0.0521	2.1898
939	W22	0.0395	0.985	0.003	0.076	22.085	0.3	0.23	0.3	0.046	2	1.514	0.0313	2.8277
940	W22	0.0589	1.045	0.0041	0.070	19.874	0.3	0.23	0.3	0.046	2	1.706	0.0457	2.3388
941	W22	0.0429	1.484	0.0061	0.141	23.867	0.3	0.23	0.3	0.046	2	3.440	0.0307	2.852
942	W22	0.0649	1.484	0.0085	0.131	21.778	0.3	0.23	0.3	0.046	2	3.440	0.0465	2.3196
943	W22	0.0517	2.008	0.0083	0.162	41.969	0.3	0.23	0.3	0.046	2	6.297	0.0358	2.6444
944	W22	0.0773	2.008	0.0125	0.162	40.108	0.3	0.23	0.3	0.046	2	6.297	0.0535	2.1613
945	W22	0.0536	2.438	0.01	0.186	50.437	0.3	0.23	0.3	0.046	2	9.286	0.0366	2.6121
946	W22	0.0801	2.438	0.015	0.188	47.215	0.3	0.23	0.3	0.046	2	9.286	0.0547	2.1372
947	W32	0.038	0.985	0.0328	0.864	4.290	0.3	0.43	0.3	0.054	2	1.514	0.0259	3.1062
948	W32	0.0603	1.045	0.0506	0.839	3.860	0.3	0.43	0.3	0.054	2	1.706	0.0395	2.5165
949	W32	0.0781	1.067	0.0627	0.803	5.496	0.3	0.43	0.3	0.054	2	1.777	0.0505	2.2249
950	W32	0.0917	1.164	0.0707	0.771	10.462	0.3	0.43	0.3	0.054	2	2.115	0.0566	2.1023
951	W32	0.1	1.164	0.0778	0.778	7.172	0.3	0.43	0.3	0.054	2	2.115	0.0617	2.0129
952	W32	0.115	1.164	0.0886	0.771	6.625	0.3	0.43	0.3	0.054	2	2.115	0.071	1.877
953	W32	0.043	1.484	0.0363	0.844	14.146	0.3	0.43	0.3	0.054	2	3.440	0.0241	3.2219
954	W32	0.0672	1.484	0.0554	0.824	13.125	0.3	0.43	0.3	0.054	2	3.440	0.0377	2.576
955	W32	0.0864	1.484	0.0707	0.818	13.275	0.3	0.43	0.3	0.054	2	3.440	0.0485	2.2715
956	W32	0.0907	1.177	0.0693	0.764	10.634	0.3	0.43	0.3	0.054	2	2.164	0.0556	2.12
957	W32	0.1287	1.484	0.0956	0.743	14.845	0.3	0.43	0.3	0.054	2	3.440	0.0721	1.8618
958	W32	0.1668	1.484	0.1135	0.681	17.845	0.3	0.43	0.3	0.054	2	3.440	0.0935	1.6354
959	W32	0.0468	1.969	0.0396	0.847	20.746	0.3	0.43	0.3	0.054	2	6.058	0.0246	3.1865
960	W32	0.0702	1.969	0.0596	0.849	20.498	0.3	0.43	0.3	0.054	2	6.058	0.0369	2.6021
961	W32	0.0926	1.969	0.0777	0.839	20.091	0.3	0.43	0.3	0.054	2	6.058	0.0487	2.2658
962	W32	0.115	1.969	0.0933	0.811	19.759	0.3	0.43	0.3	0.054	2	6.058	0.0605	2.033
963	W32	0.1577	1.969	0.1147	0.727	20.273	0.3	0.43	0.3	0.054	2	6.058	0.0829	1.7361
964	W32	0.0511	2.438	0.0422	0.826	25.117	0.3	0.43	0.3	0.054	2	9.286	0.0261	3.092
965	W32	0.0755	2.438	0.0627	0.830	24.984	0.3	0.43	0.3	0.054	2	9.286	0.0386	2.5435
966	W32	0.099	2.438	0.082	0.829	24.385	0.3	0.43	0.3	0.054	2	9.286	0.0506	2.2222
967	W32	0.1238	2.438	0.0992	0.801	24.007	0.3	0.43	0.3	0.054	2	9.286	0.0633	1.9866
968	W32	0.1743	2.438	0.1258	0.721	24.170	0.3	0.43	0.3	0.054	2	9.286	0.0892	1.6743
969	W32	0.0368	0.985	0.0301	0.817	4.889	0.3	0.38	0.3	0.054	2	1.514	0.0256	3.1234
970	W32	0.0567	1.045	0.044	0.775	5.181	0.3	0.38	0.3	0.054	2	1.706	0.0381	2.5604
971	W32	0.0742	1.067	0.0537	0.724	6.554	0.3	0.38	0.3	0.054	2	1.777	0.0493	2.2519
972	W32	0.087	1.164	0.0599	0.689	11.753	0.3	0.38	0.3	0.054	2	2.115	0.0555	2.1232
973	W32	0.1046	1.249	0.0709	0.678	7.020	0.3	0.38	0.3	0.054	2	2.436	0.0648	1.9646
974	W32	0.0425	1.484	0.0342	0.805	13.071	0.3	0.38	0.3	0.054	2	3.440	0.0249	3.1693
975	W32	0.065	1.484	0.051	0.785	12.622	0.3	0.38	0.3	0.054	2	3.440	0.0381	2.562
976	W32	0.0842	1.484	0.063	0.748	12.744	0.3	0.38	0.3	0.054	2	3.440	0.0494	2.2505
977	W32	0.1045	1.484	0.073	0.699	13.891	0.3	0.38	0.3	0.054	2	3.440	0.0612	2.0206
978	W32	0.144	1.484	0.0899	0.625	17.639	0.3	0.38	0.3	0.054	2	3.440	0.0844	1.7215
979	W32	0.0461	2.008	0.0381	0.826	23.686	0.3	0.38	0.3	0.054	2	6.297	0.0255	3.131
980	W32	0.0693	2.008	0.0555	0.800	22.947	0.3	0.38	0.3	0.054	2	6.297	0.0383	2.5544
981	W32	0.0919	1.969	0.0699	0.761	22.434	0.3	0.38	0.3	0.054	2	6.058	0.0509	2.2152
982	W32	0.1389	1.932	0.0924	0.665	23.511	0.3	0.38	0.3	0.054	2	5.831	0.0772	1.7997
983	W32	0.0495	2.498	0.0389	0.787	27.303	0.3	0.38	0.3	0.054	2	9.744	0.0267	3.058
984	W32	0.0739	2.498	0.0571	0.773	26.907	0.3	0.38	0.3	0.054	2	9.744	0.0399	2.503
985	W32	0.0969	2.498	0.0718	0.741	27.253	0.3	0.38	0.3	0.054	2	9.744	0.0523	2.1855
986	W32	0.1461	2.498	0.097	0.664	28.577	0.3	0.38	0.3	0.054	2	9.744	0.0789	1.78
987	W32	0.0357	0.985	0.025	0.699	5.451	0.3	0.33	0.3	0.054	2	1.514	0.0256	3.1244
988	W32	0.0548	1.045	0.032	0.584	5.574	0.3	0.33	0.3	0.054	2	1.706	0.0381	2.5608
989	W32	0.0726	1.067	0.0375	0.516	11.358	0.3	0.33	0.3	0.054	2	1.777	0.05	2.2358
990	W32	0.0851	1.164	0.0424	0.498	14.833	0.3	0.33	0.3	0.054	2	2.115	0.0566	2.102
991	W32	0.1048	1.219	0.0506	0.483	11.033	0.3	0.33	0.3	0.054	2	2.321	0.0685	1.9107
992	W32	0.0408	1.484	0.0284	0.697	10.311	0.3	0.33	0.3	0.054	2	3.440	0.0252	3.1506
993	W32	0.0629	1.484	0.0389	0.620	10.483	0.3	0.33	0.3	0.054	2	3.440	0.0388	2.5368
994	W32	0.0817	1.484	0.047	0.575	12.347	0.3	0.33	0.3	0.054	2	3.440	0.0505	2.2255
995	W32	0.102	1.484	0.0555	0.544	13.838	0.3	0.33	0.3	0.054	2	3.440	0.063	1.9917
996	W32	0.1428	1.484	0.07	0.490	15.574	0.3	0.33	0.3	0.054	2	3.440	0.0883	1.6829
997	W32	0.0471	1.969	0.0322	0.683	25.216	0.3	0.33	0.3	0.054	2	6.058	0.0278	3.0007
998	W32	0.071	1.969	0.0453	0.638	25.657	0.3	0.33	0.3	0.054	2	6.058	0.0418	2.4447
999	W32	0.0942	1.969	0.0564	0.599	26.483	0.3	0.33	0.3	0.054	2	6.058	0.0555	2.1225
1000	W32	0.1425	1.969	0.0742	0.520	27.758	0.3	0.33	0.3	0.054	2	6.058	0.084	1.7254
1001	W32	0.0507	2.498	0.0332	0.655	30.621	0.3	0.33	0.3	0.054	2	9.744	0.0292	2.9241
1002	W32	0.0758	2.498	0.0467	0.616	32.291	0.3	0.33	0.3	0.054	2	9.744	0.0437	2.3931
1003	W32	0.0993	2.498	0.0585	0.589	33.454	0.3	0.33	0.3	0.054	2	9.744	0.0572	2.0899
1004	W32	0.149	2.381	0.0783	0.525	36.338	0.3	0.33	0.3	0.054	2	8.859	0.0862	1.7034
1005	W32	0.0348	0.985	0.0157	0.451	9.659	0.3	0.3	0.3	0.054	2	1.514	0.0256	3.1272
1006	W32	0.0548	1.045	0.0226	0.412	10.192	0.3	0.3	0.3	0.054	2	1.706	0.0391	2.5279
1007	W32	0.0729	1.067	0.0282	0.387	15.240	0.3	0.3	0.3	0.054	2	1.777	0.0516	2.2017
1008	W32	0.0863	1.164	0.0324	0.376	15.507	0.3	0.3	0.3	0.054	2	2.115	0.0591	2.0569

Table F.1. Conditions for Transmission Tests (cont'd)

Test #	Test Series	H <sub>i</sub> (m)	T <sub>ci</sub> (s)	H <sub>t</sub> (m)	K <sub>t</sub>	K <sub>r</sub> (%)	B (m)	h (m)	h <sub>a</sub> (m)	D <sub>50</sub> (m)	Cota	L <sub>o</sub> (m)	s <sub>op</sub>	ξ
1009	W32	0.1046	1.164	0.0395	0.378	13.019	0.3	0.3	0.3	0.054	2	2.115	0.0717	1.8678
1010	W32	0.0406	1.484	0.0207	0.510	12.426	0.3	0.3	0.3	0.054	2	3.440	0.026	3.099
1011	W32	0.0627	1.484	0.0298	0.475	13.905	0.3	0.3	0.3	0.054	2	3.440	0.0402	2.4936
1012	W32	0.0818	1.484	0.0368	0.449	14.969	0.3	0.3	0.3	0.054	2	3.440	0.0525	2.1822
1013	W32	0.1029	1.484	0.0461	0.448	15.517	0.3	0.3	0.3	0.054	2	3.440	0.066	1.946
1014	W32	0.1439	1.484	0.0595	0.414	17.238	0.3	0.3	0.3	0.054	2	3.440	0.0923	1.6459
1015	W32	0.0479	1.969	0.0276	0.576	27.900	0.3	0.3	0.3	0.054	2	6.058	0.0295	2.9134
1016	W32	0.0697	1.969	0.0377	0.541	28.273	0.3	0.3	0.3	0.054	2	6.058	0.0429	2.4148
1017	W32	0.0921	1.969	0.0464	0.503	28.543	0.3	0.3	0.3	0.054	2	6.058	0.0566	2.1014
1018	W32	0.14	1.969	0.0637	0.455	29.794	0.3	0.3	0.3	0.054	2	6.058	0.0861	1.7042
1019	W32	0.05	2.381	0.0273	0.546	33.374	0.3	0.3	0.3	0.054	2	8.859	0.0302	2.8764
1020	W32	0.0746	2.381	0.0397	0.532	34.683	0.3	0.3	0.3	0.054	2	8.859	0.0451	2.3552
1021	W32	0.0978	2.381	0.0504	0.516	35.856	0.3	0.3	0.3	0.054	2	8.859	0.0591	2.0568
1022	W32	0.147	2.381	0.0705	0.479	38.984	0.3	0.3	0.3	0.054	2	8.859	0.0888	1.6775
1023	W32	0.0361	0.985	0.0065	0.180	18.912	0.3	0.27	0.3	0.054	2	1.514	0.0273	3.0282
1024	W32	0.0557	1.045	0.0105	0.189	15.962	0.3	0.27	0.3	0.054	2	1.706	0.041	2.4686
1025	W32	0.0872	1.164	0.0181	0.207	22.400	0.3	0.27	0.3	0.054	2	2.115	0.0619	2.0096
1026	W32	0.0392	1.506	0.011	0.281	20.801	0.3	0.27	0.3	0.054	2	3.542	0.0262	3.0887
1027	W32	0.0625	1.484	0.0181	0.289	18.348	0.3	0.27	0.3	0.054	2	3.440	0.0418	2.4442
1028	W32	0.1039	1.484	0.0314	0.302	18.144	0.3	0.27	0.3	0.054	2	3.440	0.0695	1.8961
1029	W32	0.0476	1.969	0.0156	0.328	37.965	0.3	0.27	0.3	0.054	2	6.058	0.0307	2.8548
1030	W32	0.0723	1.969	0.0244	0.338	34.727	0.3	0.27	0.3	0.054	2	6.058	0.0466	2.3163
1031	W32	0.1203	1.969	0.0416	0.346	33.113	0.3	0.27	0.3	0.054	2	6.058	0.0775	1.7959
1032	W32	0.0514	2.626	0.0175	0.341	45.059	0.3	0.27	0.3	0.054	2	10.769	0.0325	2.7753
1033	W32	0.0758	2.626	0.0277	0.365	42.815	0.3	0.27	0.3	0.054	2	10.769	0.0479	2.2856
1034	W32	0.1238	2.438	0.0453	0.366	42.278	0.3	0.27	0.3	0.054	2	9.286	0.0785	1.7851
1035	W32	0.0386	0.985	0.0058	0.149	23.291	0.3	0.25	0.3	0.054	2	1.514	0.0298	2.8962
1036	W32	0.059	1.045	0.0076	0.128	19.002	0.3	0.25	0.3	0.054	2	1.706	0.0446	2.3687
1037	W32	0.0894	1.164	0.012	0.134	23.511	0.3	0.25	0.3	0.054	2	2.115	0.0652	1.9587
1038	W32	0.0415	1.484	0.0092	0.221	22.990	0.3	0.25	0.3	0.054	2	3.440	0.0287	2.9525
1039	W32	0.0624	1.484	0.0128	0.205	20.591	0.3	0.25	0.3	0.054	2	3.440	0.0431	2.4081
1040	W32	0.1029	1.484	0.0225	0.219	19.946	0.3	0.25	0.3	0.054	2	3.440	0.0711	1.8755
1041	W32	0.049	2.008	0.0116	0.237	41.509	0.3	0.25	0.3	0.054	2	6.297	0.0327	2.7662
1042	W32	0.0735	2.008	0.0181	0.247	38.287	0.3	0.25	0.3	0.054	2	6.297	0.0489	2.2601
1043	W32	0.1225	1.969	0.0313	0.255	36.992	0.3	0.25	0.3	0.054	2	6.058	0.0817	1.7491
1044	W32	0.0515	2.438	0.0129	0.251	48.814	0.3	0.25	0.3	0.054	2	9.286	0.0339	2.7167
1045	W32	0.0776	2.438	0.02	0.258	44.807	0.3	0.25	0.3	0.054	2	9.286	0.051	2.2139
1046	W32	0.1285	2.438	0.0362	0.282	41.089	0.3	0.25	0.3	0.054	2	9.286	0.0844	1.721
1047	W32	0.0386	0.985	0.0032	0.083	20.520	0.3	0.23	0.3	0.054	2	1.514	0.0306	2.8588
1048	W32	0.0575	1.045	0.0044	0.076	17.569	0.3	0.23	0.3	0.054	2	1.706	0.0446	2.367
1049	W32	0.0861	1.164	0.0068	0.079	23.372	0.3	0.23	0.3	0.054	2	2.115	0.0647	1.9658
1050	W32	0.0424	1.484	0.0062	0.146	20.531	0.3	0.23	0.3	0.054	2	3.440	0.0303	2.8709
1051	W32	0.0638	1.484	0.0085	0.133	20.176	0.3	0.23	0.3	0.054	2	3.440	0.0457	2.3396
1052	W32	0.1035	1.484	0.0142	0.137	20.571	0.3	0.23	0.3	0.054	2	3.440	0.0741	1.8373
1053	W32	0.0509	2.008	0.0085	0.167	41.036	0.3	0.23	0.3	0.054	2	6.297	0.0352	2.665
1054	W32	0.0763	2.008	0.0124	0.162	39.936	0.3	0.23	0.3	0.054	2	6.297	0.0528	2.1753
1055	W32	0.1256	2.008	0.0222	0.176	39.086	0.3	0.23	0.3	0.054	2	6.297	0.0869	1.6961
1056	W32	0.0529	2.438	0.0101	0.190	48.064	0.3	0.23	0.3	0.054	2	9.286	0.0362	2.6292
1057	W32	0.0793	2.438	0.0146	0.185	45.813	0.3	0.23	0.3	0.054	2	9.286	0.0542	2.1477
1058	W32	0.1305	2.438	0.0256	0.196	43.094	0.3	0.23	0.3	0.054	2	9.286	0.0892	1.674



Table F.2. Conditions and Damage of the Stability Tests (cont'd)

Tests	H <sub>i</sub> (m)	T <sub>p</sub> (s)	B (m)	h <sub>c</sub> (m)	h (m)	D <sub>50</sub> (m)	Cotα	ξ	H/AD <sub>50</sub>	# of units Displaced			% Damage			S			S <sub>N</sub>			S <sub>A</sub>							
										FS	C	BS	Total	FS	C	BS	Total	FS	C	BS	Total	FS	C	BS	Total	FS	C	BS	Total
SN11	0.11	1.5	0.3	0.3	0.23	0.034	2	2.81	2.01	28	2	0	30	5	1	0	6	3	0	1	4	2	0	2	2	0	0	3	
SN12	0.11	1.48	0.3	0.3	0.23	0.034	2	2.76	2.03	33	3	0	36	6	1	0	7	5	0	1	6	2	0	2	4	0	0	5	
SN13	0.11	1.48	0.3	0.3	0.23	0.034	2	2.75	2.04	33	3	0	36	6	1	0	7	6	0	1	6	2	0	2	4	0	0	5	
SS1	0.14	2.01	0.3	0.3	0.38	0.034	1	6.63	2.59	51	56	4	111	14	23	1	39	6	4	1	10	3	4	0	7	6	4	0	10
SS2	0.15	2	0.3	0.3	0.23	0.034	1	6.45	2.71	F	F	F	F	F	F	F	F	F	F	F	F	F	F	F	F	F	F	F	
SP1	0.13	1.49	0.3	0.3	0.38	0.034	2	2.60	2.33	10	2	0	12	2	1	0	3	2	1	0	3	1	0	1	1	0	0	1	
SP2	0.14	1.48	0.3	0.3	0.23	0.034	2	2.50	2.47	115	16	0	131	21	5	0	27	4	5	2	11	7	1	0	8	4	1	0	11
SC1	0.06	1.06	0.3	0.3	0.23	0.034	2	2.68	1.11	0	0	0	0	0	0	0	0	2	1	0	3	0	0	0	0	0	0	0	0
SC2	0.09	1.5	0.3	0.3	0.23	0.034	2	3.13	1.62	20	0	0	20	4	0	0	4	4	1	0	6	1	0	0	1	2	0	0	2
SC3	0.13	2.01	0.3	0.3	0.23	0.034	2	3.55	2.26	85	10	9	104	16	3	2	21	9	2	0	11	6	1	1	7	9	1	1	11
SC4	0.09	1.5	0.3	0.3	0.23	0.034	2	3.11	1.64	85	10	9	104	16	3	2	21	8	2	1	11	6	1	1	7	8	1	1	11
SC5	0.06	1.06	0.3	0.3	0.23	0.034	2	2.64	1.14	85	10	9	104	16	3	2	21	8	4	3	11	6	1	1	7	8	1	1	11

Note  
F = Totally damage

# APPENDIX G

## PHOTOGRAPHS

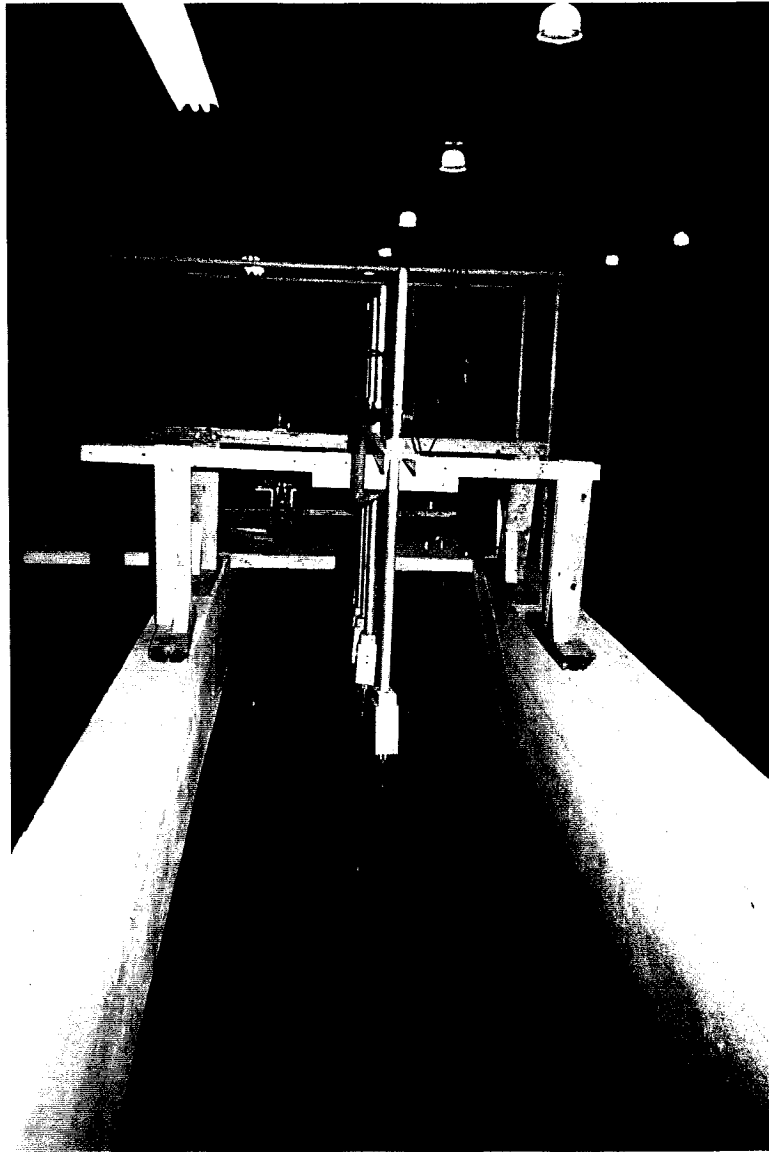


**Fig. G1.** Top view of the wave flume, looking in the direction of wave paddle.

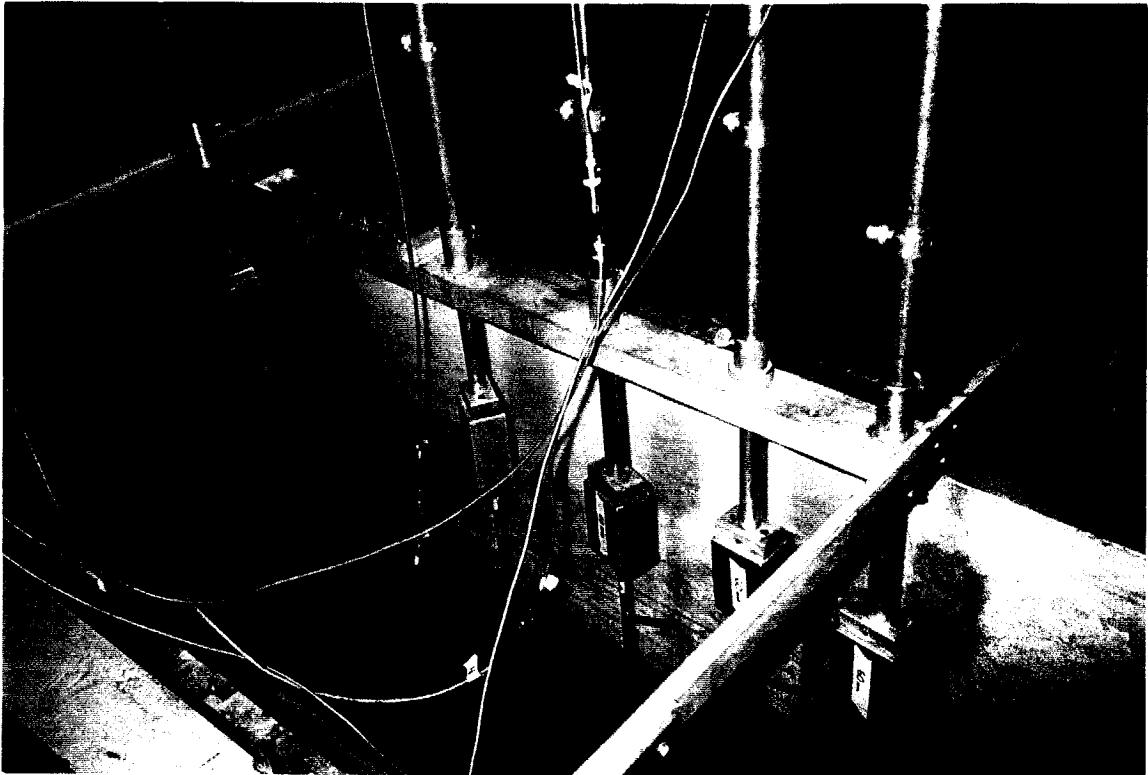


**Fig. G2.** Water level transducer, showing the array of five wave probes.

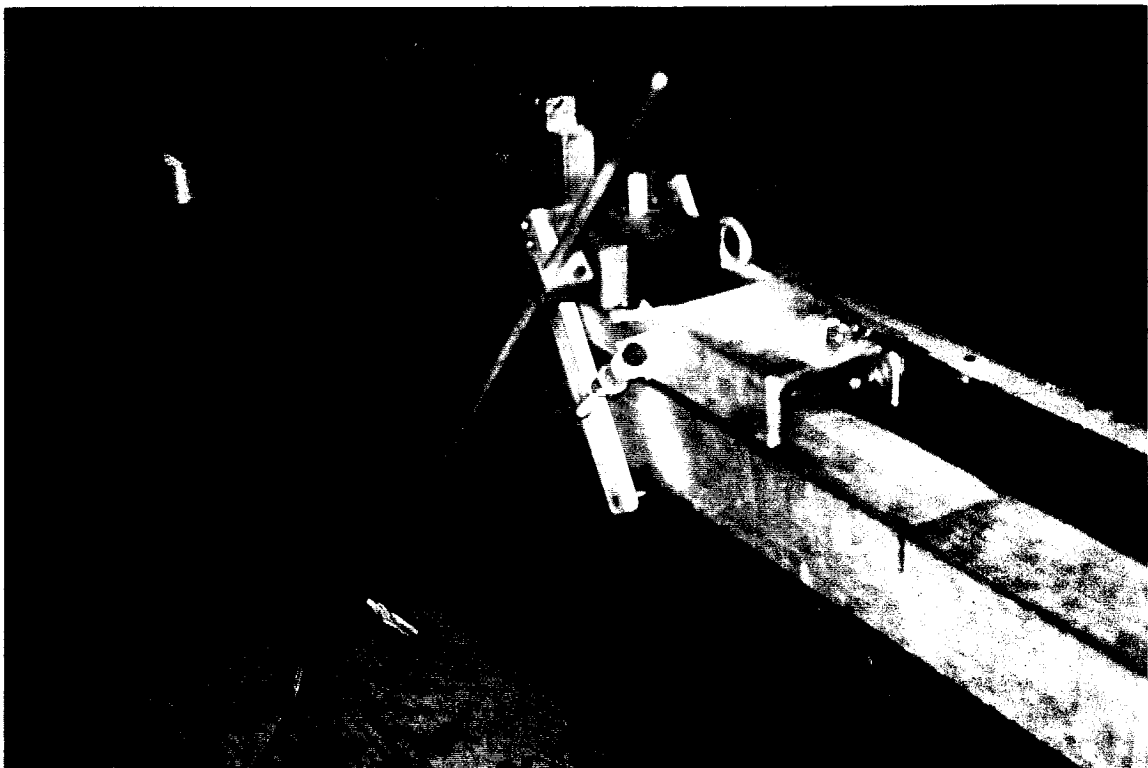


**Fig. G3.** Mechanical profiler.



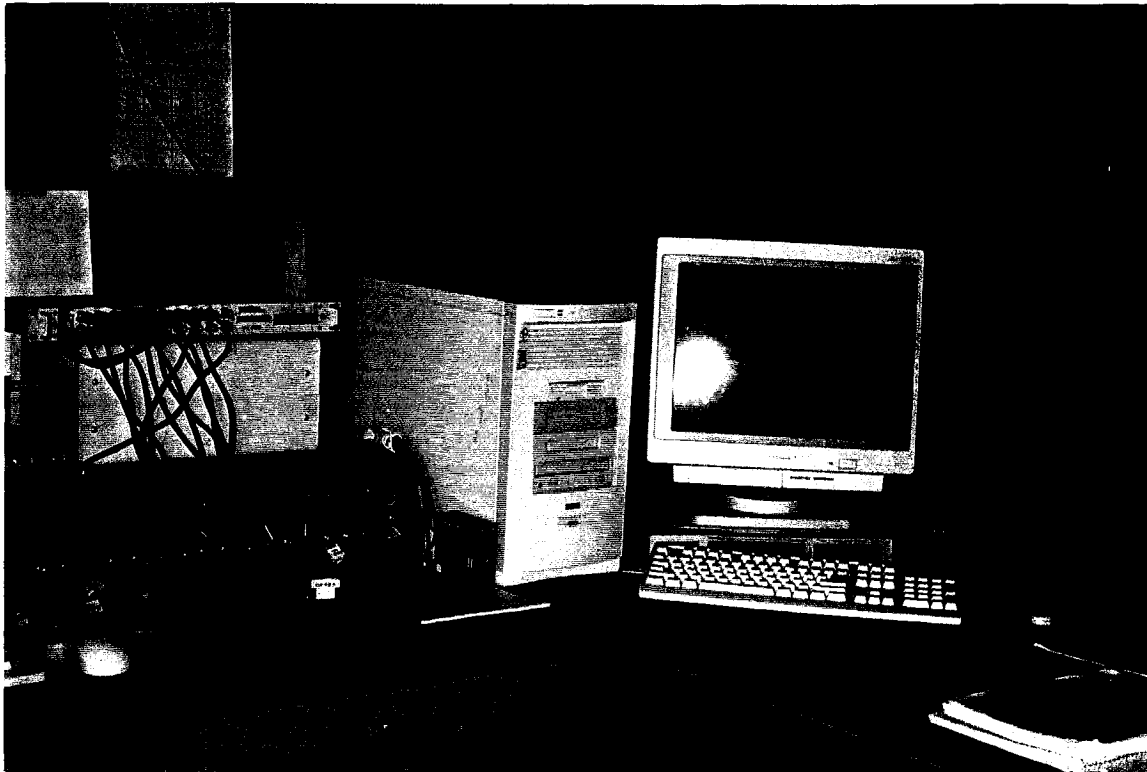


**Fig. G4.** Control terminal of wave generation and data acquisition.



**Fig. G5.** Control terminal of mechanical profiler.



Fig. G6. Breakwater before testing.

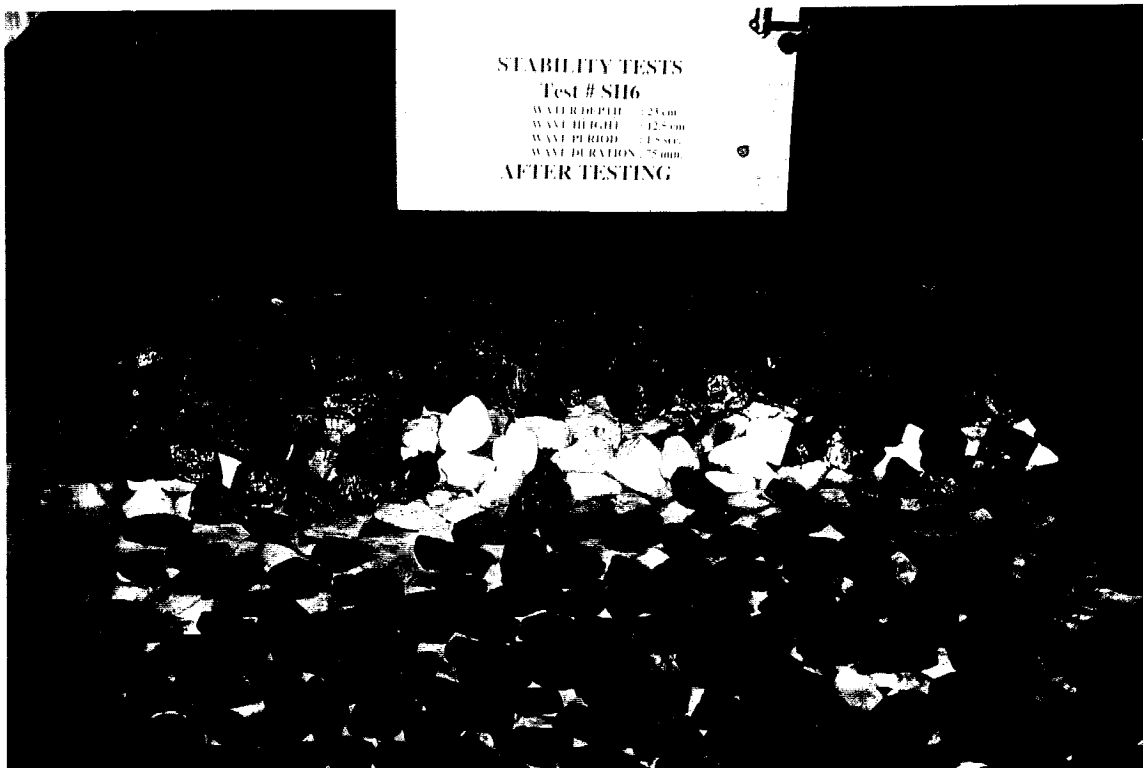


Fig. G7. Breakwater after testing.